FINNISH METEOROLOGICAL INSTITUTE
CONTRIBUTIONS

No. 40

MODELLING OF THE TRANSPORT OF NITROGEN AND SULPHUR CONTAMINANTS TO THE BALTIC SEA REGION

Marke Hongisto

ACADEMIC DISSERTATION IN APPLIED PHYSICS

Helsinki University of Technology

Dissertation for the degree of Doctor of Science in Technology to be presented with due permission of the Department of Engineering Physics and Mathematics, Helsinki University of Technology for public examination and debate in Auditorium F1 at Helsinki University of Technology (Espoo, Finland) on the 9th of May, 2003, at 12 noon.

Finnish Meteorological Institute
Helsinki 2003

ISSN 0782-6117
ISBN 951-697-572-0

Yliopistopaino
Helsinki 2003

ILMATIETEEN LAITOS

Julkaisun sarja, numero ja raporttikoodi
Contributions No. 40, FMI-CONT-40

Julkaisija Ilmatieteen laitos, Vuorikatu 24
PL 503, 00101 Helsinki

Julkaisuaika 2.4. 2003

Tekijä
Marke Hongisto

Projektin nimi
Toimeksiantaja

Nimeke

Rikki- ja typpiyhdisteiden kulkeutumisen mallittaminen Itämeren alueelle

Tiivistelmä

Työssä on kehitetty simulaatiomalli Hilatar, jolla voidaan kolmiulotteisessa hilassa laskea ja ennustaa ilman epäpuhtauksien kulkeutuminen ja sekoittuminen alailmakehässä, kemiallinen muutunta kulkeutumisen aikana ja laskeuma Euroopassa ja sen osa-alueilla. Mallin eri versioilla on arvioitu Itämeren ympärysvaltioiden rikki- ja typpiyhdisteiden pitoisuuksien ja laskeumien kehitys vuosina 1985, 1988 ja 1993-2001, tutkittu laskeuman ja pitoisuuksien vaihtelua ja arvioitu niihin vaikuttavien fysikaalisten, meteorologisten sekä mallien rakenteeseen liittyviä tekijöiden suhteellista tärkeyttä sekä mallien epävarmuustekijöiden suuruutta. Hilatar-mallilla on arvioitu mm. EU:n BASYS - Baltic Sea System Study - projektissa Itämeren typpilaskeuma, tutkittu sen vaihteluun vaikuttavia tekijöitä sekä myös simuloitu lähialueiden päästöjen kulkeutumista Suomeen pitkällä aikavälillä ja episoditilanteissa. Sen varhaisemmilla versioilla on laskettu myös Suomen ympäristökeskuksen Daiquiri-mallin laskeuma-matriisit.

Itämeren ympärysvaltioiden korkeiden epäpuhtauspitoisuuksien ja laskeuman alueellinen ja ajallinen vaihtelu on suurta. Episodimaisuuden aiheuttavat ennen kaikkea säätilanteiden vaihtelu, paikallisesti savuvanojen suuret pitoisuusgradientit, päästöjen aikavaihtelu sekä kaukokulkeumaepisodit. Pohjoismainen hapettuneen typen laskeuma on Lapissa keskimäärin kymmenesosa Tanskan tasosta, ammoniakkilaskeuma vielä pienempi. Vaikka rikkilaskeuma on suuri Kuolan saastelähteiden ympäristössä, se ei ylitä Suomen Lapissa Keski-Euroopan tasoa. Typen märkälaskeuma Itämereen on suurinta talvella ja syksyllä. Kuivalaskeuman osuus on suurin Tanskassa kesällä korkeiden ammoniakkipäästöjen takia. Vaikka eurooppalaiset päästöt laskivat 1990-luvulla, typpilaskeuma tai pitoisuudet eivät seuranneet mukana, sen sijaan rikkilaskeuma pieneni hiukan. Vallitseva suursäätila vaikuttaa eniten laskeuman vuosivaihteluun. Avoimen Itämeren ilmakuorma vuosina 1993-1998 vaihteli välillä 140-180 kt N hapettuneiden ja 100-120 kt N pelkistyneiden typpiyhdisteiden osalta. Ilmakuorman suhteellinen merkitys levien ravinteena vaatii lisätutkimuksia, sillä Itämeri on jo varsin pahoin rehevöitynyt ja primäärituotannon ravinteista suurin osa tulee sisäisestä kuormituksesta.

NO_x- ja SO_2-pitoisuudet olivat korkeimmillaan talvisin kun kemialliset- ja laskeumanielut ovat heikoimmillaan, ja inversiotilanteet ovat yleisiä. NH_3-päästöt ovat suurimmat kesällä, ja ammoniakin muutunta partikkeleiksi on nopeinta talvella kun sulfaattia on ilmassa. Typpihapon talvipitoisuudet ovat alhaisia hitaan kaasufaasi-muutunnan, lyhyiden päivien ja NH_3 reaktion takia. Laskeumien kriittiset kuormitukset ylitettiin, sen sijaan SO_2:n talvi- ja NO_2:n vuosipitoisuudet jäivät kriittisiä arvoja pienemmiksi tarkasteluaikana tausta-alueilla Pohjoismaissa, mutta SO_2-pitoisuudet ylittivät kriittiset talvikeskiarvot varsinkin vuonna 1996 laajoilla alueilla Euroopassa.

Malli-mittausvertailu osoitti että Hilatar pystyy simuloimaan rikki- ja typpiyhdisteiden maantieteellisen jakauman ja aikavaihtelun varsin hyvin Itämeren ympäristössä. Mallitulokset ja sääkentät talletetaan kahteen jatkuvasti päivitettävään tietokantaan. Aineistoja voidaan käyttää mm. selvitettäessä ilmastollisten stressitekijöiden sekä ilmansaasteiden yhteisvaikutusta kasvillisuusvaurioiden syntyyn.

Julkaisijayksikkö
Ilmatieteen laitos, Ilman laadun tutkimus

Luokitus (UDK)
504.05, 504.064.2, 551.510.42, 551.509.313.328

Asiasanat
Matemaattiset mallit, ilman epäpuhtaudet, Happamoituminen, Rehevöityminen, Ilman laadun numeerinen ennustaminen

ISSN ja avainnimike
ISSN 0782-6117
Finnish Meteorological Institute Contributions
ISBN 951-697-572-0
Kieli: Englanti
Myynti
Sivumäärä 188
Hinta
Ilmatieteen laitos / Kirjasto
PL 503, 00101 Helsinki
Lisätietoja

FINNISH METEOROLOGICAL INSTITUTE

Published by	Finnish Meteorological Institute Vuorikatu 24, P.O. Box 503 FIN-00101 Helsinki, Finland	Series title, number and report code of publication Contributions No. 40 FMI-CONT-40 Date 2.4. 2003
Author Marke Hongisto		Name of project Commissioned by

Title

Modelling of the transport of nitrogen and sulphur contaminants to the Baltic Sea Region

Abstract

In the work for this thesis, the 3D model Hilatar, which can be used to monitor and numerically forecast air pollution transport, chemical transformation and deposition in Europe and its sub-areas, has been developed. Model has been used to assess the sulphur and nitrogen concentrations and fluxes over the Baltic Sea and its surroundings in 1985, 1988 and 1993-2002 and to study their time variation caused by physical, meteorological and model structural factors, as well as other uncertainties connected to the 3D modelling. The model has been used e.g. in quantifying nitrogen flux to the Baltic Sea, and the factors that influence it, within the EU BASYS (Baltic Sea System Study) project and in studying of pollutants in episodic situations. The first model version has been used in calculating the Daiquiri-model unit matrixes for the Finnish Environmental Institute.

The temporal- and spatial variation of the concentration and deposition of air pollutants is high. Episodicity is to a large extent caused by meteorological factors, the time variation of emissions, high concentration gradients close to source areas and long-range transport from high-intensity emission areas. Considering the Nordic countries, the modelled deposition of oxidised nitrogen in Lapland is around 10 % of that in Denmark, the ammonium deposition being still smaller. Although sulphur deposition is high in the vicinity of the large industrial areas of the Kola Peninsula, is does not exceed the Central European level there. The wet flux of nitrogen to the Baltic Sea is strongest in winter and autumn. The dry nitrogen deposition share was highest in Southern Sweden and Denmark in summer due to high ammonium emissions. The effects of the decreasing emission trend could not be seen in Northern European N-deposition in 1993-98; S-deposition decreased slightly, however. The prevailing meteorological conditions were the primary cause of the inter-annual variation of regional deposition. Annual deposition to the open Baltic Sea area (391 000 km^2) over the period 1993-1998 vary in the range 140-180 kt(N) for NO_x and 100-120 kt(N) for NH_x. The relative importance of the atmospheric load for algae growth in the Baltic Sea needs to be further studied since the sea is already rather badly eutrophicated and the primary production is largely driven by the nutrients that have already accumulated in the system.

Modelled NO_x and SO_2 concentrations are at their highest during winter, due to slower chemical and terrestrial deposition sinks, maximum emissions and more frequent inversions. Ammonia emissions are highest during the summer and the conversion of NH_3 to ammonium-sulphate particles is stronger in winter when there is more sulphate in the air. HNO_3 levels are low in winter due to low reactivity, short days and reactions with NH_3. The critical deposition limits were exceeded, but the critical wintertime SO_2 and annual NO_2 concentrations were not exceeded in the Nordic background areas, although this occurred for SO_2 over large areas in Europe especially in the cold winter of 1996.

Comparison with field campaign results and long-term measurements demonstrated a rather good description of both the spatial and temporal characteristics of the S and N pollution in the Baltic Sea region. Model results and meteorological input data are stored in two continuously updated databases. They can be used in studying simultaneous effect of meteorological and air pollution stresses on vegetation.

Publishing unit	Finnish Meteorological Institute, Air Quality Research
Classification (UDK) 504.05, 504.064.2, 551.510.42, 551.509.313.328	Keywords Mathematical models, Air pollutants, Acidification, Eutrophication, Numerical air quality forecasts
ISSN and series title ISSN 0782-6117 ISBN 951-697-572-0	Finnish Meteorological Institute Contributions Language English
Sold by Finnish Meteorological Institute / Library P.O.Box 503, FIN-00101 Helsinki Finland	Pages 188
	Price Note

To the memory of my father and my Karelian ancestors.

Acknowledgement

The model and simulations for this thesis have mainly been produced in 1991-96 in the FMI Air Quality Department, then within a specific BASYS research group at Vuorikatu, and thereafter in different rooms belonging to the meteorological or climatological research groups, with beautiful views from the window and interessant colleagues. I would like to express my gratitude to my supervisor Sylvain Joffre for opening up connections to the European research community and for his continuous support, as well as to all the colleagues who have worked with the Hilatar model, its meteorological data base, graphical interfaces or web pages at Vuorikatu: Ville Savolainen, Ilkka Vallinoja, Kirsti Jylhä, Virpi Flyktman, Mikhail Sofiev and Ilja Sidoroff.

I would like to thank the EMEP MSC-W centre for providing its emission inventory and background concentrations for the simulations before June 1995, Andreas Bott for his advection algorithm, the FMI HIRLAM group for the meteorological data, and Oystein Hov for the photochemical codes.

The scientists who have collaborated within various research groups in the Air Quality Department before 1997 are also kindly acknowledged. I would especially like to thank Juha-Pekka Tuovinen, Pentti Vaajama (in memorium), Virpi Lindfors and Juhani Damski for various algorithms, programs and atmospheric boundary-layer models, which are integrated or linked into the Hilatar modelling environment.

The stack emissions inventory has been collected in joint projects with Finnish, Russian and Estonian scientists. I would especially like to thank Antti J. Häkkinen for his activity in its development. I would also like to thank Harri Pietarila, not only for providing the 1995 data set, but also for the promised next update. The early traffic emission inventory made for Estonia and Russia by Kari Mäkelä at the VTT is also acknowledged. I would also like to express warm thanks to all the FMI computer support staff, especially to Kimmo Lahtinen, and to Ritva Hänninen, Pirjo Martikainen and Esko Puheloinen from the FMI library.

The experience gained within EUROTRAC, BASYS and various NMR-funded Nordic projects has been very important. I would like to thank all the co-authors of the articles and referred papers. It has been a great pleasure to work closely with a scientist like Michael Schulz, who understands the importance of both model and measurement studies, and to learn more about modelling in joint projects with Gerhard Petersen, Olaf Krüger, Zahari Zlatev, Jan Eiof Jonsson and Joakim Langner. Within BASYS I especially enjoyed working with Lise Lotte Sørensen and her close colleagues. Support from the measurement community, especially Berndt Schneider, Elke Plate, Roman Marks and Dalia Sopauskiene, has been of a great value. Co-operation within East-European studies with Natalia Goltsova, Rein Tamsalu, Peeter Ennett, Marko Kaasik, Ylis Soukand and other Estonian and Russian researchers has given a deep insight into the environmental conditions in our neighbouring areas.

For their comments on the thesis or the manuscripts I would like to thank Rainer Salomaa, Sylvain Joffre, Rein Tamsalu, Hannu Savijärvi, Veli Matti Kervinen, Jaakko Kukkonen and Göran Nordlund. I would also like to thank the whole Institute management for providing good working conditions, and Robin King for his careful language corrections. Financial support from the Ministry of the Environment in Finland before 1997 as well as from the Finnish Academy of Sciences, the Nordic Council of Ministers, the Nessling Foundation and EU BASYS throughout the MAST programme (contract: MAS3-CT96-0058) is gratefully acknowledged.

Finally, I would like to express my sincere gratitude to my parents, Eila and Taavi Mannonen, for their love and continuous encouragement, and to apologise to them, as well as to my dear daughters, Tuuli and Eeva, for my absence during many long working days and evenings.

CONTENT OF THE THESIS

In the work for this thesis, a regional-scale model Hilatar for simulating the transport of various gaseous air pollutants and particulate matter over Europe and its northern subregions, with associated pre- and postprocessors and graphical interfaces, has been developed. The model has been used e.g. in the following:

1 estimating numerically since 1993 the long and short-range transport of sulphur and nitrogen compounds, heavy metals and dust from Europe or neighbouring countries to Finnish background areas,
2 calculating the magnitude of the air pollution fluxes to the Baltic Sea and to other ecosystems,
3 when estimating the origin, transport paths and chemical conversion of various pollutants, explaining in parallel the meteorological conditions leading to pollution episodes,
4 forecasting long-range transport of air pollutants to Finland,
5 producing animations of concentration and deposition dynamics together with meteorological fields, for demonstration purposes, teaching and system analysis.

The model performance has been tested numerically and by model-measurement inter-comparison. The results and meteorological input data are collected in two continuously-updated data bases: The first contains meteorological fields, the second gridded fluxes and concentrations of sulphur (S) and nitrogen (N) compounds over the Nordic model region (NMR area) and the European (EUR) domains. Summaries of the results are also presented on operationally updated www-pages for informing the Finnish public on the current air quality situation. The model system was used in estimating the atmospheric load to the Baltic Sea for the EU MAST BASYS (Baltic Sea System Study) Sub-project (SP) 5.

Most of the work in this thesis is published in the following papers, which are referred to in the text by their corresponding Roman numerals.

LIST OF PUBLICATIONS AND THE AUTHOR'S CONTRIBUTION TO THE PAPERS OF SEVERAL WRITERS.

I Hongisto, M., 2002. Hilatar, a limited area simulation model for acid contaminants. Part I. Model description and verification.
Atmospheric Environment 37/11 pp. 1535-1547

II Hongisto, M., Sofiev, M. and Joffre S., 2002. Hilatar, a limited area simulation model for acid contaminants. Part II. Long-term simulations results.
Atmospheric Environment 37/11 pp. 1549-1560

The paper contains the BASYS project simulation results. MH (the author) was involved in the planning of the project from an early stage. She constructed the model versions and data base interfaces, performed all numerical tests for the various model versions, pre-processed most of the input data, wrote the pre- and post-processing programs, performed most of the simulations and model-measurement inter-comparisons, analysed most of the results, took part in providing meteorological and pollution forecasts for the required track planning for the ships during the winter field campaigns.

III Hongisto M., Sofiev M., 2001. Representativeness of the coastal measurements for the open sea – experience of the model applications in the Baltic region. A contribution to the subproject CAPMAN. In P.M. Midgley, M. Reuther and M. Williams (Eds.) Proceedings from the EUROTRAC-2 Symposium 2000. Springler-Verlag Berlin, Heidelberg, New York, 2001, 5 p. 486-490

MH simulated the situations, studied coastal meteorology and gradients and analyzed the results.

IV Poikolainen J., Lippo H., Hongisto M., Kubin E. & Mikkola K., 1998. On the abundance of epiphytic green algae in relation to the nitrogen concentrations of biomonitors and nitrogen deposition in Finland. Environmental Pollution 102, S1, 85-92.

MH constructed a zoomed version of the Hilatar model with a grid of around 11 km (0.1^{o}) and simulated the concentration and deposition exposure for the biomonitoring study at the Finnish National Forest Inventory.

V Hongisto M. and Joffre S., 1997. Transport modelling over sea areas. In Ebel A., Friedrich R. and Rodhe H., (ed's). Transport and chemical transformation of pollutants in the troposphere, Vol. 7, Tropospheric modelling and emission estimation, chemical transport and emission modelling on regional, global and urban scales. Springer-Verlag Berlin Heidelberg 1997, p.52-58.

Paper V is a summary of six successive annual reports within the EUROTRAC project. MH studied, among other things, the NOx deposition in 1985 and 1988 and the effect of the MABL and dry deposition velocity parameterisation on the transport over sea-areas, estimated the influence of the Kola Peninsula sources and the Estonian and Russian emissions on Finland, and constructed a box model, containing aqueous chemistry, in order to study sulphur transformation kinetics in clouds, and to re-estimate the reaction rates for Hilatar.

MH was the responsible author for papers I-III and V.

Other publications related to the thesis are: Hongisto (1990, 1992a-c, 1993a-c, 1994, 1997, 1998, 2001, 2002a-b); Hongisto et al. (1988, 1991, 1995, 1997, 1998a-b, 1999a-c); Hongisto & Joffre (1990, 1993, 2002); Hongisto & Jylhä (1998); Hongisto & Valtanen (1992, 1993); Hongisto & Wallin (1990); Häkkinen et al. (1995); Plate et al. (1999); Schneider et al. (1999); Schulz et al. (1997, 1998, 1999); Schulz (1998); Schulz & Hongisto (1998); Sofiev et al. (1999, 2001, 2002); Tervahattu et al. (2002a-b); Tuovinen at al. (1989) and Zlatev et al. (2001).

SYMBOL NOTATIONS AND ABBREVIATIONS

A	numerical constant, a specified function of height in defining η-coordinates,
ABL	the atmospheric boundary layer
AO	Arctic Oscillation
a,b,c	numerical constants for defining hmix in stable situations or for the sulphur oxidation rate in clouds,
a_k , b_k	numerical constants in defining vertical coordinates,
BC	background concentration for mass conservation tests,
C	correction factor for diffuse radiation in calculating G,
C_c	the Cunningham slip correction coefficient,
C_D	the drag coefficient,
$C(\delta)_s$,$C(\delta)_b$	concentrations at height z=δ over smooth and broken sea, respectively,
C_o	the concentration at the air/water interface,
$c(\vec{x},t)$	the concentration of a compound, at time t and place $\vec{x}$ = x, y, z,
c_p	the specific heat at constant pressure,
clf, clf(x,z)	the fractional cloud cover,
$clf_M(x,z)$	maximum fractional cloud cover above,
D_x	molecular diffusivity of the gas x,
D_c	Brownian diffusivity of particles,
DIN	dissolved inorganic nitrogen
D(z)	the dew-point temperature,
D_p	the raindrop size distribution
DON	dissolved organic nitrogen
d	day, cumulative day,
d_p	the diameter of a particle
dzk_{ijk}	the height of the k:th vertical level of grid (i,j),
$E(D_p,d_p)$	the collision efficiency between the raindrop and the particle,
EMI_x	emission of compound x,
EDX	energy dispersive X-ray microanalyzer
e	the water vapour pressure, $=\rho_v R_v T$,
e_s	the saturation vapour pressure,
$F(z_{ref})$	flux at the reference height z_{ref},
F_x, F_δ, F_s	flux in the turbulent and the deposition layers, and between smooth and broken sea surfaces,
f_i	auxiliary functions,
f_o, f_{ox}	the coefficient of reactivity for compound x,
G	solar irradiation,
GrADS	Grid Analysis and Display System
GRIB	gridded binary
G1,G2	vertical, potential temperature gradients,
g	acceleration due to gravity
H	the Henry's law coefficient,
h_{mix},h	the mixing height,
h/L	dimensionless stability,
K_{eq}	the equilibrium constant between ammonium nitrate, gaseous ammonia and nitric acid,
$K(\vec{x},t)$	the turbulent diffusion or gradient transfer coefficient, eddy diffusivity

	in units of m^2s^{-1},
K_M, K_H, K_E	K for momentum, heat and moisture,
K_z	vertical eddy diffusivity
K_{as}, K_{ab}, K_{ms}, K_{mb}, K_{sb}	turbulent transfer coefficients in the turbulent and the deposition layers, and between smooth and broken surfaces for defining the v_d for particles,
k_{eq}	equilibrium coefficient for gaseous and particulate NH_3-HNO_3-balance,
k_i	reaction rate,
k_{SB}	the Stefan-Bolzmann constant,
L	the Monin-Obukhov length,
L	loss term in the differential equation for chemical transformation,
L_c	scavenging rate for compound c,
LAI	the leaf area index,
liq	subscript, aqueous phase concentration or conversion rate
LRT	long-range transport
lwc,lwc(x,z)	liquid water content,
M	air density, in liquid phase M=mol l^{-1},
MABL	marine atmospheric boundary layer
m	mass of air, or mass of concentration inside a grid box,
NAO	the North Atlantic Oscillation,
$N(D_p)$	raindrop size distribution
P	production term in the differential equation for chemical transformation,
PAN	peroxyacetyl nitrate
PAR	photosynthetic radiation,
PP	primary production
p(z), p_k	pressure, pressure at model level k,
p_o	a reference pressure taken as 1000 hPa,
Pr	the turbulent Prandtl number,
p_s	surface pressure,
p_{st}	standard atmospheric pressure at sea level =1013.26 hPa,
pH	negative logarithm of the H^+-ion content of the droplet,
ppm, ppb	10^{-6}, 10^{-9},
QSSA	quasi steady-state approximation
q(z)	specific humidity,
q_s	the saturation specific humidity,
q_*	the moisture scale,
R, R_d	gas constant for dry air, 287.05 [J (kg K)$^{-1}$],
R(z)	the precipitation rate at altitude z,
R_i	the rate of reaction i,
Re	the Reynolds number,
RH	the relative humidity,
Ri	the bulk Richardson number,
R_v	gas constant for moist air, 461.51 [J (kg K) $^{-1}$],
r_a	the aerodynamic resistance,
r_b	the resistance near the surface layer,
r_c	the resistance associated with pollutant-surface interaction,
r_{ac}	resistance which depends on the canopy height and density,
r_{cl}	surface resistance of leaves, twigs and bark,

r_{dc}	resistance against buoyant convection in canopies,
r_{gs}	surface resistance of the soil, leaf litter, etc.,
r_{H2O}	the minimum bulk canopy stomatal resistance of water vapour,
r_{lu}, r_{lux}	leaf surface (cuticle) resistance for compound x,
r_{ext}	external leaf surface resistance,
r_s and r_m	stomatal and mesophyll resistances,
r_{snow}	snow resistance,
r_p	the particle radius,
r_d	the particle dry radius,
r_w	the particle wet radius,
$S(\vec{x},t)$	source and sink terms (emissions, chemical transformation, and deposition) in the transport equation,
Sc	the molecular Schmidt number,
SEM	scanning electron microscope
SP	sub-project
S_θ	the solar constant at sea level,
$T(z)$, T_s ,T_2	temperature at level z, at (sea) surface or at 2 m height,
T_{rot}	the period of rotation for mass conservation tests,
T_v	virtual temperature = $T\{1.-(e/p)\ [1-R_d/R_v]\}^{-1}$,
$U_t(D_p)$	the fall speed of the rain drops with diameter D_p
u_*	the friction velocity,
u, v, u(z), $\vec{u}$	horizontal wind components and wind velocity,
$V(\vec{x},t)$, V_{10}	the mean wind velocity, wind velocity at 10 m height,
V_{gd},V_{gw}	the terminal settling velocity for dry particles and those which have grown due to the effect of humidity,
v_d	dry deposition velocity,
$v_{d,g,}$ ($v_{d,g,i}$)	gravitational settling velocity of the particles (in size class i),
w_*	the convective velocity,
w	the vertical wind velocity,
x,y	horizontal coordinates,
ZI	Zonal Index
z	vertical coordinate, vertical height,
z_{ref}	reference height,
z_o	surface roughness in general or for momentum,
z_h, z_e	surface roughness length for heat and humidity,
z_k	height of the vertical level k,
z/h	the dimensionless height,

GREEK AND SPECIAL SYMBOLS AND OPERATORS

α	the percentage of the sea surface covered by breaking waves,
ε	the numerical error in mass conservation,
ζ	dimensionless height in the surface layer, =z/L,
$\eta(z)$	hybrid terrain-following vertical coordinate levels of the HIRLAM model,
η_k	$\eta(z)$ at vertical level k,
θ_*	the temperature scale,

θ_z	the solar zenith angle,
θ_s	the slope of the local terrain,
$\theta(z)$, $\theta_v(z)$	potential temperature, virtual potential temperature,
ν	the kinematic viscosity of air,
ρ_v	density of the moist air,
ρ	density of the air,
ρ_p	density of a particle
Φ	the geopotential height,
∇	del (nabla) operator,
δ	partial derivative,
Δ	difference,
ΔA	grid side area, = $\Delta y_i \cdot \Delta z_i$, or $\Delta x_i \cdot \Delta z_i$ or $\Delta x_i \cdot \Delta y_i$
Δt	time interval,
$\Delta_{(NH_4)_{1.5}SO_4}$	formation rate of ammonium sulphate,
$\Delta_{NH_4NO_3}$	formation rate of ammonium nitrate,
κ	the von Kármán constant,
Λ_x	scavenging velocity of the compound x,
μ	the dynamic viscosity of air,
τ	the (photochemical) lifetime,
$\varphi_H(z/L)$	dimensionless potential temperature gradient in the surface layer,
$\Psi_M(\zeta)$	surface layer diabatic correction function for momentum,
$\Psi_H(\zeta)$	surface layer diabatic correction function for heat,
$\psi_E(\zeta)$	surface layer diabatic correction function for moisture,
ω	angular velocity vector for mass conservation tests, $= 2\pi / T_{rot}$.

ACRONYMNS

ADOM	initially: an Eulerian Acid Deposition Model
BASYS	the Baltic Sea System Study
BALTEX	the Baltic Sea Experiment
CAPMAN	Coastal Air Pollution Meteorology and Air-Sea Nutrient Exchange
CCE	the European Coordination Centre for Effects
EMEP/MSC-W	Co-operative Program for Monitoring and Evaluation of the Long Range Transmission of Air Pollutants in Europe, Meteorological Synthetizing Centre - West
EPAK	Epäpuhtauksien K-teoriaan perustuva leviämismalli A dispersion model for air pollutants based upon the K-theory
EURAD	European Regional Acid Deposition Model
EUROTRAC	The EUREKA project on the transport and chemical transformation of trace constituents in the troposphere over Europe in http://www.gsf.de/eurotrac/ (October 2002)
FINOX	a Finnish regional dispersion model for oxidised nitrogen
FMI	Finnish Meteorological Institute
GENEMIS	GENeration and evaluation of EMISsion data for episodes, a EUROTRAC-2 subproject. in: http://www.ier.uni-stuttgart.de/public/abt/tfu/projekte/genemis/ (October 2002)
GKSS	Forchungszentrum Geesthacht GmbH

HELCOM	The Helsinki Comission
HIRLAM	The HIgh Resolution Limited Area Model
ICP	International Cooperative Programme
IPCC	Intergovernmental Panel on Climate Change
IIASA	International Institute of Applied Systems Analysis
MARE	Marine Research on Eutrophication
MAST	MArine Science & Technology programme
NCAR	National Center for Atmospheric Research, Boulder Colorado
NMR	Nordiska Ministerrådet (in the case of financial support) Nordic Model Region (in referring to the model's geographical coverage)
RADM	Regional Acid Deposition Model
RIVM	Rijksinstituut voor Volksgezondheid & Milieu National Institute for Health and Environment in the Netherlands.
UNEP	United Nations Environmental Programme
VTT	Technical Research Centre of Finland,

1. OBJECTIVES AND HISTORY OF THE MODEL DEVELOPMENT

The increased spatial and temporal resolution of meteorological predictions, advances in the theoretical description of the physical phenomena in the atmospheric boundary layer (ABL), better understanding of exchange processes between the air and the underlying surface, satellite-data-based inventories and the rapid development of computers have all multiplied the possibilities of studying atmospheric pollution using numerical models. Studies on effects of air pollutants on ecosystems are important. The critical loads and critical concentration limits, defined as levels above which, according to present knowledge, direct adverse effects on receptors may occur (Ashmore & Wilson, 1992), are still exceeded in sensitive ecosystems (Posch et al., 2001). Discussion on the reasons for forest decline and water eutrophication is still going on. Models have made it possible to quantify the role of air pollutants for the observed damages in comparison with other anthropogenic or natural stress factors, and to evaluate the cumulative effects of long-lasting destructive stresses (coldness, drought, wetness, deposition, elevated concentrations), together with an assessment of currently-occurring events, including direct exposure to air pollutants. Long-term deposition amounts or average concentrations for a single pollutant do not necessarily correlate with visible damage.

While continuous measurements are important in monitoring the local air pollution situation, models are valuable tools in quantifying the budgets of external loads to the ecosystem, the coverage and extent of episodes and the origin of the pollutants. They can describe the meteorological conditions during pollution episodes and explain the reasons and mechanisms behind the onset of an episode. Models increase our knowledge about the background air quality over regions where continuous measurements are not available or where local factors influence monitoring results.

The goals of the work for this thesis were to construct a model – Hilatar -, that could simulate the long and medium-range transport of tropospheric contaminants from Central Europe to Finland. Hilatar was designed to be able to numerically monitor the air pollution concentrations and fluxes in background areas, to complete and explain information gathered in measurement networks and field campaigns and to estimate the nutrient load to the Baltic Sea for marine ecosystem modellers.

The author already started to construct tools for environmental decision-making in the Department of Technical Physics at the Helsinki University of Technology (Reinikainen, 1981; Mannonen, 1982; Hongisto, 1985; Routti et al., 1983) by constructing a multi-goal optimization model of the Finnish energy system. At the FMI, this expertise was applied in the planning of optimal sulphur reduction strategies for Finland (Hongisto et al., 1988 and Hongisto & Wallin, 1990). In that study, several scenarios for industrial and energy-producing systems were generated, and the unit deposition matrices calculated by the EPAK-model (Nordlund et al, 1984) were used in a model constructed for optimizing sulphur control measures so that the critical load would not be anywhere exceeded.

The static EPAK model was only able to carry out transport studies with linear chemistry, e.g. of sulphur. At that time, the role of nitrogen (N) as an acidifying and fertilising pollutant was becoming even more obvious. Because the chemical transformation of nitrogen compounds is a non-linear process, nitrogen compounds

have a longer life-time in the atmosphere, and the origin of N deposition lies for the main part outside Finland, new tools for studying the role of nitrogen in Finnish background areas were needed. Non-linearity itself implies that the transfer matrix technique is in principle an inadequate method of assessing nitrogen transport.

The first version of a dynamical model for air-pollution transport and deposition, the FINOX model, a Finnish regional dispersion model for oxidised nitrogen (Hongisto 1992a and 1993a), covered Southern Finland with a 30 km horizontal polar-stereographic grid. The meteorological fields were interpolated from surface measurements. The ABL parameters were calculated from the vertical profiles of the Jokioinen soundings with FMI local-scale plume model pre-processors originally written by P. Vaajama. The surface parameters were interpolated from synoptic measurements at around 40 stations with a 3 h time interval. The vertical wind and temperature profiles were estimated using logarithmic laws and Ulden & Holtslag (1986) non-dimensional stability correction functions. In addition to the papers related to this thesis, the FINOX model has been applied e.g. for estimating the deposition of oxidised nitrogen in 1985 and 1988 (Hongisto 1992a; Paper V) and for generating source-receptor matrices for the Finnish integrated assessment model (Syri et. al., 1998, Kangas & Syri, 2002).

The main problems with the FINOX model were connected with the local factors affecting all measurements at synoptic stations, most severely wind speed and direction as well as precipitation. Interpolation can produce mass convergence if smoothing is not performed. Also, only three sounding stations exist in Finland, one of which is outside and one on the border of the model area. The Jokioinen soundings were used to represent the stability state of the lower troposphere over the whole land area, while results of the marine ABL (MABL) model (Lindfors et al., 1991) using coastal measurements were used over the sea areas. The stability-dependent change of wind with height was estimated from empirical work reported in Hanna et al. (1982), leading to rather a theoretical model, which might not well describe Finnish ABL conditions with their frequent inversions. The 30 km grid was also sparse, and the advection method (Smolarkiewicz, 1983) produced somewhat artificial numerical diffusion. Long-range transport was taken from the EMEP/MSC-W model results as 1-layer concentrations at the model's boundaries.

A new model which could use large-scale forecast fields instead of local measurements was needed, because air pollutants transport is both spatially and temporally a long-range chain of events, most of the contaminants in background areas being long-range transported from Central Europe or elsewhere. Additionally, due to factors discussed in the previous chapter, FINOX was not actually the proper tool for studying the dynamical meteorological and other processes influencing the deposition and transport of pollutants over the sea, in coastal zones and in forested areas.

The Hilatar model, capable of using the forecast fields of the FMI operational weather prediction model HIRLAM (high resolution weather prediction model), was constructed at the beginning of the 1990's. Its gradual updating and the improvement of the physical parameterisation is a continuous process. The model has been applied to many studies of nitrogen and sulphur pollution over various parts of the Nordic area since 1991. In order to achieve an operational capability for the field campaigns in 1997-1998, the model was extended to cover the whole of Europe (Paper I). This,

initially only an on-line estimate of the long-range transported (LRT) pollutant contribution, has been further used to generate air pollution forecasts for Finnish background areas (Hongisto 2002b). The Baltic Sea area model has also been used in simulating the transport and deposition of Pb, Cd and Zn over the Baltic Sea region for the two BASYS Network field experiment periods (Sofiev et al., 2001; Schneider et al., 1999), with parameterisation partly taken from the EMEP-MSC-E heavy metal model (Galperin et al., 1994). In these heavy metal studies the Europe-wide calculations were made with the GKSS Research Centre model ADOM (Petersen, 1998; Petersen at al., 1998).

The model area, grid and computer environment have been changed several times: versions with 10-13 vertical levels reaching from 3 to 10 km, and horizontal grids of 0.1^o, 0.2^o or 0.25^o over Finland or Fenno-Scandia and the Baltic States and with grid of 0.4^o and 0.5^o over Europe have been developed. The FINOX model with its meteorological pre-processors was run on FMI VAX machines, while the Hilatar code was transferred to a Cray, then to Cedar and to the Unix work-station Lilith. The meteorological and chemical data bases have various user and visualisation interfaces, storage formats and physical and geographical coverage, depending on which machine and model version is used. In the latest version the data are kept in direct access files, from where they can be directly picked up by various computer routines, visualised or animated using the Grads graphical package (www.iges.org) or further post-processed by statistical or other programs written in Fortran.

Recently, the work has been returning to its roots. Operational use of the model makes it possible to numerically track hypothetical radioactive releases simultaneously from all the European nuclear power stations, for estimating the extent of necessary protective measures.

2. AIR POLLUTION IN THE BALTIC SEA BACKGROUND AREAS

An increased nitrogen and sulphur supply leads to eutrophication and acidification of the target areas. Because the effects of the atmospheric load on e.g. marine and terrestial ecosystems depend on the present state of the system, the conditions of the various ecosystems studied in this thesis are first briefly summarized.

2.1 Marine environment

2.1.1 Characteristics of the Baltic Sea

The Baltic Sea is a young, semi-closed brackish water basin with a relatively small volume (around 22 000 km^3) and a long (30-50 years) residence time for its water. It is very shallow, being on average 55 m in depth. The Baltic Sea Basin got its present form after the last Ice Age, when the Atlantic connection finally opened around 8500-7000 years ago. By comparison, the average depth of the Mediterranean is over 1.5 km, and it's age is around 5 million years (Kakkuri and Hjelt, 2000; Furman et al., 1998). The annual precipitation of around 200 km^3 and the riverine fresh water input of around 480 km^3 keep the salinity low.

The water of the last Baltic Sea phase, the Litorina Sea (up to 4000 years ago) was slightly more saline than at present. From sediment analysis it has been concluded that, in the initial phase of the Litorina Sea due to strong haline stratification and high organic production, extended anoxia occurred, particularly in the deep basins (Zuelicke, 1999). Sediment records show that alternating periods of prevailing anoxic and oxic conditions in the deeper waters have continued throughout the brackish state of the Baltic Sea, exhibiting a cyclicity of about 300 years. The exact reasons for these changes are not clear as yet, but they are connected with climatic variability and linked to the water exchange between the Baltic Sea and the North Sea. Intense algae blooms were common already in the Litorina Mare phase (Zuelicke, 1999; Winterhalter, 1999).

2.1.2 Vulnerability of the Baltic Sea ecosystem

The marine ecosystem of the Baltic Sea is very sensitive. Species have to be adapted to the two-layered brackish water, an environment with changing light, temperature and salinity, and varying circulation conditions between strong and mild ice winters. Its aquatic biota is very poor in species, and the food chains are vulnerable to external disturbances (HELCOM 1996; Zuelicke, 1999).

The water quality and the state of the ecosystem are the subject of several international conventions, the most important being the "Convention on the Protection of the Marine Environment of the Baltic Sea Area (Helsinki, 1974, revised 1992)". The state of the Baltic Sea is regularly assessed at 5-year intervals by HELCOM (the Marine Environment Protection Commission or the Helsinki Commission), and published in the Baltic Sea Environment Proceedings (HELCOM, 1996)

The atmospheric load has an impact on the well-being and functioning of the whole marine food chain. The role of the airborne load, composed of nutrients, harmful chemicals and organic compounds, has to be evaluated with respect to other human-induced and natural threats to the marine ecosystem. These include fisheries, mariculture, sea transport, sand and gravel dredging and heaping, dumping of waste from ships or coastal industry, disposal of municipal sewage, accidental releases from coastal petrochemical plants and oil tankers and the slow change in the light conditions of the spawning grounds due to natural upheaval of the seabed. Human-induced climatic change also affects water temperature, altering, e.g., ice cover extremes, which in turn vary water circulation and light conditions.

2.1.3 Eutrophication of the different sub-basins

Eutrophication, a result of over-fertilisation, is a chain of processes, initiated by excessive nutrient loads. Increased concentrations of nutrients in the water lead to physical, chemical and biological changes in fauna and flora, as well as changes in oxygen conditions in the water, in the sediments and on the surface of the sea-bed. The cycling of organic matter in the sea - production, consumption and decomposition - are not in balance, and accumulation of dead material into bottom occur. (Rönnberg, 2001; Summary, 2002)

With respect to nutrients, the Baltic Sea is almost closed: only around 10 % of the nutrient inputs are exported through the Danish straits, the rest ending up in internal sinks (Eilola & Stigebrandt, 1999; Zuelicke, 1999). During the last century, the amount of nutrients in the Baltic Sea increased by several orders of magnitude, leading to nutrient over-enrichment and increased production in the sea (Bonsdorff et al., 2001; Kuparinen & Tuominen, 2001).

Using several measures to quantify eutrophication, Rönnberg (2001) and Dahlgren & Kautsy (2002) have shown that it is a serious problem over the whole Baltic Sea area. The Secchi depth has decreased in coastal areas. The excessive growth of filamentous algae has harmed more slowly-growing macroalgae. Summertime primary production and chlorophyll-*a* concentrations have approximately doubled in the southern Baltic Proper since the 1970's, large amounts of drifting algae spoil coastal waters and turbidity and sedimentation rates have increased (Bonsdorff et al., 2001). While biomass and production have increased above the halocline, below it many important food chains have been disturbed or lost. An area of 100 000 km^2, about 25 % of the total bottom area of the central Baltic Sea, is anoxic, leading to a weakening denitrification capacity and further increased eutrophication (Dahlgren & Kautsky, 2002; Summary, 2002; Kuparinen and Tuominen, 2001).

Shallow sills divide the Baltic Sea into rather isolated basins. The state of every sub-basin is unique due to its characteristic features (volume, depth, water salinity and turnover time, river and atmospheric inputs and loads, cloudiness, evaporation, precipitation, temperature cycle, ice conditions and ecosystem biodiversity). The specific problems, the importance of the atmospheric load and the response of the ecosystem to external disturbances are very different in the south and the north, as well as in the eastern or western parts of the Baltic Sea.

The northernmost part, the Bothnian Bay, is normally covered for 150-180 days with ice having a maximum thickness of 50-80 cm. The annual inflow of fresh water, around 105 km^3, is high in comparison to the volume (1500 km^3) of the basin. Phosphorus (P) concentrations are low, but nitrogen (N) concentrations are rather high. The Bothnian Sea has a three times higher volume and a smaller freshwater inflow, but higher P and lower N concentrations than the Bothnian Bay. The primary production (PP) of the Bothnian Bay is phosphorus-limited, while in the Bothnian Sea both P and N can act as a limiting nutrient (HELCOM, 1996). The bottom fauna of the Gulf of Bothnia is extremely vulnerable, since only 3 species constitute 99-100 % of the bottom animals (Lange et al., 1991).

Signs of eutrophication of the Archipelago Sea area between Finland and Sweden were already visible in the 1970's (Rönnberg, 2001; Kirkkala, 1998). The Secchi depth in the middle and open areas has decreased from over 10 m in the 1950s to the present 2-5 m (Kirkkala, 1998). The deepwater salinity has a decreasing trend, and except in the northernmost parts, the oxygen situation has worsened, especially in areas with poor water exchange (Rönnberg, 2001; HELCOM 1996). P and N concentrations increased significantly in the period 1970-1993, levelling out thereafter. Most of the area is N-limited (Kirkkala, 1998, Jumppanen & Mattila, 1994).

The volume of the Gulf of Finland, 1100 km^3, is small in comparison with the flow of the Neva river (78.6 ±13.8 km^3 yr^{-1}), which constitutes up to 20 % of the total river

run-off into the whole Baltic. The Gulf is not sill-separated from the Baltic Proper, as are the other basins, and it is thus more influenced by the saline water inflows from the North Sea. The halocline is strongest in the western parts at a depth of 60-70 m, and near the largest eastern fresh-water input at 10-30 m. In summer, a strong thermocline develops at the same depth. The water is generally completely mixed down to the bottom in spring and autumn and also in up-welling areas in summertime.

The Gulf of Finland has been considered rather polluted, as the nutrient load per surface area is 2-3 times, in the eastern part even 5 times, higher than over the rest of the Baltic Sea (Rönnberg, 2001). Since the late 1980's the total nitrogen load has decreased from 193.7 kt N by 70 kt in 1997-98; however, no corresponding improvement has been observed in the state of the open Gulf of Finland (Pitkänen et al., 2001). The bottom concentrations of N show an increasing trend up to 1990, then a levelling off (HELCOM, 1996). The observed phosphate concentrations have been increasing, most propably due to increased internal loading which is a conseguence of bad oxygen conditions (Pitkänen et al., 2001). The Secchi depth at the cape of Hanko has decreased from around 9 m in 1914-1939 to the present 4 m (Jumppanen & Mattila, 1994); however, since 1993 it has been recovering. Nitrogen has been assessed as being the limiting factor for PP in summer and early autumn in the western Gulf.

A summary of the state of other Baltic Sea sub-areas can be found in Rönnberg (2001). She reports very serious changes in the oxygen, nitrogen and phosphorus concentrations, in the primary production and amount of zoobenthos in the Central Baltic, in oxygen and macrovegetation in the Belt Sea and in oxygen, drifting algae mats, zoopenthos and ichthyofauna in the Kattegatt. The condition of the Gulfs of Riga and Gdansk is generally bad. On the Swedish west-coast, very serious changes in macrovegetation and zoobenthos have been observed. The Gulf of Bothnia is the only part where only small or moderate changes have occurred. The Archipelago Region is the most damaged part of the Baltic Sea.

2.2 Forested areas, lakes and other surfaces

Critical loads are defined as the quantitative estimates of an exposure to one or more pollutants below which significant harmful effects on specified sensitive elements of the environment do not occur, according to present knowledge (Nilsson & Grennfeldt, 1988, Egmond et al., 2002). The numerical threshold values for critical levels set for individual pollutants (Ashmore & Wilson, 1992), have been collected in Table 9 of Hongisto (1998). The exceedances of critical levels are assessed and calculated on a regular basis both for terrestrial and aquatic ecosystems by the CCE (the European Coordination Centre for Effects at the RIVM, Rijksinstituut voor Volksgezondheid & Milieu - National Institute for Health and Environment). The exceedance of critical loads in Finland is discussed in Hongisto (1998) and paper II.

The critical loads for e.g. acidity or exposure to a single compound do not explain the tolerance to air pollution of forests or, indeed, any ecosystems. Vegetation is exposed to a complex mixture of potentially damaging substances (from nutrients to toxic metals) in parallel with climatic and biological stresses (including insects). All these interact with

one another and affect plants, animals and fungi in symbiosis with plants in ways that are poorly understood (but which can be additive, synergistic or antagonistic).

At the beginning of the 1990's, critical loads for both eutrophication and acidification were exceeded over large areas of Europe, often by a considerable margin (Posch et al., 2001). As a results of emission reduction agreements, exceedances are expected to be reduced both spatially and in absolute terms. In Posch et al. (2001), the increased spatial resolution of the EMEP model (a 50 km x 50 km version) revealed new sensitive ecosystems in comparison with the 150 km model used in the previous assessments. For sulphur, the most sensitive ecosystems are located in Scandinavia and Scotland, for nitrogen, the critical areas are situated in Northern Scandinavia and Finland, but also in south-eastern Europe and in a zone around the 60^{th} latitude in Russia. The exceedances are presented as ecosystem protection coverage maps. In 1990, over most of Central-Europe, from Spain to the Baltic countries and Southern Finland, over the Balkans, Greece and areas north of the Black Sea, only less than 10 % of the ecosystem was protected subject to N-deposition. The geographical area of this critical N load threshold exceedance is expected to decrease by approximately half by 2010, but the situation is still alarming. A similar phenomenon is seen with respect to S and N-based acidity. Around 1993, acidic deposition exceeded the critical loads over roughly 60 per cent of the area of Europe, in most places by significant amounts (Downing et al., 1993). The second sulphur protocol should protect about 81 %, 86 % and 90 % of the ecosystem's area in 2000, 2005 and 2010, respectively, for sulphur alone (Hettelingh et al., 1995). In 2010, 70 % of the European area should be protected against the total risk of acidification. However, nitrogen is considered to be more important than sulphur (Posch et al., 2001), especially considering its multiple effects (acidification, eutrophication and O_3 formation).

According to calculations made by IIASA (International Institute of Applied Systems Analysis), the critical acid load for sulphur, 0-200 eq ha^{-1} y^{-1}, was exceeded almost everywhere in Finland in the 1980's by a factor of 1-3. Even with the existing emission reduction programme, depending on the emission reduction scenario, the critical load for sulphur will still be exceeded in parts of Finland in 2010 (Johansson, 1999). The state of Finnish forests is rather good in comparison with that in other European countries: in 2000, the proportion of coniferous trees with > 25 % defoliation was 12-13 % in Finland, while the corresponding figure for the Czech Republic was almost 60 % (Environmental Statistics, 2002). Lakes have been more sensitive with respect to acid deposition than the forests. Of the 4900 Finnish lakes that are cosidered acid, about half have been acidified through human influence (Forsius, 1992). These, however, are also recovering slowly.

Nitrate deposition leads to eutrophication of terrestrial and marine ecosystems. The critical load for nitrogen is below 2 g (N) m^{-2} yr^{-1} for coniferous forests, 1.5 g (N) m^{-2} yr^{-1} for deciduous forests and even less for slowly-growing areas. The maximum calculated annual average nitrogen deposition for the period 1985-1993 in background areas in southern Finland is 0.85 g(N) m^{-2} yr^{-1}, decreasing to below 0.3 g(N) m^{-2} in Lapland. Near low-level emission sources the deposition gradients are significant. The critical loads are not exceeded in background areas. However, excess nutrients can affect the overwintering of plants.

The direct exposure to air pollutant concentrations is discussed in Hongisto (1998). Northern conditions weaken the resilience of the ecosystem against air pollutants. During winter the critical concentration for SO_2 is 15 $\mu g\ m^{-3}$, if the annual accumulated temperature above 5 ^oC is less than 1000 degree days. In Lapland, SO_2 exceeding 3-5 $\mu g\ m^{-3}$ can cause injury to epiphytic lichens.

Research on the direct effects of acid rain and cloud on vegetation has led to the definition of the critical load concept for both acute, short-duration exposure and for chronic, long-duration exposure of vegetation to acid mist (Ashmore & Wilson, 1992). The possible direct effect of orographic clouds in Northern Finland calls for the parameterisation of this effect in the models. In southern Finland, cold nights during the growing season can occasionally resemble high altitude conditions, although mists never occur as frequently as the orographic clouds that cover hill sides.

3 MODELLING OF AIR POLLUTION TRANSPORT AND FLUXES

3.1 Formulation of the problem

The Hilatar model (Paper I, Hongisto 1998 and Appendix 1) is an Eulerian grid-point model in which the evolution of concentrations $c(\vec{x},t)$ at time t and place $\vec{x} = (x, y, z)$ of compounds emitted into the lower troposphere is calculated by numerically solving the transport and chemical transformation equation

$$\frac{\partial}{\partial t} c(\vec{x}, t) + [\vec{V}(\vec{x}, t) \cdot \nabla\, c(\vec{x}, t)] = \nabla \cdot \left[\vec{K}(\vec{x}, t) \cdot \nabla c(\vec{x}, t)\right] + S(\vec{x}, t) \qquad (1)\ ,$$

where $V(\vec{x},t)$ is the wind velocity, $K(\vec{x},t)$ is the eddy diffusivity and $S(\vec{x},t)$ includes emissions, chemical source and sink terms and deposition. The equation is decomposed into one-dimensional diffusion, advection and chemistry sub-problems, which are solved successively by an algorithm suitable to each one.

In solving the transport equation it is assumed that:

a) The initial and advected concentrations are known along all grid borders,
b) The surface dry deposition velocity defines the lowest vertical layer boundary condition, and
c) The mass of the air, used for the determination of the vertical velocity, is conserved.

Following the principles of the method of fractional steps (Yanenko, 1971; Marchuk, 1975, 1986) equation 1 is decomposed into one-dimensional sub-problems which are solved successively, each sub-problem by an appropriate algorithm. In order to ensure mass conservation, the vertical mass of each layer is transported, instead of concentration, when the advection is solved numerically.

Turbulent diffusion is solved using the gradient transport theory, the K-theory, first applied to momentum flux in the 1870's (Businger, 1982; Boussinesq, 1877): analogical to molecular diffusion, turbulent fluxes are assumed to be proportional to local mean concentration gradients. Diffusion smoothes sharp gradients at a rate depending on the

strength of the turbulence. The limitations on the use of the K-theory are discussed in Appendix and in Hongisto, 1998).

The Hilatar model is compared with other European 3D regional air pollution models in Hongisto (1998), using the review by Moussiopoulos et al. (1997). Inter-comparison with the Nordic models is presented in Zlatev et al. (2001). All European 3D models have similarities, and the chemical conversion subroutines of the Nordic models have a common origin (the EMEP MSC-W Lagrangian model of Iversen et al. (1989) for acid compounds, and that of Simpson (1992) for photochemical compounds). In constructing the Hilatar model I partly followed the parameterisation of the RADM, Regional Acid Deposition Model (NCAR 1985), which has been implemented in Europe (the EUROTRAC Eurad model, Hass, 1991). Hilatar has some advanced features: a unique sea-area parameterisation (both an MABL model and a detailed dry deposition module for gases and particles), a high resolution (26-11 km) grid with a high-resolution (now around 22 km) meteorological input, a stack-source based emission inventory in Finland, Estonia and parts of Russia, an accurate advection algorithm, a detailed land surface classification as well as wet and dry sink process descriptions and a separate description of sulphur chemistry in clouds. At the time of the review, no other grid model had been reported, in which a long simulation period is combined with a high spatial resolution. At the present time, most meteorological institutes run 3D models operationally, and the tools have been accepted as being reliable enough for predicting air quality.

3.2 The model structure

The Hilatar model exists in several versions. The original vertical grid has been changed twice, first following the HIRLAM vertical grid change in 1992, then raising the model top from 3 km to around 10 km (in the south and over open sea areas in winter, the mixing height exceeds considerably 3 km). The horizontal resolution and the simulation area have been changed more often, the model is quite adaptable to such changes. The parameterisation schemes are updated continuously. The model version covering the whole of Europe is referred to here as the EUR-Hilatar, while the model covering the Baltic Sea drainage basin with its surroundings is referred as the NMR model.

The long-range transported (LRT) pollutants contribution is estimated by adding daily average concentrations to the air flowing into the simulation area through the boundaries. LRT values are obtained on the EMEP model grid from the EMEP MSC-W centre in Norway or from the EUR-Hilatar (simulations since June 1995). The emissions, meteorological parameters and dry and wet deposition sink terms vary every hour during the simulations.

3.2.1 Grid, surface, modelling area, linking of zooming models

Vertically, the present versions of the Hilatar model use the terrain-following hybrid HIRLAM grid: the lowest 10 layers are below 3 km, while above this height 3 additional layers below 10 km are used. Rotated spherical grid coordinates are used as its frame of reference in the horizontal and hybrid terrain-following coordinates vertically (HIRLAM, 1990). The model level heights above the surface, determined by

the average topography of the grid square, are calculated in Hilatar from hydrostatic equilibrium and the ideal gas law.

A detailed surface inventory with over 50 land-use categories with a 10 km resolution, analysed from Landsat TM images as a joint task by five Finnish research institutes, has been adjusted to the Hilatar grid. However, because this inventory did not cover areas outside Finland, the GRID Arendal on-line GIS Baltic Sea Drainage Basin land cover database, extracted from http://www.grida.no/baltic/ in 1995, and interpolated into the Hilatar grid, has been used in most 0.1^o model simulations. The land surface is categorised into 6 classes: forest, open land, open water, urban land, glacier and unknown land - in addition, information about the agricultural portion exists in the same data base. For the 22-55 km (0.2, 0.25^o, 0.4^o and 0.5^o) Hilatar models, the land-use data are the HIRLAM model surface data at the corresponding resolution, classified into forest, lakes, sea and other surfaces. The mountainous land types are separated from the class ”other surfaces” using topography and a latitude-dependent formula. The forest is assumed to be half coniferous, half deciduous.

3.2.2 Physical parameterisation of the atmospheric boundary layer

For model applications before November 1999, the turbulence parameters, i.e. the friction velocity, the Monin-Obukhov length, the temperature scale, the convective velocity and the mixing height (h_{mix}) are calculated from the HIRLAM temperature, wind and specific humidity profiles, using two different methods over sea and land areas (Paper I; Hongisto, 1998; Appendix). The meteorological parameters have been calculated for each HIRLAM grid point in the area and interpolated afterwards to the simulation grid.

Over land areas, the FMI meteorological pre-processor for local dispersion model studies (written by Pentti Vaajama) is applied, using the HIRLAM potential temperature $\theta_v(z)$ profiles, instead of the dry potential temperature from soundings. During unstable situations the mixing height h_{mix} is evaluated from the moist potential temperature profile by searching for the first inversion level, i.e., the first level at which $\theta_v(z)$ increases with height. In stable and near-neutral situations an analytical form is used.

Over sea areas, where the diabatic effect of the moisture flux on buoyancy and especially the interaction between the surface roughness and the wind are important, the iterative method described in Joffre (1988) and applied in Lindfors et al. (1991, 1993) is used.

Since the change of the HIRLAM version in November 1999, the mixing height and flux measures have been directly available, and a meteorological data pre-processor written by Kirsti Jylhä and Carl Fortelius, using Grads routines (GrADS, 2002), has been used. The friction velocity and other scaling parameters are solved analytically from HIRLAM variables.

The eddy diffusion coefficient parameterisation is based on the scaling regimes (Holtslag & Nieuwstadt, 1986) presented in Hass (1991). The ABL is scaled into different regimes, each with a specific turbulent structure. The formulae are presented in Hongisto (1998). The fractional cloud cover clf(x,z) is parameterised in terms of relative humidity RH according to HIRLAM (1990). The liquid water content of the clouds depends on

cloud type, temperature, convectivity and the possibility of cold advection over sea areas.

3.2.3 Numerical methods

The advection algorithm of Bott (1989) has been in use since 1995. The chemistry equations are solved by the QSSA (quasi steady-state approximation) method (Hesstvedt et al., 1978), and vertical diffusion by the Crank-Nicholson algorithm with a staggered grid (Tuovinen 1992).

3.2.4 Chemical conversion during transport

In the model either an inert chemistry module for dust or heavy metals is used, or gaseous and particle concentrations are calculated for the following substances:

NO_x(g), HNO_3(g), NO_3(p), PAN(g), NH_4NO_3(p), NH_3(g), SO_2(g), SO_4(p) and $(NH_4)_{1.5}SO_4$(p),

where PAN is peroxyacetyl nitrate and $NO_x = NO + NO_2$. NO is not a variable because its instantaneous value can be calculated if the ozone and peroxy radical concentrations are known. The chemistry module is the EMEP-MSC-W code (Iversen et al., 1989) with the following modifications:

- Sulphur dioxide is described by two variables: SO_2 is assumed to be emitted as $SO_{2,non\text{-}liq}$, which is in non-scavengable form for correction of the local wet deposition, and it is transformed into scavengable $SO_{2,liq}$ in a half-life of 1.5 hours. Other local deposition correction coefficients are not used.
- Inside clouds, the sulphate production rate differs from the clear sky conversion rate,
- nitrate and sulphur particles are split into two size classes,
- the most recently-available rate coefficients are applied,
- dry deposition is used as a boundary coefficient in the vertical diffusion equation, with only the gravitational settling of the particles being described in the chemistry sub-model as a sink term,
- the scavenging and dry deposition sink-terms are rewritten as described in Hongisto 1998 and Appendix, and
- the emission terms in the chemistry module are re-classified (instead of the grid sum of high and low-level emissions, individual stack sources with an estimation of the effective emission height using standard plume rise equations are employed whenever an emission inventory is available).

Tests of the chemical mechanism in Finnish conditions are described in Hongisto (1990) and Hongisto & Joffre (1990). Additionally, a 1-dimensional two-phase model with aqueous chemistry has been developed in order to assess the dependency of the chemical transformation rates inside the cloud droplets on light, temperature, moisture, oxidant concentrations, etc. (Hongisto 1993c).

3.2.5 Dry deposition

The dry deposition velocity v_d is calculated using the resistance analogy, employing the aerodynamic and molecular resistances of Voldner (1986). The surface resistance r_c for gases depends on radiation, temperature, relative humidity, amount of rain, dew or fog, pollutant exposure time and canopy height and density. Separate resistances for the gas transfer into plants through different paths and surfaces are parameterised following Wesely (1989). In winter, the snow resistance of Erisman (1994) is used. A minimum value of $r_c = 0.1$ s cm^{-1} for all gases is assumed. Over water, moisture, wave-breaking and the solubility of the gases have to been taken into account in the method (Lindfors et al., 1993),

Dry deposition sink strengths have a reversed seasonal intensity over water and land areas. Dry deposition reaches its maximum in winter if cold air is located over open water, while at that time of year the sink term has a minimum strength over land. As an example, the summer and winter variation of the 1993-98 average HNO_3 v_d fields are illustrated in Paper I, and a detailed description of the formulae is given in Hongisto (1998) and in Appendix. The v_d of SO_2 was higher in summer over forested areas in Sweden and Finland than in the south. Over the open Baltic Sea, $v_d(SO_2)$ exceeded 1 cm s^{-1} in January, being typically around half of this value during summer. Over land the wintertime grid average v_d of sulphate particles was 0.05-0.2 cm s^{-1}, exceeding 0.3 cm s^{-1} in summer, while the monthly average over water was smaller throughout the year. The average v_d of NO_2 over land was $\leq$ 0.02 cm s^{-1} in winter, and $\leq$ 0.2 cm s^{-1} in summer.

3.2.6 Wet deposition

The removal rate of pollutants by rain depends on many microphysical parameters, cloud dynamics, the pollutant characteristics and the precipitation rate and type.

Several experiments beneath the plumes of large power plants show that SO_2 is not immediately scavenged out from the flue gases. One reason may be the pH and temperature dependency of Henry's coefficients, HCl and HF emissions restricting the uptake of SO_2 into droplets, or organic surface layers covering combustion-emitted aerosols and impeding the water acceptance of the particles (Fraude & Goshnick, 1995). The emitted SO_2 is non-scavengeable. Downwind of the sources, it is linearly converted into a scavengeable form in a half-life of one-and-a-half hours.

Precipitation is assumed to occur as rain with a gradual transition to snow when temperature decreases from 270 to 260 K. The seasonal variation of vertical precipitation R(z) is from Chang (1986): R(z) at a height of 3 km is 22 and 58 % of the surface value in winter and summer, respectively.

Using the scavenging rate L_c for HNO_3 of Chang (1984, 1986), below-cloud scavenging by snow is more efficient than by rain. In-cloud scavenging equals the cloud droplet removal rate by falling raindrops. During snowfall, the values of Chang (1986) were used for particles, but because those formulae do not give similar relative L_c rates as those given by the EMEP model (Jonsen & Berge, 1995), a slightly faster rate for particles in cloud, and, in comparison to it, a bit less efficient rate below cloud, which are closer to

the Scott (1982) rates, are used (Appendix). NH_3 is scavenged by the Asman & Janssen (1987) parameterisation. In-cloud scavenging of NH_3 will proceed at about the same rate as that of SO_4^{2-} aerosols. The scavenging rates of other compounds were estimated using the ratio of the respective EMEP efficiencies, following the annual variation of the HNO_3 scavenging rate.

The EMEP and Hilatar scavenging coefficients are compared in Hongisto (1992a and 1998). The removal rates using different scavenging parameterisations depend on mixing height and precipitation. Generally, the Chang (1986) removal rate for HNO_3 is slower in summer than the Jonsen & Berge (1995) rate; in winter it is faster. The NH_3 scavenging rate of Asman is only 38 % of the EMEP value for below-cloud rain (800 m h, 1 mm hr^{-1} rain intensity), but faster in cloud. When the mixing height is low, the EMEP removal rate of HNO_3 is clearly faster than that of Chang, especially with higher precipitation amounts. With 1 mm h^{-1} rainfall, the SO_2 concentration drops by 50 % in 0.9-3.5 hours in summer and 1.7-7.7 hours in winter, depending on the cloudiness. With 3 mm h^{-1} rainfall, the corresponding times are 1.3-3.5 h in winter and <10 min - 3.2 h in summer. Precipitation scavenging is more efficient in the early part of the rainfall.

3.3 Model Input

3.3.1 Meteorological fields

The meteorological fields of the HIRLAM weather prediction model have been collected in a data base covering the Baltic Sea drainage basin since 1991, so as to be available for air pollutant dispersion modelling studies. In 1993, 1996 and 1999 the geographical area of the data has been progressively enlarged. For simulations before 1999, the meteorological input consisted of the 6-hour prediction fields with a 0.5^o horizontal resolution (HIRLAM, 1990). Since November 1999, the resolution has been 0.2^o and 0.4^o (HIRLAM, 2002 and links within). Vertically, before May 1992 data from the 7 lowest layers of the available 16 HIRLAM levels are included. In May 1992, the HIRLAM vertical grid was expanded to 31 levels, after which data from the 10 lowest vertical layers, up to 3 km, were used. Since June 1995 13 layers have been used and the model top has been raised to 10 km.

The physical parameters saved in the data base are described in Hongisto (1998) and in Appendix. Since November 1999 this data consists of 51 variables, 7 of them being 3-dimensional. The original GRIB (gridded binary) formatted files, each time step in its own file, are pre-processed on a monthly basis. The ABL parameters, pre-calculated with separate ABL processors over marine and land areas, are saved as well. The graphical interface programs use Disspla or UNIRAS libraries or Grads routines.

A post-processing package with statistical routines has been constructed for calculating averages or time series of any of the ABL or Hilatar model internal parameters (e.g. vertical wind velocities, vertical mixing coefficients, dry deposition velocities or scavenging efficiencies), over different periods. It has also been used in picking out selected time series at any measurement place, classifying the data with e.g. the time of the prediction or wind direction, calculating 1D trajectories and presenting the data overlaid on a map as animated fields, numbers, wind rose presentations, curves, isolines or other visualisations.

3.3.2 Emissions

The emission data consists of the EMEP 50-km gridded emission inventory (EMEP 2002), merged in the NMR area with the Finnish, Russian and Estonian stack inventories and areal emissions (Häkkinen et al., 1995; Mäkelä & Salo, 1994) updated with additional statistical information (see Hongisto, 1998, references herein and Appendix). Effective plume heights are estimated for the stacks, and emission-specific vertical height profiles are used for areal sources. Country-specific daily emission indices from the GENEMIS project (Lenhart et al., 1997) are used together with the monthly, daily and diurnal indices of the FMI local emission inventory (Hongisto 1998; Appendix).

The annual international ship traffic emissions in the Baltic Sea have been re-estimated using the Lloyd's Register for the base year 1990 for the EMEP MSC/W database in 1998. The new ship emissions estimate, 353 kt NO_2 (older value 80 kt) is still rather low considering the known total NO_x emissions from Finnish ships alone, which exceeded 71 kt in 2000 (Mäkelä et al., 2002). The international ship emissions of SO_2 for 1990 rose to 229 kt from an old value of 72 kt SO_2 (EMEP, 2002). The base year of the new emission inventory is the year 1990. Since then ship traffic has increased, especially in the Gulf of Finland, where several new harbours have been constructed in the 1990's.

4 MODEL VERIFICATION AND VALIDATION

4.1 Numerical accuracy

The performance of the advection algorithm was tested by calculating the change in mass and peak value of a frozen initial distribution (of cone, rectangular block or delta-peak shape) which is rotated around an axis of symmetry. The transported quantities were compared with the initial values after 12.5 days of circulation. The test equations, initial distributions and results of trials made over the European and various NMR Hilatar model domains, horizontal grids and resolutions, are presented in Paper I and in Hongisto (1993a; 1998). Over the European domain the maximum error in mass M during the rotation, M(t)/M(t=0), was ± 0.15 % of the initial mass. The error depends on the location of the initial distribution and on the ratio of the mass of the peak to the background mass, which was here 36.2 % for the cone shape, and 41.1 % for the rectangular block. M(t)/M(t=0) is related to the truncation error when the concentrations are represented in the algorithm by polynomials. The simulation time, 12.5 days, is long enough for this numerical error to be insignificant in comparison to the errors connected with the other parameterisations of the physical and dynamical features of the system.

The evolution of the peak height shows how the splitting-up method smoothes concentration distributions, primarily during diagonal transport. The cone and rectangular-shaped distributions are quite stable, e.g. for the cone, the maximum drops to 89-85 % of its initial value in 220 h, in contrast to a delta function type of

distribution, which loses 80 % of its maximum height to the neighbouring cells within 5 hours of circulation (over the European grid with 0.5^o resolution).

Similar mass tests have been performed for all model versions with various differing grids and domains (fixed 30 km Polar Stereographic grid and rotated spherical grids of 0.1^o, 0.2^o, 0.25^o, 0.4^o and 0.5^o).

The performance of the vertical diffusion algorithm is compared with an analytical solution in Tuovinen (1992). Pure mass conservation tests of the algorithm in the Hilatar grid did not show any mass loss when the upper boundary at a height of 10 km was closed. Examples of the mass transfer rate across the inversion layer and other tests can be found in Hongisto (1998). Under efficient mixing conditions, the time required to achieve a uniform mass profile is less than 2 hours for a typical daytime profile of the vertical eddy diffusivity K_z with a maximum of 50 m^2s^{-1} below the mixing height, and less than one hour if K_z is increased to 100 $m^2\ s^{-1}$. The mixing efficiency depends on the initial concentration profile and the structure of the grid.

The chemistry algorithm QSSA does not conserve mass exactly. There are three reasons for this: firstly, the relatively long time step, 225 s, during which the concentrations are assumed to keep their previous time-step values, even though they are actually consumed or produced in the chemical reactions. Secondly, the sink and source terms are independent of each other, being expressed by an exponential or linear decay, depending on the strength of the sink. Finally, the requirement of a minimum background concentration level also increases the mass slightly.

Finally, the combined advection-diffusion-chemistry equations were tested by studying the life-time and transport distances of NH_3, SO_2 and NO_x puffs over short periods in real meteorological conditions (Hongisto, 1998). To get a real transport distance estimate, simulations over several years are needed.

4.2 Model - measurement inter-comparison

Modelled daily concentrations of SO_2, NO_2, NH_3, SO_4^{2-}, NO_3^-, NH_4^+, HNO_3+NO_3^- and NH_3+NH_4^+ in air, and monthly mean wet depositions of $SO_4^=$, NO_3^- and NH_4^+ were compared with EMEP measurements extracted from the EMEP/NILU data base (www.emep.int). The EUR model grid averages were compared with measurements at around 90 European EMEP stations over the period June 1995 – September 1999 and the NMR model results with 29 EMEP stations over the years 1993 and 1996-1998 (papers I, II and Hongisto, 1998). Additionally, inter-comparison of measured and modelled Pb, Cd and Zn and various nitrogen species concentrations in aerosol and in precipitation during two 2-month BASYS network studies at four coastal stations and during two 2-week periods of Lagrange studies at two research vessels, have been performed (Sofiev et al., 2001, 1999; Schulz et al., 1999a, b and 1998; Schneider et al., 1999; Plate et al., 1999; Plate 2000). Inter-comparison with other Scandinavian models and with measurements for the 1997 reference period are presented in Zlatev et al. (2001), and with the EMEP model and measurements in Hongisto (1992a and 1998). Comparison with modelled concentrations during the episodes are presented in Hongisto (1998), Tervahattu et al. (2002), Hongisto (1992b, 2001) and Hongisto & Joffre (1994).

4.2.1 Comparison with EMEP station measurements

The model-measurement inter-comparison has been carried out independently for the two sets of model results. The statistical package of Sofiev (1999) has been used in the EUR model domain (Paper II), while the Hilatar post-processing routines (Papers I, II and Hongisto, 1998) have been employed for the NMR model results. All stations located inside the model domains were included in the comparison with no a-priori filtering of the data. In the following sections, the results of the intercomparisons are discussed for concentrations and depositions, in that order. In each case the EUR model results are followed by those for the NMR model.

Sulphur compounds

For almost all species, the EUR model demonstrated quite good agreement with measurements over Central and Northern Europe, while for Southern Europe the results were usually not so encouraging (Fig. 7 in Paper II). The best congruence was achieved in slightly different areas and stations for different species.

SO_2 was somewhat overestimated over Central Europe (by ~0.5-2 μg (S) m^{-3}) and at the Finnish north-eastern border (Fig. 7b and 8 in Paper II). It was underestimated at all Norwegian stations, at the coastal site of Utö, Finland, at most Southern Swedish stations, and in Ireland (Papers I, II). In the remaining parts of the Nordic countries overestimation occurred, mainly in winter. The correlation coefficient for daily SO_2 reached 0.4–0.6 in summer and over 0.6 in winter over North-Western Central Europe. These values are close to the maximum possible level of ~0.7-0.8 for daily averaging (Berg & Schaug, 1994). The concentration of sulphate in aerosol is generally underestimated everywhere by ~0.2-0.5 μg(S)m^{-3}, except over the Black Triangle region, where an overestimation of 0.2 μg(S)m^{-3} appears (Fig. 7b in Paper II). The daily correlation is nearly the same as for SO_2.

In the NMR model domain, the winter concentration of SO_2 is slightly overestimated at the southern stations (Figs. 3 and 5 in Paper I), but underestimated at specific marine stations influenced by ship emissions in Gotland and SW Finland, and in Lapland at stations influenced by the Kola emissions. One reason for over-estimation is the time-splitting error: near source areas the concentrations are smoothed to neighbouring cells during advection. When the concentrations were over-estimated, the difference was larger in summer than in winter. One explanation is the model's vertical resolution: the h_{mix} estimated from the HIRLAM profiles is lower than if it is estimated from soundings. Also the time-integration of the h_{mix} has an effect. Meteorological input are read at 6 hr time intervals, but h_{mix} has its maximum late in the afternoon. Thus, it is higher between 12 and 18 UTC than the time interpolation can estimate. At coastal stations, model underestimation can also be caused by emissions that are too low, and by stability differences between land and sea during the cold months. If the sea is open and cold air advects over it, mathematical averaging makes the partly-frozen shores too unstable, and the modelled pollutants are mixed through too deep a layer.

Over the NMR area, the correlation of modelled and measured SO_2 concentrations was weak at some marine stations, at eastern stations with a low measurement frequency,

and also at clean and elevated sites, but it was above 0.6 for most Finnish and south-western stations. The sulphate in the air was underestimated in 1993 as well as in 1996-1998 at all stations, on average by 44 % in 1996 and 64-61 % in 1997-98 (Fig. 6 in Paper I). Sulphate particles are smaller than nitrate particles, and are thus transported over longer distances, so more non-European and natural contributions can be expected than for nitrate. The geographically highly variable inattributable contribution, estimated for the EMEP model results, is three times larger for sulphate than for oxidised nitrogen deposition (Barrett and Berge, 1996).

Over the highly polluted Black Triangle region, where the observed wet deposition exceeded 100 mg (S) m^{-2} mon^{-1}, the European model overestimated the sulphur load by up to ~160 mg (S) m^{-2} mon^{-1} (Fig 7b, Paper II). The model overestimates wet sulphate deposition in general in Central Europe, but usually by not more than 30 % of the mean value. For the rest of the domain, the absolute deviation is within ± 15 mg (S) m^{-2} mon^{-1}. Usually, overestimation occurred during small-deposition events, which is an indication of over-predicted light precipitation and scavenging that is too efficient during light-rain events. High deposition events were underestimated. The correlation coefficients for monthly sums varied from –0.1 for Portugal up to 0.8 for several Norwegian stations.

In the NMR model area, wet deposition of sulphur, in mg m^{-2}, was overestimated in 1996-1998 at the Finnish north-eastern border, in Lithuania and sometimes in Denmark, but was under-predicted in Norway, at Utö, Finland and at most of Southern Swedish stations (Fig. 9 in paper I). Overestimation occurred mainly in winter. The summertime deposition should in fact be slightly under-estimated, since during rainy periods dry deposition is included in the measured values. The absolute deviation was highest in Norway, where the HIRLAM rain was also under-predicted at the same stations. The underestimation on the Atlantic coast is also partly due to a missing non-European contribution and an incomplete ship emission inventory. Again, the strong wet deposition peaks were generally underestimated, while during low deposition events the deposition was sometimes higher than that measured. There was no difference between stations collecting weekly or daily samples in the monthly results.

Oxidised nitrogen

The NO_x concentrations were somewhat underestimated (by less than 0.5 μg m^{-3}) over Scandinavia, Germany and the UK (Fig 7a, Paper II). At some stations the modelled and measured concentrations were almost equal. Within the NMR area, the underestimation was most pronounced at coastal stations in spring and close to emission areas during inversion situations, because the minimum mixing height was set to 150 m and the low-level emissions were initially mixed through at least the two lowest model layers. At some stations, where concentrations are very low, NO_x was also slightly overestimated. In the summer and spring of 1998 and in 1996, NO_2 was overestimated slightly at some southern Swedish and Norwegian stations. The reasons are the same as for the SO_2: too low a mixing height in HIRLAM, smoothing in transferring of the emissions from the EMEP to the HIRLAM grid, a high and clean mountainous measurement site or the time-splitting method in advection. Also at the high elevated sites the comparison was made with modelled surface soncentrations because a terrain-following grid was used. The correlation of daily values was lower

than that for SO_2, being especially poor at marine, northern or eastern stations in the NMR area.

The correlation of the sum HNO_3+NO_3^- was above 0.5 over the Baltic Sea region and the UK (EUR model results, Fig. 7a, Paper II). Measurements in other parts of Europe were too scarce for any firm conclusions. The absolute level of concentrations is overestimated by up to 100 % (Figs. 5 and 7, Paper I). In the NMR domain the overestimation increases northwards, although average concentrations decrease to 10 % of the level at the southern stations. The chemistry module might produce too much nitrate, there are unknown chemical sinks or e.g., dry deposition (at least to the sea surface) might be too slow due to minimum value for the surface resistance set for all particles and highly soluble gases. The seasonal variation of nitrate is stronger than that measured.

Nitrogen wet deposition was overestimated by 30 % over most of the European domain, mainly during small deposition events, and underestimated at a few stations spread out over Europe. The difference was higher in Southern Europe. The temporal correlation was considerably better than that for air concentrations, exceeding 0.5 for more than half of the stations. Systematic low correlation appears only in Southern Europe.

Over the NMR area, wet deposition of oxidised nitrogen was under-predicted in Southern Norway and Sweden, and also in Northern Norway; however, it was slightly over-predicted elsewhere. The overestimation was strongest in the wet year 1998, while 1996 was rather well predicted, as was also 1993. The NO_x deposition measured at Finnish EMEP stations by the FMI is systematically lower than that at stations of the Finnish Environmental Institute (Vuorenmaa et al., 2001).

Reduced nitrogen

In the NMR area, NH_3 was only measured in Latvia in 1997 and on the Kola Peninsula in 1996. NH_3 concentrations were generally underestimated, especially in summer, and the correlation between modelled and measured values was poor. NH_4^+ was slightly underestimated (~0.3 μg (N) m^{-3}) in the European domain, by up to 25% in remote regions but by less than 10% in Central Europe. $(NH_4)_{1.5}SO_4$(p) and NH_4NO_3(p) were the only ammonium particles modelled, however ammonium can exist also in other forms. Ammonium in the air was only measured at four stations and underestimated there (Fig. 8, Paper I). The sum NH_3+NH_4^+ was underestimated at remote Scandinavian sites, while in some parts of Europe the deviation had the opposite sign. The time correlation for NH_4^+ varied over a wide range, with a maximum (0.5) over the southern Baltic region. The correlation for total ammonium was high over the whole Baltic Sea region (~0.6) and the UK, but statistically insignificant in the south.

Ammonium wet deposition was usually underestimated by about 20 % in Central Europe, being, however, overestimated during low deposition events. Time correlation in the Nothern Central Europe, England and Nordic countries was about 0.5. There are also a few stations in France, Spain and the Black Triangle region where the agreement was very good. Over the NMR domain, it was under-predicted, except near Denmark in 1997 and 1998, indicating that the scavenging efficiencies might be too low.

No clear annual cycle in the deposition was detected. The monthly deposition peaks at Norwegian mountain stations, at the marine station of Hoburg and directly downwind of the large source areas were underestimated.

4.2.2 Comparison with BASYS field campaign measurements

Within the BASYS subproject "Atmospheric Load", two joint network studies were performed in summer (15 June - 11 August 1997) and in winter (3 February - 31 March 1998), covering substantially different meteorological situations. Measurements of concentration and deposition patterns with intercalibrated instruments were performed at four coastal stations: Hel, Poland (18.82E, 54.60N), Hoburg, Gotland (18.10E, 56.92N), Kap Arkona, Germany (13.43E, 54.68N) and Preila, Lithuania (21.22E, 55.33N) (see Fig. 1 in Schulz, 1998). Measurements included ambient air concentrations of particulate SO_4^{2-}, NO_3^-, Cl^-, NH_4^+, Na^+, K^+, Ca_2^+ and trace metals, gaseous NO_2, NH_3, HNO_3, Hg, and the size-segregated aerosol concentration of major ions as well as trace metals, and wet deposition sampling.

During the two Lagrangian experiments (2-15 July 1997 and 1-15 March 1998), simultaneous measurements were also carried out on two ships, the "Alexander von Humboldt" and the "Professor Albrecht Penck" of the Institute of Baltic Sea Research, Warnemünde. The aim was to follow the change in the composition of the air mass when the wind blows from the ship to a coastal station, to derive the removal velocities over the sea, and to assess coast-to-sea gradients with measurements for better extrapolation of coastal data to open sea conditions.

The ships were oriented so as to measure along the same trajectory, the one downwind of the other, in such a way that at least one coastal station could also be in the same air mass path. The positions were determined by HIRLAM weather forecasts and air mass trajectories for all coastal stations and ships (Savolainen, 1997; Hongisto & Jylhä, 1998). The meteorological conditions during the field campaigns are described in chapter 5.6.2. The instruments aboard the ships were inter-calibrated several times during the experiment. The measurements were performed over periods of the same but varying length at both coastal stations and on board the ships, depending on the expected change of the trajectory direction (Schulz, 1998).

As the sampling stations are located around the Southern Baltic Proper, it was expected that a concentration gradient could be discovered. Hoburg and Preila are receptor sites, where polluted central European air masses arrive after some transport over the sea. They should resemble pure marine sites during on-shore flow conditions, at least with respect to ambient air concentrations.

A comparison between ship and coastal data, where their positions were sufficiently close, revealed that the coastal measurements were very often equal within a range of 10 - 20 % during on-shore wind conditions. The air concentrations measured on the two ships resembled each other very much, once the transport of the air mass had been considered correctly. Such a "marine" point measurement may thus be judged representative for the dimensions of a typical marine model grid box (box length 25 - 50 km) used in the BASYS simulations (Schulz, 1998).

In Fig. 1 (Schulz et al., 1999a) the modelled and measured wet deposition components are compared for the summer and the winter periods. Dry deposition values were not compared, it is difficult to measure and has been suggested to be of minor importance. Better agreement is found for nitrate than for ammonium, the largest discrepancies being at Hel and Kap Arkona for both N compounds. For the more remote stations of Preila and Hoburg the agreement is closer. This suggests that, close to an intensive source area, a wet deposition estimate is more difficult to obtain, while the long-range transport and removal in remote marine regions is correct.

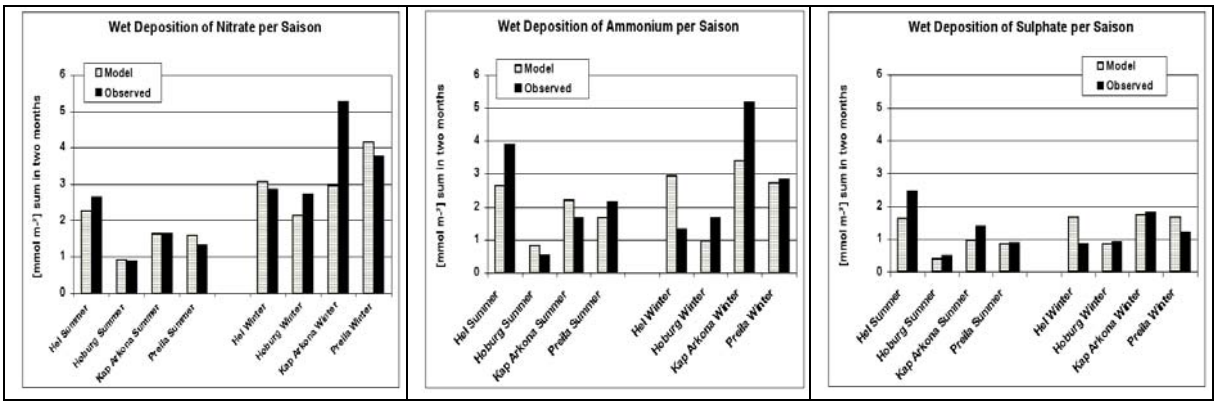

Fig 1. Comparison of the modelled and observed wet deposition of nitrate, ammonium and sulphur during the BASYS summer and winter network study

The discrepancy between modelled and measured compounds was highest for NO_2, (see figures in Plate, 2000) – the mean measured network concentrations were 0.8 μg (N) m^{-3} in summer and 1.36 μg (N) m^{-3} in winter, while the model gave higher concentrations (1.0 and 3.0 μg (N) m^{-3} respectively). In Brorström-Lunden et al. (1999) the measured values were reported as being much higher. The reason for the summertime difference at coastal stations can lie with the wind direction, the high coastal emission density and the initial mixing of the emissions inside the whole grid cube in the model. However, in the summer Lagrange period the ship measurements of NO_2 were higher than the model results, a fact explained in Brorström-Lunden et al. (1999) as being due to contamination. If situations with offshore or very low winds and with a stable boundary layer either over land or over the sea are ignored, the concentrations measured on board were within 10-20 % of the coastal measurements.

Both measurements and model results confirmed that pollution events occur episodically in the Baltic region. The inter-comparison of the 2-day average concentration of particulate nitrate (Schulz et al., 1999a) is presented in Fig. 2 for all stations during the two network studies. The highest concentrations were observed almost simultaneously at all stations at the beginning of the winter period and again at its end. Very low concentrations occurred in the middle of the summer period. Considerable fluctuations on the scale of the sampling frequency are seen to be superimposed on the general concentration level at all stations. The general level and also the fluctuations are simulated rather well by the model, which confirms the validity of the deposition estimate, which was the main target of the BASYS field campaign. The largest overall difference was found at the Gotland site in the middle of the winter episode. During these partly stormy conditions, the model overestimated the

particulate nitrate consistently, indicating a missing sink in the model, or the presence of some of the other reasons which were discussed in the previous chapter 4.2.1.

The good agreement and correlation between the model results and measurements shows that the aerosol cloud inhomogeneity can be described in fine detail on the resolution of the HIRLAM model even during very variable weather conditions. The station measurements are representative for the two-day period. The high peak, simulated at the end of July at Kap Arkona, was not measured. The model simulations show that the episode was born in the western parts of Central Europe. Nitrogen rich air circulated towards southern Norway and Sweden, also reaching, however, the German coastal station of Kap Arkona. Most probably the coastal meteorology and the wind direction were the reasons for the overestimation of the episode.

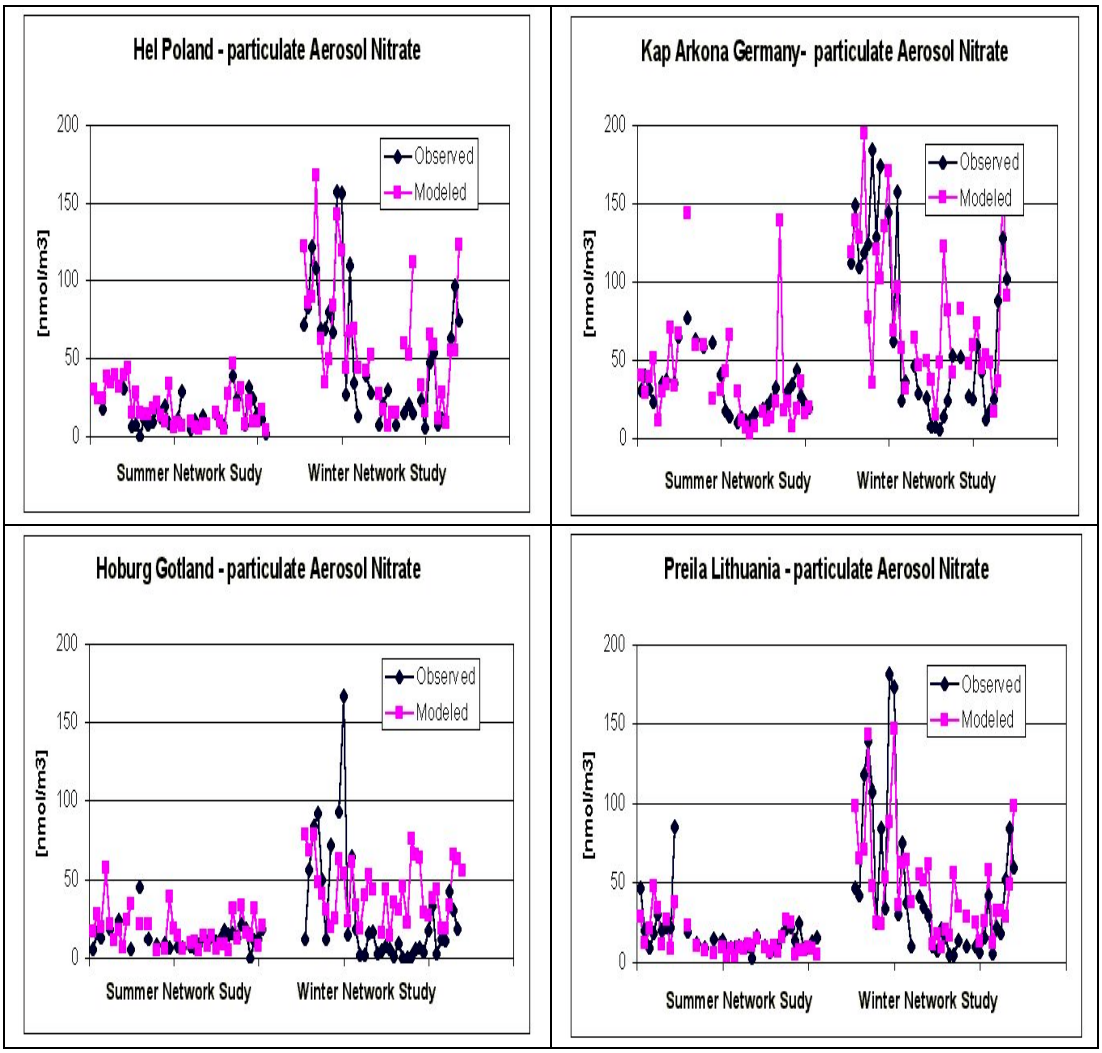

Fig. 2. Comparison of the modelled and observed concentrations of aerosol nitrate in the air at the stations of Hel, Kap Arkona, Hoburg and Preila, during the BASYS summer and winter network study.

Comparison of the mean modelled and measured concentrations of HNO_3 and nitrate averaged over the four stations' data (Schulz et al., 1999a) are shown in Fig. 3. From

the long-term average comparisons over all EMEP stations (Chapter 4.2.1) it was evident that the model produces too much nitrate and nitric acid. This is not confirmed in all the BASYS coastal measurements. In particular, the measured HNO_3 wintertime concentrations could be higher than those modelled. This phenomenon might be connected to, in addition to missing emissions, to the different marine air chemistry; but is not explained by it. The observed depletion of chlorine from the sea salt particles: HNO_3 is lost by the reaction with the NaCl on the surfaces of sea salt particles, produces $NaNO_3$ particles, which have on average a large dry-diameter, which increases under the moist marine conditions. It is possible that these particles have such a high wet diameter (not measured in general), that the sea areas are more effective deposition areas for nitrate, than what is parameterized in the current transport models.

The nitrate deposition and aerosol nitrate concentrations were not well correlated, despite the fact that the latter is the main precursor of the deposited nitrate (Schulz et al., 1999). Deposition is a result of a large-scale, long-term process and not by any means necessarily connected to the instantaneous surface concentration. The course of events might be similar to those of the more studied sulphur oxidation (e.g. Stein & Lamb, 2000). Material transported to the upper layers of the ABL can be accumulated in the cloud droplets in the model upper layers during LRT and can be chemically converted in the wet phase. The cloud droplets can evaporate, temporarily releasing their contents, and condense again several times, before raining down. Other uncertainties are brought about by the episodicity of the occurrence of precipitation intensity and the non-linearity of the scavenging coefficients. It was seen that nitrate concentrations may accumulate in the air during long dry periods, e.g. in winter after 18.2.1998, when the highest ambient air concentrations were observed, along with little deposition.

At the most clearly marine site of Hoburg, Gotland, the largest and most consistent discrepancies are found in the middle of the winter period. During the episode 11.-13.3 a nearly constant southern flow connected the Polish station of Hel with Hoburg. A decrease in nitrate concentration can be seen both in the model and in the observations. The physical processes causing it include chemical transformation, dilution, especially during the night, to a larger volume over the sea and loss by dry deposition. During these days the model predicts, both at the coast and at Hoburg, too much aerosol nitrate, too little nitric acid and too much total ammonium (NH_x). This suggests that the modelled ammonia concentrations are too high, maybe because of uncertainties in emissions, favouring ammonium nitrate particle formation. These fine particles have a considerably longer lifetime than nitric acid or coarse nitrate, and might be responsible for the elevated nitrate concentrations at Hoburg. The actual species partitioning among the different oxidised nitrogen compounds is therefore as important as the dry deposition process.

The largest differences between the measurement sites were observed, a) when there was no flow connection between sites, b) when mixing conditions over the measurement sites were different due to different ABL stability conditions over land and sea, or c) in a stable ABL with very light winds. The comparison of Hg concentrations between Kap Arkona and the two ship positions for the whole winter experiment period led to the overall conclusion that significant differences exist between the coast and the open sea (Schulz et al., 1999a).

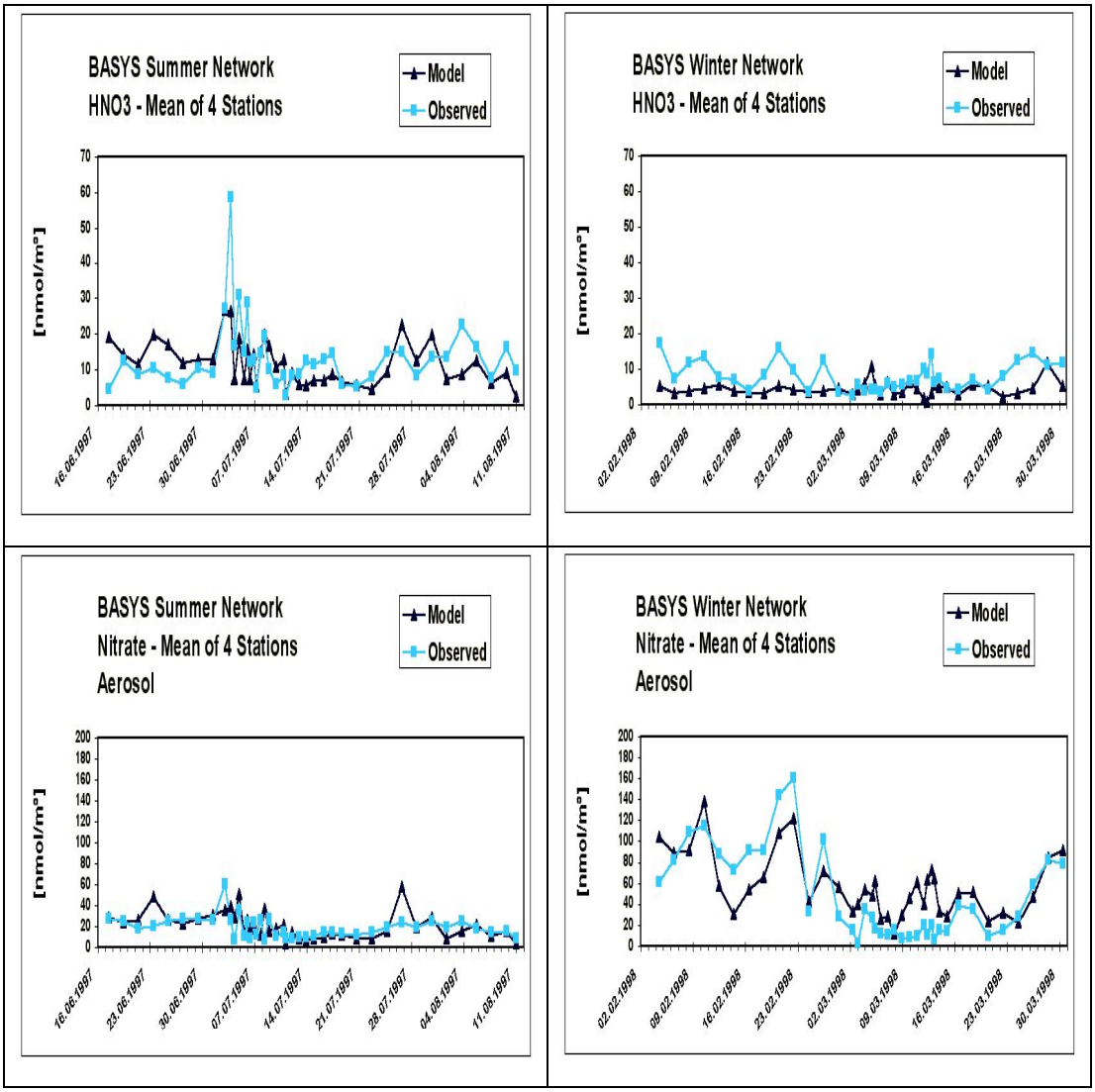

Fig. 3. Comparison of HNO_3 and nitrate, summer and winter network study

4.2.3 Annual flux comparison with BASYS field measurements

The estimate of the annual deposition over the Southern Baltic Proper derived from the BASYS network field measurements was compared with the Hilatar model result in Schulz et al. (1999a). The annual nitrogen wet deposition load estimate for the Southern Baltic Proper, derived from measurements, was 542 mg N m^{-2} a^{-1}, while the first model estimate, made with the EUR-Hilatar and the 1995 EMEP emission inventory, was 486 mg N m^{-2} a^{-1}. The Hilatar model underestimated the four-month network study measurement results by just 10 %. Later, the 1998 EMEP inventory has been completed by new source categories, and e.g. the European NO_x emissions have been increased by 15 %. This partly explains why the modelled deposition was lower than the measurements indicate.

5 MODEL RESULTS

5.1 Acid pollution in the Baltic Sea area

5.1.1 Deposition

Because the model has been constructed for air pollution studies in Finland and its neighbourhood, the European simulation results are not discussed here. The European deposition levels are much higher and concentrations often exceed critical limits, but due to different climatology, the whole air pollution situation is different.

The inter-annual variation of the average sulphur and total nitrogen deposition distributions over the NMR model domain (Paper II, Figs 2 and 3, Hongisto, 2002), depends on meteorological factors. The deposition distributions have the expected north-south gradient, superimposed on a west-east gradient for sulphur due to the Estonian and Russian sources. Over the Baltic Sea, the winter and autumn total deposition of nitrogen is about 1.5 times higher than the corresponding summer and spring values, due to the seasonal differences in rain amounts over water.

The 6-year average dry deposition of nitrogen was highest in summer in Southern Sweden and on the Danish islands (its share exceeding 50 % of the total deposition), due to high summertime ammonium emissions. It decreased northwards and with height in high altitude areas. The relative standard deviation of monthly N deposition was highest over the Atlantic in the winter and spring months (it could exceed 100%) or in remote or mountainous areas (Paper II). The absolute deviation of the deposition was highest over coastal and southern areas.

The seasonal variation of sulphur deposition was higher than that for nitrogen. The dry deposition share of the total atmospheric load was highest over the Southern Baltic Sea (frequently exceeding 60 %, except in spring). Over other northern areas except the Kola Peninsula it was most of the time below 10 %. The variability in the deposition is very large close to some of the strong stack sources.

From 1993 to 1996, European SO_2-emissions decreased by 15 %, those of NO_2 by 7 % and of NH_3 by 5 % (EMEP, 2002). This decrease was not even over all countries (Paper II), and inter-annual variation depended on the weather conditions (emissions increased in the Nordic countries during the cold year of 1996 compared to 1995). NH_3-emissions decreased most in the Eastern European countries, even by as much as 45% in Lithuania.

The decreasing emission trend over the period 1993-98 could be detected as a slight average decrease in S-deposition; however, the inter-annual variation was large due to weather conditions (Paper II). The slight reduction in nitrogen emission is not reflected in the deposition values for any area. The annual regional variation was affected more by the prevailing meteorological conditions. According to simulations with the new HIRLAM model version and redefined ABL parameters, deposition increased in 2000, returning to the 1998 level in 2001 (Hongisto, 2002).

5.1.2 Concentrations

The surface concentrations of nitrogen compounds (Paper II; Hongisto, 2002a) decrease northwards with increasing distance of transport from the most intensive source areas. SO_2 and SO_4^{2-} concentrations show high peaks in the vicinity of the northern and eastern sources. NO_x and SO_2 concentrations are highest during winter due to the maximum emissions, slow reactivity, lower scavenging and dry deposition velocity rates compared to summer, and frequent wintertime inversions. The summertime daily average ABL height over land is more than six times higher than that in winter, even though a minimum ABL height of 150 m was set. Ammonia emissions are highest during summer. In winter, NH_3 concentrations are low because it is also more effectively converted into ammoniumsulphate particles when there is more sulphate in the air. HNO_3 levels are low in winter due to the short days, low OH concentrations and a temperature-independent reaction with NH_3 producing ammonium nitrate near the surface.

NO_x and SO_2 winter concentrations decreased until 1995, increasing again in 1996, while during summer, the NO_x concentration exceeded the period average in the eastern parts of the model at the end of the period, in the western parts at the beginning of it. The particulate concentrations at the NMR model boundaries were highest in 1993-1994 (when the EMEP LRT model was in use) and during the cold year 1996 (with EUR-Hilatar LRT). Generally no trend can be detected, the concentrations of individual compounds over a specific geographical area seeming to depend on meteorology: precipitation, the main advection direction relative to the main source areas, cloudiness and the availability of reactants.

Modelled critical values for SO_2 (a winter average of 20 μg m^{-3}) were not exceeded in the background areas of the NMR model area (Hongisto, 2002). However, they were exceeded in winter 1996 over large areas of Central Europe (the broad Black Triangle area, Hungary) but also over the Balkan countries, as well as in the UK Midlands and the western Po Valley. The same overall picture occurred in 1997 and 1998, but the exceedance areas were smaller and more scattered. Critical concentrations of NO_2 (30 μg m^{-3} as an annual average) were not exceeded during those years in any background areas, not even in the European model domain.

5.2 Correlation with green algae abundance

The state of the forests in Finland is monitored with a network of permanent sample plots in the National Forest Inventory (last national report: Ukonmaanaho & Raitio, 2001). In southern and central Finland the network consists of clusters of four circular sample plots in a 16 x 16 km grid, while a slightly sparser grid (24 x 32 km, 3 clusters) is used in Northern Finland. Map surveys of epiphytic lichens on conifers have been made in 1985 and 1995 for 14 species sensitive to SO_2.

Green algae are single-celled organisms that take their nutrients directly from rainwater and air. They require sufficiently high temperatures and humidity, and enough light. Nitrogen has been suspected to be the most important growth-limiting factor for green algae, since they occur in the vicinity of various nitrogen sources (Ferm et al., 1990).

In Finland, green algae on conifers have become considerably more abundant in the years 1985-1995 and their area of distribution has expanded northwards. They live in symbiosis with lichens, the epiphyllic microbial cover often also including various bacteria and fungi. For Paper IV, the NO_x, ammonium and sulphur concentrations and deposition patterns at all National Forest Inventory sites were computed for the year 1993 with the 11 km Hilatar model version. The abundance of green algae and the nitrogen concentration in mosses were compared against the air quality and climatological data and site factors.

In the study, a slight correlation was found between the N concentrations in moss and the abundance of green algae (r=0.54), as well as between the N concentration in moss and the NO_x, NH_3 and S deposition (r1=0.47, r2=0.44 and r3=0.44). The greater were the deposition of NO_x, NH_3 and S, the greater was the proportion of those sample plots having an abundance of algae. However, the effect of air pollutants could not be separated from the climatic effects (e.g. temperature increase; the effect of increased precipitation was not studied, although increased moisture favours green algae growth). The green algae were found to be abundant in areas having less deposition than in Sweden, and their correlation with NO_x deposition was not as high as that found in Sweden (Bråkenhielm & Quinghong, 1995). In conclusion, the slight rise of mean annual temperature, long-term stable N deposition and the clear fall in sulphur deposition were all found to be factors that promote the growth of the algae.

5.3 Transport over sea areas and fluxes onto the Baltic Sea

The Baltic Sea separates Finland from the intensive Central European and Estonian source areas. Dispersion conditions in the MABL differ in many respects from those in the overland situation. When an air mass flows from the land to the sea, this generally leads to a reversal in the thermal stability, a step-like change in the ABL height, enhanced mixing due to the differences in surface roughness, and a moisture increase capable of activating chemical reactions (Joffre, 1985, 1988). The effects of sea spray and natural marine emissions, leading to a different chemical transformation environment, have been found to be important for the exchange of gases and particles between the air and the sea surface (Hertel 1995; Andreae & Cruzen, 1997; Geernaert, 1997; Pryor & Sørensen, 1999; Schulz et al., 1999a). It has also been shown that fast chemical reactions disturb the turbulent diffusion flux, and that actually the classical definition of the deposition velocity based on the ratio of constant flux to the concentration is not valid (Geernaert, 1997; Sørensen et al., 2000). In short, over the Baltic Sea, the average mixing, the transport time and most sink and source terms differ from their respective values over land.

In coastal regions, the meteorological conditions partly exhibit the features of sea areas. Most of the marine factors, e.g. moisture, windiness and, during cold seasons, milder temperatures, together with the change in the surface roughness and increased turbulence, which produce more vertical mixing and reduce the aerodynamic resistance, increase the efficiency of the dry deposition sink. The highest deposition loads, as well as the largest bias between model calculations and measurements, are to be found at stations located in coastal areas. These effects have been discussed, e.g., in an EUROTRAC project in which the transport of Estonian, St. Petersburg and Karelian emissions over the Gulf of Finland was studied with an 0.1^o resolution model

(Paper V) and in a CAPMAN (Coastal Air Pollution Meteorology and Air-Sea Nutrient Exchange) contribution within EUROTRAC-2 (Paper III).

5.3.1 Annual deposition to the Baltic Sea, 1993-1998

The annual deposition to the open Baltic Sea area (391 000 km^2, limited to 57° 44' 8" N near Skagen) over the period 1993-1998 for oxidised and reduced nitrogen lay in the ranges of 140-180 kt (N) NO_x and 100-120 kt(N) NH_x (Fig. 4). The distribution of these totals over the various HELCOM sub-areas, the reasons for the load variability and its characteristic features are discussed in Hongisto & Joffre (2002), Hongisto (1998), Hongisto et al. (1999a-b), Schulz & Hongisto (1998), Schulz (1998), Zuelicke (1999) and BASYS (1999). The total N-deposition to the Baltic Sea open water area exceeded 270 kt(N) before 1995, dropping to below 240 kt in 1997, but increasing again to 295 kt(N) in 1998. Neither N-deposition to the Baltic Sea nor concentrations at coastal stations have decreased during the 6-year period.

The seasonal distribution of the 6-year average total nitrogen deposition over the Baltic Sea is illustrated in Fig. 5. The annual deposition (Fig. 1. in Hongisto & Joffre, 2002) was below 300 mg(N) m^{-2} over most of the northern part of the Gulf of Bothnia, increasing towards the Finnish coast and decreasing towards Sweden. The deposition exceeded 400 mg(N) m^{-2} over the Finnish archipelago, growing to 1200 mg (N) m^{-2} near the south-western coast. The inter-annual variation of the geographical distribution in 1993-98 is not very large; the dry deposition of oxidised nitrogen (NO_x) declined, however, from its 1993-94 levels, while wet deposition increased.

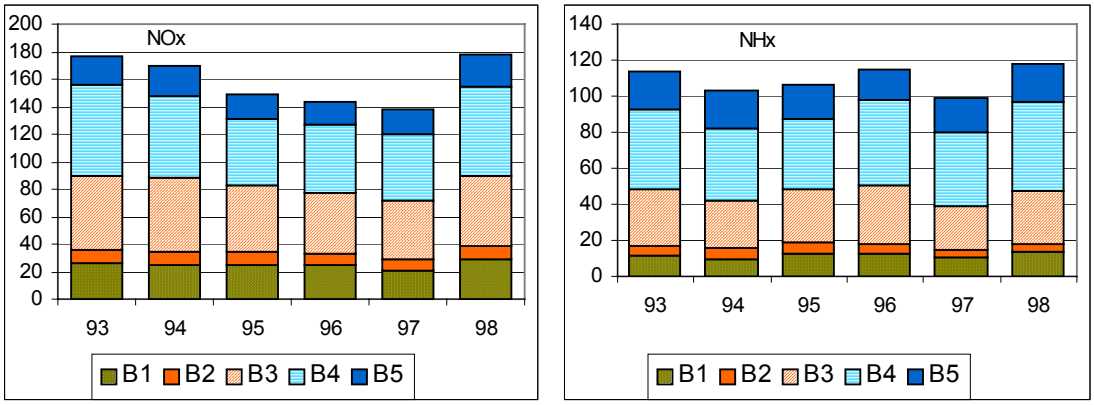

Fig. 4. Annual deposition in kt (N), 1993-1998, for oxidised nitrogen NO_x, and reduced nitrogen NH_x, to the Baltic Sea subareas: B1 – Gulf of Bothnia, B2 - Gulf of Finland, B3 – North Baltic Proper, B4 – South Baltic Proper and B5 – Kattegat/Belt Sea.

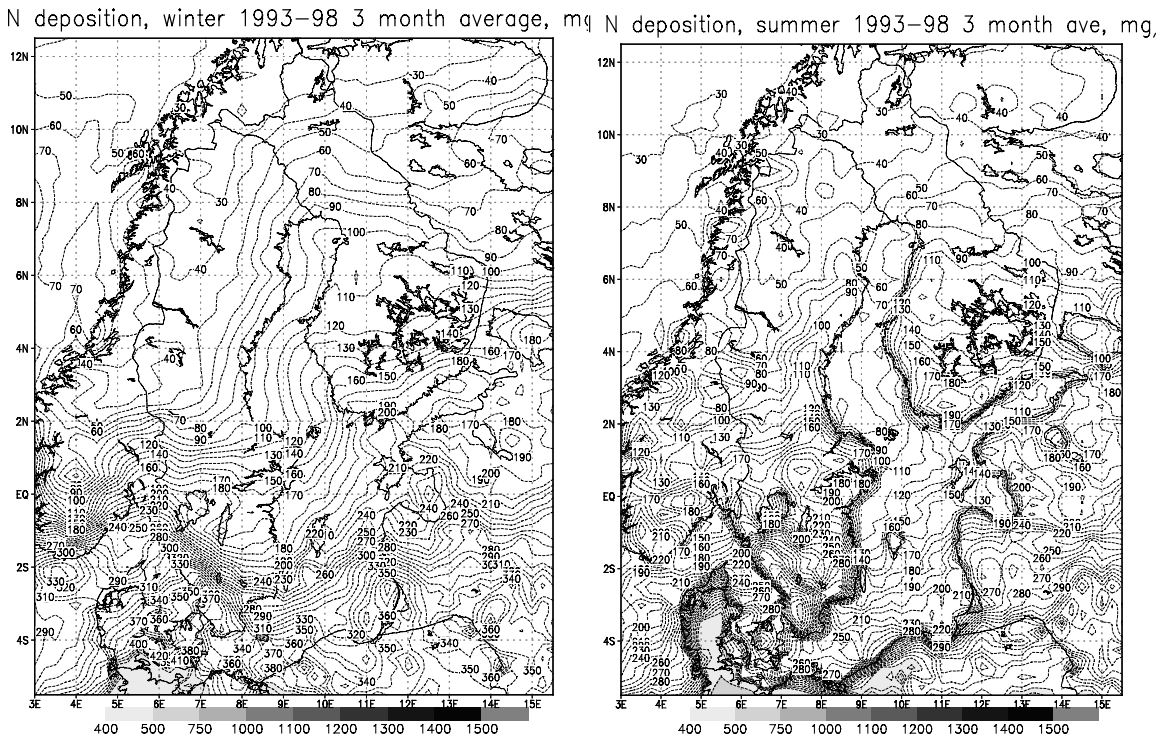

Fig. 5. The seasonal distribution of the 6-year average total nitrogen deposition over the Baltic Sea

These results are within the range of the EMEP MSC-W calculations that indicate a decline in the total deposition load from 320 kt to 230 kt (N) between 1987/88 and 1995 (Bartnicki et al., 1998), and a slight increase to 241 kt (N) in 1998 (Bartnicki et al., 2001). The EMEP MSC-E estimate for the 1987-1991 load is somewhat higher, 298 - 343 kt (N) (Dedkova et al., 1993). Earlier total N-deposition estimates were 400 kt (N) for the early 80's (Lindfors et al., 1993) and 300 kt (N) for the late 80's (HELCOM, 1991).

Over the same calculation periods, the Hilatar load exceeded the estimate of the 150 – 50 km resolution EMEP model (Bartnicki et al., 1998, 2001) by 11 % in 1993, 7-8 % in 1994-95, 4 % in 1996 and 2 % in 1998. The EMEP estimate for the year 1997 is not comparable to the Hilatar estimate due to incomplete precipitation fields (Bartnicki et al., 2001). The largest differences were in the southern Baltic Proper. On the other hand, ammonia deposition over the Gulf of Finland was higher in the EMEP model. On average, the 1996 Hilatar dry flux estimate was 69–92 % of the EMEP estimate for NH_x/NO_x, and 114-101 % for wet flux, respectively. This can be explained by model differences in resolution (150 vs 28 km), meteorological input and time variation in emissions. An emission-corrected comparison with BASYS Network-period measurements (Schulz et al., 1999a-b) gave around the same deposition.

Although deposition density was higher in the southern Baltic Sea, 50% of the total atmospheric N-load fell om the northern sub-areas B1-B3, i.e. the Gulfs of Bothnia and Finland and the Northern Baltic Proper, compared with 35 % on B4, the Southern Baltic Proper, and 12 % on B5 (Kattegatt – Belt Sea). The load consists mainly

(around 80 % for NO_x, 65 % for NH_x) of wet deposition, although dry deposition can be dominant during dry summer months, as in July 1994 (75% for NH_X and 71% for NO_X). The seasonal variation was rather even, with inter-annual and monthly variation being significant, however.

Short and long-term time-variations were significant, and the load did not depend linearly on concentrations or precipitation. The total nitrogen deposition, found to a large extent to be long-range transported from Central Europe, depended strongly on the climatological conditions prevailing over Central and Northern Europe. Inter-annual differences in wintertime deposition depended on the frequency and latitude of the cyclone tracks. When low-pressure centres move along a northern route, high NO_x deposition originating from the main emission areas occurs simultaneously with frontal precipitation.

The effect of the updated 1990 ship emissions was significant for the Baltic Sea load estimate. When the year 1993 was re-simulated using these new ship emissions, the annual NO_x depositions to the Baltic Sea rose by +8% (total), +12% (dry) and +7% (wet) compared to previous runs. Dry deposition increased most in June (+19 %).

5.3.2 Episodicity of the load to the Baltic Sea

The episodic nature of most atmospheric processes is a well-recognised feature that can be detected by all measurements with sufficient resolution (Leinonen et al. 1994-2001, Ruoho-Airola & Salmi, 2001). Most of the monthly wet deposition is collected during a few days, which are usually not those of maximum accumulated precipitation. At coastal stations, the spring and summer months are especially dry.

The simulated 6-h deposition over the Baltic Sea during 1993-98, illustrated in Fig. 6, displays the typical peaks characterising episodes of air pollution. There are no long dry periods that cover the total sea area. The Baltic Sea is large, and being situated in a mid-latitude zone typified by alternating polar, marine or continental air masses, meteorologically opposite situations can prevail simultaneously over any parts of it, with either a west-east or north-south divide.

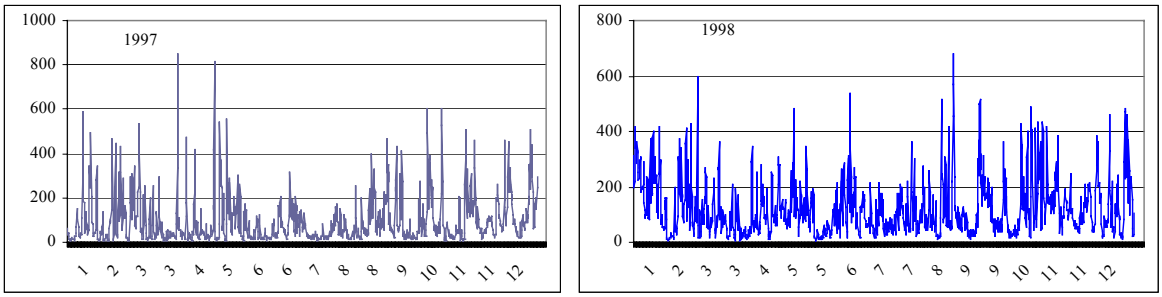

Fig. 6. Total deposition to the Baltic Sea Area, NO_x episodes (in kg $(6h)^{-1}$) in 1997 and 1998.

During 1996-1998 30 % of the annual NO_x deposition to the whole Baltic Sea was received within 30 days, 20 % in 17 days, 10 % in 7 and 5 % in 3 days. The number of

episodes varies from year to year (Fig. 7), as illustrated by the frequency of exceedance of 400 t in 6h for NO_x and for NH_x to the total Baltic Sea. This diagram also partly provides an answer to the annual variation of NO_x deposition.

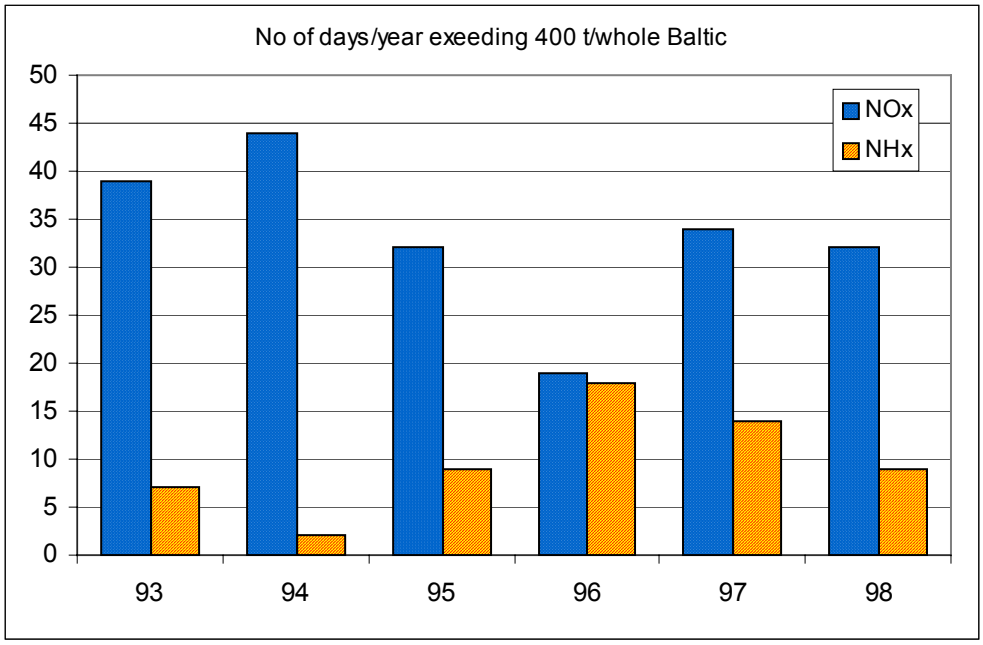

Fig. 7. Annual number of high deposition episodes exceeding 400 t (N) in 6h for NO_x and NH_x over the whole Baltic Sea

The frequency of exceedance of a given share of the monthly deposition over the whole Baltic Sea is lower than that over any single marine point during one 6h event. The episodicity of wet deposition is also weaker in the model compared to daily measurements. The smoothing of plumes over the grid volume, slightly over-predicted weak precipitation and efficient scavenging at low rain rates give a rather high deposition background, and peaks that are not as sharp as those measured. In general dry deposition was also rather episodic.

5.4 Influence of meteorological conditions on the load to the Baltic Sea, 1993-1998

5.4.1 Flow direction and pressure anomalies

Atmospheric circulation patterns determine the flow direction during rainy periods over the different Baltic Sea sub-basins, strongly influencing the time variation of the nitrogen deposition. This influence was studied within the BASYS project using German Weather Service weather maps (DWD 1993-1998), in which meteorological situations are classified according to the surface pressure distribution over Europe, western Russia and the Atlantic, using the Hess-Brezovski weather types (Hongisto & Joffre, 2002).

The flow direction over the sub-basins does not stay constant during a given weather event, as local pressure anomalies turn the wind. If a cyclone crosses the Baltic Proper, which is common during south-westerly flow, the trajectory analysis fails to identify the source areas for a period in which trajectories are turning rapidly over all the nearby source areas, and the wind blows from the opposite direction after the event has passed. South-westerly flow is strongest when cyclones move over the Atlantic north of the Norwegian coast. The weather types (Table 1) were grouped according to the main flow sectors with respect to the sub-basins B3-B5. Sub-basins B1-B2 were generally more affected by the north-eastern sector than the southern parts.

A zonal circulation pattern prevailed from 1993 to spring 1995 and also in 1998, while for almost the whole of the two intermediate years the large-scale circulation changed to a meridional type (high west-east pressure difference) that was strongest in 1996 (Fig. 8). A similar distribution also appeared in the seasonal variation of the duration of the grouped weather types (Fig. 9). The share of primarily south-westerly (SW-S) flows was 76-82 % of the winter days during 1993-95 and again in 1997-98, but dropped to 27 % during winter 1996. The period spring 1995–summer 1996 was exceptional, with high incidences of northerly and north-easternly flows and cooler air outbreaks, which were usually also rather dry.

Table 1: Main flow direction over sub-basins B3-B5 classified according to the large-scale weather types of Hess-Brezovski (1993).

Main wind direction	Weather types
Primarily W-SW types:	Wz, SWa, SWz, Wa,
Sometimes W-SW types or mainly SW,S	Ws,Ww, NWz, HM,BM,TrW, Sa,Sz
Mainly N,NE,E,SE	TM, NEa, NEz, HFz, HNFa, HNFz, SEa,Sez, TB
Mainly NW, N, NE	NWa, Na, Nz, HNa,HNz, HB,Nea
Mainly E,SE,S	TrM, Hfa

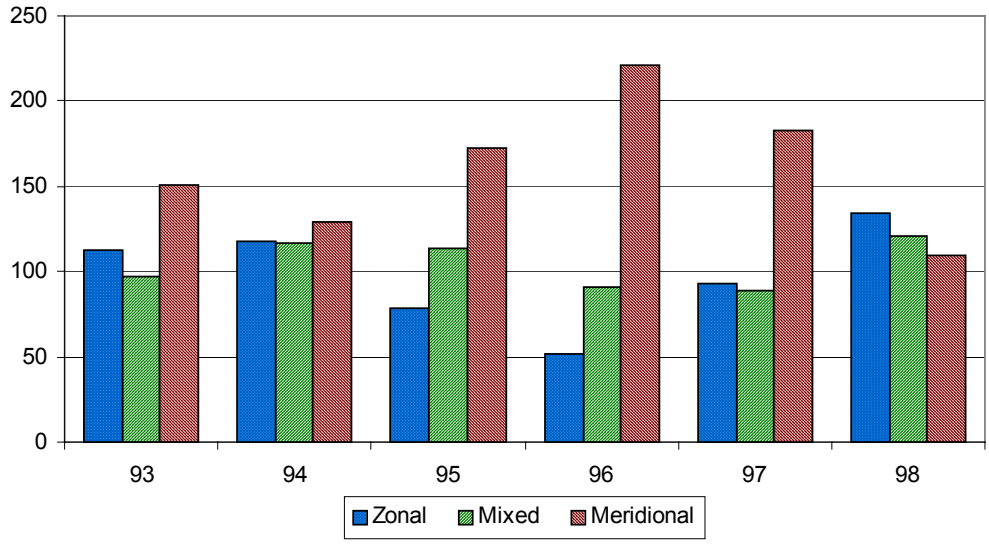

Fig. 8. Occurrence of large-scale weather types during 1993-1998. No. of days in year.

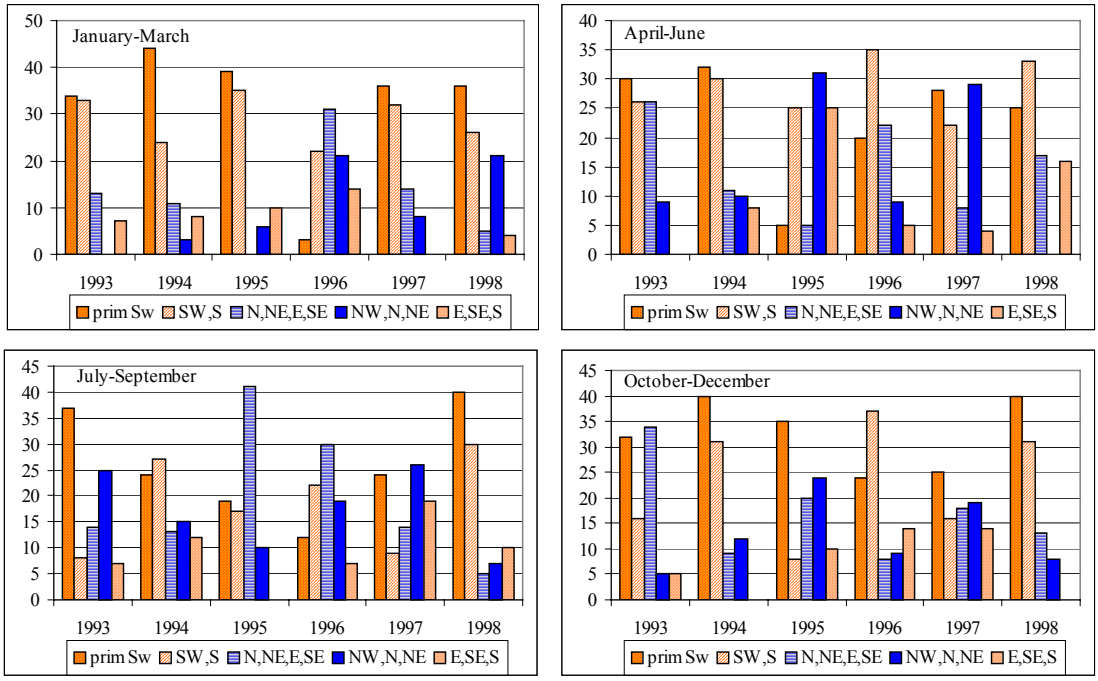

Fig. 9. Duration (as days in 3 months) of large-scale flow regimes over the Baltic Sea sub-areas B3-B5, 1993-1998.

Generally the wind sectors NW-N-NE-E are clean with respect to nitrogen pollution. In winter 1996, the wind blew from these clean air sectors for 57 % of the time. A strong, almost permanent high-pressure centre was situated over Russia in January and February, also extending several times over Scandinavia and the Baltic Sea. This northerly flow share reached 59 % in summer 1995, being lowest in winter 1995 (7%), and 13-18 % in summer 1998, in winters 1993 and 1994, and in autumn 1996.

This primary dependence of deposition on air mass origin is illustrated in Fig. 10 with the correlation between monthly NO_x and NH_x deposition and the duration of weather types with opposite wind direction. The correlation coefficients for days with a primarily S-SW wind direction over the whole sea area with NO_x dry deposition was 0.66/0.48/0.36/0.02 in winter, spring, summer and autumn, respectively.

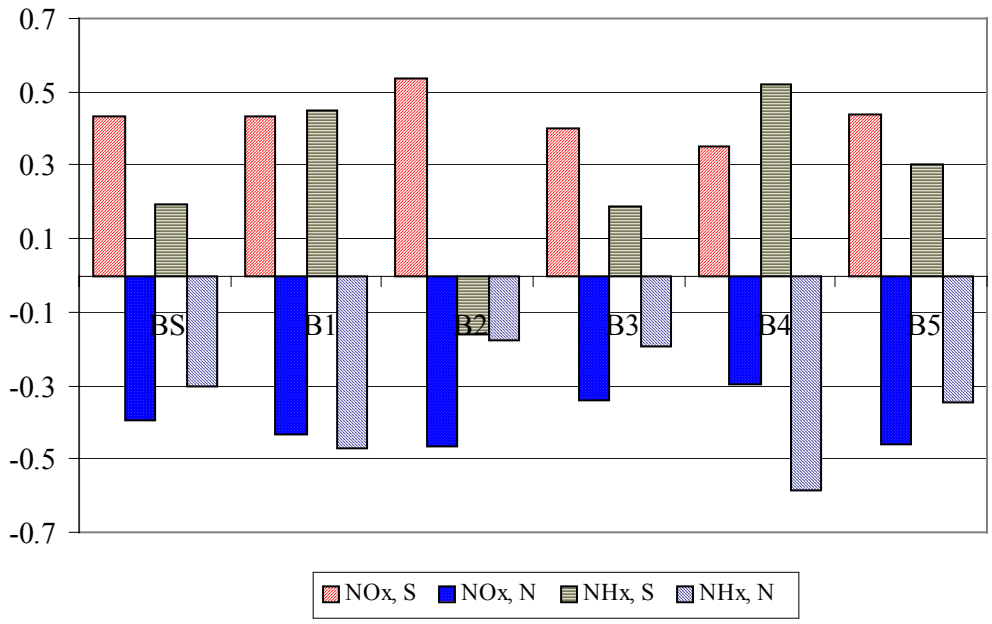

Fig. 10. Correlation of NO_x and NH_x total deposition with combined northerly (N=N,NW,NE) and southerly (S=S,SE,SW) wind directions for the whole Baltic Sea and its individual sub-basins

5.4.2 The North Atlantic Oscillation

The North Atlantic Oscillation (NAO) index is positive when the sea-level pressure difference between the Icelandic low and the Azores high is above normal, intensifying both westerly water and air flow across the North Atlantic towards Scandinavia. In addition to wind conditions, the NAO determines the temperatures on both sides of the ocean, and the effect is most strongly felt in winter and early spring. A geographically more general index for the same phenomena is the Zonal Index (ZI), the average pressure difference between latitudes 35° and 55° averaged over longitudes 20°W–40°E. Both are encompassed by the Arctic Oscillation, AO, reflecting the variability of empirical orthogonal functions of the monthly sea-level pressure distribution poleward of 20°N. The wintertime AO has had an upward trend during the past several decades, indicating a strengthening of the wintertime polar vortex from sea level to the lower stratosphere (Thompson and Wallace, 1998).

The 6-year average correlations of the monthly NAO index with NO_x- and NH_x-deposition to the Baltic Sea were 0.43 and 0.22, respectively. The index correlated especially with the wet deposition in winter and springtime, but not well during other seasons. The correlation with ZI was somewhat higher (Fig. 11). The NAO index could be in conflict with the length of the Baltic ice winter: during winter 93/94 it was positive from November to April, although the ice winter was of medium strength. The annual zonal index correlated well with NO_x deposition to the Baltic Sea (0.68), but not with ammonium deposition (0.29). The seasonal variation was the same as with NAO.

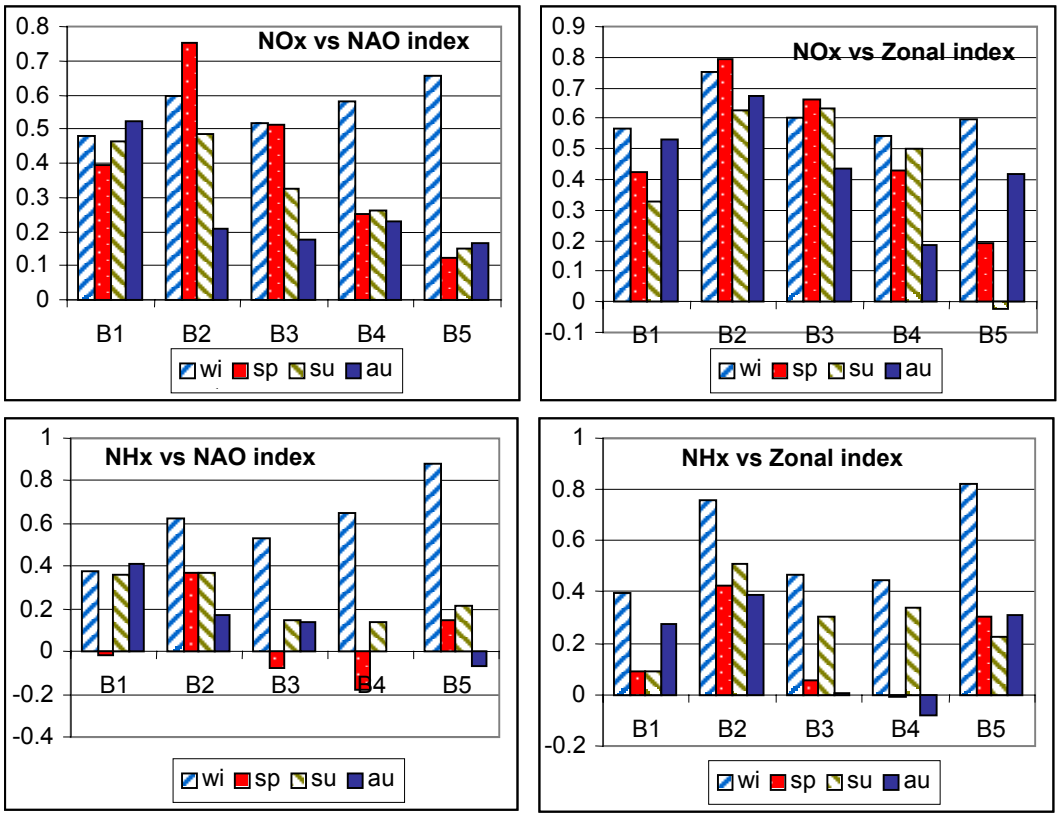

Fig. 11. Seasonal correlation of NO_x and NH_x deposition, in the different Baltic Sea Basins, with NAO and ZI indexes. Wi, sp, su and au are winter, spring, summer and autumn, respectively.

5.4.3 Precipitation

Most of the precipitation to the Baltic Sea fell during the autumn and summer months, with rather a high monthly variation, standard deviations usually being more than 50 % of the average monthly value.

During winters 93-95, when mainly south-westerly flows prevailed and NO_x deposition was high, precipitation was also higher than normal, except during the cold February of 1994. Maximum rain amounts over the Baltic Sea occurred, however, in 1998, autumn 1997 and 1994. Compared to the 1961-1990 normal, the period spring 1995-spring 1996 was dry over sub-basins B3-B5, the accumulated precipitation being below 25 % in January 1996 over most of the Baltic Sea, and 20-50 % of the normal amount during October-December 1995. The cold summers 1993 and 1998 were dry, the precipitation being 58 and 75 % of the seasonal average. Ammonium deposition reached its maximum during the wet months of November 1996 and October 1998.

Total NO_x deposition is non-linearly related to the precipitation amount. The highest monthly deposition in each sub-area was reached with on average 50 % of the precipitation maximum, which usually corresponded to around 60 % of the maximum monthly deposition. The episode frequency is highest in winter, while 31-33 % of the rain was received in the autumn. Over the individual basins the monthly NO_x deposition correlated with the precipitation sum with a coefficient of 0.46-0.71.

Meteorological variability is not reflected as clearly in the deposition of sulphur and ammonium. In the case of sulphur, this is because the northern and north-eastern sources of are significant. For ammonium, the transport distance is also shorter and it has its highest emissions during summertime, when the precipitation is not as strongly correlated with the wind direction.

5.4.4 Ice winters

The winters of 1992/93 and 1994/95 were extremely mild, the maximum extent of the ice cover being around 70 000 km^2 and the ice season about 8 weeks shorter than during the average winter (1960/61–1989/90). The winters of 1996/97 and 1997/98 were mild (with 128 000 km^2 max. ice cover extent), while in 1993/94 and 1995/96 the ice cover extent was average (206 000–262 000 km^2) and the ice season 2-4 weeks longer than normal (Seinä et al., 1996; MTL 2002). The winter of 1994/95 was the warmest, as was also the winter of 1993/94 until the very cold February of 1994. The winter months of 1996 were the coldest over this 1993-1998 period. On 57% of the time, winds blew from the sector between north and south-east, precipitation was less than 50 % of the normal and NO_x deposition below 50 % of the 1993-1998 average winter deposition. There was no large variation in the spring temperatures.

An ice cover decreases dry deposition flux to the sea, because over an open sea turbulence keeps the dry flux high. Ice cover is also a sign of frequent cold winds from the nitrogen-clean sector. Thus wet deposition is also lower than if the sea is open. The anti-correlation coefficients between the total NO_X-deposition and the monthly average fractional ice cover over the Gulf of Finland basin B2 was -0.54 and over the Gulf of Bothnia -0.48. It was higher if the spring months are ignored (for B2 -0.62, for B1 -0.52 excluding May). During the stable spring months the retreat of the ice cover did not increase the deposition as high as it was in winter, when conditions are convective over the open sea. Dry deposition anti-correlated with ice over B2 (–0.48), over northern B1 (-0.40) and southern B1 (-0.34). The frequency of the deposition episodes decreased with increasing ice cover.

5.4.5 Boundary-layer parameters

The variability of ABL height, wind strength, mixing conditions and relative humidity affect the vertical dilution, transport speed and chemical conversion rate of contaminants transported over the sea. This is illustrated in Fig. 12 in terms of seasonal averages at the centre of sub-basin B3, the Northern Baltic Proper. During winter or late autumn with northerly flow over the warmer open sea, the mixing height was high, vertical mixing efficient and pollutant concentrations were diluted more efficiently. However, dry deposition velocities were also high. During winter 1995 with frequent southerly flows, the vertical-mixing efficiency was only a third of that of the cold winter 1996, when the 3-month average wind velocity was, however, almost 3 m/s lower than in 1995 or 1997. Spring is meteorologically the most stable period over the Baltic Proper. Summers show high inter-annual variation in the eddy viscosity coefficient K_z.

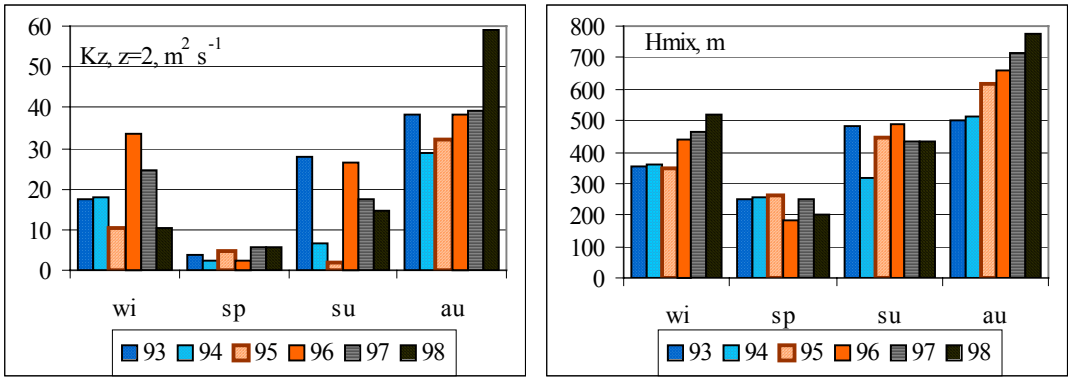

Fig. 12. Seasonal and inter-annual variability of eddy viscosity Kz (at level z=2, ~ 110 m) and ABL height at the centre of the Northern Baltic Proper, sub-basin B3

5.5 Ability of the coastal measurements to represent the open sea area

Marine and land areas follow a reversed meteorological cycle. The ABL is more stable during winter over land but also during spring and early summer over water, if warm air spreads over the still cold sea. Turbulence is strong in convective situations over land in summer, as well as over the sea in autumn and early winter.

Coastal areas are difficult both for models and for field work. The collection efficiency of precipitation and wet deposition gauges can be rather poor in windy places, thus underestimating measured deposition. Meteorological gauges are also quite close to the surface, and when the sea is frozen, at windy locations re-emitted light dry snow might be collected by the gauges instead of precipitation. This is clearly seen at Utö, where, during the winter months, the meteorological gauge can collect twice as much, or even more, water than the air quality gauge that is located very near, but at a higher place.

In most cases the emission density is higher in the coastal zone. The emissions are mixed inside the whole grid cube, while in fact it depends on the wind direction whether the emitted plume is detected at all. With a clean offshore wind, sub-grid mixing in the model leads to overestimation of the concentrations upwind over the sea, where measurements give a better estimate of them. The grid-averaging of some marine and continental ABL parameters, if their values differ very considerable between stable and unstable areas, also affects dilution. Their grid-averaging should depend on wind direction, too. This was clearly seen during the cold November of 1993 (Hongisto, 1998).

In mid-latitudes sea breezes usually travel from 5 to 50 km inland. However, in some cases very deep inland penetrations, of even 100 km from the shoreline, occur at latitudes of about 50 ^{o}N (Tijm et al., 1999). This can temporarily turn the wind direction against the mean flow. In fine resolution (10-25 km) weather prediction models, weak sea breezes can be resolved, while in coarser ones (e.g. HIRLAM 0.5^{o} wind fields) the sea breeze is generally a sub-grid circulation phenomena and should not affect grid average values.

The seasonal differences in the 6-year average total deposition gradients (Fig. 5) are large. The short-term gradients are very site-specific, depending on the wind direction

with respect to the coastal emissions and their intensity. The dependence of the representativeness of the coastal measurements for the open sea upon the meteorology, averaging period and location with respect to emission areas, was assessed by extracting monthly coast-to-sea gradients along 10 cross-sections from the 26 x 26 km^2 resolution model data base and by integrating the modelled load and concentrations over the main sub-basins of the Baltic Sea and comparing these with the coastal measurements (Paper V).

Over the West-Norwegian coast, precipitation was stronger both over the mountains and over the North Atlantic in comparison to the coastal zone. Dry deposition is also higher over the open sea than over the coastal zone, so that coastal measurements only represent coastal, not marine conditions. The wintertime total deposition was 20-40 % (NO_x) and 10-29 % (SO_x) higher over the Atlantic at a distance of 50 km from the Norwegian coast. For NH_x the difference was ± 15 %. Over the North Sea a similar gradient was detected for NO_x and SO_x. Wintertime total NH_x-deposition (up to 60 %), and dry deposition of all compounds were, however, higher over Denmark than over the surrounding sea areas. In summer both dry and wet deposition of all compounds were lower over the North Sea and southern Baltic Sea than over the surrounding land, with a slight general increase over water towards the east.

In several west-east cross-sections taken over the Baltic Proper and the Bothnian Bay, the 6-year average wintertime deposition was also smaller over coastlines in comparison with the surrounding water areas. Over the sea it increased towards the east, the relative gradient being strongest over the Bothnian Sea, where the east-coast deposition exceeded the levels near the Swedish coastline by 64 / 78 / 116 % for NO_x, NH_x and SO_x, respectively.

Generally, both wet and dry deposition decreased towards the north-west over the Baltic Sea, but the gradient depends on emission intensity: along the Central European coast deposition is stronger than over the Southern Baltic proper, but over the North Sea it is higher than over Southern Norway. Short-term gradients depend on the meteorology and the on/offshore wind, either increasing or decreasing towards the open sea. In conclusion, extrapolation of coastal measurements to the open sea areas is not straightforward; a good meteorological analysis has to be performed for such a study.

5.6 BASYS Lagrange and Network studies

Within BASYS the Baltic Sea was truly studied as a unified system in which the various parts interact with each other. The major findings of the work of the different subprojects are summarised in the BASYS final report conclusions (Zuelicke 1999).

5.6.1 Network and Lagrange studies

Simulations of atmospheric pollution concentrations and load estimates, as well as meteorological analyses, were performed to accompany the experimental findings

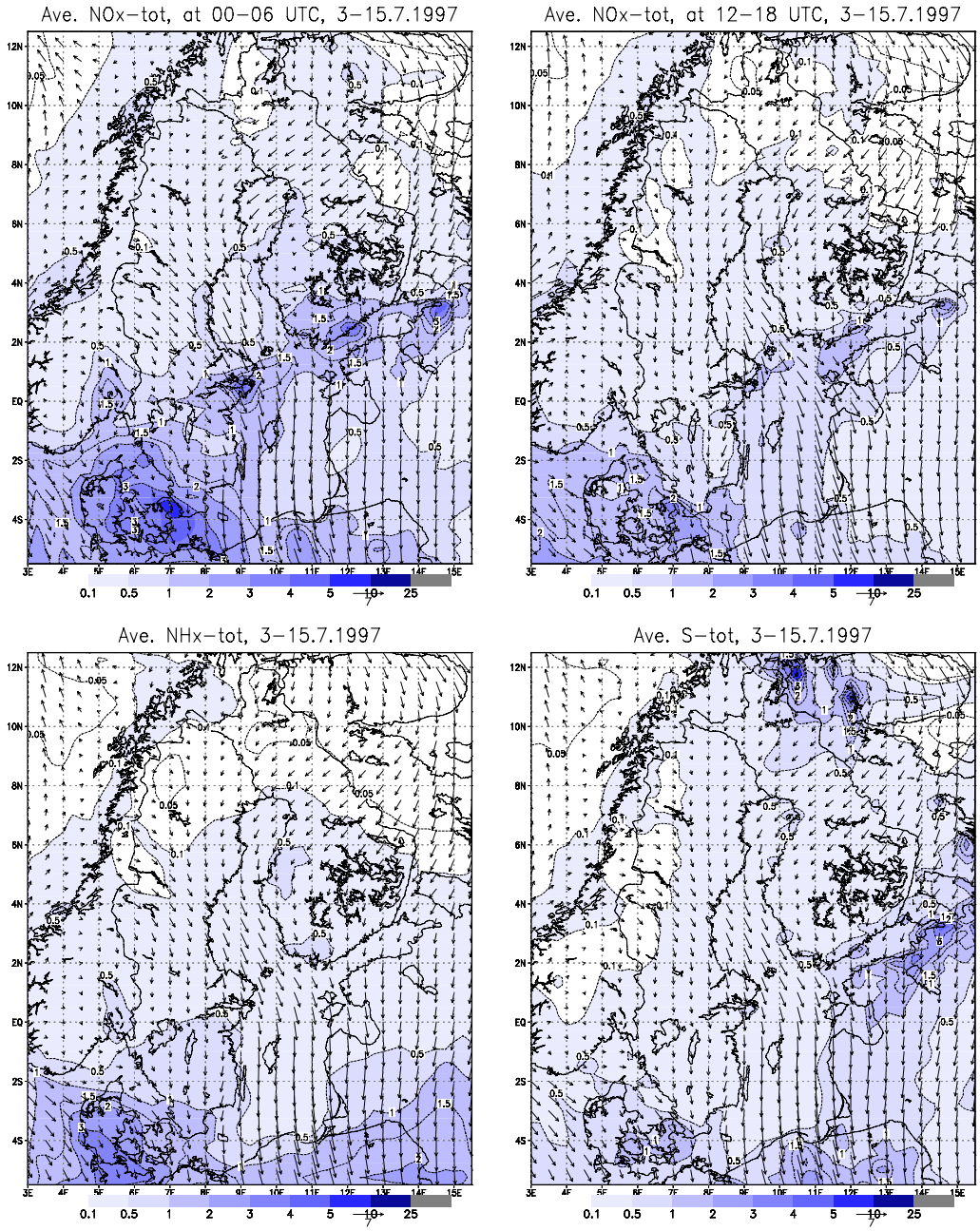

Fig. 13. Modelled average NO_x-, NH_x and total S concentrations during the BASYS summer Langange field campaign.

(Schulz et al., 1999a-b; Schulz & Hongisto, 1998; Schulz 1998). The measured nitrate, nitric acid and NO_2 concentrations were twice as high at the most western station of Kap Arkona, Rügen, Germany than at the most eastern station of Preila, Lithuania, due to the currently higher traffic emissions in Western Europe. The same results were obtained by the model (Fig. 13).

The highest ammonium concentrations were observed at the southern stations of Hel and Kap Arkona. A possible explanation lies in the high emissions of sulphur in Central Europe. The formation of sub-micron ammonium sulphate has been shown to be an effective carrier of ammonium through LRT.

The measured nitrate-to-sulphate ratios were significantly higher in the samples from Kap Arkona and even in those from Hoburg compared to those from the south-eastern Baltic Sea region. This can be seen from the model results in Fig. 14. Nitric acid, the main precursor of particulate nitrate, has a large variability as compared to the sum of HNO_3 plus NO_3^-. The low concentrations of NO_x at Preila and Hel indicate that the major source of oxidised nitrogen is to be found in Western Europe, with its high traffic emissions.

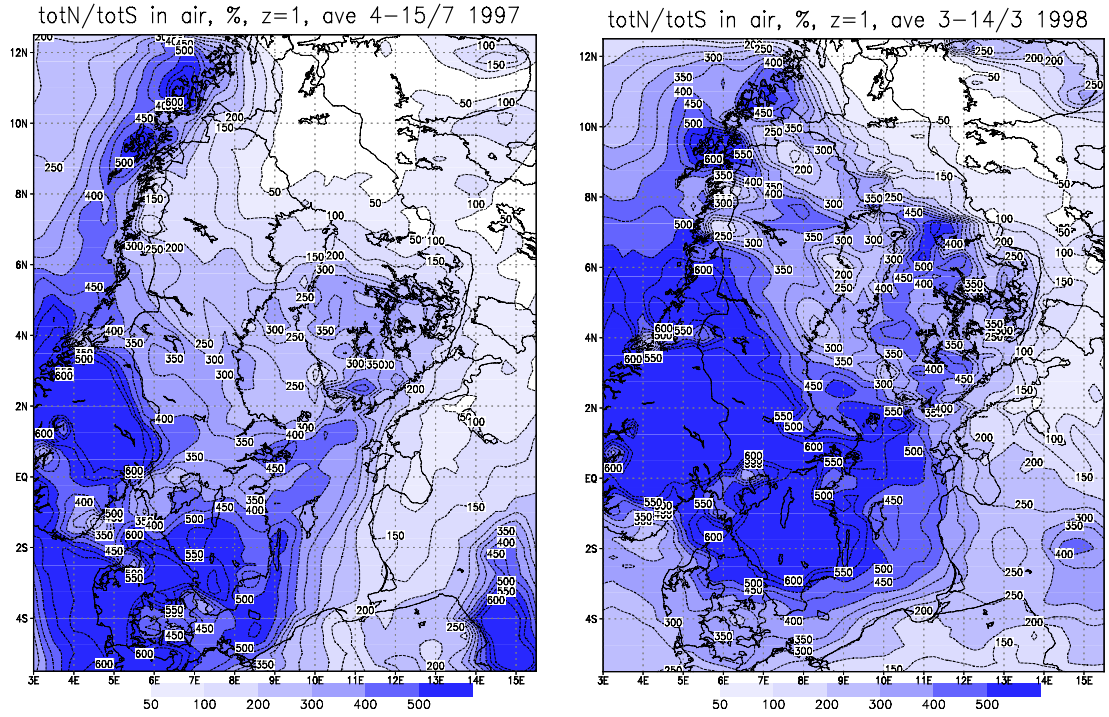

Fig. 14. Modelled average N-to-S concentration ratios during the BASYS summer and winter Lagrange experiments.

In clean areas, the sodium-to-chloride ratio in marine aerosol is almost equal to that of seawater. Nitric acid changes the chemical composition of natural sea salt particles. In summer at the four coastal stations and aboard the ships 40 - 70 % of the chloride in sea salt was found to be replaced by nitrate as a consequence of polluted air mixing with marine air. This constitutes a dramatic shift in species composition (Schulz et al., 1999a). The chlorine released from the sea salt particles influences the ozone cycle over coastal areas. This should be incorporated into the models. The reason for the observed high O_3 concentrations at coastal stations has traditionally been explained by a decreased sink through dry deposition.

The shift in species composition of oxidised nitrogen in marine air affects removal times. The net effect on the air-sea flux of nitrate via dry deposition depends on the meteorological conditions. HNO_3 is a highly soluble gas and has a perfect sink in seawater, unless it has already reacted with natural or anthropogenic contaminants.

5.6.2 Process Study: Micrometeorological Experiment

The Hilatar model calculations were also compared with the process study measurements, aimed at understanding and parameterising the processes governing the air-sea exchange of ammonia and nitric acid, namely turbulent transport and the chemical reactions affecting the production and/or destruction of these gases in the surface layer. The experiments were carried out using a mast at the southern end of the island of Östergarnsholm, near Gotland, in May 1997 and August 1998.

During the six days of the May 1997 field campaign, measured hourly concentrations of NO_2 exceeded 60 ppb during a number of hours, but were usually in the range 20 - 30 ppb, dropping at night below 2 ppb. The Hilatar model concentrations, using the 1990 ship emission inventory, were much lower. According to the measurements, the site, which had been expected to represent background conditions, seemed to be temporarily as polluted as some suburban areas. It is also interesting that for the same periods the model's under-prediction of HNO_3 concentrations was small, although they are usually significantly over-predicted over land.

The measurement location seems to be more influenced by the diurnal ABL variation over the land rather than over the sea, and by a close-lying source. To explain the Östergarnsholm concentrations, a shorter time-step for the meteorological input, careful analysis of the break-up of the night-time inversion layer, simulation of the circulation of pollutants within the sea breeze cycle, and – most important – updating of the ship emission inventory, seem to be necessary.

5.6.3 Simulations of the air pollution for the BASYS field campaigns

The aim of the Lagrangian study was to estimate, from measurements made on the research ships and at coastal stations, the chemical transformations taking place during transport, as well as the air-sea exchange, the mass dispersion and the gradients along the trajectories, and to simulate this situation with the model.

In 1997, both Lagrangian experiment periods were first simulated with the 0.25^o Hilatar model without LRT concentrations, as the European model was still under construction. In March 1998 the concentration distributions were predicted in order to evaluate the best measurement places. However, throughout the whole period, data communications with the ships were very bad, and the experiment director considered the sending of meteorological data to have a higher priority.

The summer Lagrange-period 3-15. July, 1997

At the beginning of July 1997, the large-scale weather pattern over Europe was characterised by a low over the British Isles and a ridge extending from the

Mediterranean to North-Eastern Europe. Although Scandinavia was affected by several cyclones, the precipitation amounts over the Baltic Sea remained rather low (Fig. 15). Hydrostatically stable conditions prevailed during the first week, and the friction velocity and mixing height values at the stations were low. The average mixing height over land had a clear diurnal variation, as seen in Fig. 16. Apart from the first three days, the prevailing wind direction was on average northerly (8-9.7 NW, 13-15.7 NE). This situation became established after the passage of a cold front over Scandinavia on the 8th of July, when a large part of Northern Europe came under the influence of an extended high-pressure area without rain.

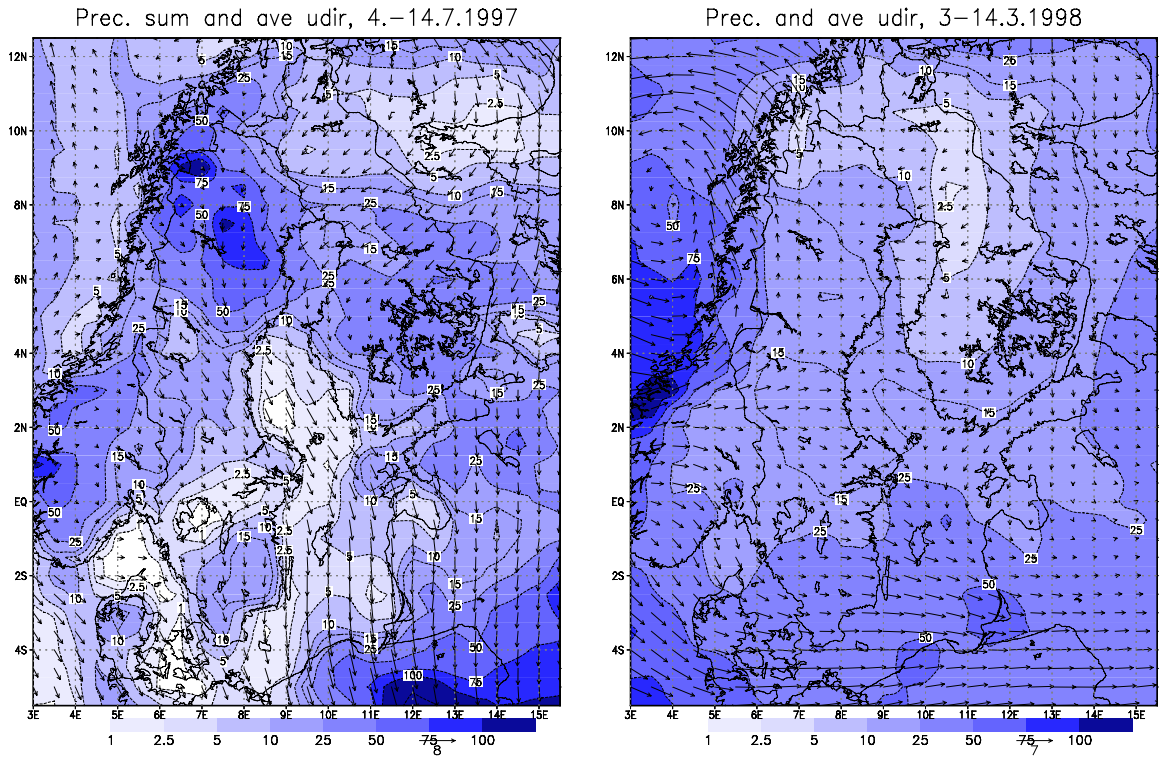

Fig. 15. The precipitation amounts during the summer and winter Lagrange periods, mm.

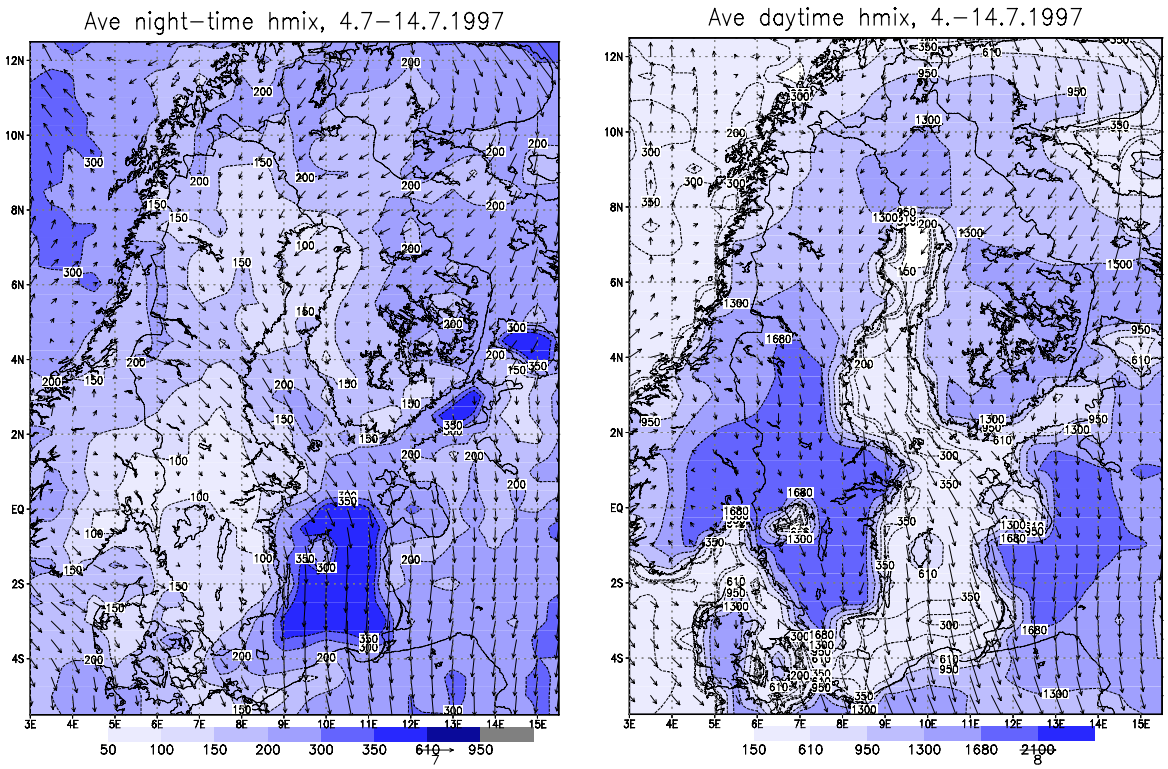

Fig. 16a. Average mixing height during the summer Lagrange period.

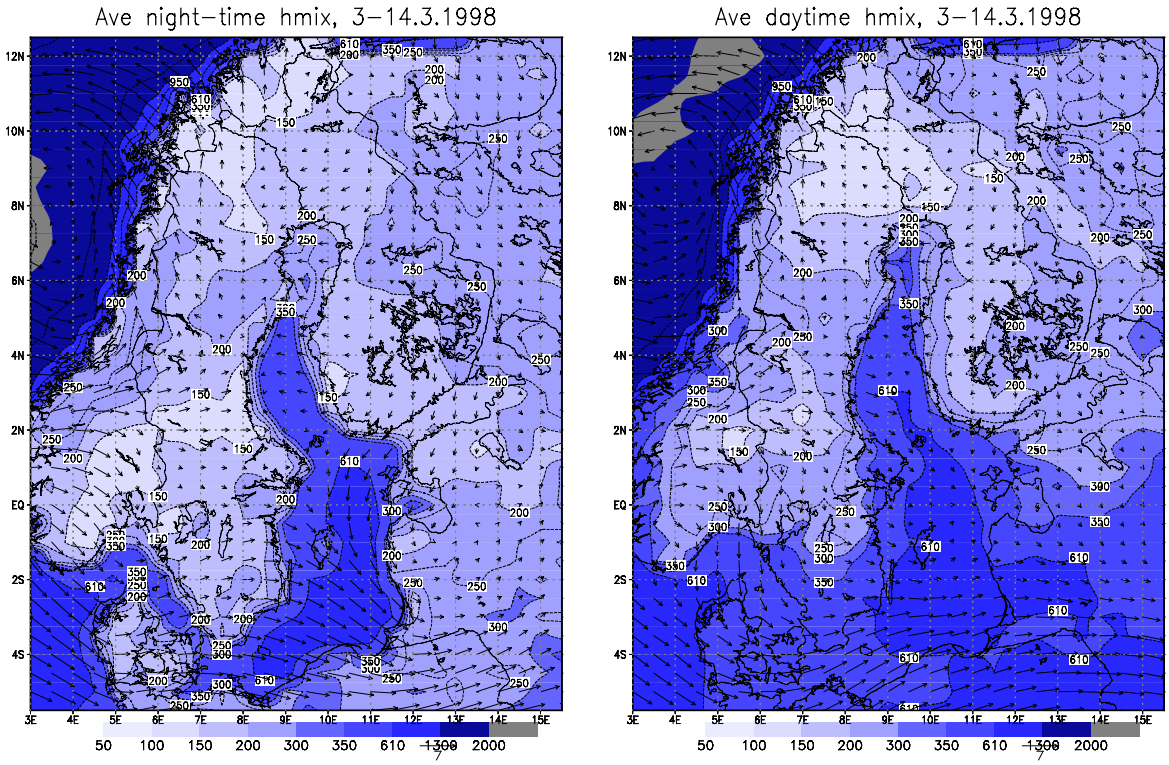

Fig. 16b. Average mixing height during the winter Lagrange period.

Over the period, the maximum NO_x concentrations were reached in the morning when traffic emissions were intense, the OH radical levels were still low and the mixing

height shallow. The difference between the morning and the afternoon concentrations is illustrated in Fig. 13. In the afternoon, the more diluted NO_x concentrations reached 600 m, while concentrations of conversion products rose as high as to 1-1.2 km. From the vertical cross-section of NO_x compounds along a north-south line from Finland to Poland, passing east of Gotland (Fig. 17) one can distinguish signs of chemical sinks: in the southern part HNO_3 is converted into nitrate by reaction with ammonia. In general the modelled concentrations over the Southern Baltic Sea were low.

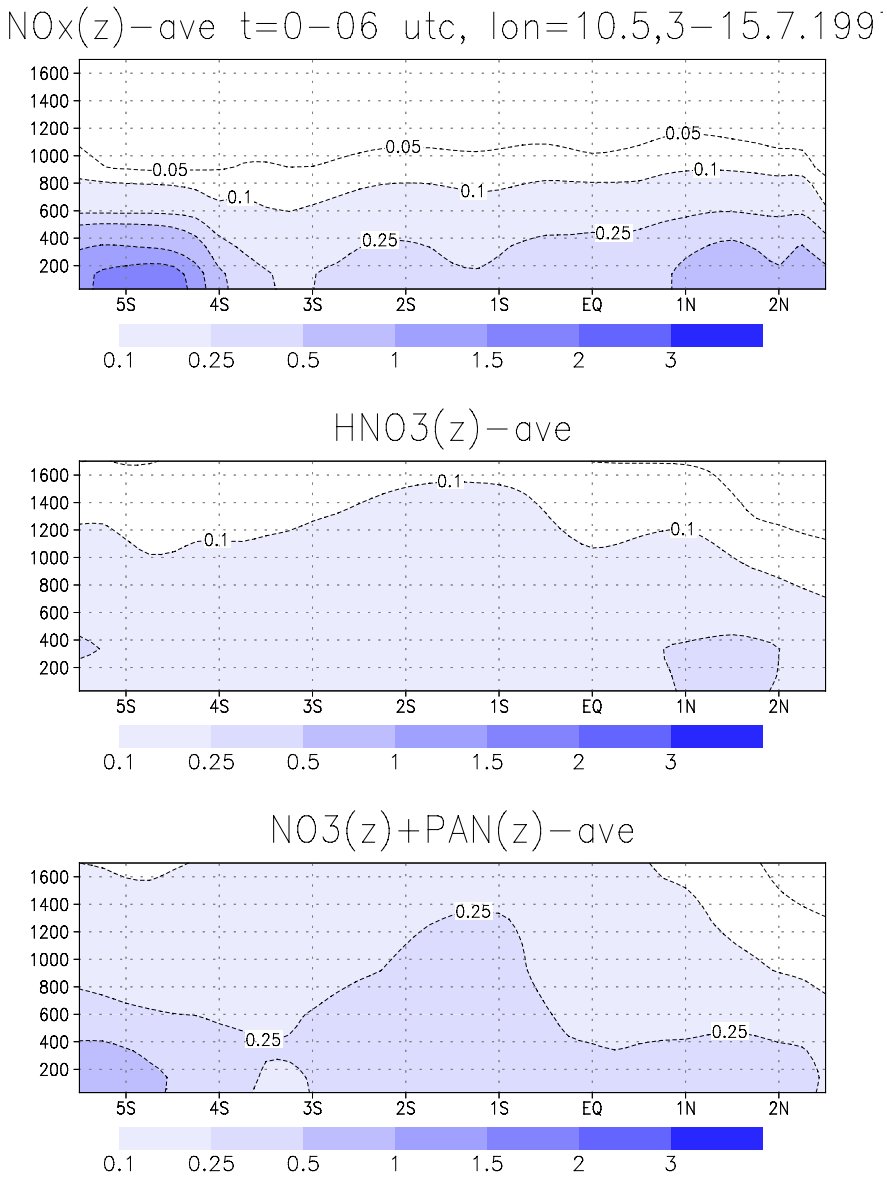

Fig. 17. Vertical cross-section of average summer Lagrange period NO_x-originated concentrations along a north-south line from Finland to Poland, passing east of Gotland.

The best tracer of pollution transport modelled on the 26 km grid has been found to be sulphur dioxide. During the 11th and 12th of July (Fig. 18), sulphur plumes from the

Kola peninsula can be shown to have been transported relatively far south over the Baltic sea. At the end of the period the Estonian and St. Petersburg emissions may have had an influence on the Preila measurements while, in general, flow was from clean areas. At the end of the period the ships sailed northwards in order to intercept the Stockholm plume. According to the total N concentration patterns, the Stockholm plume seems to have reached mv. Alexander von Humboldt on the 11th of July. Unfortunately, the horizontal resolution of the emission inventory in Sweden was rather poor, making it difficult to clearly distinguish the plume as that of the city.

The grid average precipitation at the beginning of the month might be overestimated (no rain was detected on board the ships - the modelled grid average wet deposition amounts were, however, very low). The period was rather dry: wet deposition, received mainly during the first few days, when the ships were not yet at sea, represented only less than one third of the total deposition of both NO_x and NH_3. Dry deposition also showed a clear gradient at the coastline, the explanation being the summertime dry deposition velocity differences over water and land surfaces. During the study period the sea seemed neither to lessen the rain amounts (as in spring, except over some places with convective rain) nor strengthen it (as in autumn). Over the Southern Baltic, the deposition of reduced nitrogen clearly exceeded that of oxidised nitrogen because of its stronger dry deposition flux to water.

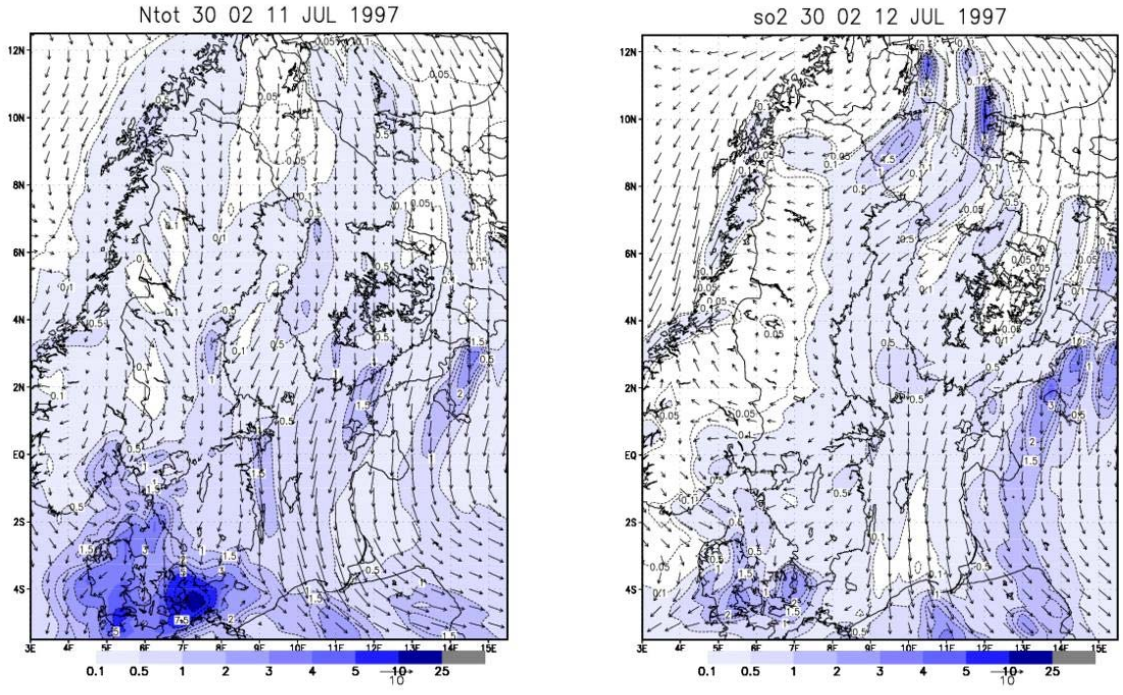

Fig. 18. Stockholm plume on the 11th of July, and an example of the influence of the Kola Peninsula, St. Petersburg and Narva emissions on the 12th of July.

The winter Lagrange experiment 2-14. March, 1998

During the winter period, there was an extended low-pressure area over northern Europe with a rather strong westerly flow prevailing over the Southern Baltic. Several cyclones moved in succession north-eastwards over the Baltic Proper, frequently changing the wind direction and origin of the air masses at the measurement sites by 180^{o} after the 6^{th} of March. On 10^{th} of March, a major high pressure area formed, extending from the western Mediterranean to Scandinavia. This feature moved slowly eastwards and on 14^{th} March it was followed by a cold trough and an associated low-pressure area with rather strong winds over the Baltic Sea. Precipitation over the southern Baltic Sea was considerably heavier than during the summer Lagrange experiment (Fig. 15). The average mixing height over the sea was on average three times higher than over land, and the diurnal cycle over the land was much weaker than in summer (Fig. 16).

Modelled average NO_x-, NH_x and total S concentrations during the BASYS winter Langange field campaign are presented in Fig. 19. At the beginning of the period (up to 7^{th} of March) and on 11-13 March the flow was from the south (SE-SW) and nitrogen-rich air was circulating over the Baltic Sea, as is illustrated in Fig. 20. On the other days, although the wind blew from cleaner northern areas, long-range transported compounds stayed rather a long time in air (Fig. 21).

Over the Gulf of Finland, more than 80 % of the total nitrogen deposition was oxidised nitrogen, consisting mainly of the wet component. This share decreased to 50 % near Denmark. Total deposition did not have a clear or strong gradient towards the open sea for either nitrogen components, though generally the descending deposition gradient was directed from south to north and from east to west due to precipitation (Fig. 22).

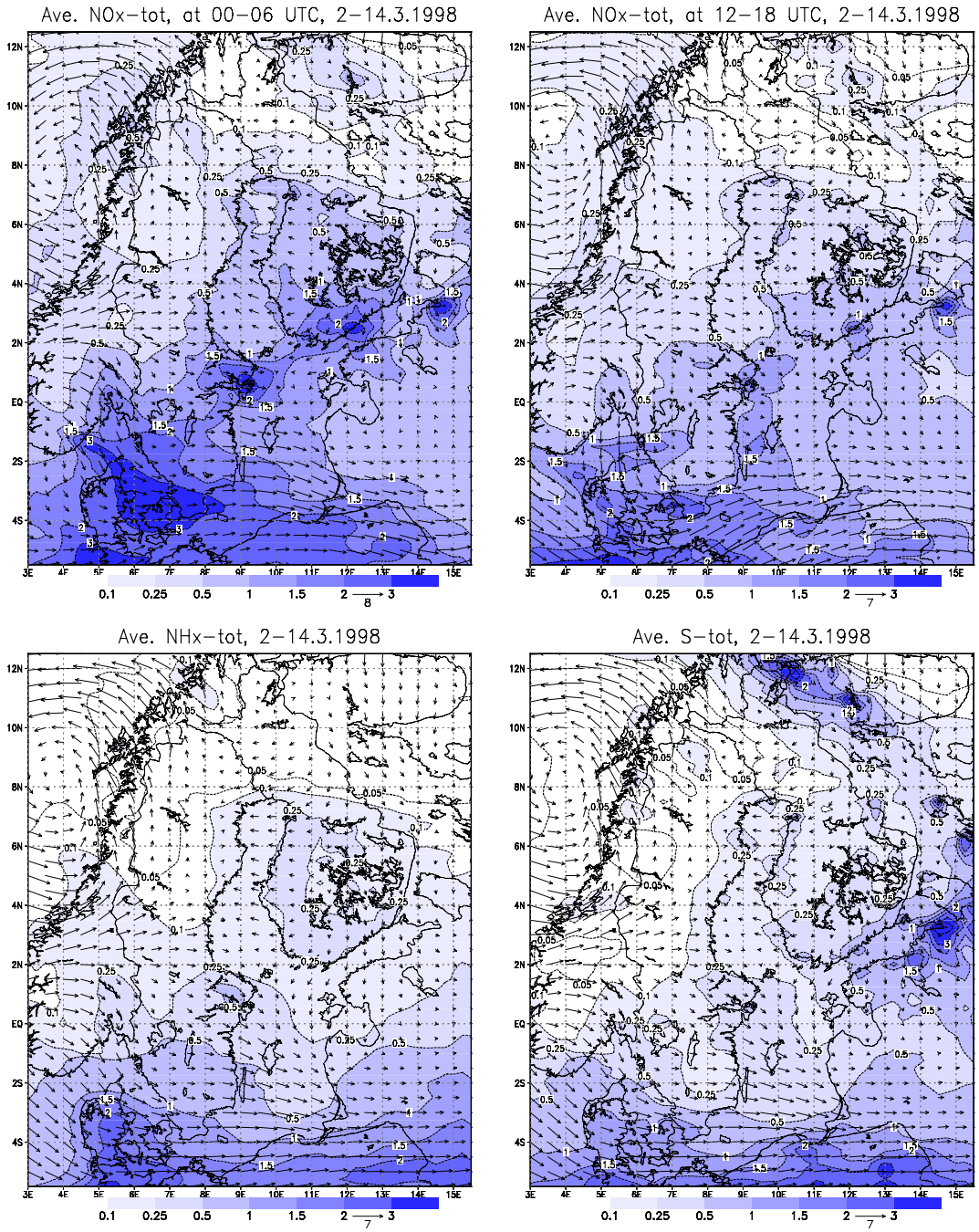

Fig. 19. Modelled average NO_x-, NH_x and total S concentrations during the BASYS winter Langange field campaign.

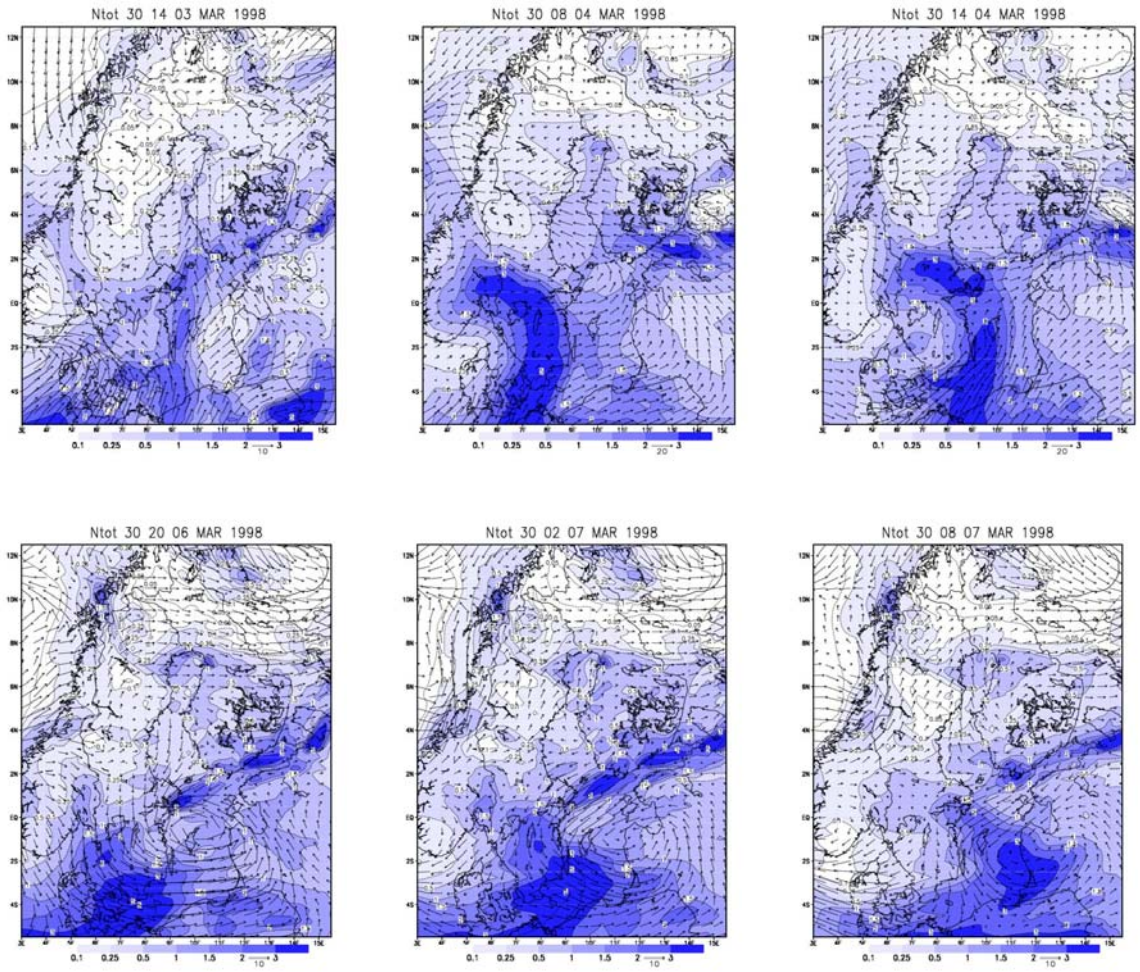

Fig. 20. Two typical time series of total nitrogen transport over the sea from western emissions areas towards the north-east, connected to the movement of fronts and cyclones at the beginning of the wintertime Lagrange period.

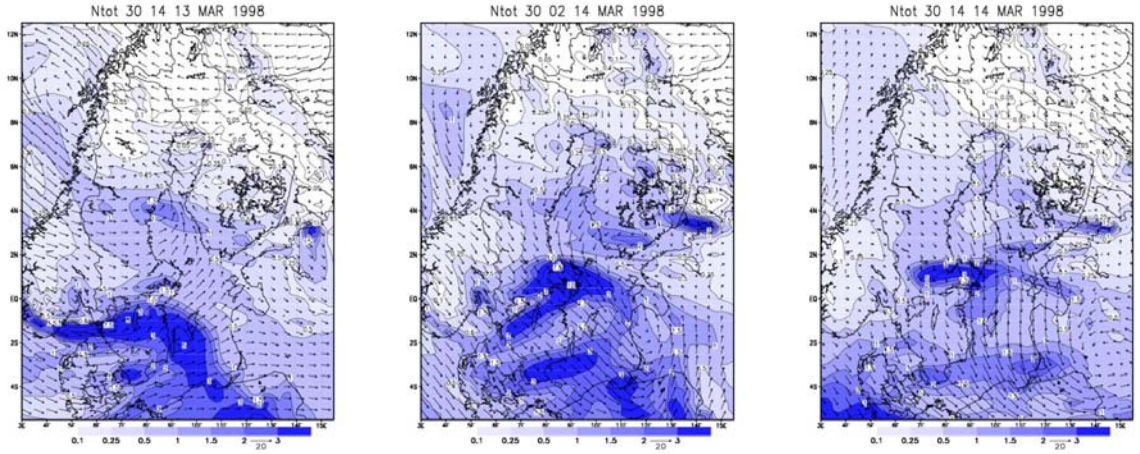

Fig. 21. At the end of the wintertime Lagrange period, LRT total nitrogen compounds originating from south-western areas stayed in the air even though the wind direction changed.

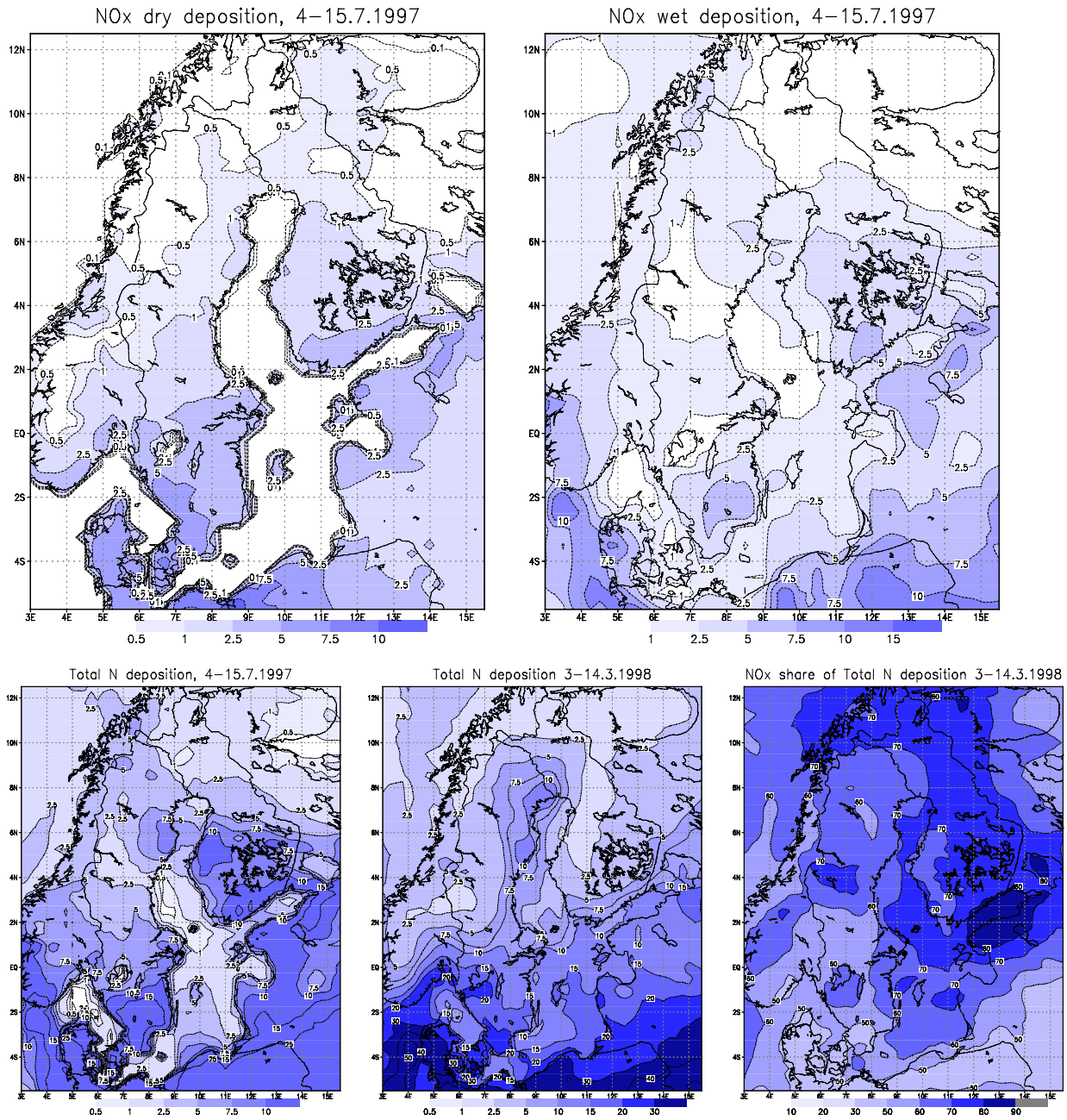

Fig. 22. Deposition of total nitrogen in the summer and winter Lagrange experiment

5.7 Quantification of the alkaline deposition load from Estonian industry

For estimating the transport of the alcaline dust from the Estonian and Slantsy oil shale industry area to Finland, a specific dust model, based on the old Hilatar version developed for former Soviet-Estonian projects in the 1990's, was constructed. It uses the new HIRLAM fields of 0.2° (around 22 km) horizontal resolution, with an updated meteorological pre-processor and sink terms. The plume rise equations for particles are those derived for buoyant hot gases, thus the nocturnal effective stack height may be too high for dust. During daytime the error is small, because anyway the emissions are mixed even higher due to convection.

Dust emissions from the county of Idä-Viru in Estonia have decreased from 179 kt in 1990 to 78 kt in 1996 and further to 50 kt in 2000 (Kallaste et al., 1992; Statistics 2001). In 2000, the Lääne-Viru emissions amounted to 820 t, including the Kunda Nordic Cement Ltd. factory emissions, which alone exceeded 82.6 kt in 1990. Oil shale is also used in Russia in the vicinity of the Estonian border. The Slantsy emissions, around 65 kt in 1990, were of the same magnitude as the former Leningrad dust emissions (Pöyry, 1990). Both emissions have decreased in the 1990's by an unknown amount. For the simulations, a dust emission intensity estimate for 1999 of 1110-1170 g s^{-1} for the large Estonian power plants was used. With an 85 % utilisation rate this would correspond to the official annual emissions of 65 kt dust, with a 6 % share being from small sources. For St. Petersburg and Slantsy an emission of 500 g s^{-1} was assumed (N. Goltsova and M. Kaasik, personal communication), which might be slightly high.

The stack heights of the Estonian Power Plant are 250 m, and of the Baltic Power Plant 160 m. The effective plume rise was estimated using the Briggs plume rise formulae and the statistical dimensions of the plume at a distance of 5 km from the sources.

The gravitational settling velocities v_g and dry deposition velocities v_d of the particles are highly size-dependent. Over sea areas, v_d is around 10 times larger for 10 μm than for 1 μm particles, and v_g varies between 0.0035 - 0.305 cm s^{-1} for particles with diameters of 1-10 μm and density of 1 g cm^{-3}. The small particles have much longer transport distances. For model-measurement comparison the annual depositions were first calculated for particles of 1, 2.5, 5, 7.5 and 10 μm diameter, for each class separately.

According to Aunela et al. (1995), the average diameter of the dust particles from the Estonian power plants is around 10 μm and only 25 % of the mass resides in particles with diameter below 7.5 μm. Thus, a diameter of 10 μm and the corresponding sink terms were used in the final simulations. When one assumes that the Ca content in the deposition is the same as in the emissions, i.e. 20 %, the Calcium originating from the Estonian and Slantsy dust emissions in 2000 and 2001 takes the form presented in Fig. 23.

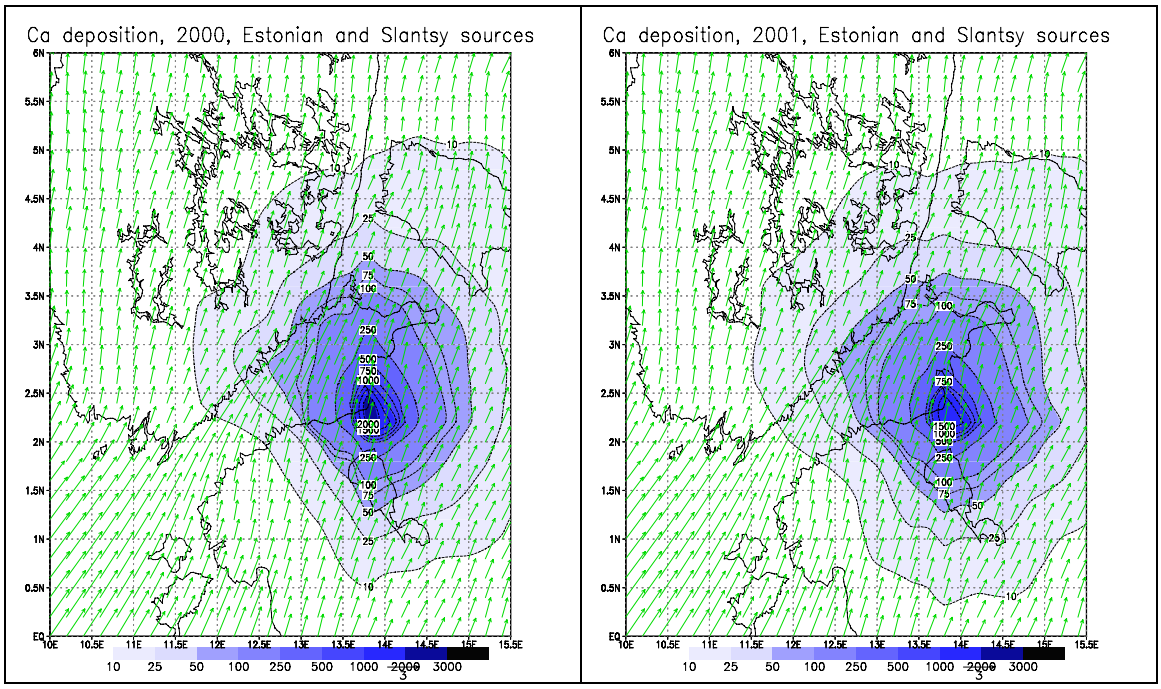

Fig. 23. Ca deposition caused by the Estonian and Slantsy dust emissions in the years 2000 and 2001, mg(Ca)m^{-2}

The simulated deposition is compared to the monthly Ca wet deposition at the coastal stations of Virolahti and Utö in Finland, in 2000 (Fig. 24). Around half of the annual deposition, during winter months an even higher share, can be explained by the Estonian and Slantsy emissions. The Virolahti station lies at the corner of a grid square and the gradients are rather sharp, thus the average deposition of four grids is used in the comparison.

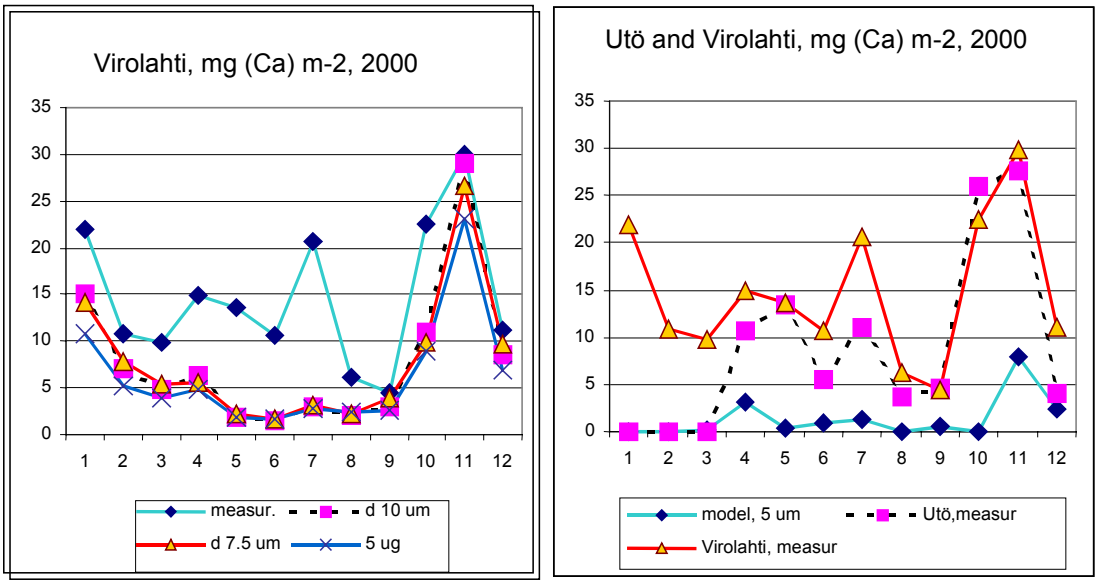

Fig. 24. Comparison of the monthly wet deposition of Ca from the Estonian and Slantsy sources with the Virolahti measurements, mg (Ca) m^{-2} $month^{-1}$ in 2000, assuming different particle diameters (5, 7.5 or 10 μm) for the emissions.

During summer, the Estonian emissions represent only a small fraction of the measured deposition. Finnish anthropogenic Ca emissions were around 12 500 t in 1987, although the error marginal in this figure is high (Anttila 1990). According to more recent emission estimates (Jalkanen et al., 2000; Lee & Pacyna, 1999) the present anthropogenic emissions are at the same level as they were in 1987. Natural emissions are high. The erosion and resuspension of Ca-containing particles depends on the chemical composition of the ground and ploughing times of the fields. In the late 1980's, around 1 Mt $CaCO_3$, with a total Ca amount of around 400 000 t, was used for the liming of fields. Vegetation also contains Ca, and it, together with pollen, can find its way into wet deposition containers. The Ca content of needles is 0.12-0.27 % and of sea salt particles 1.16 % (Anttila, 1990). Virolahti is also a mining area, and the possible transport of dust from open quarries to the air quality gauges remains to be estimated. As the station is surrounded by fields and is situated in the vicinity of a house, a cowshed and an uncovered road, a rather high share of the summertime Ca deposition may have a local natural origin.

5.8 Estimating the origin of pollution episodes

5.8.1 Storms in August 2001

The model's capability of monitoring air quality operationally has been assessed e.g. by studying concentration and deposition patterns in stormy conditions (Hongisto, 2001). In August 2001 a rather exceptional storm (17-28.8) brought to Finland, in addition to downpours of rain, a deposition rich in nitrogen and sulphur compounds. The precipitation zone was connected with a low-pressure centre that moved slowly from Southern Scandinavia towards the Baltic States. The south-easterly flow over the Gulf of Finland increased, with the wind finally exceeding the storm threshold, 21-22 m s^{-1}. The flow was typical for the season, i.e. very warm and moist, which increased the frontal rain near the Finnish coast.

A rather narrow but strong precipitation zone aligned from south-east to north-west moved over Southern Finland. The Hilatar model estimated that 35 % or even more of the monthly total deposition was received in this zone over the Northern Baltic Proper within 12 hours. The surface wind over Southern Finland blew directly from the industrial areas located in north-eastern Estonia, so it would have been natural to expect that those emissions would have contributed to the deposition. However this was not the case: by dynamic simulations it was shown that the measured deposition was of Central-European origin.

The episode started to develop over Central Europe on 26.8, when hot and moist maritime air was carried from the direction of the English Channel eastwards, generating an inversion over the Northern Central-European industrial areas. The mixing height decreased and surface winds calmed over an area including e.g. the Black Triangle region. Local concentrations reached high levels also because dry deposition decreased in the stable ABL and there was no rain near the source areas. Pollutants generated during the episode circulated over the Baltic States and the Baltic Sea Proper towards the north, and were then scavenged down within the front connected to the low-pressure system. The episode is illustrated in Fig. 25.

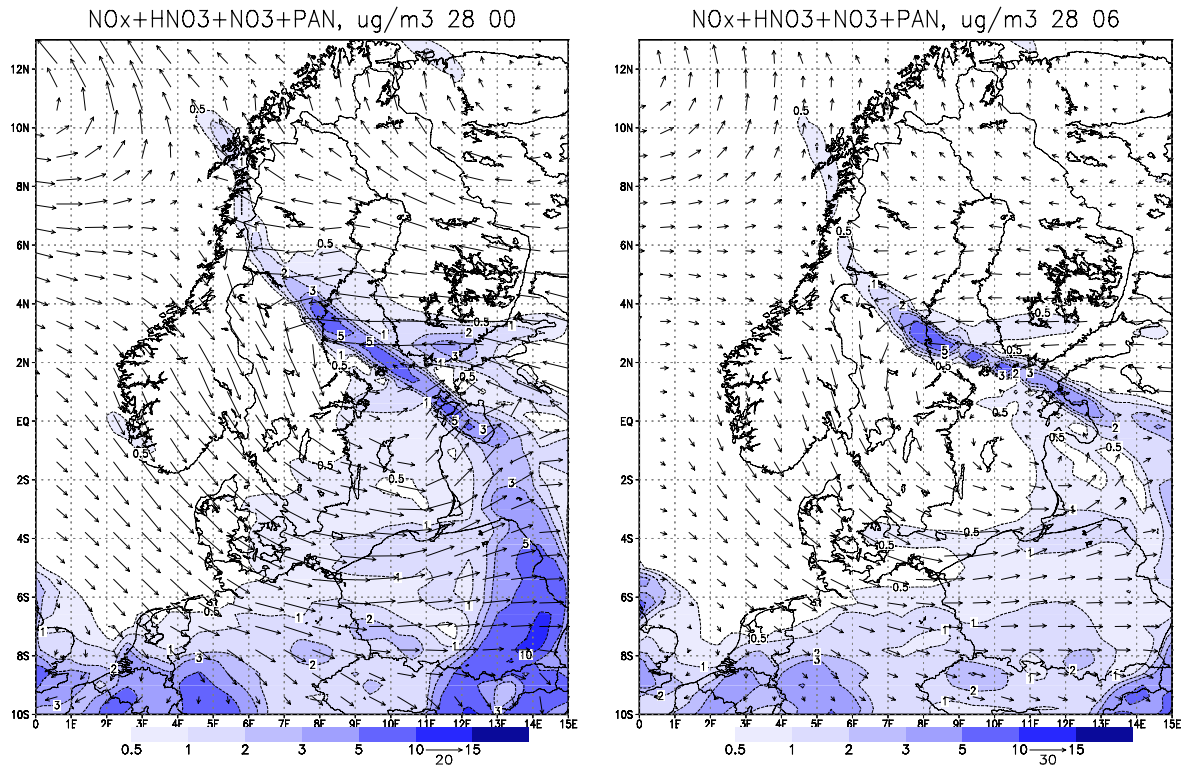

Fig. 25. Modelled NO_x, HNO_3, NO_3 and PAN surface concentrations, µg m^{-3} 26-28.9

From this episodic study it was concluded that for understanding the origin of deposition events, local meteorological fields or measurements of surface concentrations do not provide the answer. LRT is a wide-scale chain of physico-chemical events: the situation can originate far away, with the conditions for the episode starting to develop several days earlier. It also seems that the Hilatar model is capable of estimating the origin of pollutants, and would be a valuable tool in operationally forecasting air pollution and deposition in Finland.

5.8.2 Dust episode in September 2001

During a rather long period, from 17th to 24th September 2001, high concentrations of particulate matter were observed at more than 10 monitoring stations along both coasts of the Gulf of Finland, in Stockholm and in Uppsala (Aarnio et al., 2001; Tervahattu et al., 2002). However, high PM_{10}-levels were not registered at inland stations in Finland or north or south of Central Sweden. The situation was analysed by the Hilatar model, but because the published report is written in Finnish it was not included in the list of papers for the thesis. However, the results are discussed here as they are important for evaluating the model's capability to forecast episodes.

The episode started to develop when a rather strong Siberian blocking high remained in almost the same position for more than one week. With the continuing flow along its southern flank, very warm air was transported from the semi-arid Central-Asian areas towards Fennoscandia. North of the Black Sea this flow met another warm stream originating from the Mediterranean and North African areas. The warm air

layer over Finland was exceptionally deep, and in Central Finland and the Oulu district temperature records were broken (Ilmastokatsaus 2001).

When the warm front reached the neighbourhood of Finland, the ABL in Estonia, St. Petersburg and the Leningrad region became stable. The HIRLAM ABL height dropped locally to below 50 m. The nocturnal inversion and signs of a low-level jet were detected at the Kivenlahti mast west of Helsinki (the maximum wind velocity exceeded 30 m s^{-1})

In a case like this, low-level jets (LLJ) are believed to be caused by an inertial oscillation in space when relatively warm air flows out over colder water or when the land cools and becomes stable (Källstrand, 1998, Bladackar, 1957). Over the Baltic Sea such cases are normal in spring and early summer when water-air temperature differences of up to 15-20 ^{o}K are not unusual (Smedman et al., 1996). The lowest 100 m of the MABL of the Baltic Sea is probably stably stratified during 2/3 of the year. LLJ's may also be caused by synoptic-scale baroclinity, fronts, land and sea breeze (Savijärvi & Alestalo, 1988) and advective accelerations. In Doppler radar observations, low-level jets can also be found in connection with every front crossing Southern Finland (on average every second day, something which may cause significant errors in dispersion studies, according to Kaurola et. al. (1989) and Kesti et al. (1989). Low-level jets or jet-like wind profiles have frequently been detected in spring along the Baltic Sea coast in several field campaigns (from 48 % to 2/3 of the measured profiles, Källstrand, 1998).

During this episode, according to the Kivenlahti measurements, the nocturnal wind direction turned by 50-55^{o} to the east between heights of 26 and 327 m; during the daytime the corresponding wind veer was 29-38^{o}. In the Northern Hemisphere the wind direction turns clockwise, i.e. veers with height as a result of the pressure gradient, the Coriolis force and surface friction. The turning angle increases with the strength of the inversion. In a stable situation the difference between the geostrophic and the surface wind is 30-50^{o} (Hanna et al., 1982).

The predicted HIRLAM wind direction did not change as much with height near the surface. The HIRLAM wind direction (at z=1, ~31 m) deviated from the Haapasaari (Kotka) measurements by 43-20^{o} between 02 and 20 hrs on 18.9, and from the Rankki (Kotka) measurements by 82-54^{o}. The difference decreased along the coastal measurement points towards the west and was almost undetectable at Turku. At the grid point corresponding to Kivenlahti the nighttime difference between the measured and forecast wind direction was 20^{o} at a height of 140 m, and 40^{o} at 330 m. HIRLAM predicted the maximum direction change to occur higher, between 600 and 900 m or even just below 1300 m. The daytime difference between the modelled and measured directions was smaller.

Simulation results

The origin of the measured concentrations was first estimated by backward simulations. The magnitude of the concentrations in the four lowest model layers at the Turku, Kotka and Helsinki grid-points was fitted to the measured values during the episode, no emissions were allowed and the weather and other parameters were read in

reversed order from the direct access files. The aim was to eliminate the grid-size effect and uncertainties in the calculation of the effective plume height, and to directly estimate the origin of the particles and their dilution due the model structure when crossing the sea area. The results show that both the Helsinki and Turku concentrations were transported from over the Narva region by the low-level winds, while the Narva dust plume reached Kotka if the winds at level z=4 (around 600 m) are used. Daytime turbulence conditions near Kotka were strong, so dust transported to the area by upper level winds could have been mixed down.

To further identify the source areas, forward simulations were made first for the Estonian sources (Estonian Power Plant, Baltic Power Plant and 6 minor sources in the Idä-Viru and Lääne-Viru counties), and then also taking the poorly-known Slantsy and St. Petersburg emissions into consideration. The principal transport height of the Estonian high stack emissions over the Gulf of Finland was level z=3 (335 m). In the emission grid the dust was only mixed down to the surface at noon and in the afternoon, otherwise the plumes stayed above or inside the inversion layer. Mixing down occurred, however, in the morning too, on the Finnish side of the Gulf. In comparison to measurements the modelled concentrations were underestimates, although the dilution of the plumes over such a stable sea should be minor. In the model, this might be caused by the artificial dispersion produced by the advection algorithm for diagonal winds.

When the Russian sources were taken into account, the modelled surface concentrations were closer to the measured ones, because the Slantsy stack heights are low. The simultaneous rise of the concentrations on both the northern and southern coasts of the Gulf of Finland on 18.9 after noon is presented in Fig. 26. The flow was channelled, the high-level Estonian plumes thus meeting the flow originating from St. Petersburg over the Finnish coastline, while the low-level emissions also remained for a while above Estonia. It seems that all emissions located between Narva and St.Petersburg could have been contributed to the increased concentrations at the Finnish coastline.

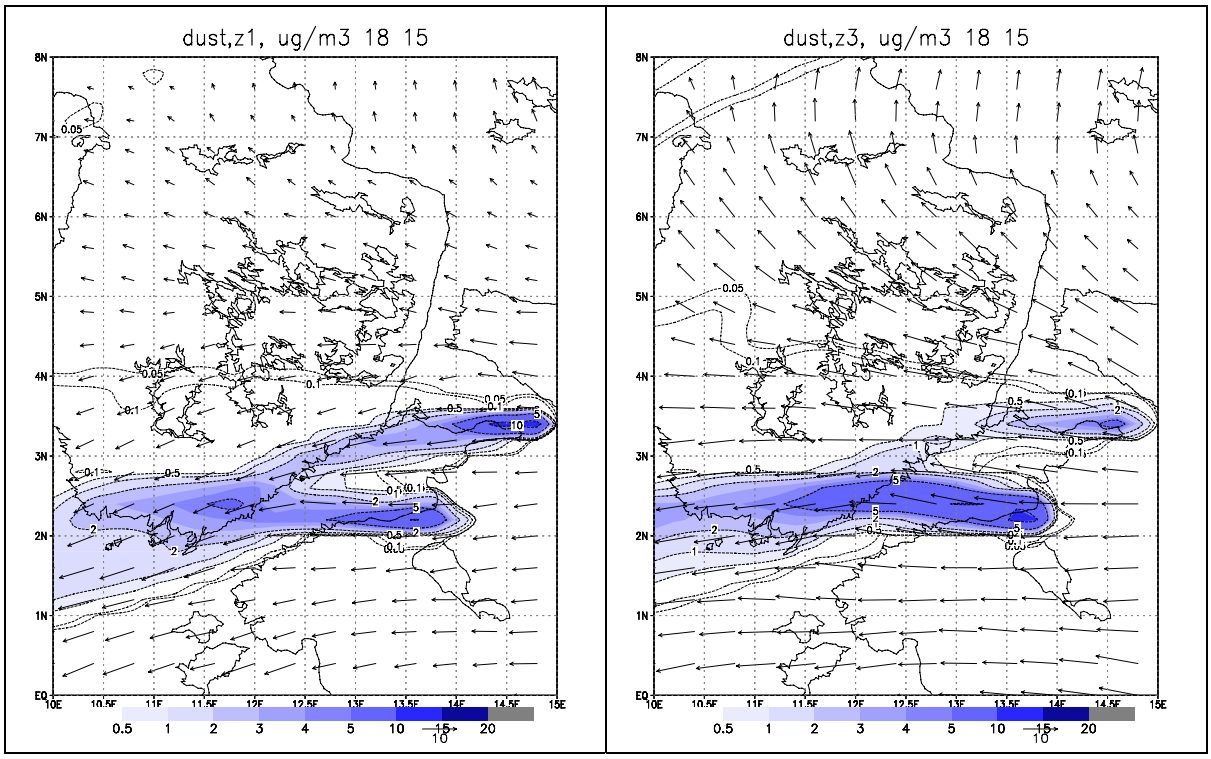

Fig. 26. Modelled dust concentrations from the Estonian, Slantsy and St. Petersburg sources at levels 1 (~31 m) and 3 (~335 m), 17.00 18.9. 2001

Because the measured dust concentrations were higher than the simulated concentrations, and such a significant rise in the SO_2 concentrations, emitted also by the Estonian power stations, was not detected, also other dust source areas along the backward trajectory from the measurement places could have been contributet to the episode. For this reason, the simulation area of the dust model was extended to cover the whole of Europe. Simulations with various artificial sources, put on it's eastern border, confirmed, together with analysis of the meteorological maps (DWD 2001a), that the fine dust collected detected on the particle surfaces was most probably coming from the Ryn Peski desert in Kazakhstan. In that area the annual precipitation amounts to 100-200 mm, summers are hot and evaporation strong (Clim, 1981). During the year 2001, the precipitation in July-September was 25-50 % from the average 1961-1990 reference period value, in August 2001 below 25 % (DWD 2001b). The area had been suffering from drought. 16th of September was also rather windy. Unfortunatelly, Ryn Peski is located outside the European simulation area, thus no real simulation results can be presented here.

The composition of the Kotka and Helsinki samples, analyzed by the SEM/EDX (scanning electron microscope coupled with an energy dispersive X-ray microanalyzer, Tervahattu et al., 2002) was similar to the results of the similarly analysed earlier reference samples collected near Narva and Kunda. But, those particles were analyzed on needels collected in a dry pine forest, and could also contain a small crust component (Tervahattu, personal communication). The chemical composition from the episode samples deviated slightly from the Häsänen et al. (1997) samples, collected at the time when Kunda and oil shale power plant emissions were much higher.

A simultaneous analysis of the particulate matter collected by the impactors at the FMI site at Herttoniemi, Helsinki (high Ca content and elevated potassium concentrations in the fine fraction), indicate an Estonian origin for the particles. Increased concentrations of many toxic elements (Cd-, Cr-, Pb- and As in the $PM_{2.5}$–fraction, Al and Fe in coarse particles and Mn in both fractions) in the samples were also typical of the Narva emissions (Häsänen et al., 1997, Jalkanen et al., 2000, Teinemaa et al., 2002). V and Ni concentrations, indicating emissions from oil-fuelled combustion, were not detected. Many particles were spherical, typical of emissions from fuel combustion, with very small, propably long-range transported particles condensed on their surface, could clearly been identified on their surface.

Observed nitrate concentrations were higher in the coarse fraction. This may be caused by the interaction of gaseous nitric acid with particles. HNO_3 may react with, in addition to sea-salt, soil-derived particles (Pakkanen, 1996; Pakkanen et al., 1996; Song & Carmichael, 1999). During episodes with Ca-rich particles, $Ca(NO_3)_2$ is formed in the reaction of nitrate and Ca-compounds on the surface of the particles.

Conclusions to be drawn from the September 2001 dust episode

According to the model simulations, the source for the episode could have been situated, in addition to in Estonia, in the zone between Narva and St. Petersburg and even further away. The large-scale weather analysis shows that the exceptionally warm air transported over the semi-arid areas north of the Caspian Sea could have been contained also suspended fine matter. This matter could have been condensed on the surface of the dust particles emitted in Estonia and Russia. In the SEM images, such condensed matter was also detected covering the spherical particles normally created in combustion. The diameter of the particles would have been increased, placing most of the particles in the coarse fraction. A parallel biological analysis, carried out at Helsinki University, supports this hypothesis of LRT from more distant areas. This LRT event could not be simulated because the suspected desert is located outside the simulation area. However, the Hilatar model area is smaller than the HIRLAM or ECMWF weather prediction areas, thus for such long-range transport studies the geographical coverage of Hilatar can be extended in the future.

From the preceeding example, it can also be concluded that if there had been any radioactive releases at the graphite-moderated Sosnovyi Bor nuclear reactor during such a meteorological situation, it would have been difficult to warn people in Southern Finland in time. The Estonian and Russian plumes remained narrow, the transport time was short and the whole coastal zone was exposed. The weather model was unable to detect the low-level jet that most probably existed, the modelled turning of the wind occurred at too great a height, the wind velocities were too low and diagonal advection very effectively smoothed the highest peaks in such a stable situation. Although those fine-scale phenomena were lost, dynamically the transport over the stable marine sea area and mixing along the coastline seemed to be well described.

6 MAIN CONCLUSIONS AND FINDINGS

In the work for this thesis, several models with grids of 0.1-0.5^{o}, together with their pre- and post-processors, were constructed. The models were nested with the EMEP MSC-W trajectory model, the European Hilatar model and the European ADOM model for heavy metals. The models were used in estimating the long- and short-range transport of atmospheric pollutants over several years. Model results and their dependency on various factors were analyzed.

Over the NMR domain, the period average deposition distributions have the expected north-south gradient, superimposed on a west-east gradient for sulphur due to the north-western Russian sources. The share of the dry N deposition was highest in summer in Southern Sweden and on the Danish islands (exceeding 50 %), due to high summertime ammonium emissions.

The decreasing emission trend could not be seen in the NMR domain N-deposition since 1993, although a slight average decrease in S-deposition was indeed detected. The annual regional variation was affected more by the prevailing meteorological conditions.

No concentration trend was detected, the concentrations of individual compounds over a specific geographical area seeming to depend on the meteorology: precipitation, the prevailing wind direction relative to the main source areas, cloudiness and the availability of reactants. Modelled critical values for SO_2 (a wintertime average of 20 μg m^{-3}) were not exceeded in the Nordic countries; however they were exceeded, especially in winter 1996, over large areas of Central Europe. Critical concentrations of NO_2 (30 μg m^{-3} as an annual average) were not exceeded during these years in any background areas.

Annual deposition fluxes of oxidised and reduced nitrogen to the open Baltic Sea area over the period 1993-1998 vary in the ranges 140-180 kt NO_x and 100-120 kt(N) NH_x. No decrease during the period up to 2001 has been observed. Short and long-term time-variations were significant. The total nitrogen deposition depended strongly on the climatological conditions prevailing over Central and Northern Europe. Inter-annual differences in wintertime deposition depended on the frequency and latitude of the cyclone tracks and the co-occurrence of south-western winds with precipitation events.

Nitric acid changes the chemical composition of natural sea salt particles. The BASYS summer network study revealed that 40 - 70 % of the chloride in sea salt is replaced by nitrate. During the BASYS network campaign the model underestimated the measured HNO_3 concentrations over the coastal stations, while over the land stations the modelled HNO_3 and HNO_3+NO_3 concentrations always exceeded those measured. HNO_3 reacts with NaCl, and the resulting conversion product particles ($NaNO_3$) have a stronger sink to the Baltic Sea than is parameterized in the current models. This might be the missing sink of nitrogen in all acid deposition models. The chlorine released from the sea salt particles is also important, because it influences the ozone cycle over coastal areas. The reason for the observed high O_3 concentrations at coastal stations, traditionally explained by a decreased sink due to dry deposition over water, might be partly wrong.

The deposition over the Baltic Sea is not geographically homogeneous. In a general sense, it decreases northwards, while increasing eastwards over water. During autumn and winter, the deposition increases towards the open sea, while during spring and summer it decreases. Depending on the season, wind direction, and intensity of emission density of the area, coastal measurements can either over- or under-represent the open-sea load.

6.1 The model's capability to predict loads and concentrations

One of the main goals of the thesis work was to construct a model that can be used in operational numerical monitoring of various air pollutants in background areas. To fulfill this goal, the model performance has been carefully evaluated by verification of the program codes, parameterisation and numerical methods, by model-model inter-comparison and by comparison of both long and short-term concentrations in air and precipitation with measurements.

The ability of the Hilatar model to describe the dynamical transport and dispersion of contaminants by atmospheric eddies, frontal patterns as well as in and below-cloud scavenging is highly dependent on the accuracy of the HIRLAM fields. The spatial resolution should be at least 0.1^{o} in order to capture, at least to some extent, the sub-grid phenomena, such as the sea breeze or high coastal gradients of precipitation. The chemical package should also contain more species and reactions. The unknown amounts and timing of some natural or biological emissions may also affect the model results.

When, for comparison, some ABL parameters were calculated using data from three sounding Finnish stations, HIRLAM profiles gave lower mixing-height values. This was also the case when the BASYS Lagrange experiment soundings were used. HIRLAM generally overestimated precipitation at coastal sites, although, the grid average precipitation cannot be compared directly to local measurements. Rain is sensitive to local factors and it can have a coastal gradient whose direction varies seasonally.

Model-measurement inter-comparisons, both with BASYS field campaign results and long-term EMEP measurements, demonstrated a rather good description of both the spatial and temporal characteristics of the S and N pollution in the Baltic Sea region. During selected episodes, the model did not explain all the measured fluctuations, because both the input measures and the values of the results are grid averages, which are not always expected to follow point measurements.

Errors connected with numerical methods are small. Time-splitting, however, results in horizontal numerical diffusion, especially during diagonal advection, which is greater the lower the grid resolution is. This means a levelling of pollution peaks and an increasing background level in clean areas. The coarse resolution both in the model's vertical grid and in the input data also increase inaccuracy.

The model fails to explain the high NO_x concentrations at coastal stations, indicating the weaknesses in the Baltic Sea ship emission inventory, the importance of the

missing sea salt reactions and inadequacy of the theoretical description of the MABL. The MABL does not obey the Monin-Obukhov laws if the waves and the wind have different directions, which is the normal case over a wave surface (Smedman et al., 1999, Drennan et al., 1999). The mixing height over water can also be extremely low, something which cannot be described with the vertical resolution of the meteorological input data. Low-level jets are common over areas with large temperature differences, as over the stable cold sea in spring when the wind blows from warm southern areas. The change in wind direction with height, e.g. during the strong inversion conditions of the episode in September 2001, was 20-40^{o} less at a height of 140 and 330 m in HIRLAM than that observed; the turning was modelled to occur at higher levels (Tervahattu et al., 2002). According to measurements, the coastal wind also often blows against the forecast direction, because the sea breeze is ignored in meteorological models with low resolution (Källstrand et al., 2000).

The marine fluxes can be bi-directional: depending on the concentration difference between the air and the water, the ammonium flux is either directed upwards or downwards (Asman et al., 1994, Barrett, 1998). This is common for CO_2 and several compounds. For example, during both the summer and winter BASYS measurements, the sea water was supersaturated with Hg, and its flux was directed upward (on average by close to 20 ng Hg m^{-1} day^{-1} in both winter and summer (Brorström-Lunden et al. 1999).

The model tends to underestimate NO_x and overestimate NO_3 and HNO_3 concentrations. During episodes, this is a consequence of the dilution, both initially and horizontally, of sharp peaks during advection; it may also be due to chemical conversion rates that are too high. For background values, this is the result of a zero non-European contribution and missing natural emissions.

The model can also be used in identifying source areas of unknown episodes by backward simulations. The grid concentrations at the measurements points are fixed to the monitored values, the wind direction should be reversed and the meteorological data read in the reverse order. The study of the September 2001 episode is the first case in which an Eulerian model has been used in such a way; it gives all the information a normal trajectory analysis provides, and additionally takes into account dispersion during transport.

An increase in the frequency of atmospheric blocking events, which set up persistent weather patterns that last for weeks to months at a time, defined in terms of large positive 500 hPa geopotential height deviations from the corresponding latitudinal mean, also decrease forecasting capabilities, because blocking is not a normal solution to a dynamical flow problem. The WMO time series for 1949-1993 suggests a tendency for an increase in wintertime blocking intensity and duration in the Atlantic-European sector (Philips, 1995), accompanied by warmer and drier winters in the latitudinal zone 40-70^{o}N and conditions that are colder and wetter than normal both south and north of the blocking.

6.2 Significance of the atmospheric load for the eutrophication of the Baltic Sea

One of the goals of this thesis work was to calculate quantitative estimates of the atmospheric N load to the Baltic Sea, and study its variation. However, the significance of the load on a system which already seems to be badly eutrophied (Chapter 2) has to be discussed in the context of the work of other scientists in the BASYS project. The ultimate question arises: how can we prevent the further eutrophication of the Baltic Sea?

Between 1950 and 1970 the nitrogen and phosphorus loads to the Baltic Sea increased by 3- and 5-fold, respectively (Dahlgren & Kautsy, 2002 and references therein). Since the 1950's the N:P ratio has changed from ~6 to ~9 (in 1999). Thus the nitrogen limitation for primary production has become somewhat less severe. Since 1970 the fluvial loads have varied mainly due to runoff changes, whereas the atmospheric nitrogen input has still been increasing. The concentrations of total P and N in the open Baltic Sea have increased accordingly, with some delay. The strongest increase was observed some 10 to 15 years after the drastic rise in loads, and concentrations remained constant throughout the eighties. Both airborne and riverine loads from the former Soviet countries decreased after 1990. However, little to no changes have been observed in concentrations in the sea during the nineties. Thus, the response of the biogeochemical cycles in the Baltic Sea to the changing external load has not been linear (Zuelicke 1999).

The summertime nitrogen fixation by blue-green algae in the Central Baltic Sea, 1540 – 1820 mg N m^{-2} a^{-1}, constitutes an external N source of the same magnitude as the land runoff to the Baltic Sea Proper (1,500 mg N m^{-2} a^{-1}). New production based on available nitrogen has increased from about 110 to 340 mg (C) m^{-3}, and the potential primary production of the cyanobacteria based on available phosphorous – after nitrogen depletion – has risen by 50% from about 200 to 295 mg (C) m^{-3} (sub-project (SP) 1a, SP2, Zuelicke 1999)

The occurrence of the cyanobacteria blooms in summer has been related to increased anthropogenic fertilisation of the Baltic Sea. However, blue-green algae are some of the oldest biological cells in the world, already existing 4-3.5 G-years ago (Kakkuri & Hjelt, 2000). Indications of intensive blooming already 7000 years ago have been detected in the BASYS project (Zuelicke, 1999). Blue-green algae growth is strongest in the Baltic Sea if the water temperature exceeds 16 ^{o}C (Kononen & Leppänen, 1997). They can benefit from increased temperature and decreased visibility conditions. The growth of the populations starts in the deeper layers, where they can stand lower visibility conditions than green algae. Blue-green algae can use both organic nitrogen (amino-acids) and carbohydrates, and can grow in conditions where light becomes the growth limiting factor.

The effects of HELCOM nutrient reduction scenarios were studied within BASYS SP 8, running a 1D multi-basin model over a 20-year period with 50 % reduced N and P inputs. Budget calculations showed that only about 10 % of the N-demand and 3 – 4 % of the P-demand of the primary production is supplied from the land. This means that eutrophication is largely driven by nutrients that have already been accumulated in the system. Thus, reactions to load reductions were found to be very slow. Considering the entire N-limited Baltic Proper, N-reduction alone would be largely compensated by

strongly increased N-fixation. Simultaneous reduction of N and P would reduce nitrogen fixation, but total primary production would not be much reduced even after 20 years. The most effective measure appears to be the reduction of P alone; however, the system still remains N-limited after 20 years (SP8).

It is difficult to come to firm conclusions on the role of the atmospheric load. Also the budget calculations, presented in Table 2 for the Baltic Proper, show that the external nitrogen load (here in the form of dissolved inorganic nitrogen DIN) needed to produce the total annual PP, is only a fraction of the nitrogen needed. Every N molecule is used several times, although there are some seasonal differences in the cycling of nutrients and deposition amounts. Nitrogen fixation is a significant N source. According to BASYS SP2, SP5 and SP8 results, nitrogen fixation constitutes about 23 % of the vernal new production, the same magnitude as the land runoff. Most of the sedimented matter is produced during the vernal bloom, while biological activity is low. During the summer, recycling is efficient, only about 10 % of primary production being lost by sinking from the euphotic zone: 90 % of the PP is thus sustained by nutrient regeneration. Part of the recycled N may come from newly-fixed dinitrogen by decay of cyanobacteria. Stable isotope investigations of sinking material have revealed that up to 50 % of the nitrogen deposition to the seafloor can be derived from fixed nitrogen (SP2, Zuelicke 1999).

Marine scientists are still discussing the magnitude of the external load. For example, in the budget calculations of Eilola & Stigebrandt (1999) it has been argued that dissolved organic nitrogen (DON) is also a significant source of nitrogen for primary production: both bacteria and phytoplankton can use DON and DIN simultaneously for growth. According to Eilola & Stigebrandt (1999), P is the limiting factor for springtime PP over the Baltic Proper. DIN is not accounted for in the budget, Table 2.

Table 2. Budgets for the Baltic Proper.

total annual PP	20-30 Mt C yr^{-1}	100 g C m^{-2} yr^{-1}	
N-requirement	3500- 5000	kt N yr^{-1}	
N fixation	130-390	kt N yr^{-1}	(Larssen et al., 1999)
run-off from land	200	kt N yr^{-1}	(HELCOM, 1996)
atmospheric load	180 kt (155-200)	kt N yr^{-1}	(this work, Schulz et al., 1999)
total external	485-790	kt N yr^{-1}	
additional turning of bottoms to anox state, release of N in 1994/1995 Gotland Basin	316	kt N yr^{-1}	

According to BASYS, the response to external load reductions is different near shores. There, P is often the growth-limiting nutrient, a situation which changes gradually to N limitation further offshore. Thus there may be some feedback from the offshore systems to most coastal systems. According to Sarkkula et al. (1998), the land-based loads (riverine, municipal and industrial) and their reductions have a clear, straight-

forward effect on nutrient concentrations and phytoplankton biomass in coastal waters. The effects are seen soon after the load reductions (within a year).

According to BASYS, the observed changes in nutrient concentrations are connected to climate variability. If no salty water pulses occur, the deep waters suffer from oxygen deficiencies, leading to nutrient releases from the sediments. During the switch from an oxic to an anoxic condition in the Gotland Basin in 1994/1995, dissolved inorganic P and N increased almost instantaneously by 2 and 3.3 mmol m^{-3}, respectively, in the water column 100 m above the bottom, with a further rise thereafter. This is equivalent to a release of 6.2 t P and 4.6 t N per km^2 of sediment area becoming anoxic – the total release being 17800 t P and 316220 t N a^{-1} (SP1a). After several years of deep-water anoxia, the concentrations of inorganic dissolved P and N increase 3.5 and 8-fold, respectively, which may lead to elevated diffusive fluxes into the upper layers. In the late seventies, when the nutrient concentrations in the open Baltic Proper rose from about 0.25 to 0.5 mmol m^{-3} (DIP) and from 1.5 to 4.9 mmol m^{-3} (DIN), this rapid increase coincided with the reduction of saltwater intrusions from 13 events every 10 years to 4 events since 1976/77.

The nutrients accumulated on the sea bottom are not all available for new production. At least over the most eutrophied areas, the Archipelago Sea and the Gulf of Finland, they are available on those occasions when the vertical exchange reaches the bottom. However, approximately 2/3 of the Baltic Sea floor situated above the halocline, are swept by currents and waves resulting in little to no deposition of organic matter in the sediments near shore-areas. A large portion of the deposited matter is transported into the deeper areas, the Arkona, Bornholm and Gotland Basins, as well as into the Gdansk Deep. According to BASYS SP 3 and 4, the deeper parts of the Baltic Sea are the main dumping grounds for organic-rich matter from natural and man-made sources.

Marine concentrations also depend on the sink processes, which are rather poorly known. Denitrification, by which molecular N_2 is released back into the atmosphere, is the most important sink for N in the Baltic Sea. Only 15 % of the external N load is exported to the North Sea, and for the entire Baltic Sea on average 18 % of it is buried in the sediments. The N loss via denitrification, estimated by budget and models, accounts for about 70 %. However, measurements have yielded only about 30 % (Zuelicke, 1999). Denitrification is caused by living organisms, and is fastest in well-oxidised conditions; the settling of detritus on the sediment surface decreases the rates considerably (SP3b). Areas where increased amounts of organic matter are accumulating are the most susceptible with regard to loss of potential denitrification in the Baltic Sea. According to Zuelicke (1999) large parts of the Gulf of Finland are on the verge of loosing this potential (SP3b).

The significance of the atmospheric load is different in each sub-basin due to the different magnitudes of the riverine and dispersed loads from the land. In the following, the ratio of atmospheric to riverine load in the different basins is summarised.

Gulf of Bothnia

The nitrogen load from rivers and the direct discharges of coastal municipalities and industries at the beginning of the 1990's was 38 kt N to the Bothnian Bay, and 47 kt N

to the Bothnian Sea (HELCOM, 1996). Additionally the river load to the Archipelago area was 9.9 kt N. For comparison, the Hilatar-calculated atmospheric load was around half of the sum above, 38/35/38/38/32/42 kt N in 1993-1998, respectively. The oxygen content of the deep basins is decreasing. However, the situation is not alarming, and no internal releases from the bottoms due to non-oxic conditions have occurred (Rönnberg, 2001).

Gulf of Finland

According to Bartnicki et al. (1998), the atmospheric load to the Gulf of Finland decreased from 18 kt in 1992-1994 to 12 kt in 1997. This work provides values of 13.9/ 15.5/ 15.2 /12.8 / 12.3 / 14.1 kt in 1993-1998, respectively. The atmospheric share of the total external nitrogen input to the Gulf of Finland has been only 10-13 %. The simulated airborne load was the highest in the year 2000, exceeding 890 mg (N) m^{-2} yr^{-1}, 2.4 mg (N) day^{-1}, at the mouth of the Gulf, and decreasing eastwards. In comparison, however, the benthic fluxes from sediments measured on the August 1999 cruise in Finnish coastal waters were 8 – 37 mg (N) day^{-1} and 7.5 – 21 mg (P) day^{-1} (Pitkänen et al., 2001). If anoxic conditions develop, the internal release of nutrients can exceed the total external load.

Belt Sea, Kattegatt and the Sounds

The nitrogen load from rivers and the direct discharges of coastal municipalities and industries at the beginning of the 1990's was 130 kt N, while the atmospheric load was 40/43/36/34/39/45 kt in 1993-1998, respectively. However, in different reports the various sub-areas may have slightly different borders.

The Baltic Proper

Atmospheric deposition is especially important in the central basins, where the influence of river discharge and other sources is naturally smaller. The river and direct coastal load to the Baltic Proper has been around 210 kt (HELCOM 1996), depending on the weather conditions of the year. In this study, the atmospheric deposition was found to be 197/179/166/174/155/195 kt N in 1993-1998, respectively, of which 53-59 % occurred in the southern Baltic Proper.

The obvious changes in ship traffic emissions since 1990, the base year for the Baltic Sea ship emission inventory, indicate that the modelled geographical distribution of the nitrogen load is too low in the northern parts of the Baltic Sea. Account should be taken of the economic collapse of the former Soviet states and their changed structure upon recovery. At least 3 large new harbours have been constructed in the Gulf of Finland. During the BASYS project, when the calculated nitrogen concentrations were compared with the process study measurements (Sørensen, 1997; Sørensen et al., 1999), it was found impossible to reproduce the measured NO and NO_2 concentrations in spring, because then the MABL was very stable, the h_{mix} shallow, and the measurement site was located close to a ship route. The situation recurred during the summer Lagrange period (IVL measurements), and is continuously observed at the marine EMEP station of Utö near the Finnish Archipelago, which is affected in almost all wind directions by surrounding ship routes.

The springtime radiation levels over seas are high due to reflection from the sea surface. This might influence OH-radical levels, which in turn, when the MABL is shallow, could produce significant concentrations of HNO_3 downwind of the ship routes via the gas-phase reaction with NO_2. If springtime NO_2 levels really are generally as high as those measured at Östergarnsholm during the BASYS process study, the increased formation of HNO_3 over marine areas could partly explain the missing NO_3 sink from all European nitrogen models. Dry deposition velocity of HNO_3 is fast. With a v_d of 2 cm s^{-1} (a moderate estimate) and a surface HNO_3 concentration of 10 μg m^{-3}, the dry deposition flux to the surface exceeds 400 mg N m^{-2} mon^{-1} in July (18 hours of light /day). This is significant in comparison to the annual fixing rate.

Many uncertainties remain in the marine chemistry. We do not know, e.g., how much NO_2 is emitted from the ships, how close to the sea surface the plumes stay, how much and how rapidly HNO_3 is converted, what are the OH radical levels in the MABL, what is the role of wet chemistry if humid particles are in the air, how large the downward N flux is and what happens to the released chlorine. But we do know that 40 - 70 % of the chloride in sea salt is replaced by nitrate, and that this nitrate comes from HNO_3. The current measurement programs should cover a larger variety of compounds and fluxes in the vicinity of ship routes.

The timing of the atmospheric load to marine ecosystems is important. In winter atmospheris load is accumulated on ice. However, the release of nutrients from ice is not modelled in current marine ecosystem models although it could have at least some effect on the spring bloom.

Approximately 50% of the primary production (PP) in the Baltic Sea takes place in an area having a depth of between 0 and 10 m, which amounts only to ~10% of the entire Baltic Sea area. Because the summertime coastal gradients of the load are high, the atmospheric load over the productive shallow areas is also higher than in the open water areas.

7 FUTURE WORK

The construction of an operative version of the model that contains ozone chemistry is the most urgent task. The grid of the Hilatar ozone model has to be changed to the most recent HIRLAM grid (which will be 0.3^o in 2002), it's chemistry should be completed with aerosols, S, NH_x and Cl compounds, the QSSA method might need to be changed and the model has to be tested. For all air pollution prediction models, over Finland the resolution has to be further increased and the stack emission inventory has to be updated.

According to BASYS and MARE studies, eutrophication of the Baltic Sea is a serious problem that is hard to control over open water areas, since internal sources seem to be the most important factors feeding the primary production. In order to study the role of internal and external nutrient sources in eutrophication, a work project to combine Hilatar interactively with the hydrodynamic-ecosystem model FinEst (Tamsalu 1998)

is currently in the process of implementation. Hilatar results and the meteorological data base fields are already used off-line in the FinEst simulations.

In order to improve the description of chemical transformations in the marine atmosphere, current measurement programs should cover a larger variety of nitrogen compounds and fluxes in the vicinity of ship routes. Chlorine depletion and aerosol processes affect removal times and have, in addition to effects on coastal O_3 levels, climatic consequences. Additionally, meteorological field campaigns should be intensified in order to estimate the effect of waves on air-sea exchange.

If the model is to be used to forecast contaminant releases in emergency situations, both the horizontal and vertical resolution of HIRLAM have to be improved in order to capture the vertical structure of the wind and the absolute levels of pollutants in stable dispersion conditions.

Air pollution problems are closely linked to climatic problems, as can be seen from the Asian Brown Cloud study (UNEP & C^4, 2002). Air pollution problems are global and the various effects are the results of several natural and manmade actions inter-coupled with each other. The increasing trend in global average temperature (a rise of 0.1 ^oC in the lowest 8 km layer every 10 years since 1950), together with changes in various climatic variables, have already affected many physical and biological systems on the earth. Both the heat content of marine areas as well as the sea level have increased, while the extent of ice and snow coverage has decreased, glaciers have shrunken and permafrost has thawed (IPCC, 2001). Changes in precipitation and the frequency and extent of extreme climatic phenomena may cause material damage, increase food prices and cause famine. Although climate variations have always occurred for natural reasons, the chemical composition of the atmosphere is now being continuously changed by human activities. Further studies of climate change and the pollution of the soil, air and water, that are decreasing the biodiversity of all ecosystems, are most important for the future of human existence on our earth.

References

Aarnio, P., Myllynen, M., Koskentalo, T., 2001. Ilmanlaatu pääkaupunkiseudulla vuonna 2000. Pääkaupunkiseudun julkaisusarja C 2001:8. Pääkaupunkiseudun yhteistyövaltuuskunta (YTV), Helsinki. 30 s + 5 appendices, (in Finnish).

Andreae M.O. & Cruzen P.J., 1997. Atmospheric aerosols: Biogenic sources and role in atmospheric chemistry. *Science, Vol. 276, 16. May 1997*, p. 1052-1058.

Anttila, P., 1990. Characteristics of alkaline emissions, atmospheric aerosols and deposition. In Kauppi P., Anttila P. and Kenttämies K., (eds.). Acidification in Finland. Springer Verlag, p. 111-134.

Ashmore M. R. & Wilson R. B. (editors), 1992. Critical levels of air pollutants for Europe. Background papers prepared for the United Nations Economic Commission for Europe, workshop on critical levels, Engham, U.K. 23-26 March, 1992, 205 pp.

Asman W.A.H., Harrison, R.M. and Ottley C.J., (1994), Estimation of the net air-sea flux of ammonia over the southern bight of the North Sea. *Atmospheric Environment*, **28**, 3647-3654

Asman W. A. H. & Janssen A. J., 1987. A long range transport model for ammonia and ammonium for Europe. *Atmos. Environ. Vol. 21, No. 10* p. 2099-2119

Aunela L., Häsänen E., Kinnunen V., Larjava K., Mehtonen A., Salmikangas T., Leskelä J. and Loosaar J., 1995. Emissions from Estonian oil shale power plants. *Oil shale* 12, p. 165.177.

Barrett, K. & Berge, E., (eds.), 1996. Transboundary air pollution in Europe, Part 1: Estimated dispersion of acidifying agents and of near surface ozone. *EMEP MSC-W Status report 1996, Report 1/96. The Norwegian Meteorological Institute, Research Report no. 32*, 152 + 29 p.

Barrett K., 1998. Oceanic ammonium emissions in Europe and their transboundary fluxes. *Atmos. Environ.* Vol 32, No. 3, pp. 381-391.

Bartnicki, J., Gusiev A & Lükeville A., 2001. Atmospheric supply of nitrogen, lead, cadmium, mercury and lindane to the Baltic Sea in 1998. EMEP Centers joint note for HELCOM. EMEP MSC-W.
in http://www.emep.int/helcom2001 (October 2002, updated: 27th April 2001)

Bartnicki, J., Barrett, B., Tsyro, S., Erdman, L., Gusev, A., Dutchak, S., Pekar, M., Lukewille, A., Krognes, T., 1998. Atmospheric supply of nitrogen, lead, cadmium, mercury and lindane to the Baltic Sea. EMEP Centers joint note for HELCOM. EMEP MSC-W Note 3/98.

Berg T, & Schaug J, ed., 1994. EMEP workshop on the accuracy of measurements with WMO-sponsored sessions on Determining the Representativeness of measured parameter in a given grid square as compared to model calculations, Passau 1993. EMEP/CCC 2/94

Bladackar A.K., 1957. Boundary layer wind maxima and their significance for the growth of nocturnal inversions. *Bull. Amer. Meteor. Soc*. 38, 283-290.

Bondsdorff E., Rönneberg C. and Aarnio K., 2001. Ecological properties in relation eutrophication in the Baltic Sea – do we know enough ? *Hydrobiologia* 2001. (in press)

Bott A., 1989. A positive definite advection scheme obtained by nonlinear renormalization of the advective fluxes. *Mon. Wea. Rev. Vol. 117, May 1989*, p. 1006-1015.

Boussinesq J., 1877. Essai sur la theorie des eaux courantes. *Mem. Savants Etrange*, Paris, 23, 46.

Bråkenhielm S. & Quinghong L., 1995. Spatial and temporal variability of algal and lichen epiphytes on trees in relation to pollutant deposition in Sweden. *Water, air and soil pollution* 79, 61-74.

Brorström-Lunden E., Ferm M., Iverfelt Å., Munthe J. and Wängberg I., 1999. A5.5 Scientific Report, 1999

Businger J.A., 1982. Equations and Concepts. in Nieuwstadt F.T.M. & van Dop H. (eds.). Atmospheric turbulence and air pollution modelling. D Reidel Publishing company, Dordrecht. p. 1-36.

Clim, 1981. Climatic Atlas of Asia. Maps of mean temperature and precipitation, prepared by the Voeikov Main Geogphysical Observatory, Leningrad. WMO, UNESCO, Goscomgidromet USSR, UNEP.

Chang T. Y., 1984. Rain and snow scavenging of HNO_3 vapour in the atmosphere. *Atm. Env. Vol. 18, No. 1* p. 191-197.

Chang T.Y., 1986. Estimates of nitrate formation in rain and snow systems. *J. Geophys. Res*, Vol. 91, No. D2, p. 2805-2818.

Dahlgren S. & Kautsy L., 2002. Distribution and recent changes in benthic macrovegetation in the Baltic Sea basins, a literature review. Meddelanden från Växtekologiska avdelningen 2002-1. Botaniska institutionen, Stockholms Universitet. 36 p.
in: http://www.mare.su.se (October 2002)

Dedkova, I., Erdman, L., Grigoryan, S., Galperin, M., 1993. Assessments of airborne sulphur and nitrogen pollution of the Baltic Sea Area from European countries for 1987-1991. EMEP MSC-E, Moscow. 67 pp.

DWD 1993-1998. Die Grosswetterlagen Europas. Amtsblatt des Deutschen Wetterdienstes. Von Jahrgang 46 bis Jahrgang 51, nummers 1-13.

DWD, 2001b. 1993-1998. Die Grosswetterlagen Europas. Amtsblatt des Deutschen Wetterdienstes. Jahrgang 54, nummers 7-9.

DWD 2001a. Europäischer Wetterbericht. Amsblatt des Deutschen Wetterdienstes. Vol 26, Nummers 258-264, 15. - 21. 9. 2001.

Downing R. P., Hettelingh J-P. and de Smet P. A. M., (eds.) 1993. Calculation and mapping of critical loads in Europe. Status Report 1993. Coordination centre for effects, RIVM Report No. 259101003, Bilthoven, 163 p.

Drennan W.M., Kahma K.K. and Donelan, A.,M. 1999. On momentum flux and velocity profiles over waves. *Boundary Layer Meteor*. 92, p. 489-515.

Egmond v K., Bresser T. and Bowman L., 2002. The European nitrogen case. *Ambio Vol*. 31, No 2., March 2002, p. 72-78

Eilola K. & Stigebrandt A., 1999. On the seasonal nitrogen dynamics of the Baltic proper biogeochemical reactor. *J. of Marine Research*, 57, 693-713.

EMEP 2002. On-line emissions data dase for the European Countries.
In: http://www.emep.int (October 2002)

Environmental Statistics, 2002. Environment and Natural Resources 2002:3. Official Statistics of Finland, Yliopistopaino, Helsinki, 200 p.

Erisman, J.W, 1994. Evaluation of a surface resistance parameterisation of sulphur dioxide. *Atm. Environ.Vol. 28, No. 16*, p. 2583-2594.

Ferm A., Hytönen J., Lähdesmäki P., Pietiläinen P. and Pätilä A., 1990. Effects of high nitrogen deposition to forests: Case studies close to fur animal farms. In Kauppi P., Anttila P. and Kenttämies K., (eds.). Acidification in Finland. Springer-Verlag Berlin Heidelberg p. 635-668.

Forsius M., 1992. Acidification of lakes in Finland. Regional estimates of lake chemistry and critical loads. *Publications of the Water and Environment Research Institute 10, 1992* National Board of Waters and the Environment

Fraude, F. & Goshnick, J., 1995. Obstructed wetting of combustion aerosol particles in the presence of organic pollutants. in: *Anttila, P., Kämäri, J. and Tolvanen, M. (eds), Proc. of the 10th World Clear Air Congress,* **2**. The Finnish Air Pollution Prevention Society, Helsinki.

Furman E., Dahlström H. and Hamari R., 1998. Itämeri, Luonto ja ihminen. Kustannusosakeyhtiö Otava, Helsinki,159 p.

Galperin M., Sofiev M., Erdman L. and Chechukina T., 1994. Model evaluation of airborne trace metal transport and deposition. Short model description and preliminary results. EMEP/MSC-E Report 3/94. Moscow, 50 p.

Geernaert L.L.S., 1997. Experimental study of the processes in air-sea exchange of gaseous nitrogen compounds. PhD thesis, University of Copenhagen, 101 p.

GrADS, 2002. Grid Analysis and Display System (GrADS). On-line documentation manuals.
In: http://www.iges.org/grads/grads.html (October 2002)

Hanna S.R., Briggs G.A. and Hosker R.P.Jr., 1982. Handbook on atmospheric diffusion. Technical Information Center, U.S. Department of Energy, DOE/TIC-11223. 102 p.

Hass H., 1991. Description of the EURAD Chemistry-Transport-Model Version 2 (CTM2). *Mittailungen aus dem Institut fur Geophysik und Meteorologie der Universität zu Köln*. Herausgeber Ebel A., Neubauer F.M., Speth P. Heft 83, 100 p.

HELCOM, 1991. Airborne Pollution Load to the Baltic Sea 1986-1990. *Baltic Sea Environ Proc., No. 39.*
In: http://www.helcom.fi/helcom/publications.html#bsep (October 2002)

HELCOM, 1996. Third periodic assessment of the state of the marine environment in the Baltic Sea 1989-1993. Background document. Baltic Sea Environ. Proc. No. 64B, 252 p.
In: http://www.helcom.fi/helcom/publications.html#bsep (October 2002)
In: http://www.baltic.vtt.fi/balticinfo/index.html (October 2002)

Hertel O., 1995. Transformation and deposition of sulphur and nitrogen compounds in the marine boundary layer. Dr. of Sci. thesis. Ministry of Environment and Energy, National Environment Research Institute, Department of Emissions and Air Pollution. Denmark. 102 p. + appendixes.

Hesstvedt E., Hov Ø. and Isaksen S.A., 1978. Quasi-steady-state approximations in air pollution modelling: Comparison of two numerical schemes for oxidant prediction. *Int. J. Chemical Kinetics, vol X,* p. 971-994.

Hettelingh J-P., Posch M., de Smet P. A. M. and Downing R. J., 1995. The use of critical loads in emission reduction agreements in Europe. *Water, Air and Soil Pollution 85/4,* p. 2381-2388.

Hinds, W.C., 1982. Aerosol Technology, properties, behaviour and measurement of airborne particles. John Wiley and Sons, 1982. 424 p.

HIRLAM, 1990. HIRLAM Forecast model level 1. On-line documentation manual. Per Kållberg, (ed.), *SMHI S - 60176*, Norrköping, Sweden, June 1990.

HIRLAM 2002a. HIRLAM, a High Resolution Limited Area Model, International Project Description.
in http://www.knmi.nl/hirlam/ (October 2002)

HIRLAM 2002b. Suomessa käytettävä sääennustemalli (in Finnish)
In. http://www.fmi.fi/tutkimus_mallit/mallit_5.html (October 2002)

Holtslag A.A.M. & Nieuwstadt F.T.M., 1986. Scaling the atmospheric boundary layer. *Boundary-Layer Meteorology 36*, 201-209.

Hongisto M. & Joffre S. 2002. 6-year simulations of dispersion of acid contaminants over Fennoscandia and Baltic Sea area. 20 p. submitted to be published in Atm. Environ.

Hongisto, 2002a. On-line results on Hilatar simulations.
In: http://www.fmi.fi/research_air/air_25.html). (October 2002)

Hongisto, 2002b. Kaukokulkeumaennuste. Forecast for Long-Range Transport of Acid compounds from Europe to Finland using the Hilatar model.
In: http://www.fmi.fi/tutkimus_mallit/mallit_17.html (October 2002, manual update)

Hongisto M., 2001. Ilman laatu elokuun myrskyjen aikana: kaukokulkeumatilanteiden operatiivinen tarkkailu.. Magazine of the Finnish Air Pollution Prevention Society, *Ilmansuojelu* 4/2001, p. 19-26., Eiriprint, Jarkoskuva Oy, Helsinki (in Finnish)

Hongisto, M., G. Peterson, O. Krüger, K. Jylhä and M. Sofiev, 1999a. Capacity to predict atmospheric inputs by models. Ext. Abstract in Zuelicke C., (ed.) Proc. of the Third BASYS Annual Sci. Conf. 20-22. Sept, pp. 136-147.
In: http://www.io-warnemuende.de/Projects/Basys/bio/con3/con3top.htm#T3-5 (October 2002)

Hongisto, M., Sofiev M., Jylhä K. and Joffre S., 1999b. BASYS Sci. Rep. High resolution numerical simulation of nutrient and trace element deposition to the Baltic. BASYS Final Scientific Report. (IO Warnemünde, DE). 18 p.
In: http://www.io-warnemuende.de/Projects/Basys/reports/final/en_home.htm A5.7 (October 2002)

Hongisto, M.,. Sofiev M., Jylhä K. and Joffre S., (1999c). Long-term and episodic simulation studies of nitrogen compounds to the Baltic Sea. I*n Zuelicke C., (ed.) Proc. of the Third Basys Annual Sci. Conf. IOW Warnemunde, 20-22 Sep 1999*
In: http://www.io-warnemuende.de/Projects/Basys/reports/final/en_home.htm Appendix A, (October 2002)

Hongisto M., 1998. Hilatar, a regional scale grid model for the transport of sulphur and nitrogen compounds. FMI Contributions no 21, Helsinki, 152 p. Yliopistopaino, Helsinki, 1998.
http://www.fmi.fi/research_air/air_25.html (October 2002)

Hongisto M., Jylhä K. and Flyktman V., 1998a. Preliminary simulations of the BASYS Lagrange periods with the Hilatar model. In: Gryning S.-E. & Batchvarova E. (ed.) *Air Pollution Modelling and its Application VII, Proceedings of the 23rd NATO CCMS International Technical Meeting, September 28 - October 2, 1998, Riviera Holiday Club, Varna, Bulgaria. NATO – challenges of modern society Vol 24*. Kluwer Academic / Plenum Publishers New York, p. 195-204

Hongisto M., Jylhä K. and Joffre S., 1998b. Simulations of the Basys 5 Network/Lagrange periods with the Hilatar model. Proc. of the Second BASYS Annual Sci. Conf., Appendix A.5.11
In: http://www.io-warnemuende.de/Projects/Basys/reports/pro2year/en_home.htm (October 2002)

Hongisto M. & Jylhä K., 1998. Backward trajectories for stations Hel, Hoburg, Kap Arkona and Preila. BASYS Atmospheric load subproject, Network Study 3.2. – 3.4.1998. FMI Air Quality Research, Basys project

Hongisto M., 1997. Nitrogen deposition to the Baltic Sea. Simulation results with the model Hilatar. in Pacyna J.M., Broman D. and Lipiatou E. (ed's) Sea-Air exchange, processes and modelling. European Commission - DG12 - MAST: EUR 17660 EN, Luxembourg: Office for Official Publications for the European Communities, p. 247-256

Hongisto M., Savolainen V. and Joffre S., 1997. Numerical simulation of atmospheric load. Proc. of the First BASYS Annual Sci. Conf. 29.9-1.10, 1997 Warnemunde, Germany. IOW Warnemunde p. 17
http://www.io-warnemuende.de/Projects/Basys/events/con1post.htm#5

Hongisto M., Kangas L., Nordlund G., Markkanen K., Häkkinen A.J., Kartastenpää R. and Kivivasara J., 1995. Model calculations of the influence on Finland of air pollution sources in the areas of St. Petersburg, Leningrad Oblast Karelia and Estonia. Anttila P., Kämäri J., Tolvanen M., (ed´s) in Proc. of the 10th World Clean Air Congress, Espoo, Finland, Vol 2, 306. The Finnish Air Pollution Prevention Society, 1995.

Hongisto M. & Joffre S., 1994. Transport Modelling over Sea Areas. EUROTRAC Annual report 1993, Vol. 5 EUMAC, Fraunhofer Inst., Garmish-Partenkirchen (D), p. 67-72.

Hongisto M., 1994. Hilatar and FINOX, 3-dimensional grid models for regional air pollutant dispersion studies. In Nielsen C.,J. (ed.), Third Nordic symposium on atmospheric chemistry, Proceedings of NORSAC '93, NILU OR 20/94 p. 164-169.

Hongisto M., 1993a. A simulation model for the transport, transformation and deposition of oxidised nitrogen compounds in Finland. Technical description of the model. Finnish Meteorol. Inst. Air quality publications No. 14, Helsinki, 55 p.

Hongisto M., 1993b. Regional air pollution modelling in Finland. Extended abstracts of papers presented at the WMO region VI conference on the measurement and modelling of atmospheric composition changes including pollution transport, Sofia, Bulgaria, 4-8 October 1993. WMO Global Atmospheric Watch No. 91, WMO/TD-NO. 563, p.149-152.

Hongisto M., 1993c. Description of the 1-dimensional two-phase model with aqueous chemistry. Vesikemiamallin rakenne. non-published report (in Finnish)

Hongisto M. & Joffre S., 1993. Transport Modelling over Sea Areas. EUROTRAC Annual report 1992, Vol. 5 EUMAC, Fraunhofer Inst., Garmish-Partenkirchen (D), p. 66-70.

Hongisto M. & Valtanen K., 1993. Development of a long-range transport model for sulphur and nitrogen compounds connected with the weather prediction model HIRLAM - Rikin ja typen yhdisteiden kaukokulkeutumismallin kehittäminen HIRLAM-sääennuste-mallin yhteyteen. Ilmatieteen laitos, Ilmanlaatuosasto, Raportteja 1993:1, 49 p. (in Finnish).

Hongisto M. & Valtanen K., 1992. Transport Modelling over Sea Areas. EUROTRAC Annual report 1991, Vol. 5 EUMAC, Fraunhofer Inst., Garmish-Partenkirchen (D), p. 41-46.

Hongisto M., 1992a. A simulation model for the transport, transformation and deposition of oxidised nitrogen compounds in Finland. 1985 and 1988 simulation results. Finnish Meteorol. Inst. Contributions No. 9, Helsinki, 114 p.

Hongisto M., 1992b. Meteorological conditions prevailing during 1991 sulphur pollution episodes in Northern Fennoscandia. In Tikkanen, E., Varmola M., Katermaa T., (editors): Symposium of the state of the environment and environmental monitoring in Northern Fennoscandia and the Kola Peninsula, October 6-8, 1992, Rovaniemi. Extending abstracts, Arctic Centre, University of Lapland, Rovaniemi, p. 28-30.

Hongisto M., 1992c. Statistical methods in modelling the concentration and deposition levels of NOx pollutants over Southern and Central Finland. In Conference on Environmetrics in Finland, Abstracts of the 4th International Conference on Statistical Methods for the Environmental Sciences, August 17 to 21, 1992, Helsinki University of Technology, Otaniemi, Espoo, Finland. p. 40-41.

Hongisto M., Joffre S., Lindfors V. and Damski J., 1991. Transport Modelling over Sea Areas. EUROTRAC Annual report 1990, Vol. 5 EUMAC, Fraunhofer Inst., Garmish-Partenkirchen (D), p. 25-30.

Hongisto M., 1990. Modelling the influence of meteorological and other factors on the chemistry of oxidised nitrogen compounds. In: Restelli, G. & Angeletti, G. (eds.) Physico-chemical behaviour of atmospheric pollutants, Kluwer Academic Publishers, p. 588-593.

Hongisto M. and Wallin M., 1990. Evaluation of Finnish Sulphur Reduction Strategies for the year 1995. In Kauppi P., Anttila P. and Kenttämies K., (eds.). Acidification in Finland. Springer-Verlag Berlin Heidelberg p. 1195-1208.

Hongisto M. & Joffre S., 1990. Transport Modelling over Sea Areas Annual report 1989, Vol. 5 EUMAC, Fraunhofer Inst., Garmish-Partenkirchen (D) p. 22-27

Hongisto M., Wallin M. and Kaila J., 1988. Rikkipäästöjen vähentämistoimenpiteiden taloudellisesti tehokas valinta. Ilmatieteen laitos, Ilmanlaatuosasto, Raportteja N:o 1988:4. 80 p.

Hongisto M., 1985. Examination of long-term energy-economic alternatives with the national energy system optimization model. Technical University of Helsinki, Department of Technical Physics, Licenciate thesis. 125 s. (in Finnish)

Häkkinen A.J., Markkanen K., Hongisto M., Kartastenpää R., Milayaev V.B., Yasensky A., Kuznetsov V.I., Kopp I.Z. and Kivivasara J., 1995. Emissions in St. Petersburg, the Leningrad area and Karelia. In: Tolvanen M., Anttila P., Kämäri J. (Eds). Proc. of the 10th World Clean Air Congress, Espoo, Finland, Vol 1, 103. The Finnish Air Pollution Prevention Society, 1995.

Häsänen E., Aunela-Tapola L., Kinnunen V., Larjava K., Mehtonen A., Salmikangas T., Leskelä J., Loosaar J., 1997. Emission factors and annual emissions of bulk and trace elements from oil shale fueled power plants. *The Science of the Total Environment* 198: 1-12.

Ilmastokatsaus, 2001. *Climatological overview, Ilmastokatsaus* 9/2001. Finnish Meteorological Institute. 12 p. (in Finnish)

IPCC, 2001. IPCC Third Assessment Report – Climate Change 2001: Part 1, The Scientific Basis. Chapter 2. Observed climate variability and change. IPCC Secretariat, C/O World Meteorological Organization, Geneva, Switzerland
In: http://www.grida.no/climate/ipcc_tar/wg1/048.htm (http://www.ipcc.ch) (October 2002)

Iversen T., Saltbones J., Sandnes H., Eliassen A. and Hov Ø., 1989. Airborne transboundary transport of sulphur and nitrogen over Europe - Model descriptions and calculations. *EMEP MSC-W Report* 2/89. DNMI, Oslo.

Jalkanen L., Mäkinen A., Häsänen E. and Juhanoja J., 2000. The effect of large anthropogenic particulate emissions on atmospheric aerosols, deposition and bioindicators in the eastern Gulf of Finland region. *Sci. Tot. Environ*. 262: 123-136.

Joffre S.M., 1985. The structure of the marine atmospheric boundary layer: A review from the point of view of diffusivity, transport and deposition processes. *Finnish Meteorological Institute, Technical report No. 29*, 119 p.

Joffre S.M., 1988. Parameterisation and assessment of processes affecting the long-range transport of airborne pollutants over the sea. *Finnish Meteorological Institute, Contributions No. 1*, 49 p.

Johansson M., 1999. Integrated models for the assessment of air pollution control requirements. Monographs of the Boreal Environmental research No. 13, Karisto Oy, Hämeenlinna, 73 p. + appendices.

Jonsen J.E. & Berge E., 1995. Some preliminary results on transport and deposition of nitrogen compounds by use of the Multilayer Eulerian Model. *EMEP/MSC-W, Note 4/95*, 25 p.

Jumppanen K. and Mattila J., 1994. The development of the state of the Archipelago Sea and the environmental factors affecting it. Lounais-Suomen Vesiensuojeluyhdistys, Julk. 82, 206 p. (in Finnish)

Kallaste T., Roots O., Saar J. and Saare L., 1992. Air pollution in Estonia 1985-1990. Environmental Data Centre, National Board of Waters and the Environment, Environmental report 3. Helsinki. 61 p.

Kakkuri J. & Hjelt S.-E., 2000. Ympäristö ja geofysiikka. Tähtitieteellinen yhdistys Ursan julkaisuja 76. Tallinna, 188 p.

Kangas L. & Syri S., 2002. Regional nitrogen deposition model for integrated assessment of acidification and eutrophication. *Atm. Environ.,* 36, p. 1111-1122

Kaurola J., Koistinen J., Leskinen M., Puhakka T. and Saarikivi P., 1989. Mesometeorologisten tekijöiden vaikutus epäpuhtauksien leviämiseen erityisesti Suomenlahden rannikolla. Osa 2. Mesoilmiöiden yleisyys Etelä-Suomessa ja Doppler-säätutkan mahdollisuudet niiden havainnoimisessa. Helsingin yliopisto, meteorologian laitos, 51 p.

Kesti P., Jylhä K., Koistinen J., Puhakka T. and Saarikivi P., 1989. Mesometeorologisten tekijöiden vaikutus epäpuhtauksien leviämiseen erityisesti Suomenlahden rannikolla. Osa 1. Eräiden mesoilmiöiden tuuli- ja sadekentät. Helsingin yliopisto, meteorologian laitos, 54 p.

Kiirikki M., Westerholm L. and Sarkkula J., 2000. Suomenlahden levähaittojen vähentämis-mahdollisuudet. *Suomen Ympäristö* 416, Suomen ympäristökeskus, 32 p.

Kirkkala T., 1998. How are you, the Finnish Archipelago ? Miten voit Saaristomeri. Ympäristön tila Lounais-Suomessa 1. Lounais-Suomen ympäristökeskus, 72 p. (in Finnish)

Kuparinen J. & Tuominen L., 2001. Eutrophication and self-purification: Counteractions forced by large-scale cycles and hydrodynamic processes. *Ambio* Vol XXX No 4-5, August 2001.

Källstrand B., Bergström H., Højstrup J. and Smedman A.-S., 2000. Mesoscale wind field modifications over the Baltic Sea. *Boundary-Layer Meteorol.,* 95, 161-188.

Källstrand B., 1998. Low level jets in a marine boundary layer during spring. *Contr. Atmos. Phys*. August 1998, p. 359-373.

Lee, D. S. & Pacyna, J. M., 1999. An industrial emissions inventory of calcium for Europe. *Atmosp. Environ.* 33, p. 1687-1697.

Leinonen L. (ed.), 1994-2001. Air Quality measurements - Ilmanlaatumittauksia 1993-2000. Official Statistics of Finland. Finnish Meteorological Institute, Helsinki, around 250 p. each. Available in the Air Quality Data base of the FMI Air Quality Department.

Lenhart L., Heck T. and Friedrich R., 1997. The GENEMIS inventory, European emission data with high temporal and spatial resolution. In: *Ebel A., Friedrich R. and Rodhe H., (ed's). Transport and chemical transformation of pollutants in the troposphere Vol. 7, Tropospheric modelling and emission estimation, chemical transport and emission modelling on regional, global and urban scales.* Springer-Verlag Berlin Heidelberg 1997, p. 217-222.

Lindfors V., Joffre S.M. and Damski J., 1991. Determination of the wet and dry deposition of sulphur and nitrogen compounds over the Baltic Sea using actual meteorological data. FMI *Contributions* **4**.

Lindfors V., Joffre S.M., Damski J., 1993. Meteorological variability of the wet and dry deposition of sulphur and nitrogen compounds over the Baltic Sea*. Water, Air, and Soil Pollution 66*, 1-28.

Mannonen M., 1982. KETO-82, the national energy system optimization model, users quide. Technical University of Helsinki, Department of Technical Physics, Report TKK-F-A496 (1982). (in Finnish)

Marchuk G.I., 1975. Methods of numerical mathematics. Springer-Verlag, New York, 316 p.

Marchuk G.I., 1986. Mathematical models in environmental problems. In: Lions J.L., Papanicolaou G., Fujita H. & Keller H.,B.*, Studies in mathematics and its applications, Vol 16.* Elsevier Science Publishers B.V., North-Holland-Amsterdam, 217 p.

Martens C.S., Wesolowski J.J., Harriss R.C. and Kaifer R. 1973. Chlorine loss from Puerto Rican and San Fransisco Bay area marine aerosols. *J. Geophys. Res.* Vol. 78, No. 36, p. 8778-8792.

Moussiopoulos N., Berge E., Bøhler T., de Leeuw F., Grønskei K-E., Mylona S. and Tombroy M., 1997. Ambient air quality, pollutant dispersion and transport models. European Environmental Agency, Copenhagen, 94 p.

MTL, 2002. Merentutkimuslaitoksen jääpalvelu, kylmää tietoa jäissä liikkujille.
in: http://ice.fmi.fi/ (October 2002)
in: http://www2.fimr.fi/fi/palvelut/jaapalvelu.html (October 2002)

Mäkelä K. & Salo M., 1994. Traffic emissions in Russia and the Baltic States. St. Petersburg, Leningrad Oblast, Republic of Karelia, Estonia, Latvia and Lithuania. *VTT Research notes 1569*.49 p.

Mäkelä K., Tuominen A. and Pääkkönen E., 2002. Suomen liikenteen päästöjen laskentajärjestelmä LIPASTO 2001. MOBILE raportti M2T9916-13. VTT Rakennus- ja yhdyskuntatekniikka, tutkimusraportti RTE 3164/02, Espoo. 39+6 p. (In Finnish)
In: http://www.vtt.fi/rte/projects/lipasto/meeri/paasto00.htm (October 2002)

NCAR, 1985. The NCAR Eulerian Regional Acid Deposition Model. The NCAR Acid Deposition Modelling Project, ADMP-85-3, NCAR Technical Note NCAR/TN-256+STR. National Center for Atmospheric Research, Boulder Colorado, 178 p.

Nilsson J. & Grennfeldt, P. (eds.), 1988. Critical loads for Sulphur and Nitrogen. Nord 1988:97. Nordic Council of Ministers, Copenhagen. 418 p.

Nordlund G., Lumme E., Pietarinen M. and Tuovinen J-P., 1984. Laskentamenetelmä rikin laskeumaosuuksien erittelemiseksi. Ilmatieteen laitos, Helsinki, 39 p.

Pakkanen T. A., 1996. Study of formation of coarse particle nitrate aerosol. Atmospheric Environment 30: 2475-2482.

Pakkanen T. A., Kerminen V.-M., Hillamo R. E., Mäkinen M., Mäkelä T., Virkkula A., 1996. Distribution of nitrate over sea-salt and soil derived particles – implications from a field study. *Journal of Atmospheric Chemistry* 24: 189-205.

Petersen G., 1998. Numerical simulation models for airborne heavy metals in Europe. A review. In: Linkov I. and Wilson R. (eds.). Air pollution in the Ural Mountains. Environmental, health and policy aspects. NATO-Advanced Science Institute Series, Partnership Sub-Series 2: Environment – Vol. 40, pp. 81 – 97.

Petersen G., Munthe J., Bloxam R. and Kumar A.V., 1998. A comprehensive Eulerian modelling framework for airborne mercury species. Development and testing of Tropospheric Chemistry Module (TCM). in Lindberg, S.E., Petersen G. and Keeler G., (eds.). Special Issue on atmospheric transport, chemistry and deposition of mercury. *Atm. Environ*., Vol. 32, No. 5, pp. 829-843.

Philips D. (ed.), 1995. The global climate system review. Climate system monitoring June 1991 – November 1993. WMO No. 819, 150 pp.

Pitkänen H., Lehtoranta J. and Räike A., 2001. Internal nutrient fluxes counteract decreases in external load: The case of the estuarial Eastern Gulf of Finland, Baltic Sea. Ambio, vol. 30, no. 4-5, p. 195-201., 0044-7447 (2001)

Plate E., 2000. Variabilität der Zusammensetzung anorganischer Aerosole – insbesondere der reaktiven Stickstoffverbindungen – in küstennahen Gebieten der Nordsee und Ostsee. Dissertation zur Erlangung des Dortorgrades des Fachbereichs Chemie der Universität Hamburg. Schriftenreihe Angewandte Analytik. Institut für Anorganische und Angewandte Analytik Nr 37, Universität Hamburg, 215 p.

Plate E., Schulz M. Ferm M., Hongisto M., Jylhä K. and Sofiev M., 1999: Variation of nitrogen aerosols in Baltic Sea regions - a comparision of modelled and measured data In *Zuelicke C., (ed.) Proc. of the Third Basys Annual Sci. Conf. IOW Warnemunde, 20-22 Sep 1999*, p.70
In: http://www.io-warnemuende.de/Projects/Basys/reports/final/en_home.htm Appendix A. (October 2002)

Posch M., Smet P.A.M., d. Hettelingh J-P. and Downing R.J., 2001. Modelling and mapping of critical thresholds in Europe. CCE status report 2001, RIVM Rapport 259101010, 162 p.
in http://www.rivm.nl/cce/

Pryor S. and Sørensen L.L., 2000. Nitric Acid- Sea salt reactions: Implications for nitrogen deposition to water surfaces. Journal of Applied Meteorology 39, 725-731

Pöyry., 1990. Environmental situation and project identification in Leningrad and Leningrads region. Nordic project fund, J Pöyry ref M2019. 68 p + appendices

Reinikainen M., 1981. The multi-goal optimization model for the Finnish energy system. Dimplom Engineering work, Technical University of Helsinki, Department of Technical Physics. 104 s. (in Finnish)

Routti J.(ed.), Hongisto M, Kuikka T. and Myllyvirta J. and Pirilä P., 1983. Long-term model for the Finnish energy-economy system. Ministry of Trade and Industry, Energy Department. Technical University of Helsinki, Report D:44, Helsinki 1983.Valtion painatuskeskus., 82 p. (in Finnish)

Ruoho-Airola T. and Salmi, T., 2001. Episodicity of sulphate deposition in Finland. Water, Air and Soil Pollution 130: 529-534.

Rönnberg C., 2001. Effects and consequences of eutrophication in the Baltic Sea. Specific patterns in different regions. Licenciate thesis, department of Biology, Environmental and Marine Biology, Åbo Akademi University, 132 p. + appendices

Sarkkula J., Koponen J., Inkala A. and Kuusisto M., 1998. Demonstrative modelling of nutrient load impacts to the baltic Sea. Finnish Environment Institute 1998 . - 24 p.

Savijärvi H. & Alestalo M., 1988. The sea breeze over a lake or gulf as the function of the prevailing flow. *Beitr. Phys. Atmosph.*, Vol. 61, p. 98-104.

Savolainen V., 1997. Forward trajectories for stations Hel, Hoburg, Kap Arkona and Preila, and ships "Alexander von Humboldt" and "Professor Albrecht Penck". BASYS Atmospheric load subproject, Lagrange study 2-15 July 97. FMI Air Quality Research, Basys project

Schneider B., Wangberg, I., Munthe J., Iverfeld A., Petersen G., Krüger O., Schmolke S., Ebinghaus R., Czeburnis D., Hongisto M. and Sofiev M., (1999). Coast-to-sea gradients of atmospheric trace element fluxes. *Ext. abstr. in Zuelicke C., (ed.) Proc. of the Third Basys Annual Sci. Conf , IOW Warnemunde, 20-22 Sep 1999*. pp.105-108
In: http://www.io-warnemuende.de/Projects/Basys/bio/con3/con3top.htm#T2-12 (October 2002)

Schulz M., Ferm M. Hongisto M., Jylhä K., de Leeuw G., Marks R., Nadstazik A., Plate E., Tamm S., Sopauskiene D. and. Ulevicus V., 1999a. Atmospheric nitrogen input to the Baltic Sea *In Zuelicke C., (ed.) Proc. of the Third Basys Annual Sci. Conf., IOW Warnemunde, 20-22 Sep 1999 a, p. 60-67.*
In: http://www.io-warnemuende.de/Projects/Basys/bio/con3/con3top.htm#T2-2 (October 2002)

Schulz M.[1], Cachier H.[2], Ebinghaus R[5], Ferm M.[3], Hongisto M.[4], Iverfeldt A.[3], Jylhä K.[4], Krüger O.[5], Kusmierczyk-Michulec J.[6], de Leeuw G.[7], Marks R.[6], Moermann M.[7], Munthe J.[3], Nadstazik A.[8], Ruellan S.[2], Petersen G.[5], Plate E.[1], Ulevicius V.[9], Schneider B.[10], Schmolke S.[5] and Sopauskiene D.[9], 1999b. Evolution of the aerosol composition in the BASYS Network study and Lagrangian experiments in summer 1997 and winter 1998. *J. Aerosol. Sci.* Vol. 30, Suppl 1., pp. S97-S98

[1]Institut für Anorganische und Angewandte Chemie, Universität Hamburg, D, [2]CFR, Gif-Sur-Yvette/F, [3]IVL, Gothenburg/S, [4]FMI, Helsinki/F, [5]GKSS, Geesthacht/D, [6]IO-PAS, Sopot/PL, [7]TNO, Den Hague/NL, [8]UG-IO, Gdansk/PL, [9]IPV, Vilnius/LIT, [10]IOW, Warnemuende/D

Schulz M., 1998 (ed'). BASYS 2-year progress report (01.08.1996-31.07.1996) - SCIENTIFIC REPORT - Subproject 5: Atmospheric Load and its subproject appendices. *In Zuelicke C., (ed.) Proc. of the Second Basys Annual Sci. Conf., Stockholm Marine Research Centre Sweden, 23-25 Sep 1999*
in http://www.io-warnemuende.de/Projects/Basys/reports/pro2year/html/sci2v1s5.html (October 2002)

Schulz M.* & Hongisto M.[+], 1998. Improving the Atmospheric Nitrogen Load Assessment for the Baltic Sea. BASYS Newsletter Number 9, November 1998 p. 28-36.
in http://www.io-warnemuende.de/Projects/Basys/newslett/news9.htm (October 2002)
*University of Hamburg / Institut für Anorganische und Angewandte Chemie
[+]Finnish Meteorological Institute, Air Quality Research

Schulz M., Plate E., Tamm S., Stahlschmidt T., Rebers A. (IAUH), Schneider B., Lakaschus S., Petersohn I., Kubsch H., (IOW), Iverfeldt A., Ferm M., Munthe J., Brorstroem-Lunden E., Schager P., Wangberg I. (IVL), Schmolke S., Ebinghaus R., Kock H.H., Otten S. (GKSS-C), Sopauskiene D., Ulevicius V., Stapcinskaite S., Juozaitis A., Ceburnis D., Zukiene S., Urba A. (IPV), Marks R., Kuœmierczyk-Michulec J., Kruczalak K., Michulec C., Sokólski M. (IO-PAS), Nadstazik A., Dudziñska B., Modzelewska M., Bedowski J. (IOPAS/UG), Savolainen V., Hongisto M. and Joffre S. (FMI), 1997. 1-year progress report (01.08.1996-31.07.1997) Scientific report, Appendix A: Documentation, Subproject 5: Atmospheric Load.
in: http://www.io-warnemuende.de/Projects/Basys/reports/pro1year/doc/doc12s51.htm (October 2002)

Scott B. C., 1982. Theoretical estimates of the scavenging coefficient for soluble aerosol particles as a function of precipitation type, rate and altitude. *Atmos. Environ. Vol. 16, No. 7,* p.1753-1762.

Seinfeld J. H., 1986. Atmospheric chemistry and physics of air pollution. John Wiley & Sons, 738 p.

Seinfeld J.H. & Pandis S.N., 1998. Atmospheric chemistry and physics. John Wiley and Sons, Inc. pp. 1016-1027.

Seinä A., Grönvall H., Kalliosaari S. and Vainio J., 1996. Ice seasons 1991-1995 along the Finnish coast. *Meri, Report Series of the Finnish Institute of Marine Research*, No. 27.

Simpson D. 1992. Long-period modelling of photochemical oxidants in Europe. Calculations for July 1985. *Atmos. Environ.* 26A, No. 9, pp. 1609-1634.

Smedman A., Högström U., Bergström H., Rutgersson A., Kahma K and Pettersson H., 1999. A case study of air-sea interaction during swell conditions. *J. Geophys. Res*., 104(C11), 25833-25851.

Smolarkiewicz P.K., 1983. A simple positive definite advection scheme with small implicit diffusion. *Mon. Wea. Rev. Vol 111*, p. 479-486.

Sofiev M**.**, Kaasik M. and Hongisto M., 2002. Model simulations of the alkaline dust distribution from Estonian sources over the Baltic Sea basin. submitted to WASP (Sept. 2001)

Sofiev M. Petersen, G., Krüger, O., Schneider, B., Hongisto M. and Jylhä, K., 2001. Model simulations of the atmospheric trace metals, concentrations and depositions over the Baltic Sea. Atmospheric Environment 35, p. 1395-1409.

Sofiev M., 1999. Statistical Package (un-published program documentation)

Sofiev M., Petersen G., Krüger O., Hongisto M. and Jylhä K., 1999. Nested simulations of the heavy metal distribution over the Baltic Sea area. *In Zuelicke C., (ed.) Proc. of the Third Basys Annual Sci. Conf.,IOW Warnemunde,* 20-22 Sep 1999, p.70-71.

Song C. H. & Carmichael G. R., 1999. The aging process of naturally emitted aerosol (sea-salt and mineral aerosol) during long range transport. Atmospheric Environment 33: 2203-2218.

Sørensen L.L. [(1)], Geernaert G.[(2)], de Leeuw G.[(3)], Plate E. [(4)], Smedmann A-S. [(5)] and Pryor S. [(6)], 1999. Surface flux process study in *Zuelicke C., (ed.) Proc. of the Third BASYS Annual Sci. Conf. in* http://www.io-warnemuende.de/Projects/Basys/bio/con3/con3top.htm#T2-6 (October 2002)
[(1)]Risø National Laboratory, Wind Energy and Atmospheric Physics Department, Roskilde, Denmark, [(2)] National Environmental Research Institute, Roskilde, Denmark, [(3)] TNO Physics & Electronics Laboratory, The Hague, Netherlands. [(4)] University of Hamburg, Instute of Inorganic and Applied Chemistry, Martin-Luther-King-Platz 6, D-20146 Hamburg,Germany. [(5)]Uppsala University, Meteorological Institute, Uppsala, Sweden. [(6)] Indiana University, Climate and Meteorology program, Department of Geography, Bloomington, USA

Sørensen L. L., 1997. BASYS process study measurements over Ostergarnsholm, spring 1997. The measurment data base.

Sørensen L.L., Pedersen B., Lund M., 2000. Flux divergence of reactive nitrogen over the coastal ocean. In: Transport and chemical transformation in the troposphere. Proceedings. EUROTRAC-2 symposium 2000, Garmisch-Partenkirchen (DE), 27-31 Mar 2000. Midgley, P.M., Reuther, M.J., Williams, M. (eds.), (Springer-Verlag, Berlin, 2001) p. 54-61

Summary, 2002. Environmental Conditions in the Baltic Sea Region. Summary of the state of the Baltic Sea, in connection to Baltic Marine Environment Bibliography.
In: http://www.baltic.vtt.fi/demo/balful.html (October 2002)

Syri S., Johansson M. and Kangas L., 1998. Application of nitrogen transfer matrixes for integrated assessment. *Atm. Environ***. 32 No 3,** 409-413.

Statistics, 1984. Statistics of radiosonde observations 1961-1980. Meteorological yearbook of Finland, Vol. 61-80, part 3. Finnish Meteorological Institute, 175 p.

Statistics, 2001. Statistical tables on Idä-Viru and Lääne Viru emissions and oil shale use in 1995-2000 from the Estonian Ministry of Environment.

Stein A. F. & Lamb D., 2000. The sensitivity of sulfur wet deposition to atmospheric oxidants. *Atmos. Environ.* 34, 1681-1690.

Stull R. B., 1988. An introduction to boundary layer meteorology. Kluwer Academic Publishers, Dordrecht, The Netherlands, 666 p.

Tamsalu R. (ed.), 1998. The coupled 3D hydrodynamic and ecosystem model FINEST. Report series of the Finnish Institute of Marine Research, Meri No. 35, 166 p.

Teinemaa E., Kirso U., Strommen M.R., Kamens R.M., 2002. Atmospheric behaviour of oil-shale combustion fly ash in a chamber study. *Atmos. Environ.* 36: 813-824.

Tervahattu H., Hongisto M., Kupiainen K., Aarnio P., Sillanpää M., Saarikoski S., 2002. Hiukkasten kaukokulkeuma syyskuussa 2001. Pääkaupunkiseudun julkaisusarja C 2002:7. Pääkaupunkiseudun yhteistyövaltuuskunta YTV, Helsinki (in Finnish)

Tervahattu H., Hongisto M., Aarnio P., Kupiainen K. and Sillanpää M., 2002. Identification of trans-border particle pollutant episode in Finland. submitted

Thompson D.W.J. & Wallace J.M., 1998. The arctic oscillation signature in the wintertime geopotential height and temperature fields. *Geophys Res. Lett*. **25**(9), 1297-1300.

Tijm A.B.C., van Delden A.J. and Holtslag A.A.M., 1999. The inland penetration of sea breezes. *Contr. Atmos. Phys.,* November 1999, p. 317-328

Tuovinen J-P., 1992. Turbulenttisen diffuusion K-teoriaan perustuva ilmansaasteiden leviämismalli. Teknillinen korkeakoulu, Tietotekniikan osasto, Teknillisen fysiikan koulutusohjelma. Diplomityö, (A dispersion model of air pollutants based on the K theory of turbulent diffusion). 109 p. (in Finnish)

Tuovinen J.P., Hongisto M. and Nordlund G., 1989. Modelling of regional transport, transformation and deposition of oxidised nitrogen compounds. in L.J.Brasser and Mulde W.C., Man and his Ecosystem. Proceedings of the 8th World Clean Air Congress, The Hague, the Netherlands, 11-15 September. Volume 3. Elsevier Science Publishers B.V., Amsterdam. p. 221-226

UNEP and C^4, 2002. Impact study: The Asian Brown Cloud: Climate and other Environmental Impacts. UNEP and C^4, Center for Clouds, Chemistry and Climate UNEP/DEWA/RS.02-3, UNEP, Nairobi.
In: http://www.rrcap.unep.org/abc/impactstudy/ (October 2002)

Ukonmaanaho L. & Raitio, H., 2001. Forest condition monitoring in Finland. National report 2000. Metsäntutkimuslaitoksen tiedonantoja 824, 2001. 157 p.

van Ulden A.P. & Holzlag A.A.M., 1985. Estimation of atmospheric boundary layer parameters for diffusion applications. *J. Climate Appl. Meteor. Vol. 24,* p.1196-1207.

Voldner E.C., Barrie L.A. & Sirois A., 1986. A literature review of dry deposition of oxides of sulphur and nitrogen with emphasis on longrange transport modelling in North America. *Atmos. Environ. Vol. 20, No. 11,* p.2101-2123.

Vuorenmaa J., Juntto S & Leinonen L., 2001. Rainwater quality and bulk deposition in Finland in 1998. Suomen ympäristö 468, Finnish Environmental Institute, Finnish Meteorological Institute. 115 p.

Wesely M.L., 1989. Parameterisation of surface resistances to gaseous dry deposition in regional-scale numerical models. *Atm. Environ., Vol 23, No. 6,* p. 1293-1304.

Winterhalter B., 1999. The state of the past, present and future Baltic Sea, based on the results of BASYS SP-7 Paleo-environment studies. BASYS Final Scientific Report. Appendix A: 7.2
In: http://www.io-warnemuende.de/Projects/Basys/reports/final/en_home.htm (October 2002)

Yanenko N. N., 1971. The method of fractional steps. The solution of problems of mathematical physics in several variables. Springer-Verlag, Berlin, 160 p.

Zlatev Z., Bergström R., Brandt J., Hongisto M., Jonson J.E., Langner J. and Sofiev M., 2001. Studying sensitivity of air pollution levels caused by variations of different key parameters. TemaNord 2001:569. Nordic Council of Ministers, Expressen Tryk & Kopicenter, Copenhagen. 47 p.

Zuelicke C., (ed.), 1999. BASYS Final Scientific Report.
In: http://www.io-warnemuende.de/Projects/Basys/reports/final/en_home.htm (October 2002)

APPENDIX

DESCRIPTION OF THE MODEL COVERING THE BALTIC SEA SURROUNDINGS WITH 10 VERTICAL LAYERS.

1. DESCRIPTION OF THE HILATAR MODEL

In this work, the structure and physical parameterisation of the grid model HILATAR, for simulating the transport, dispersion, chemical transformation and deposition of nitrogen and sulphur pollutants, is introduced. The text is a slightly updated part of the report (Hongisto, 1998).

Emitted air pollutants are mixed in the lower troposphere, carried by the wind, oxidised into other compounds during transport and scavenged down by rain or by dry deposition when air masses flow over vegetation or other surfaces. The residence times of the compounds depend on the season, latitude, meteorological conditions, emission height, reaction kinetics during the transport, available oxidants, surface type below the pollutant clouds etc.

With its preceding version, the FINOX-model (Finnish regional dispersion model for oxidised nitrogen, NO_x compounds, HONGISTO, 1992 and 1993), the HILATAR model has been constructed mainly for acid deposition studies. The modelling area covers Finland, Scandinavia, the Baltic countries and parts of the other countries surrounding the Baltic Sea. The grid size can be varied, so that for regional studies selected sub-areas are simulated separately with a higher grid resolution. The model flow chart is presented in Fig 1.

The evolution of compounds emitted into the lower troposphere is simulated by numerically solving a set of differential equations which describe the advection of air pollutants by the wind, their diffusion by atmospheric turbulence, their chemical conversion to other species and deposition to the ground on a grid of 11-28 km horizontal resolution, having 7-10 vertical layers below 3 km. The daily average concentrations of the long-range transported pollutants, obtained on the EMEP-model grid from the EMEP MSC-W centre in Norway, are added to the air flowing into the simulation area through the boundaries. The emissions, meteorological parameters and dry and wet deposition sink terms vary every hour during the simulations.

The meteorological input parameters are taken from the meteorological database collected since 1991. It consists of the 6-hour predictions of the HIRLAM (HIgh Resolution Limited Area Model) numerical weather model which is in routine use at the FMI. The turbulence parameters, such as the friction velocity, the Monin-Obukhov length, the temperature scale, the convective velocity and the mixing height are calculated afterward from the temperature, wind and specific humidity profiles. Because turbulent fluxes and sink terms were not assumed to be horizontally continuous, two separate boundary layer models have been applied over sea and land areas.

1.2 The model structure

The HILATAR model is an Eulerian grid-point model in which the concentrations of a compound, $c(\vec{x},t)$ at time t and place $\vec{x}$ = x, y, z are calculated by numerically solving the transport - transformation equation (1)

$$\frac{\partial}{\partial t}c(\vec{x},t)+[\vec{V}(\vec{x},t)\cdot\nabla\, c(\vec{x},t)]=\nabla\cdot\left[\vec{K}(\vec{x},t)\cdot\nabla c(\vec{x},t)\right]+S(\vec{x},t) \qquad (1)$$

where the second term on the left-hand side represents advection, $V(\vec{x},t)$ is the mean wind velocity (with horizontal and vertical components) and $S(\vec{x},t)$ includes emissions, source and sink terms of chemical transformation and deposition. The turbulent diffusion term $\nabla\cdot[K(\vec{x},t)\cdot\nabla c(\vec{x},t)]$ is written using the gradient transport theory, or the K-theory. The turbulent fluxes are assumed to be proportional to local mean concentration gradients according to equation (2), where $K(\vec{x},t)$ in units of m^2s^{-1} is called the eddy diffusivity, turbulent diffusion, turbulent transfer or gradient transfer coefficient (STULL, 1988):

$$\overline{c'V'_i} = -\, K_i\frac{\partial}{\partial i}c(\vec{x},t), \qquad i = x,y,z \qquad (2)$$

In solving equation (1) the following boundary conditions are used:

a) The initial and advected concentrations are known along all grid borders,
b) The surface dry deposition velocity defines the lowest vertical layer boundary condition, and
c) The mass of the air, used for the determination of the vertical velocity, is conserved.

Equation (1) is solved by the method of fractional steps described in YANENKO (1971) and MARCHUK (1975,1986). Following the principles of this method, the equation is decomposed into one-dimensional diffusion, advection and chemistry sub-problems which are solved successively, each sub-problem by an algorithm suitable to it. In order to ensure mass conservation, the vertical mass of each layer is transported instead of concentration when the advection is solved numerically.

There are some limitations on the use of the K-theory: the characteristic length and time scales for the changes in the real concentration field (including chemical transformation) should be large, compared with the corresponding scales for turbulent transport (SEINFELD, 1986). In the real atmosphere there are in some cases large eddies, associated with the rise of warm air parcels that carry heat from hot to cold places regardless of the local gradient, and the transport can then also occur up the gradient. The latter case implies that if the K-theory is applied, negative K values should be used. After STULL (1988), it is not recommended to use K-theory in convective mixed layers. In numerical grid models (e.g. HIRLAM, the ECMWF model, EURAD model) it is, however, used in all situations. In HILATAR, where horizontal diffusion is omitted, in the large-eddy situation the K-coefficients are large, the mixing in a vertical grid column is rapid, the profiles become well mixed (smooth), and the results do not appear to be non-physical.

1.3 Description of the grid

The HILATAR model uses the HIRLAM grid: vertically the lowest 10 layers are used, and horizontally the HIRLAM grid is divided by two or five in order to increase the resolution. The HIRLAM uses rotated spherical grid coordinates as its frame of reference in the horizontal and hybrid η terrain following coordinates vertically (HIRLAM, 1990). The η levels are related to the pressure by

$$\eta = \frac{p}{p_o} + A\left(1 - \frac{p_o}{p_s}\right) \tag{3}$$

where p_s is the model surface pressure, p_o is the reference pressure taken as 1000 hPa and A is a specified function of height. The model surface is the model topography (at η = 1), smoothed out in such a way that it fits the horizontal grid resolution. Near the model surface, the value of A is zero, so that here the η-surfaces follow the terrain. Further up in the atmosphere, A varies with height until A=η at the top of the model (on average 31 km above the surface of the earth), where η follows the pressure levels. The η parameter varies between [0,1], being 0 for p=0 at the upper model boundary, 1 at $p = p_s$ on the surface. If p(z) is solved from equation (1), $p(z)= A(z)p_o + p_s(\eta(z)-A(z))$. In HIRLAM the vertical grid is defined by using the pressure p_s at model level k: $p_k = (a_k + b_k p_s)$ and $\eta_k = (a_k/p_{st}+b_k)$, where the standard atmospheric pressure at sea level p_{st} = 1013.26 hPa. a_k=0 and b_k=1 at k=31, which is the η-layer close to the surface, and a_k=1 and b_k=0 for k=1, the highest layer of the model.

The vertical height of the HIRLAM levels above the surface of the earth (described by the average topography of the grid square) is calculated in HILATAR from the hydrostatic equilibrium $\frac{dp}{dz} = -\rho g$ and the ideal gas law: $p = \rho R_d T_v$, where T_v= virtual temperature = $T\{1.-(e/p)\ [1-R_d/R_v]\}^{-1}$, where $e = \rho_v R_v T$ is the water vapour pressure, R_v= 461.51 [J/(kg K)], and R_d = 287.05 [J/(kg K)]. T_v at level z can be approximated by $T_v(z) = T(z)\ \{1 + 0.61\ q(z)\}$, where q(z) is the specific humidity.

Thus $dz = -dp/(\rho g) = -R_d T_v/(\rho g)$, and by integration $z_k - z_{k-1} = -\frac{R_d}{g}\int_{p_{k-1}}^{p_k} T_v d(\ln p)$. In HIRLAM the geopotential height Φ is used instead of the height z,

$\Phi = \int_0^z g dz$, with $\Phi(z=0) = 0$ [J/kg]. Starting from the surface topography (expressed as Φ), $\Phi(z_k) = \Phi(z_{k-1}) + \frac{R_d \cdot T_v}{g} \ln\left(\frac{p_{z-1}}{p_z}\right)$, $z_k = \Phi(z_k)\ g_o^{-1}$ and we take $g = g_o = 9.80665$ m s^{-2}.

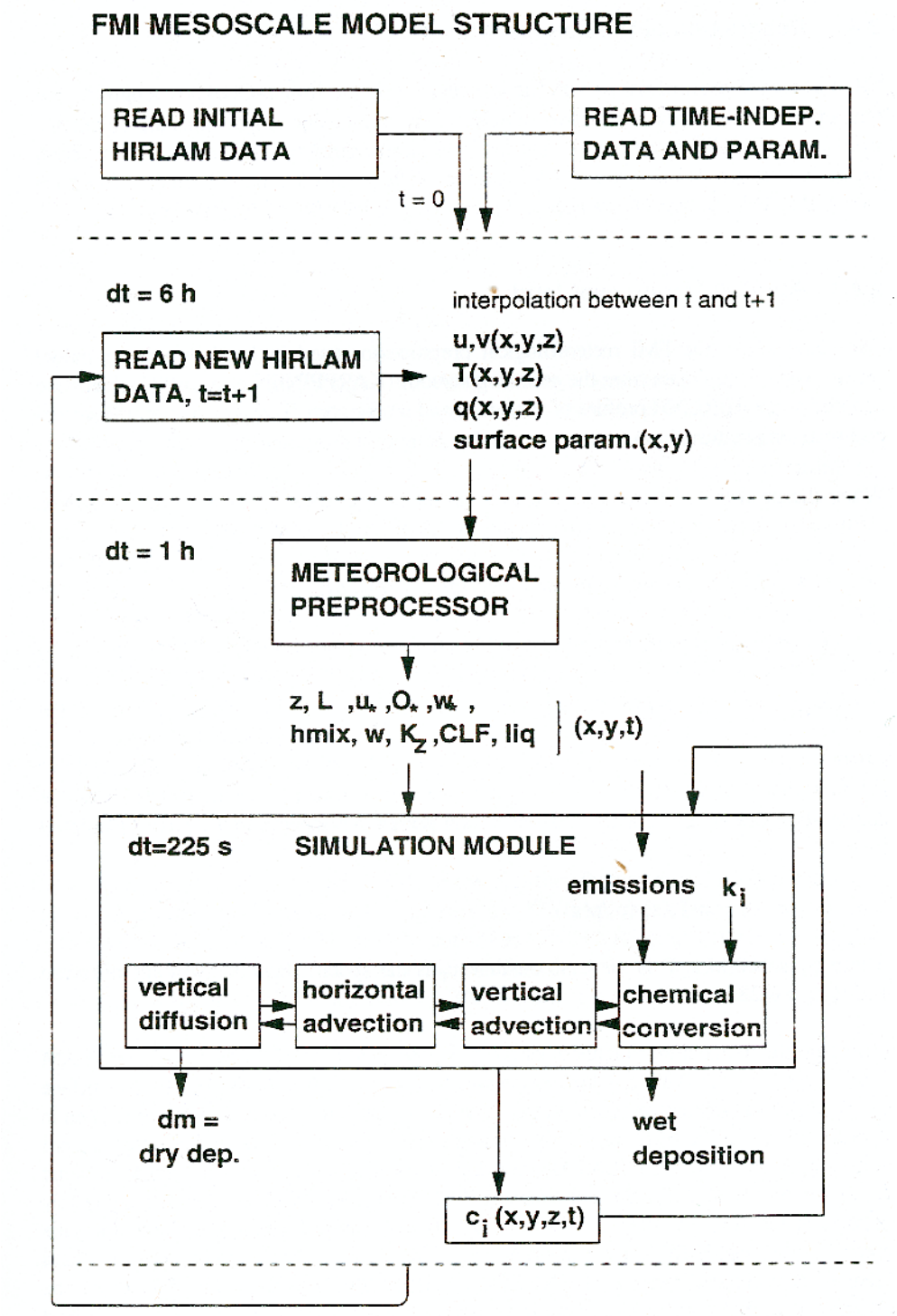

Fig. 1. Flow chart of the HILATAR model

1.4 Description of the boundary layer

The turbulence parameters, i.e. the friction velocity u_*, the Monin-Obukhov length L, the temperature scale θ_*, the convective velocity w_* and the mixing height (hmix) are calculated from the HIRLAM temperature, wind and specific humidity profiles, using two different methods over sea and land areas. The meteorological parameters have been calculated for each HIRLAM grid point in the area and interpolated afterwards to the simulation grid.

1.4.1 Parameterisation over land

Over land areas, the FMI meteorological pre-processor written by Pentti Vaajama for local dispersion model studies, and using vertical data from the sounding stations, has been adapted to use HIRLAM profiles of wind u(z), temperature T(z) and humidity. The potential temperature $\theta_v(z)$, instead of the dry potential temperature, is used.

When the profiles and the local surface roughness z_o are known, u_*, θ_* ja L are solved from:

$$u(z) = (u_* /\kappa)[\ln(z/z_0) - \Psi_M (z/L) + \Psi_M (z_0/L)], \quad (4)$$

$$\theta_v (z_1) - \theta_v (z_s) = (\theta_* /\kappa)[\ln(z_1/z_s) - \Psi_H(z_1/L) + \Psi_H(z_s/L)], \text{ and} \quad (5)$$

$$L = T_s u_*^2 /(\kappa g \theta_*) \quad (6)$$

where the subscript s refers to the 2 m height (close to the surface) value, z_1 is the height of the first model level (at about 31 m), κ is the von Karman constant (=0.4), g is the acceleration due to the gravity and the virtual potential temperature $\theta_v(z)$ is calculated from

$$\theta_v(z) = T_v(z) (p_o/p(z))^{R/cp} \quad (7)$$

where p_o is 100 kPa, R is the gas constant, c_p is the specific heat at constant pressure and $R/c_p = 0.286$.

Over land the momentum roughness length z_o is used as in the HIRLAM model (HIRLAM 1990, 1996). In the 0.25^o (28 km) resolution model, it is directly the HIRLAM surface roughness of the forecast model with the same resolution (the 0.25^o model has only been in operational use at the FMI since 1996, thus meteorological fields for earlier dates do not exist). In the 0.1^o (11 km) HILATAR model, z_o is calculated using the land use data, being set to 1 m for forest, 1.5 m for mountains, 0.0002 m over snow and according to a monthly dependent function for other surfaces and a wind-dependent formula over sea- and lake areas. The original HIRLAM z_o values are rather large over land areas when compared to the HEIKINHEIMO & HELLSTEN (1992) estimates, where the effective z_o in the close vicinity of coastal areas was typically 0.002 m, in Southern Finland typically 0.03-0.1 m.

The diabatic correction functions are from van ULDEN & HOLTSLAG (1985):

$$\Psi_M(\zeta) = [1-16(\zeta)]^{0.25} - 1, \quad \text{when } \zeta < 0, \tag{8}$$

$$= -17\{1-\exp[-0.29(\zeta)]\}, \quad \text{when } \zeta > 0,$$

$$\Psi_H(\zeta) = 2\ln\{0.5*(1+[1-16(\zeta)]^{0.5})\}, \quad \text{when } \zeta < 0, \text{ and} \tag{9}$$

$$= -5(\zeta) \quad \text{when } \zeta > 0,$$

where $\zeta = z/L$.

According to observational studies, the wind velocity, temperature and moisture do not reach their surface values at the same height (which is characterised by z_o) (BRUTSAERT, 1982). Over inhomogeneous surfaces, the roughness length for heat can be up to four orders of magnitude smaller than that applied for momentum. In SASS, (1992) case study simulations for estimating road temperatures are described. The z_o was varied from 1 to 10^{-5} m, and the best consistency with measurements was obtained with the smallest z_o. It is evident that use of the physical roughness is not the best way to describe the connection of temperature or moisture profiles with the ground below, as it is for the wind profile, since other surface characteristics (e.g. capability to absorb or emit heat or moisture etc.) may even be more important. In the ABL module, $\Psi_h(z/L)$ is defined to be independent of z_h. In BRUTSAERT (1982) several alternative formulae for determining the roughness for scalar, water vapour or sensible heat have been proposed.

1.4.2 Parameterisation over sea areas

Over sea areas, where the diabatic effect of the moisture flux on buoyancy and especially the interaction between the surface roughness and the wind are important, the iterative method described in JOFFRE (1988) and applied in LINDFORS et al. (1991) is used. The method starts by defining a 10-m wind velocity - V_{10} - dependent roughness length z_o from a first approximation of the friction velocity. This is made using the drag coefficient C_D:

$$C_D = (0.49 + 0.065\, V_{10})\, 10^{-3} \quad \text{if } V_{10} > 11 \text{ m s}^{-1}, \tag{10}$$

$$C_D = 0.0012 \quad \text{if } V_{10} \le 11 \text{ m s}^{-1},$$

$$C_D = 0.0015 \quad \text{if the sea is covered with ice.}$$

As a first guess

$$u^* = C_D^{0.5}\, V_{10}, \tag{11}$$

and

$$z_o = 0.0144\, u_*^2/g + 0.13\, \nu/u_*, \tag{12}$$

$$z_h = 20\, z_o \exp(-7.3\, \kappa\, Re^{1/4}\, Pr^{1/2}), \quad \text{if } Re > 0.15,$$

$$z_h = 30\, \nu/u_* \exp(-13.6\, \kappa\, Pr^{2/3}), \quad \text{if } Re \le 0.15,$$

$$z_e = 20\, z_o \exp(-7.3\, \kappa\, Re^{1/4}\, Sc^{1/2}), \quad \text{if } Re > 0.15,$$

$$z_e = 30\, \nu/u_* \exp(-13.6\, \kappa\, Sc^{2/3}), \quad \text{if } Re \le 0.15,$$

where z_h is the roughness length for temperature and z_e for humidity. The Reynolds number is $Re = u_* z_o/\nu$, the molecular Schmidt number Sc is the ratio of the kinematic viscosity of air ν to the molecular diffusivity of the gas D_x, $Sc = \nu / D_x$, where $\nu = 0.15$ $cm^2\ s^{-1}$, the turbulent Prandtl number $Pr = 0.711$, $D_{NO2} = 0.14\ cm^2\ s^{-1}$, $D_{HNO3} = D_{SO2} = 0.12\ cm^2\ s^{-1}$, $D_{pan} = 0.085$ and $D_{NH3} = 0.227\ cm^2\ s^{-1}$

The first value for the stability parameter ζ is defined using the bulk Richardson number Ri as $\zeta = Ri$, if $Ri \leq 0$, (neutral or unstable ABL), and $\zeta = Ri \cdot (1-Ri)^{-1}$, if $Ri > 0$, (stable ABL). $Ri = (g/T) \cdot (\theta - T_s) \cdot z_{ref} / V_{10}^2$, the potential temperature $\theta = T \cdot (1000/p)^{R/Cp}$, and T_s is the HIRLAM sea surface temperature. The diabatic correction functions for momentum ψ_M, heat ψ_H and moisture ψ_E are the STULL (1988) functions;

$$\psi_M = \psi_H = \psi_E = -5\ \zeta\ , \qquad \text{if Ri or } \zeta > 0, \quad (13)$$

$$\psi_M = 2\ \ln\{(1+X)/2\} + \ln\{(1+X^2)/2\} - 2\ \text{Arctan}(X) + \pi/2, \qquad \text{if Ri, } \zeta < 0$$

$$\psi_H = \psi_E = 2\ \ln\{(1+X^2)/2\} \qquad \text{if Ri, } \zeta < 0, \text{ and}$$

$$X = (1-16\ \zeta)^{1/4}\ .$$

The revised estimates for u_*, T_*, q_* and L_* are, using different values for the surface roughness for heat (z_h), momentum (z_o) and moisture (z_e):

$$u_* = \kappa\ V_{10}\ \{\ln(z_a/z_o) - \psi_M\}^{-1} \qquad (14)$$
$$\theta_* = \kappa\ (\theta - T_s)\ \{\ln(z_a/z_h) - \psi_H\}^{-1}$$
$$q_* = \kappa\ (q - q_s)\ \{\ln(z_a/z_e) - \psi_E\}^{-1}$$

$$L_* = (L^{-1} + L_q^{-1})^{-1}\ , \qquad (15)$$

where:

$$L = T_2 u_*^2 / (kg\theta_*) \qquad (16)$$
$$L_q = u_*^2 T_v / (0.61\ g\ \kappa\ T_2\ q_*)$$

where again subscript s refers to the sea surface value, and subscript 2 to the value in air at a height of 2 metres, and both values are from the HIRLAM data base. The iteration proceeds by defining new z_o, z_h and z_e, new ζ, etc., until a satisfactory convergence for u_* is reached.

The diabatic correction functions for moisture and heat are assumed to be identical and similar to those of van ULDEN & HOLTSLAG (1985) over land areas. For momentum, ψ_M differs from the profile function over land. The initial method has been left unchanged, because it has not been proven which profile function is the best in marine or continental conditions, and the boundary layer parameter estimation methods are independent of each other. Also the stability situation is generally different over land and sea areas: thus; in any case, the profile functions will not be, and do not have to be, the same. The profile functions are only used for iteration of the stability parameters from existing profiles, not for calculation of any vertical quantity (wind, moisture or temperature, which are taken directly from HIRLAM). In coastal areas the friction

velocity and other ABL parameters are surface-coverage-weighted averages of sea and land values.

1.4.3 Height of the mixing layer, and vertical velocity

The mixing layer height is calculated with the FMI local dispersion model ABL pre-processor algorithm using the HIRLAM virtual potential temperature, instead of the original dry potential temperature profile $\theta_v(z)$ from soundings. During unstable situations hmix is evaluated from the moist potential temperature profile by searching for the first inversion level where $\theta_v(z)$ increases with height. In stable and near-neutral situations an analytical form is used. Hmix is a function of the $\theta_v(z)$ vertical gradient $\delta\theta_v/\delta z$ =G1 between the lowest model level and a height of 2m above the surface, as follows:

$$\text{hmix} = a / (G1 + b) \qquad \text{if } G1 \geq 0.01\ ^{o}\text{K m}^{-1}, \tag{17}$$

$$\text{hmix} = z_{i-1} + [DH - \theta_v(z_{i-1})] / G2 \qquad \text{if } 0 \leq G1 < 0.01\ ^{o}\text{K m}^{-1},$$

where

$$DH = \theta_v(2\text{ m}) + G1 \cdot a / (G1 + b), \tag{18}$$

$$G2 = [\theta_v(z_i) - \theta_v(z_{i-1})] \cdot [z_i - z_{i-1}]^{-1},$$

$a = 4.5\ ^{o}\text{K}$, $b = 0.005\ ^{o}\text{K m}^{-1}$ and z_i is the first model level at which $\theta_v(z_i) > DH$.

During stable situations, hmix can vary from 900 m to very low values, depending on the inversion strength; in the simulations a minimum value of 150 m has been used.

In the HILATAR model, the vertical velocity w between the original HIRLAM η layers is calculated afterwards from the HIRLAM horizontal wind fields, starting from the surface (where w = 0), and forcing the mass flux sum across all the sides of each model box boundary to be conserved:

$$\sum_i \frac{\Delta m_i}{\Delta t} = \sum_i \frac{\Delta(V_i \rho_i)}{\Delta t} = \sum_i (\Delta A_i \cdot \Delta\rho_i \cdot \Delta\vec{u}_i - \Delta A_{i-1} \cdot \Delta\rho_{i-1} \cdot \Delta\vec{u}_{i-1}) = 0. \tag{19}$$

where i = x,y,z, at each grid cell face, $\vec{u}$ = u,v,w and $\Delta A = \Delta y_i \cdot \Delta z_i$ in the x-direction with wind component u, etc. The vertical wind velocity w is solved from the equation assuming that below 3 km the air is incompressible (ρ = p/RT stays constant, thus instant horizontal and vertical pressure and temperature gradients, between two adjacent cells within a 11 - 28 km horizontal and a 30-500 m vertical distance, are assumed to be negligible).

1.5 Vertical diffusion

K can be defined differently for momentum (K_M), heat (K_H) and moisture (K_E). It has been concluded from some experiments that, during neutral situations, the most likely values are $K_E = K_H = 1.35\ K_M$. Several approaches for parameterisation of the eddy diffusivity are listed in STULL (1988), and for a FMI local scale model in NIKMO et al. (1997).

The eddy diffusion coefficient parameterisation used here is based on the scaling regimes (HOLTSLAG & NIEUWSTADT, 1986) presented in HASS (1991). The ABL is scaled into different regimes, each with a specific turbulent structure, according to the dimensionless stability h/L and the dimensionless height z/h, where h is used for hmix.

In the surface layer, which is defined as the first 10 % of the ABL (z/h < 0.1), the fluxes are nearly constant, and in a neutral and stable boundary layer K_z is

$$K_z = u_* \kappa z (1 - z/h)^2 [\ \varphi_H(z/L)\ ]^{-1}, \tag{20}$$

where

$$\begin{aligned} \varphi_H(z/L) &= 0.74\ (\ 1 - 9\ z/L\ )^{-0.5}, && \text{if } z/L \le 0 \\ &= 0.74 + 4.7\ z/L, && \text{if } 0 < z/L < 1. \end{aligned} \tag{21}$$

During stable and near-neutral conditions, the surface layer formulation is applied to the rest of the ABL; however, neutral conditions are assumed when h/L < 1. For stable conditions above the surface layer, if z/L > 1, $\varphi_H(z/L)$ is prevented from becoming too large by applying the formula of HOLTSLAG et al. (1990):

$$\varphi_H(z/L) = 4.7 + 0.74\ z/L. \tag{22}$$

In the convective boundary layer, the convective velocity w_* is the scaling velocity during unstable conditions (L<0), and

$$K_z = w_* \kappa z [\ 1 - z/h\ ], \tag{23}$$

where

$$w_* = [\ (g/\theta_v)h\ H_s]^{1/3} = u_*\ [-h/(\kappa L\ )\ ]^{1/3}, \tag{24}$$

according to the Obukhov length definition in STULL, (1988). Because the EMEP model ABL height is occasionally higher than that calculated from the HIRLAM profile, weak mixing across the boundary layer was necessary so that the background concentrations, calculated with the EMEP-model, which were partly mixed into the free troposphere, could make a contribution to the dry deposition and surface concentrations, not only to wet deposition. Thus at the mixing layer height K_z was set to be 0.5 $m^2\ s^{-1}$. Above the ABL, a constant value of 2 $m^2 s^{-1}$, was used for K_z in the reported applications; the HASS's (1991) formulation did give rather high values in some situations, and it can be adopted into the model in the near future.

1.6 Chemistry submodel

1.6.1 Reactions and equations

In the model the following gaseous and particle concentrations are calculated:

NO_x(g), HNO_3(g), NO_3(p), PAN(g), NH_4NO_3(p), NH_3(g), SO_2(g), SO_4(p) and $(NH_4)_{1.5}SO_4$(p),

where PAN is peroxyacetyl nitrate and NO_x = NO + NO_2. NO is not a variable because its temporal value can be calculated if ozone and peroxy radical concentrations are known. The chemistry module is the EMEP-MSC-W code (IVERSEN et al., 1989) with the following modifications:

- Sulphur dioxide is described with two variables; SO_2 is assumed to be emitted as $SO_{2,non\text{-}liq}$, which is in non-scavengable form for correction of the local wet deposition, and it is transformed to a scavengable $SO_{2,liq}$ in a half-life of 1.5 hours,
- Inside clouds, the sulphate production rate differs from the clear sky conversion rate,
- local deposition correction coefficients are not used,
- nitrate and sulphur particles are split into two size classes,
- the most recently-available rate coefficients are applied,
- dry deposition is used as a boundary coefficient of the vertical diffusion equation; only the gravitational settling of the particles is described in the chemistry submodel as a sink term,
- the scavenging and dry deposition sink-terms are rewritten as described in the other chapters, and
- the emission terms in the chemistry module are re-classified (instead of the grid sum of high and low level emissions, individual stack sources with an estimation of the effective emission height using standard plume rise equations are employed whenever an emission inventory is available).

The conversion equations with the respective transformation rate coefficients are

$$\frac{d}{dt}[NO_2] = EMI_{NO_x} + k_{t,pan}\cdot[CH_3C(O)O_2NO_2]\cdot[PAN] - \left\{k_{OH,NO_2}\cdot[OH] + k_{pan,CH_3CO_3}\cdot[CH_3C(O)O_2] + k_{O_3,NO_2}\cdot[O_3] + \Lambda_{NO_x}\right\}\cdot[NO_2], \quad (25)$$

$$\frac{d}{dt}[PAN] = k_{pan,CH_3CO_3}\cdot[CH_3C(O)O_2]\cdot[NO_2] - \left\{k_{t,pan}\cdot[CH_3C(O)O_2NO_2] + \Lambda_{PAN}\right\}\cdot[PAN],$$

$$\frac{d}{dt}[HNO_3] = k_{OH,NO_2}\cdot[OH]\cdot[NO_2] + k_{NO_3}\cdot[NO_3] - \left\{k_{HNO_3} + \Lambda_{HNO_3} + \Delta_{NH_4NO_3}\right\}\cdot[HNO_3],$$

$$\frac{d}{dt}[NO_3] = k_{HNO_3}\cdot[HNO_3] + k_{O_3,NO_2}\cdot[O_3]\cdot[NO_2] - \left\{k_{NO_3} + \Lambda_{NO3}\right\}\cdot[NO_3],$$

$$\frac{d}{dt}[NH_3] = EMI_{NH_3} - \Lambda_{NH_3}\cdot[NH_3] - \left\{\Delta_{(NH_4)_{1.5}SO_4} + \Delta_{NH_4NO_3}\right\}\cdot[NH_3],$$

$$\frac{d}{dt}[SO_2]_{non\text{-}liq} = EMI_{SO_2} - \{k_{OH,SO_2} \cdot [OH] + k_{SO_2}\} \cdot [SO_2]_{non\text{-}liq},$$

$$\frac{d}{dt}[SO_2]_{liq} = -\{\Lambda_{SO_2} + k_{OH,SO_2} \cdot [OH] + k_{SO_2aq}\} \cdot [SO_2]_{liq} + k_{SO_2} \cdot [SO_2]_{non\text{-}liq},$$

$$\frac{d}{dt}[SO_4]_{1,2} = EMI_{SO_4} - \left\{ \Lambda_{SO_4} + \Delta_{(NH_4)_{1.5}SO_4} + \frac{v_{d(grav)1,2}}{hmix} \right\} \cdot [SO_4]_{1,2} + k_{OH,SO_2} \cdot [OH] \cdot [SO_2]_{liq+non\text{-}liq} + k_{SO_2aq} \cdot [SO_2]_{liq},$$

$$\frac{d}{dt}[NH_4NH_3] = \Delta_{NH_4NO_3} \cdot [NH_3] + \Delta_{NH_4NO_3} \cdot [HNO_3] - \Lambda_{NH_4NO_3} \cdot [NH_4NH_3],$$

$$\frac{d}{dt}[NH_4SO_4] = \Delta_{(NH_4)_{1.5}SO_4} \cdot [NH_3] + \Delta_{(NH_4)_{1.5}SO_4} \cdot [SO_4]_{1,2} - \Lambda_{(NH_4)_{1.5}SO_4} \cdot [NH_4SO_4],$$

where

EMI_x	=	emission of compound x,	$[(molec \cdot m^3) \cdot s^{-1}]$
Λ_x	=	scavenging velocity below and in cloud for compound x,	$[s^{-1}]$,
$k_{i,j}$	=	reaction rate of compound i with compound j,	
$k_{t,j}$	=	decay rate of compound j with temperature,	
$\Delta_{(NH_4)_{1.5}SO_4}$	=	formation rate of ammonium sulphate,	
$\Delta_{NH_4NO_3}$	=	formation rate of ammonium nitrate,	
$v_{d(grav),i}$	=	gravitational settling velocity of the particles in size class i.	

1.6.2 Reaction rates

The reactions are either uni-, bi-, or termolecular. The EMEP reaction rate coefficients have been re-evaluated by the LACTOZ (EUROTRAC sub-project Laboratory Studies of chemistry Related to Tropospheric Ozone) steering group. The HILATAR-model rate constants have been changed following the recommendations of the evaluation report (WIRTZ et al., 1994).

The OH-reaction with x=SO_2 and x=NO_2 is pressure-dependent, and the termolecular reaction rates are calculated from FINLAYSON-PITTS & PITTS (1986):

$$k_{OH,x} = \frac{k_{o,x} \cdot [M] \cdot 10^{-6}}{1 + \frac{k_{o,x}[M]}{k_{\infty,x}}} \cdot F_c^{\,b} \qquad [cm^3 \cdot s^{-1} \cdot molec^{-1}], \tag{26}$$

where $b = \left\{ 1 + \left[\log\left(\frac{k_{o,x} \cdot [M]}{k_{\infty,x}} \right) \cdot N^{-1} \right]^2 \right\}^{-1}$,

$$M = 2.45 \cdot 10^{-19} \cdot \left(\frac{300}{T} \right) \cdot \left(\frac{p}{1013{,}25} \right) \quad [molec \cdot cm^3],$$

T is in units of K, and p in mb, $N = 0.75 - 1.27 \log_{10} F_c$ and $F_c = 0.45$.

For y = PAN, rate constants as a function of gas density are presented in a reduced, fall-off regime form (LIGHTFOOT et al., 1992):

$$\log\frac{k}{k_{\infty,y}} = \log\left\{\left(\frac{k_{o,y}}{k_{\infty}}\right)\cdot\left(1+\frac{k_{o,y}}{k_{\infty,y}}\right)^{-1}\right\} + \log F_c \cdot \left[1+\log\left(\frac{k_{o,y}}{k_{\infty,y}}\right)/N(F_{c,y})\right]^{-2} \quad (2$$

with $N(F_{c,y}) = 0.75 - 1.27 \log F_{c,y}$ and $F_{c,y} = 0.3$.

The uni- and bimolecular reaction rates are:

k_{SO_2} = transformation rate of SO_2 from non-scavengable to scavengable sulphur dioxide; $k_{SO_2} = \ln 2 / \tau$ with $\tau = 1.5$ h,

$k_{SO_2}aq$ = transformation rate of SO_2 into SO_4 in cloud, described below,

$k_{O_3,NO_2} = 1.2 \cdot 10^{-19} \cdot e^{-2450/T}$, $\left[m^3 \cdot s^{-1} \cdot molec^{-1}\right]$

$k_{NO_3} = 0.5 \cdot 10^{-5}$, $\left[s^{-1}\right]$

$k_{HNO_3} = 1 \cdot 10^{-5}$, $\left[s^{-1}\right]$,

Reaction between NO_2 and O_3 leads to formation of nitrate radical, $NO_3^{\cdot}$, which is rapidly photolyzed or reacts with NO back to NO_2 during the day. During the night the reaction with the rate k_{O_3,NO_2} proceeds with the following steps: $NO_2 + O_3 \rightarrow NO_3^{\cdot} + O_2$; $NO_3^{\cdot} + NO_2 <-- > N_2O_5$; $N_2O_5 + H_2O \rightarrow 2\ NO_3^- + 2\ H^+$, where the first step is the rate-determining for the net reaction (see e.g. SANDNES, 1993), and the reaction proceeds on the surface of wetted particles. This is quite an old formulation, in the photochemical models alternative reactions of the nitrate radical e.g. with VOC are important (DIMITROULOPOULOU & MARS, 1997). For the termolecular OH-reaction rates with NO_2 and SO_2, the parameters are those of Table 2.

Table 2. Parameters needed in defining termolecular reaction rates.

Compound	$k_o \cdot [M]$	unit
NO_2	$2.6 \cdot 10^{-30} \cdot (T/300)^{-2.9}$	$\left[cm^6 \cdot s^{-1} \cdot molec^{-2}\right]$
SO_2	$4.0 \cdot 10^{-31} \cdot (T/300)^{-3.3}$	$\left[cm^6 \cdot s^{-1} \cdot molec^{-2}\right]$
	k_o /[M]	
PAN, decomposition	$4.9 \cdot 10^{-3} \cdot e^{-100.6 \cdot 10^3/RT}$	$\left[cm^3 \cdot s^{-1} \cdot molec^{-1}\right]$
PAN, recombination	$4.9 \cdot 10^{-3} \cdot (T/298)^{-7.1}$	$\left[cm^3 \cdot s^{-1} \cdot molec^{-1}\right]$
	k_∞	
NO_2	$3.2 \cdot 10^{-11}$	$\left[cm^3 \cdot s^{-1} \cdot molec^{-1}\right]$
SO_2	$2.0 \cdot 10^{-12}$	$\left[cm^3 \cdot s^{-1} \cdot molec^{-1}\right]$
PAN, decomposition	$3.7 \cdot 10^{16} \cdot e^{-113 \cdot 10^3/RT} \cdot M$	s^{-1}
PAN, recombination	$1.21 \cdot 10^{-11} \cdot (T/298)^{-0.9}$	$\left[cm^3 \cdot s^{-1} \cdot molec^{-1}\right]$

where RT = 8.3144 T(x,z) [J $^oK^{-1}$ $mole^{-1}$] and the OH reaction rates for NO_2 and SO_2 are originally from deMORE et al. (1992). In comparison, the EMEP (and old Finox-model) NO_2 oxidation rate with the OH radical was $k_{OH,NO_2} = 1.1\text{-}1.4 \cdot 10^{-17}$, $\left[m^3 \cdot s^{-1} \cdot molec^{-1}\right]$.

The ammonium sulphate and nitrate formation rates are calculated as described in the EMEP MSC-W acid deposition model (IVERSEN et al., 1991). Gaseous ammonia in the air reacts immediately with sulphate aerosols forming ammonium sulphate particles, $(NH_4)_{1.5}SO_4$, which is a notation for the sum of $(NH_4)_2SO_4$ and NH_4HSO_4. The process proceeds until one of the precursor components, NH_3 or $SO_4^=$ has been totally used. The rest of the gaseous ammonia reacts with nitric acid. The resulting ammonium nitrate NH_4NO_3, is, at temperatures below 170 ^oC, in equilibrium with ammonia and nitric acid:

$$\left[HNO_3\right] + \left[NH_3\right] \Leftrightarrow \left[NH_4NO_3\right], \tag{28}$$

and exists either in particle (at 25^{o}C below 62 % RH) or in dissolved form. The equilibrium constant is related to the partial pressures of NH_3 and HNO_3. The reaction is recursive: if the relative humidity, RH, decreases enough (to below a critical value), the gaseous components are released. At equilibrium:

$$p_{[NH_3]} \cdot \; p_{[HNO_3]} = K_{eq}. \tag{29}$$

The NH_3 concentration can be solved from the last expression. The resulting equilibrium concentration will be

$$\left[NH_3\right] = \frac{\left[NH_3\right] - \left[HNO_3\right]}{2} + \sqrt{\frac{\left\{\left[NH_3\right] - \left[HNO_3\right]\right\}^2}{4} + K_{eq}} \tag{30}$$

The equilibrium coefficient K_{eq} is a function of temperature T and relative humidity RH. For particulate NH_4NO_3, K_{eq} is in ppb^2, and according to FINLAYSON-PITTS & PITTS (1986) and SEINFELD (1986): $\ln K_{eq} = 84.6 - 24220\ T^{-1} - 6.1 \ln (T/298)$.

When the relative humidity RH increases, e.g. at T = 25^{o}C, RH > 62 %, ammonium nitrate particles are dissolved. The point of deliquescence for a given temperature for the relative RH_d (%) is: $\ln RH_d = 856.23\ T^{-1} + 1.2306$, and the equilibrium coefficient k_{eq} in $(molec\ cm^{-3})^2$ is :

$$\ln k_{eq} = 70.78 - 24220\ T^{-1} - 6.1 \ln (T\ 298^{-1}), \tag{31}$$

and:

$$\ln K_{eq} = \ln k_{eq}, \qquad \text{if } RH < RH_d, \tag{32}$$

$$= \quad \ln k_{eq} - \frac{20.75 + \ln k_{eq}}{101 - RH} \cdot \frac{RH - RH_d}{101 - RH_d}, \qquad \text{if } RH \geq RH_d.$$

Ammonia also reacts with OH according to: $NH_3 + OH \rightarrow NH_2 + H_2O$, with k = $1.6 \cdot 10^{-13}$ (molecules $cm^{-3})^{-1}$ s^{-1} (FINLAYSON-PITTS & PITTS, 1986). However, in the model neither the NH_2-radical nor its decay products are variables, and the lifetime of NH_3 for this reaction is 72 days (with $[OH]=1 \cdot 10^{-6}$ cm^{-3}), for which reason this reaction pathway has not been considered relevant.

1.7 Transformation rates in clouds

1.7.1 Mechanisms

Already HEGG (1985) estimated that the oxidation of sulphur dioxide (SO_2) to sulphate particles in clouds is the dominant SO_2 conversion mechanism in the troposphere, and recently (e.g. in PHAM et al., 1995; CHIN et al., 1996; FEICHTER et al., 1996) it is suggested that from 70 to 95 % of the total sulphur is oxidised inside clouds. The aqueous chemistry associated with the clouds and precipitation scavenging tends to be non-linear. Precipitation scavenging is strongly affected by the dynamics of the specific weather systems. The deposition process becomes non-linear especially in winter, when the SO_2 oxidation rate in clouds is limited by the oxidant availability, or near highly-polluted areas where the droplets may become saturated with pollutants, and still further because the scavenging efficiencies of SO_2 and sulphate are not equal. The dry-deposition process is also non-linear in high concentration areas (NAPAP, 1991).

Nitrogen oxides (NO_x) are scavenged only after they have been converted to nitric acid or particles. The oxidation involves both gas-phase chemistry and the reactions of the products on the surface of wetted particles. The principal daytime conversion mechanism with the hydroxyl radical, as too the night-time conversion path, are non-linear (NAPAP, 1991).

Numerous field studies have identified acidic sulphate aerosols and some gases e.g. SO_2 and HNO_3 as well as organic acids, as major precursors for the formation of acidity in cloud or rainwater (WALCEK & TAYLOR, 1986). The conversion rate of SO_2 to sulphate in the clouds is rapid; MÖLLER & MAUERSBERGER (1992) estimated that the liquid phase sulphate production is between 10^2 and 10^4 times more effective than in gaseous production, in the same air volume, depending on season, time of day and oxidant. When comparing liquid with homogeneous gas phase transformation rates, the aqueous phase rate has to be averaged in time and space. Also the high reaction rate is sustained for relatively short times, since the individual reactions are frequently pH or reactant-limited.

The rate of aqueous phase sulphur oxidation depends on the concentrations of the dissolved reactants and on the pH of the droplet. Possible mechanisms are sulphate production by uncatalyzed oxidation with O_2, oxidation by hydrogen peroxide, ozone,

methyl hydrogen peroxide, peroxyacetic acid, or by iron or manganese-catalyzed reactions (MÖLLER, 1980).

The transformation rate of SO_2 into SO_4 in a cloudy environment is approximated by a gas-phase reaction. It was estimated by the following method: the 1-2 day average SO_4 production rate of a specific cloud module has been compared with the SO_4 yield rate of the HILATAR gas phase reaction module, and the first-order reaction rate which gave the best fit between the models at 60 ^{o}N latitude, when season (oxidant concentrations), temperature, pH, cloudiness and cloud type (liquid water content) were varied, was selected. Its first-order rate takes into account the annual variation of both main oxidants' (O_3 and H_2O_2) concentrations, and the temperature dependence of the solubility of the faster oxidant, H_2O_2.

1.7.2 Cloud submodule

The cloud submodule, containing the variables and the sink and source terms of the HILATAR chemistry module with two-phase chemistry of both nitrogen and sulphur, is a 1D box model without any dilution or transport features. It was developed in order to study the dynamics and transformation of sulphur compounds with alkalic particles in the plumes of Estonian oil shale power plants.

The reaction rate in air at level z with maximum fractional cloud cover above, $clf_M(x,z)$, is $k_{OH,SO_2} = k_{OH,SO_2} \square(1.-0.25*clf_M(x,z))$. All reactions are assumed to happen in the gas phase, if the temperature T(x,z) > 250 ^{o}K. Above 250 ^{o}K, at level z with fractional cloud cover clf(x,z) and liquid water content liq(x,z), the best fit between the models inside the cloudy part has been found to be k_{SO_2aq} in units s^{-1}:

$$k_{SO_2aq} = clf(x,z) \cdot f_2(x,z,t,d) \cdot liq(x,z) \cdot \min(1., \frac{(T(x,z) - T_1)}{T_0 - T_1}) \qquad (33)$$

where $f_2(x,z,t,d) = c(x,t) \cdot f_1(ox) \cdot (a + b \cdot t(d))$, $t(d) = \sin(\pi \cdot |(d-1.)/365|)$, d = cumulative day, c(ix,t) = 30 after sunrise, 9 with no light, a, b, T_o and T_1 are 15, 10, 273 and 250, respectively, and $f_1(ox) = [H_2O_2](x,t) \cdot k_{H_2O_2}{}^{1.4}$,

where $k_{H_2O_2} = k_{1,SO_2} \cdot H_{1,H_2O_2} = 1.66 \cdot 10^{-2} \cdot e^{1964 \cdot \left[\frac{1}{T} - \frac{1}{298}\right]} \cdot 1.76 \cdot e^{3120 \cdot \left[\frac{1}{T} - \frac{1}{298}\right]}$,

$H_{1,H2O2}$ is the Henry's law constant for H_2O_2, $K_{1,SO2}$ is the sulphur oxidation rate inside droplets, from WALCECK & TAYLOR (1986). The H_2O_2 background concentration varies from 0.1 ppb (December and January) to 1 ppb (July and August) and this concentration is latitude dependent.

The results of the model simulations depend on the emission ratios used. In the southern part of the model domain, where there are more NH_3 emissions, the conversion is slower, because the pH is higher. Tests have been made in varying pH conditions. The pH-dependent rates could not be used in real transport simulations, because only a fraction of the compounds that contribute to the pH of a cloud droplet are included in the chemistry module - i.e. there are not enough data about alkalic dust emissions.

1.7.3 Numerical conversion rates

The rate formula (33) has been used in weighting the sulphur production rate inside and outside the clouds. Inside cloudy areas, the model typically gives volume average rates of the order of $4 \cdot 10^{-5}$ s^{-1} during summer days and $1.5 \cdot 10^{-5}$ s^{-1} during winter days, $1.2 \cdot 10^{-5}$ s^{-1} during summer nights and $0.2 \cdot 10^{-5}$ s^{-1} during winter nights. These reaction rates are averages over the cloud volume and 24-48 hour time. In cloudy areas these conversion rates are about 100 times higher than the EMEP-MSC-W model sulphur oxidation rates, but comparable to the mean tropospheric oxidation rates of MÖLLER (1980) in s^{-1}: $R_{particle} = (0.1\text{-}10) \cdot 10^{-5} \cdot [SO_2]$, $R_{aq} = 5 \cdot 10^{-5} \cdot [SO_2]$, $R_{hom} = 0.12 \cdot 10^{-5} \cdot [SO_2]$ and $R_{h\nu} = 0.01 \cdot 10^{-5} \cdot [SO_2]$. Here $R_{particle}$, R_{aq}, R_{hom} and $R_{h\nu}$ refer to surface reactions of SO_2 with particles, liquid phase oxidation, homogeneous gas-phase reactions (with OH, HO_2 or RO_2-radicals) and photochemical oxidation, respectively. They are modest in comparison with the aqueous phase rate constant expressed as a pseudo first-order reaction of gaseous SO_2 used in BENKOVITZ et al. (1994) (the reaction with H_2O_2 is considered to occur instantaneously, with O_3 the rate is $1.68 \cdot 10^{-3}$ s^{-1} with pH = 4.5 and $[O_3]$ = 37 ppb). Maybe, over remote areas, e.g. oceans, the reactions are not oxidant-limited; however, this kind of 11-min half-life was assumed to be impossible to maintain during long-range transport over polluted areas.

In the upper layers, where the temperature is lower, the conversion rates fall to zero in clouds without liquid water (with temperatures below 250 ^oK). The monthly grid average conversion rates at the first model layer in January varied between 0.1-2.5 $\cdot 10^{-6}$ s^{-1}, in July from $2 \cdot 10^{-6}$ up to $1.2 \cdot 10^{-5}$ s^{-1}.

If the HILATAR model sulphur oxidation rates are compared with the EMEP-model rates, which vary between $0.11 \cdot 10^{-7}$ s^{-1} in winter and $5 \cdot 10^{-6}$ s^{-1} during summer, the geographical differences are significant. During summertime, the EMEP rate lies in the middle of the monthly average variation of the HILATAR model, but the winter average EMEP conversion rate was slower than the mild and moist January 1993 HILATAR model SO_4-production rate in the near-surface layers.

1.7.4 Cloud cover

In HIRLAM (1990), the fractional cloud cover clf(x,z) is parameterized in terms of relative humidity RH according to

$$clf(x,z) = [RH(x,z) - RH_{cr}]^2 / [1 - RH_{cr}] \qquad (34)$$

where $RH_{cr} = 0.9$, $RH(x,z) = q(x,z)/q_s(x,z)$, q is the specific humidity, q_s, the saturation specific humidity. RH(x,z) is calculated by

$$RH(x,z) = \left(\frac{R_v}{R_d} \frac{p(x,z) \cdot q(x,z)}{e_s(T(x,z))}\right) \cdot \frac{(p(x,z) - e_s(T(x,z))}{p(x,z) - \frac{R_v}{R_d} p(x,z) \cdot q(x,z)} \qquad (35)$$

$e_s(T(x,z))$, the saturation vapour pressure at temperature T(x,z) expressed in ^oC is

$$e_s(T(x,z)) = 6.107 \cdot 10^{a\,T(x,z)/[b + T(x,z)]} \quad (36)$$

with a= 7.5 and b=237 if T(x,z) > -5., otherwise a=9.5 and b=265.5.

The liquid water content (lwc) of the clouds is assumed to be lwc = 0.1 g m^{-3} in the basic case (clouds without precipitation), lwc = 0.3 g m^{-3} if large-scale precipitation is predicted, and lwc = 1 g m^{-3} if convective precipitation is predicted, or if kind > 15, where kind is defined on the main pressure levels (850 and 700 mb) as kind = T(850)-T(500)+TD(850) - {T(700)-TD(700)}, where TD(z) is the dew-point temperature. Over sea areas, when T(850) - T_s >11 ^oK, and T_s > 273 ^oK, and T(850) < 268 ^oK, where T_s is the sea surface temperature, cold advection over sea areas and lwc = 0.8 g m^{-3} are assumed. During windy conditions over open sea areas, the surface moisture of the lowest levels is slightly increased by requiring that clf(x,1) is the maximum of clf(x,1) and $0.8 \cdot u_*$ and clf(x,2) is the maximum of clf(x,2) and $0.1 \cdot u_*$.

The 1961-1980 average heights of 850 and 700 mb were according to Jokioinen soundings at 1350-1460 m and and 2842-3025 m (STATISTICS, 1984). The heights of each model level depend in the pressure, temperature and humidity, and they are approximately over Finland (without the surface) 31, 141, 335, 601, 922, 1288, 1690, 2114, 2559, 3015, 5000, 7000 and 10000 m.

1.8 Advected background concentrations at the boundaries

The emission sources outside the simulation area are taken into account by including, in the air flowing across the borders, an LRT (long-range transported) background term. This is the daily average concentration of each compound calculated with the EMEP MSC-W trajectory model (BARRETT et al., 1995) on a grid of 150 km horizontal resolution. The concentrations are assumed to be evenly distributed below the EMEP-model mixing height. Above this height the advected concentrations are assumed to have a low background concentration value. The EMEP model boundary layer height represents the 12 o'clock UTC value, and its diurnal variation is assumed to be similar to the time variation of the mixing height given by the HILATAR-model pre-processor at the corresponding place.

1.9 Dry deposition parameterisation

Dry deposition, i.e. the removal of gaseous and particulate pollutants or fog from the atmosphere to the earth's surface, by vegetation or other biological or mechanical means, is a significant removal process for nitrogen and sulphur oxides and their conversion products from the air. Direct measurement of dry deposition is difficult; it is most frequently estimated by calculating the dry deposition velocity using meteorological data and surface resistance parameterisation, or using concentration profile measurements. The dry deposition portion varies significantly depending on the measurement place and time. Its share of the total flux depends strongly on the distance from the source areas, because it is directly related to ambient air concentrations. Dry deposition has been estimated to vary annually from an average of 22-30 % of the total $SO_4^=$ and NO_3^--deposition in Eastern Canada (SIROIS & BARRIE, 1988) to 25-59 and 31-70 % respectively in the Eastern USA (MEYERS et al., 1991), without cloud water

interception. In general, budget estimates indicate that, inside a large region such as North America or Europe, approximately one third of the emissions is deposited by wet deposition, one-third by dry deposition, and the remaining part is transported out of the region (WHELPDALE & KAISER, 1996).

The vertical flux down to the earth's surface is parameterised by the dry deposition velocity v_d, which is defined by

$$v_d(z_{ref}) = F(z_{ref}) / c(z_{ref}), \tag{37}$$

where $c(z_{ref})$ is the average concentration at the reference height z_{ref}, and $F(z_{ref})$ is the flux to the surface. Equation (37) is used as the boundary condition at the lowest level in the vertical diffusion algorithm.

1.9.1 Resistance method

The concept of resistance had already been introduced in 1951 for characterising the evaporation and transfer of water vapour between the stomata and leaf surfaces, in order to avoid the use of bulk transfer equations when all the microphysical terms needed are not available (BRUTSAERT, 1982). Today the resistance analogy is widely used in estimating dry deposition velocities v_d. The resistance terms are r_a, the aerodynamic resistance, which describes the turbulent transfer of the substance to the near-surface layer, r_b, which is the resistance to penetration across the atmospheric near-surface layer (where molecular transport dominates over turbulent transport) by convection, diffusion or inertial processes, and r_c, the resistance associated with pollutant-surface interaction, as follows:

$$v_d = (r_a + r_b + r_c)^{-1} . \tag{38}$$

Theory of the atmosphere-surface exchange has been developed first for gases with no surface source (i.e. SO_2 and O_3) and extended to the other pollutants. The parameterisation used in HILATAR model is constructed using the articles of VOLDNER et al. (1986), WESELY (1989), PADRO et al. (1991) and PADRO (1993), and ERISMAN (1994). Over sea areas the LINDFORS et al. (1991) method is used. The resistances r_a and r_b are calculated from

$$r_a = \frac{1}{\kappa \cdot u_*}\left[0.74 \cdot \ln(\frac{z_{ref}}{z_o}) - \Psi_c(\frac{z}{L}) \right] \tag{39}$$

$$r_b = \frac{2}{\kappa \cdot u_*}\left(\frac{Sc}{Pr}\right)^{2/3}, \tag{40}$$

$$r_a + r_b = \frac{1}{\kappa \cdot u_*}\left[\ln(\frac{\kappa u_* z}{D}) - \Psi_c(\frac{z}{L}) \right], \text{ for soluble gases over the water surface of lakes} \tag{41}$$

The symbols and terms are those used in chapter 2.4 and z_{ref} is 15 m. The diabatic correction function for a scalar concentration $\Psi_c(z/L)$ is replaced with that for heat $\Psi_h(z/L)$ as is usually done in dry deposition models, since they both represent a scalar. In the expression for r_a, the roughness z_o for momentum, the only roughness in HIRLAM, has been used.

The surface of all grid squares has been classified into the following types: agricultural land, lakes, sea, forests and mountains; that remaining is classified as "other surfaces", i.e. the rest of the 11 types of WESELY (1989). The roughness parameter used for forests is 1 m, while it is 0.02 cm for snow and ice, 0.7 cm for grass in spring, 3 cm in summer and 1 cm during the autumn. For lakes, a wind-dependent formula (42) from VOLDNER (1986) is used. It resembles the roughness formula already proposed by Charnock in 1955 (see e. g. STULL, 1988):

$$z_0 = \nu(9.1\ u_*)^{-1} + 0.016\ u_*^2/g. \qquad (42)$$

The expression (43) for the resistance r_b of gases is used for all other land types except snow or water. For gaseous deposition to snow-covered surfaces, $r_b = 2$ s cm^{-1} is used.

Over rough surfaces (z_o=1, forest), at a reference height of 15 m, the value of the aerodynamical resistance r_a drops below 10 s m^{-1} during near-neutral situations (- 0.01 m^{-1} < 1/L < 0.01 m^{-1}) if 0.5 m s^{-1} > u_* > 0.9 m s^{-1}, and in unstable conditions (1/L = -0.1) if u_* > 0.15 m s^{-1}. If the surface roughness is smaller, the aerodynamic resistance is larger in the same conditions. Over agricultural land, where the surface roughness varies with the season, r_a > 10 s m^{-1} if u_* < 1 m s^{-1} during all seasons. During the time of low aerodynamic resistance (< 10 s m^{-1}), the maximum dry deposition velocity can increase to over 10 cm s^{-1}, unless other resistances reduce it.

1.9.2 Land use data

For determining the surface resistance, detailed information on the land use is required. The WESELY (1989) r_c-parameterisation is available for the following land use categories: 1) urban, 2) agricultural and 3) range land, 4) deciduous, 5) coniferous and 6) mixed forest, 7) water, 8) barren land or desert, 9) non-forested wetland, 10) mixed agricultural and range land and 11) rocky areas with low growing shrubs.

A detailed inventory with over 50 land-use categories with a 10-km resolution analysed from Landsat TM images by 5 institutes, mainly in the Finnish National Board of Survey and Environment Data Centre of Finland, has been applied to the HILATAR grid. However, because the inventory did not cover areas outside Finland, for the 11 km (0.1^o) model, the GRID Arendal on-line GIS Baltic Sea Drainage Basin land cover database, from http:://www.grida.no/baltic/, has been used in most simulations. In this land use is categorised in 6 classes: forest, open land, open water, urban land, glacier and unknown land - in addition, information about the agricultural portion exists in the same data base. For the 28 km (0.25^o) HILATAR model, the land-use data are the HIRLAM 0.25 ^{o} model surface data classified into the following primary surface types: forest, lakes, sea and other surfaces. In both cases the mountainous land types are separated out from the class ”other surfaces” with topography and latitude-dependent formula. Half of the forest is assumed to be

coniferous, half deciduous. The other surfaces are further separated roughly into agricultural land, towns and the remaining WESELY (1989) surface types using a latitude-dependent maximum fraction of each surface type as a weighting factor.

1.9.3 Surface resistance

The surface resistance r_c of canopies depends on the solar radiation, surface temperature, relative humidity, amount of rain, dew or fog and pollutant exposure time. It is defined, in a combination of the parameterisation of WESELY (1989), HICKS et al. (1987) and ERISMAN (1994), by the following formula:

$$r_c = \left[\frac{1}{r_s + r_m} + \frac{1}{r_{lu}} + \frac{1}{r_{ext}} + \frac{1}{r_{dc} + r_{cl}} + \frac{1}{r_{ac} + r_{gs}} \right]^{-1} \qquad (43)$$

whereby the transport of the pollutants to the canopy is approximated as following five parallel routes:

- into the plants via stomata and through the mesophyll (resistances r_s and r_m),
- into the plants through the cuticula cells (leaf surface resistance r_{lu}), or in wet situations through external leaf surfaces (r_{ext}),
- into the lower canopy against the resistance of buoyant convection in canopies (r_{dc}) and against the surface resistance of leaves, twig and bark (r_{cl}),
- into the ground against the resistance r_{ac}, which depends on the canopy height and density and against the surface resistance of the soil, leaf litter etc., (r_{gs}).

If the surface is covered with snow, for other surface types except towns and forests, r_c is replaced by the specific snow resistance r_{snow}.

Although it is known that HNO_3 is adsorbed quickly and almost irreversibly on most surfaces, particularly when they are wet, (see MEIXNER et al. 1988a), the minimum surface resistance for HNO_3 is assumed to be 0.1 s cm^{-1} for all surfaces, as recommended in WESELY (1988), in order to avoid too high dry deposition fluxes. In the following formulae the units of the resistances are s cm^{-1} unless otherwise stated.

Stomatal resistance

The gases are transferred into plants via diffusion through leaf stomata; the stomatal resistance is thus inversely proportional to the diffusivity of the substance. The surrounding guardian cells control the opening of the stomata by changing their physical form. The stomatal resistance depends on the amount of photosynthetic radiation (PAR), on the leaf temperature, on water pressure inside the leaf surface, on the relative humidity and the moisture content of the ground, on the CO_2-concentration near the leaf surface and the exposure to air pollutants, on leaf age, season and vegetation type.

Much of the knowledge on plant behaviour is based on evaporation studies used e.g. for meteorological research on the surface exchange of humidity (TOURULA, 1993). The exchange processes are complicated to model, since each plant responds individually to radiation changes by closing the stomata during a time varying from a few seconds to even 40 minutes, while the opening is quicker. The relative humidity affects the stomatal resistance via several feedback's and delays; dense vegetation can remain moist for a while, even when the relative humidity is decreasing. When the ground dries, the plants have to limit their evaporation rate to keep their water potential at a safe level.

The density of the canopy, parameterised in some models by the leaf area index LAI, is important for estimating the flux to the canopy through stomata. LAI represents the total area of the leaves projected on a horizontal plane in proportion to the area of the plants. Depending on the formulation of the in-canopy resistance in the model, it seems to have different definitions. The one-sided LAI varies between 5 (summer) to 1 (winter) in Canadian deciduous forests and between 8 (early spring) to 11 (end of summer) in coniferous forests in the Netherlands, as used in ERISMAN (1994) - on the other hand e.g. FOWLER (1994) applied smaller values for it. The land type data did not contain sufficient information on LAI. If this is the case then, according to ERISMAN et al. (1994), the WESELY (1989) parameterisation of the stomatal resistance is recommended, and this approach has been used here.

The stomatal resistance r_{SX} for compound x is calculated as a function of the surface temperature T_S and solar irradiation G (W m^{-2}) in the temperatures range 0 - 40 ^oC by

$$r_{sx} = r_{H_2O} \cdot \frac{D_{H_2O}}{D_x} \cdot \left\{ 1 + \left[\frac{200}{G + 0.1} \right]^2 \right\} \cdot (f_t \cdot f_w), \qquad (44)$$

where $f_t = 400./\{T_s \cdot (40 - T_s)\}$.

r_{H2O} is the minimum bulk canopy stomatal resistance of water vapour from WESELY (1989) for each season and land use type. The temperature dependency function f_t is from HICKS et al. (1987). The optimal temperatures for gas exchange depend on the vegetation type, being 25 ^oC for maize and oak and 9 ^oC for spruce. The f_t-formula used here gives about the same optimal conditions for respiration in a temperature range 14-26 ^oC, a 91 % respiration at 10 ^oC and 30 ^oC and a decrease to 40 % at 1^oC and 39 ^oC. Below 0 ^oC and above 40 ^oC the stomata are assumed to be closed.

Drought is recommended to be described with a step function, depending according to HICKS et al. (1987) on the leaf water content, so that over the threshold limit $f_W = 1$, and is linearly dependent on the leaf water content. Experimentally-determined dependency coefficients for each surface and detailed knowledge of the wetness storage capacity of the ground in different conditions was not available, thus at the present time the accuracy of the dry deposition module will not be increased by implementing the drought dependency. In future studies the accumulated rain sum and number of drought days can be used for estimating the effect of drought on the dry deposition velocity.

The solar irradiation G in W m^{-2} is computed from

$$G = cn \cdot S_{\theta} \cdot \exp\left\{ -B \cdot \frac{p}{p_o \cdot \cos(\theta_z)} \right\} \cdot [\cos(\theta_z) + C] , \quad (45)$$

where cn = 1, S_θ = the solar constant at sea level (in W m^{-2}), B inverse mass of the atmosphere, (in atm^{-1}), θ_z = the solar zenith angle and C = corrective factor for diffuse radiation, 0.103 - 0.138.

Gases, which are soluble in water or have a high oxidation potential, can be deposited to the extra-cellular water inside plant leaf stomata. This is described by the mesophyll resistance r_m. It is insignificant for SO_2 and O_3 (and is assumed to be zero). For the other substances, it depends on the reactivity and solubility of the pollutant according to:

$$r_{mx} = \left[\frac{H}{3000} + 100 \cdot f_0 \right]^{-1} \quad (46)$$

where H is the Henry's coefficient and f_o is the coefficient of reactivity. Gases have been classified as being extremely reactive (f_o=1), such as ozone, slightly (f_o=0,1) or not at all reactive (f_o=0, such as SO_2). For moist and water surfaces the solubility is a function of the acidity or pH. Henry's constant at pH = 7 (neutral) has been used. When f_o is 0.1 or 1, or when H > 10, r_{mx} is small.

Cuticle resistance

According to WESELY (1989) the resistance of the outer surfaces in the upper canopy, the leaf cuticle resistance r_{lu}, can be assumed to be the same for SO_2 and O_3. The other gases (subscript x) are assumed to diffuse through the leaf surface cuticle either as SO_2 or as O_3, and r_{lux} is calculated from

$$r_{lux} = \frac{r_{lu}}{10^{-5} \cdot H^* + f_{0x}} . \quad (47)$$

Resistance to deposition to soil and to the lower canopy

Recently it has been shown (MEYERS & BALDOCCHI, 1993a) that when the surface is moist, up to 20-30 % of SO_2 deposition to a deciduous forest is received at the forest floor. The deposition to the soil decreases with increasing pH and increases with relative humidity; it is also sensitive to temperature and snow cover.

r_{cl} (surface resistance of leaves, twigs and bark) and r_{gs} (surface resistance of soil, leaf litter etc.) have been experimentally determined for ozone and SO_2, and have been found to depend on the temperature according to 1000 exp[-T_s-4] for all substances. For the other gases, r_{clx} and r_{gsx} are evaluated from:

$$r_{clx} = \left[\frac{H^*}{10^5 \cdot r_{clS}} + \frac{f_{ox}}{r_{clO}} \right]^{-1}, \qquad \text{and} \qquad r_{gsx} = \left[\frac{H^*}{10^5 \cdot r_{gsS}} + \frac{f_{ox}}{r_{gsO}} \right]^{-1} \tag{48}$$

where r_{clS}, r_{clO}, r_{gS} and r_{gsO} are numerical values from WESELY (1989).

Canopy resistance

r_{ac} (the resistance dependent upon the canopy height and density) and r_{dc} (the resistance of buoyant convection) describe the transport through the upper canopy to the surface by large-scale intermittent eddies, and could be combined with r_{clx} and r_{gsx}. r_{ac} is assumed to be zero for bare land and lakes, while for other surfaces numerical values for each surface are taken from WESELY (1989). The resistance r_{dc} describes the effect of sunlight on buoyant convection and mixing inside the canopy, and also the effect on the dry deposition of the wind on the sides of hills, and is formulated as:

$$r_{dc} = 100 \cdot \frac{\left[1 + \frac{1000}{G + 10} \right]}{1 + 1000 \cdot \theta_s} \tag{49}$$

where θ_s, the slope of the local terrain, is ignored at the moment.

1.9.4 Rain and fog

For dry periods MEYERS & BALDOCCI (1993b) measured and reported a surface uptake resistance for SO_2 of the order of 700 s m^{-1}. Early measurements proved that, during rainy periods, the surface resistance of SO_2 is very small, similar to that for open water, especially for agricultural vegetation, and corresponding resistances have been implemented in the models (WALCEK et al., 1986).

Rain and fogwater cover the stomata, and the direct exchange of gases is prevented. According to the studies made at the Argonne National Laboratory (WESELY, 1988), dew generally covers 2/3 of the leaf surface, and the stomatal resistance r_{sx} increases by a factor of three. In addition, the upper canopy resistance is affected: for dew-coated surfaces, the resistance r_{lu} for SO_2 decreases, and for O_3 increases, as follows:

$$r_{luS} = 100 \text{ s m}^{-1}, \text{ and } \quad r_{luO} = \left[\frac{1}{3000} + \frac{1}{3 \cdot r_{lu}} \right]^{-1}. \tag{50}$$

According to WESELY (1989), in contrast to the situation in fog, the surface resistance for SO_2 increases during rain. He assumes that the rain water has already been saturated by S(IV). The resistance for O_3 also increases.

$$r_{luS} = \left[\frac{1}{5000} + \frac{1}{3 \cdot r_{lu}} \right]^{-1}, \text{ and } r_{luO} = \left[\frac{1}{1000} + \frac{1}{3 \cdot r_{lu}} \right]^{-1} . \quad (52)$$

For other substances

$$r_{lux} = \left[\frac{1}{3 \cdot r_{luS}} + 10^{-7} \cdot H^{*} + \frac{f_{ox}}{r_{luO}} \right] \quad (53)$$

where r_{luO} is the respective value for rain or dew. This formula is used for other gases than SO_2.

All measurements do not support this hypothesis of increased resistance during wet periods. According to the main conclusions of the NMR workshop on dry deposition (LÖVBLAD et al, 1993), appropriate algorithms for providing estimates of the surface resistance for SO_2 as a function of surface wetness were still not yet available for plant canopies in 1993. Water film chemistry is very important for the dissolution of SO_2 - at low concentrations r_c might be low, at high concentrations it depends on the amount of other neutralising compounds in the air, because an increase in acidity due to the dissolution and oxidation of SO_2 in water films will reduce SO_2 dry deposition to wetted surfaces. The surface wetness may be provided by dew, guttation, rain, fog, clouds or the deliquescence of aerosols deposited on the surfaces (at 60 % RH for NH_4NO_3, 80 % RH for $(NH_4)_2SO_4$). The NMR working group recommended the use for SO_2 of a negligible surface resistance of 10 s m^{-1} if RH > 90 %.

ERISMAN (1994) compared long-term measurements of dry deposition velocities for different locations and canopies during winter and summer conditions with those calculated, and concluded that the WESELY (1989) parameterisation yields significantly lower modelled dry deposition values than those measured. He derived an external parameterisation for SO_2 dry deposition on wet leaves, which has also been adopted in the modified EMEP model dry deposition module (SELAND et al., 1995). The formulation of this modified cuticular resistance in different temperature ranges is:

r_{ext}	=	1 s m^{-1}	during or just after precipitation, T > -1 ^{o}C,
r_{ext}	=	25000 exp { -0.0693 RH}	if RH < 81.3 %, T > -1 ^{o}C,
r_{ext}	=	0.58 10^{12} exp { -0.278 RH}	if RH > 81.3 %, T > -1 ^{o}C,
r_{ext}	=	200 s m^{-1}	if -1 > T > -5 ^{o}C,
r_{ext}	=	500 s m^{-1}	if T < -5 ^{o}C,
r_{ext}	=	0 s m^{-1}	some hours after precipitation has stopped.

r_{ext} grows from zero (rainy period) to 88-89 s m^{-1} (at relative humidity RH = 81.3%), but then to 782 s m^{-1} (if RH= 50 %) or to 3126 s m^{-1} (if RH=30 %). The drying times for vegetation were 2 h and 4 h after daytime rain in the warm season and in winter, respectively, and correspondingly 4 and 8 h during the night-time (ERISMAN, 1994). In the HILATAR model no drying times were included, since the meteorological

input is provided at 6 h intervals, nor was any saturation effect of the wet surfaces by acid contaminants or the neutralisation capacity of the plant considered.

The resistance of surfaces covered by snow was modified from the WESELY (1989) formulation to be 500 s m^{-1}, according to ERISMAN (1994), if T < -1 ^{o}C, and 70(2-T) when 1 < T < -1 ^{o}C. The coverage of the forests with snow is assumed to depend on the snow depth.

The dry deposition velocity over moist surfaces depends on the acidity of the droplets. The deposition of NH_3 neutralises an acid deposition. Thus, simultaneous deposition of SO_2 and NH_3 should result in higher SO_2 and NH_3 dry deposition rates to water surfaces than would be found by SO_2 and NH_3 alone. This process, referred as co-deposition, will be incorporated into the model in the near future.

1.9.5 Dry deposition over the sea

Over sea areas we use the method described in LINDFORS et al. (1991). For gases, the resistance method is used, where the diabatic correction function ψ_e is used in defining r_a with equation (42). R_b was set to $R_m = (\kappa u_*)^{-1} \ln(z_o/z_{oc})$, where $z_{oc} = z_{oe}$ is from equations (12). R_s was set to zero for soluble gases like HNO_3, NH_3 and SO_2 (a similar assumption was made by VOLDNER (1986) and also over a frozen sea. For NO_2, the surface resistance values of VOLDNER (1986) were used.

For particles, the LINDFORS et al. (1991) parameterisation is a modified version of the WILLIAMS (1982) method. Below a reference height the atmosphere is divided into two layers, and v_d is obtained through the resistance analogy. The upper layer is dominated by turbulence, while transfer in the thin quasi-laminar deposition layer just above the sea surface is separated into two parallel paths. Via one path, diffusion and impaction transport material to the smooth sea surface, while the other path, operative over that fraction of the sea surface which is broken with the formation of sea spray, is controlled by the scavenging of particles by impaction and coagulation with spray droplets. In addition, terminal settling takes place in both layers. The interaction between the smooth and broken sea surface areas is represented by a lateral transfer coefficient.

The dry flux of particles in the turbulent layer is given by (SLINN et al., 1978; SLINN & SLINN, 1980 and WILLIAMS, 1982):

$$F_z = (1-\alpha)\cdot K_{as}\cdot[C(z_{ref})-C(\delta)_s] + \alpha\cdot K_{ab}\cdot[C(z_{ref})-C(\delta)_b]+ V_{gd}\cdot C(z_{ref}) \qquad (54)$$

where the percentage a of the sea surface covered by breaking waves is $\alpha = 1.7\cdot10^{-6}\cdot V_{10}^{3.75}$ (WU, 1979), and $C(\delta)_s$ and $C(\delta)_b$ are the concentrations at the top of the quasi-laminar layer ($z=\delta$) over the smooth and broken sea, respectively. K_{as} and K_{ab} are the turbulent transfer coefficients defined by $K_{as} = K_{ab} = \kappa\cdot u_* / [\ln(z_{ref}/z_{oc})-\psi_E(z_{ref}/L_*)]$ with the roughness length $z_{oc}=D_c/(\kappa\cdot u_*)$. The Brownian diffusivity of the particles is given by $D_c = (k_{SB}T_aC_c)/(6\pi\mu r_p)$, where k_{SB} is the Stefan-Bolzmann constant, T_a is the air temperature, C_c the Cunningham slip correction coefficient, μ is the dynamic viscosity of air and r_p is the particle radius.

The terminal settling velocity in the Stokes region is obtained from the balance between the air resistance force and the gravitational force; at high Reynolds number an iterative method is used.

Within the deposition layer, the dry flux is given by WILLIAMS (1982) by

$$F_\delta = (1\text{-}a)\cdot K_{ms}\cdot[\, C(\delta)_s - C_0\,] + a\cdot K_{mb}\cdot[\, C(\delta)_b - C_0\,] + (1\text{-}a)\cdot V_{gw}\cdot C_s + a\cdot V_{gw}\cdot C(\delta)_b \quad (55)$$

where K_{ms} and K_{mb} are the transfer coefficients for a smooth and a broken surface, C_o is the concentration at the air/water interface and V_{gw} is the terminal settling velocity for particles which have grown due to the effect of humidity. The smooth surface transfer coefficient is defined by $K_{ms} = u_*^2 \;/\; (\kappa\cdot V_{10})\cdot[\, 10^{-(2/St)} + Sc^{-½}]$, where the Stokes number $St = u_*^2\cdot V_{gw}/g\nu$. K_{mb} is classified with wind velocity: K_{mb} =0, if $V_{10} \leq 5$ m s^{-1} , K_{mb} = 1 cm s^{-1} in the V_{10} range of 5 - 15 m s^{-1} and K_{mb} = 5 cm s^{-1} if $V_{10} >$ 15 m s^{-1}.

The terminal settling velocity in the humid region is obtained in the same way as for dry particles. When the relative humidity exceeds 80 %, condensation increases the dry particle diameter r_d to approximately $r_w = \alpha(S)\cdot r_d^{\beta(S)}$ where the parameters α and β depend on the saturation ratio S and the particle composition. Over salty water, the growth of the particle is restricted by Raoult's law, which sets an upper limit for the relative humidity of about 98.3 %.

The interaction between the smooth and broken surface areas yields a third dry flux path which takes care of the lateral transfer between these two regimes. This flux is estimated after WILLIAMS (1982) by:

$$F_{sb} = K_{sb}\cdot[\, C(\delta)_s - C(\delta)_b], \quad (56)$$

where it assumed that $K_{sb} = K_{ab}$.

The dry deposition velocity is resolved from flux equations (56-58) by assuming that the surface is a perfect sink and particle resuspension is ignored.

At sea, interactions with sea salt may cause the particle-size distribution associated with sulphur and nitrogen compounds to be shifted towards larger sizes, thereby increasing the dry deposition.

1.9.6 Upward fluxes

In numerous field studies it has been established that, while HNO_3 is always deposited to terrestrial ecosystems (due to its high solubility and surface reactivity), the vertical fluxes of NO, NO_2 and NH_3 are bi-directional, depending on their atmospheric mixing ratios and the prevailing meteorological conditions (see e.g. JOHANSSON, 1989, WESELY et al., 1989, SLEM & SEILER, 1991, CARDENAS et al., 1993 and ASMAN et al., 1994). In WILLIAMS & FEHSENFELD (1991) it has been suggested that for agricultural areas where fertilization is heavy, the areal values of NO flux into the atmosphere can be comparable to those of urban areas. The biosphere-atmosphere exchange, involving biological emissions, deposition and possibly also chemical transformation (see MEIXNER et al., 1988b), is as yet poorly understood. Laboratory

studies have shown three mechanisms that may lead to the production of NO in soils: microbial nitrification, denitrification and chemodenitrification (chemical decomposition of nitrite). In addition, the photolysis of nitrite may be important over ocean surface waters and flooded rice fields (JOHANSSON, 1989). According to PADRO & EDWARDS (1991), JOHANSSON (1989) and WILLIAMS & FEHSENFELD (1991) the emissions of NO_x depend on soil temperature, solar radiation, soil moisture content, soil nutrient level and plant cover. According to the dry deposition chamber measurements of HÖFKEN et al. (1988), at a temperature of 20 ^oC the NO_2 flux is directed upwards at NO_2 concentration levels of 2-5 ppb when the soil humidity is 2 %, and with a 20 % soil humidity at 2-10 ppb NO_2 levels. In the HILATAR model the natural biological emissions of nitrogen oxides are ignored, but, because the resistance analogue model employed cannot describe the NO_x fluxes in all situations, it is assumed that at concentrations below the 1 ppb level there is no dry deposition of NO_2 to any surface.

For the dry flux of ammonia, too, the model can only give an upper limit estimate, because atmospheric $NH_3(g)$ is in Henry's law equilibrium with the dissolved $NH_3(aq)$, NH_4^+ and H^+ in sea water. It has been shown experimentally (ASMAN et al., 1994) that near coasts and estuaries, if there are significant nitrogen discharges via the rivers and low gas-phase concentrations, the dry flux of ammonia is directed upwards (a common situation over remote and temperate marine areas), and the dry deposition of reduced nitrogen is zero.

1.9.7 Resistances for particles over land

For particles, deposition depends strongly on particle size, since transfer to the surface involves Brownian diffusion, inertial impaction/interception and sedimentation. The mass size distribution of nitrate particles is generally assumed bimodal, with one mode centred in the 0.1-1 μm range and the other in the 2-10 μm range, with a substantial fraction of the mass in the large particle mode. This leads to the adoption of a lower r_b than is indicated by earlier measurements for the generally smaller sulphate particles. For nitrate the r_b values of Table 3 are used, while for other particles the r_b-values are twice as big. According to measurements by BYTNEROWICZ et al. (1987), nitrate deposition velocity values as high as 3.7 cm s^{-1} have been detected in West Germany for a certain kind of spruce forest, though general recommendations are of the order of 1.-1.2 cm s^{-1} for a spruce forest and 0.7 cm s^{-1} for a pine/deciduous forest. However, the separation of the gaseous phase from the measurements is difficult. To avoid too high deposition velocity values for particles, a surface resistance of 0.1 s cm^{-1} has been used.

Table 3. Near-surface resistance values used for nitrate, s cm^{-1} (VOLDNER et al., 1986)

surface	winter		spring		summer		autumn	
	day	night	day	night	day	night	day	night
conifer. forest	0.7	1.5	0.7	1.5	0.7	1.5	0.7	1.5
deciduous forest	5.0	10.0	1.5	3.0	0.5	1.0	1.0	2.0
grass/ice	5.0	12.5	2.0	3.0	1.5	3.0	1.5	3.0

1.9.7 The gravitational settling velocity for the dust model

For the dust model, the gravitational settling velocity for particles, $v_{d,g}$, is $\rho_p d_p^2 (18\nu)^{-1}$, where ν is the viscosity of the air, $1.81 \cdot 10^{-4}$ g·(cm·s)$^{-1}$, and ρ_p and d_p are the density and diameter of the particle (Hinds, 1982). For particles with $d_p = 10$ μm and $\rho_p = 1$ g cm^{-3}, $v_{d,g} = 0.305$ cm s^{-1}. Several sink rates were used depending on the model application. In the emission module, two size classes for sulphur particles are used, and for the conversion products, nitrate particles are assumed to be on average larger than sulphate particles.

1.10 Parameterisation of wet deposition

For the majority of pollutants scavenging by precipitation is the most effective atmospheric cleansing mechanism: if a gaseous compound is not soluble and does not produce scavengeable products, its life-time can increase to years. The removal rate of pollutants depends on many microphysical parameters, cloud dynamics and the pollutant itself, as well as on the precipitation rate and type, thus also being a function of e.g. altitude and temperature.

In determining scavenging rates for the HILATAR model, formulas of the nitrogen compounds from the FINOX model have been used as a base, and similar expressions are derived for SO_2 by using relative scavenging efficiencies of several models.

In wintertime the formulae used describe the scavenging of pollutants by snow systems, which contain a negligible amount of supercooled liquid water. According to ROGERS & YAU (1989), these conditions are also met with in summertime at higher altitudes, if the temperature is lower than about -10 ^{o}C. In the model, precipitation is assumed always to be rain when the temperature T(z) exceeds 270 ^{o}K, snow when T(z) is below 260 ^{o}K, and between these limits it is assumed to be linearly distributed between rain and snow.

In the HILATAR model, it is assumed that wet deposition does not uniformly remove material from the air in each vertical layer up to the top of the modelling volume. In addition to the scavenging efficiency variation with precipitation type etc., the precipitation rate itself decreases with height. The height dependency varies with time according to a sine function between the limits presented in CHANG (1986), the winter minimum occurring on 15th February and the summer maximum on July 15th. Below about 1 km, the precipitation rate as about the same as that measured at the surface. Above cloud base, the rate decreases quite rapidly with height, varying between 56-78 % at 2 km, and 22 - 58 % at 3 km, of the surface precipitation values in winter and summer, respectively; the removal rate in the upper part of the cloud with generally low concentrations is thus small.

1.10.1 Scavenging of the nitrogen compounds

According to the early studies, CHANG (1986), cloud chamber experiments and direct measurements indicate that in the presence of O_3, NO_2 converts in clouds at a significant

rate to aqueous nitrate. Thus, in addition to the EMEP-model uniform night-time gas-phase transformation to particles, the same chemical pathway occurs in clouds: NO_2 reacts with O_3 producing NO_3 and N_2O_5, which are not destroyed in the weak photolytic conditions inside storm clouds, and which are scavenged as effectively as HNO_3. Because this sink term is not used in most of the models, the scavenging of NO_x-compounds is ignored; however if by adding this missing sink the model's chemistry could improved. At the moment the model produces too much nitrate when its results are compared with measurements. If only the in-cloud scavenging would be included, the NO_2 surface concentrations would not be affected.

The scavenging rates L_c (in s^{-1}) for highly (irreversible) soluble gases, such as HNO_3, are given by the CHANG (1984,1986) formulae:

$$\begin{aligned} L_c\,(HNO_3) &= 0.33\cdot10^{-4}\cdot R(z)^{0.42} + 1.0\cdot10^{-4}\cdot R(z)^{0.58} && \text{rain, below-cloud, } (s^{-1}), \\ L_c\,(HNO_3) &= 0.88\cdot10^{-4}\cdot R(z)^{0.33} + 1.9\cdot10^{-4}\cdot R(z)^{0.64} && \text{snow, below-cloud, } (s^{-1}), \\ L_c\,(HNO_3) &= 4.0\cdot10^{-4}\, R(z)^{0.74} && \text{in-cloud } (s^{-1}), \end{aligned} \qquad (57)$$

where R(z) is the precipitation rate (mm h^{-1}) at altitude z, and the in-cloud scavenging value is the same as that for the cloud droplet removal rate by falling raindrops. Thus, highly soluble gases are removed from the air more efficiently inside than below cloud, and the removal of HNO_3 by snow is an efficient process.

CHANG uses the same scavenging formulas for OH, HO_2, NO_3, N_2O_5 and HNO_3.

For soluble aerosol particles SCOTT (1982) has derived a washout coefficient formula by examining the collisions between the falling raindrop and the aerosol, which is a much faster removal process than that published in CHANG (1986) for aerosol nitrate particles:

$$\begin{aligned} L_c &= 3.50\cdot10^{-4}\cdot R(z)^{0.78} && \text{rain, SCOTT (1982), } (s^{-1}), \\ L_c &= 2.8\cdot10^{-5}\cdot R(z)^{0.74} && \text{rain, CHANG (1986), } (s^{-1}), \\ L_c &= 2.44\cdot10^{-4}\cdot R(z), && \text{snow, SCOTT (1982), } (s^{-1}), \\ L_c &= 1.0\cdot10^{-4}\cdot R(z)^{1.2}, && \text{snow, CHANG (1986), } (s^{-1}). \end{aligned} \qquad (58)$$

In the EMEP multilayer Eulerian model (JONSEN & BERGE, 1995), NH_3 is assumed to be removed in clouds from the atmosphere at the same rate as HNO_3, and particles at a rate half that of HNO_3. The sub-cloud scavenging rate for gases is half, for particles a 1/7-part of the respective in-cloud scavenging rates. The same scavenging rates have also been used in PERSSON et al. (1994). DAVIS et al. (1992) have used aircraft concentration and surface precipitation measurements for calculating the scavenging ratios of different gaseous and particulate pollutants. The results for the in-cloud scavenging ratios were $8.5\cdot10^5$, $5.6\cdot10^6$ and $4.3\cdot10^5$, for SO_4^{2-}, NO_3^- and NH_4^+-particles, respectively, and $3.4\cdot10^5$, $2.4\cdot10^6$ and $9.7\cdot10^4$ for total sulphate, nitrate and ammonium. RUIJGROK et al. (1992) measured at Arnheim, Holland similar scavenging ratios for sulphate and nitrate particles. They also found that winter scavenging values for nitrate were half the summer values.

ASMAN & JANSSEN (1987) use for the scavenging of NH_3 the formulae

$$L_c = 2.64\, R(z)^{0.68} \qquad \text{below-cloud, } (s^{-1}) \qquad (59)$$

$$L_c = 5000\ R(z)^{0.64}\ hmix^{-1} \qquad \text{in-cloud,} \qquad (s^{-1})$$

where R is in units of m s^{-1} and hmix in m. In-cloud NH_3 scavenging will proceed at about the same rate as the in-cloud scavenging of SO_4^{2-} aerosol particles, which act as condensation nuclei. Asman and Janssen use the latter formula in their model for both in and below-cloud scavenging, in HILATAR, both (59) sink rates are used.

With a 1 mm h^{-1} rain intensity and 800 m mixing height, the removal rate of HNO_3 and NH_3 will be $4.86 \cdot 10^{-4}$ s^{-1} (in-cloud) and $2.43 \cdot 10^{-4}$ s^{-1} (below-cloud) in the EMEP formulation, while according to CHANG (1986) the rates will be $4.0 \cdot 10^{-4}$ s^{-1} (in-cloud, HNO_3), $1.33 \cdot 10^{-4}$ s^{-1} (below-cloud, rain, HNO_3) and $2.78 \cdot 10^{-4}$ s^{-1} (below-cloud, snow, HNO_3); the Asman rates are $0.92 \cdot 10^{-4}$ s^{-1} (below-cloud, rain, NH_3) and $4.0 \cdot 10^{-4}$ s^{-1} (in-cloud, NH_3). When the mixing height is low (usually in wintertime), the EMEP removal rate of HNO_3 is clearly faster than that of CHANG, especially with higher precipitation amounts.

1.10.2 Scavenging of the other compounds

The scavenging rates of those compounds, for which an analogous parameterisation scheme was not available, have been estimated using the ratio of the EMEP scavenging efficiencies of the various compounds. The ratio of the scavenging efficiencies of particles and HNO_3 from the JONSEN & BERGE (1995) and older EMEP-model descriptions is $1.4 \cdot 10^6$ (HNO_3) / $1.0 \cdot 10^6$ (particles). HNO_3 is scavenged faster than particles. In Table 4, the CHANG (1984, 1986) formulas for particles and HNO_3, and the SCOTT estimate for particles are compared, the numerical results are:

Table 4 scavenging efficiency comparison, s^{-1}

precipitation rate	HNO_3	NO_3 SCOTT	NO_3 CHANG
2 mm/h	$1.93 \cdot 10^{-4}$	$6.1 \cdot 10^{-4}$	$0.46 \cdot 10^{-4}$
10 mm/h	$4.67 \cdot 10^{-4}$	$21.1 \cdot 10^{-4}$	$1.50 \cdot 10^{-4}$

Thus, the particles are scavenged 3 times faster than HNO_3 in weak precipitation (2 mm/h) and more than 4 times faster at the stronger rate (10 mm/h) if the SCOTT formulae are used; however, at a 4-3 times slower rate with the CHANG parameterisation. The CHANG (1986) formulae do not give relative scavenging efficiencies similar to those of the EMEP model. In the HILATAR model, the HNO_3-scavenging rate in all situations, and the Chang parameterisation for particles during snowfall are used; for particle scavenging by rain the scavenging rate can be chosen, and a formula $L_c = 0.7 \cdot 10^{-4} \cdot R(z)^{0.78}$ is used in the simulations described.

In conclusion, in the HILATAR model the values used in the simulations are:

$$\begin{aligned} L_c\ (\text{particles}) &= 3.0 \cdot 10^{-4} \cdot R(z)^{0.78} && \text{rain, below cloud } (s^{-1}), \\ L_c\ (\text{particles}) &= 4.0 \cdot 10^{-4}\ R(z)^{0.74} && \text{rain, in-cloud, } (s^{-1}), \\ L_c\ (\text{particles}) &= 1.0 \cdot 10^{-4} \cdot R(z)^{1.2}, && \text{snow, } (s^{-1}). \end{aligned} \qquad (60)$$

The same formulation has been used for all particles in the acid model.

For the dust model, the scavenging formulae have been slightly modified. The scavenging efficiency for particles depends on the raindrop size distribution D_p, the type of rain, the fall speed of the drops $U_t(D_p)$ and the aerosol diameter d_p. According to Scott (1981), the in-cloud scavenging rate is $L_c(z)= 0.35\ 10^{-3}\ R(z)^{0.78}\ (s^{-1})$, where R(z) is the rain intensity at height z, mm hr^{-1}. According to Chang (1984), the theoretical maximum for the two most commonly-used raindrop size distributions $N(D_p)$ is $L_c(z)= 0.4\ 10^{-3}\ R(z)^{0.74}\ (s^{-1})$ - $L_c(z)= 0.46\ 10^{-3}\ R(z)^{0.86}\ (s^{-1})$.

Below cloud the scavenging formula

$$L_c(d_p) = \int_0^\infty 0.25\ \pi\ D_p^2\ U_t(D_p)\ E(D_p,d_p)\ N(D_p)\ dD_p$$

can be solved numerically. There the collision efficiency between the raindrop and the particle, $E(D_p,d_p)$, is the only size-dependent parameter. It reaches a minimum value of 10^{-4} - 10^{-3} when d_p is 10^{-1} - 1 μm, and a maximum of around one when $d_p \geq 10$ μm or very small (Seinfeld & Pandis, 1998). For one-size class aerosols
$L_c(d_p) = 1.5\ E(D_p,d_p)^{-1}$, varying between 0.8-8 R(z) hr^{-1} for 10 μm particles if the raindrop diameter is D_p = 0.2 to 2 mm (Seinfeld & Pandis, 1998).

The SO_2 in-cloud removal rate is assumed to vary of the respective HNO_3 scavenging rate, with an annual variation modulated by the expression $0.21 + 0.07 \cdot \sin(2 \cdot \pi \cdot (d-120)/365)$ - which gives the same summer/winter ratio as that of the EMEP model.

Emitted SO_2 is not dissolved immediately into liquid droplets: the results of several experiments where the scavenging efficiency of rain has been measured beneath the plumes of large power plants (TEN BRINK et al., 1988, JYLHÄ, 1995), show that SO_2 is not immediately scavenged out from the flue gases, and this feature is usually taken into account in local dispersion models. One physical reason can be the pH and temperature dependency of the Henry's coefficients, the HCL and HF emissions from coal-fuelled power plants restricting the uptake of SO_2 into precipitating droplets. FRAUDE & GOSHNICK (1995) have analyzed organic layers which often cover the surface of urban and combustion-emitted aerosols, and which seem to impede the water acceptance of the particles. This also inhibits the fast scavenging of pollutants in power plant plumes. In the HILATAR model, the emitted SO_2 is assumed to be initially non-scavengeable, but downwind of the emission sources is linearly converted into a scavengeable form with a half-time of one-and-a-half hours.

1.11 Numerical methods

The nature of the problem and the grid configuration set some restrictions on the algorithms capable of solving the combined advection-diffusion transport of the pollutants. For the elementary one-dimensional sub-problems the grid is limited, so the boundaries have an influence on the solutions, at least in the case of the advection algorithm. On a horizontal grid of 11-28 km, stack emissions give an uneven distribution

of concentrations with sharp gradients. This can lead to slight numerical diffusion in the model.

1.11.1 Advection

The positive definite advection scheme of SMOLARKIEWICZ (1983) has been used for the horizontal advection sub-problem in all applications reported before September 1995, after which the positive definite, area-preserving flux-form advection algorithm of BOTT (1989) has been operational in the model. Both methods are based on the explicit, forward in time, positive definite and numerically efficient upwind differencing. The upstream method is accurate only to the first order in space and time and produces rather strong numerical diffusion, which is reduced using various procedures. The Smolarkiewicz algorithm uses corrective advection fluxes, which reduce the truncation error produced by the upstream solution. In comparison with other positive definite algorithms, the mass conservation was poor (BARTNICKI et al. 1990). Because of significant numerical diffusion, a lot of the mass was transferred through the boundaries; in CHOCK (1991) it was also found to be highly diffusive. The Bott scheme is another improvement of the CROWLEY (1968) method of polynomial fitting for higher-order accurate schemes. It works as follows: the integrated flux forms of TREMBACK et al. (1987) are first normalized with a view to reducing the phase speed errors. Negative values of the transported quantity are then suppressed by non-linearly limiting the normalized fluxes, and the resulting advection equation is numerically solved by means of the usual upstream procedure. The results of simulations with the same meteorological and other input data have been compared in some test cases with the HILATAR model, and the Bott algorithm shows the best performance. The Bott scheme was originally written for an equidistant numerical grid. Its numerical tests in the actual horizontal HIRLAM grid are described in chapter 4. Vertical transport is described by a simple mass transfer balance discretization method.

1.11.2 Vertical diffusion

The vertical diffusion is solved by the Crank-Nicholson differentiation algorithm with a staggered grid (TUOVINEN, 1992; PRESS et al., 1986). The method, numerical tests and comparison with an analytical solution with and without dry deposition is described in detail in TUOVINEN (1992) and NIKMO et al. (1997). The original algorithm has been vectorized, and mixing is allowed through the full depth of the ABL. Weak mixing of the LRT pollutants down across the mixing height is allowed, and above the ABL height continuous mixing is assumed. The parameterisation of K_z was described in section 2.5. The mass conservation of the algorithm has been tested.

Under efficient mixing conditions, the time required to get a uniform mass profile is less than 2 hours for a typical K_z-profile with a maximum of 50 $m^2 s^{-1}$ below the mixing height, and less than a hour if K_z increases to 100 $m^2 s^{-1}$. The mixing efficiency depends on the initial concentration or mass profile, and the structure of the grid. The behaviour of the vertical diffusion algorithm is demonstrated by two examples.

Let us first consider how fast mass is transferred through the mixing layer if $K_z = 0.5$ $m^2 s^{-1}$ across the inversion layer is used. The concentration profile below the ABL height on

level 5 is assumed to be uniform, while above it the concentration reaches a peak value of 10 times the background value. We use the average HIRLAM grid levels and a K_z-profile of 0.5, 10, 20, 50 $m^2 s^{-1}$ at levels 1 to 4, 0.5 $m^2 s^{-1}$ at level 5 and 2 $m^2 s^{-1}$ above it. The pollutant mass content of the thinner layers below the mixing height, near the surface, will be doubled in the first hour, and increased to a threefold value at the end of the first day. Finally, from the mass content of the layer 6, which is above the mixing layer, only about 23 % is mixed down through the mixing layer, while 44 % rises to the upper layers within the two-day simulation period (the mass distribution depends on the layer widths). Thus if we have estimated the value of the mixing height too low, (which might be the case sometimes) this parameterisation does correct the situation slightly, however slowly, during the transport further. Below the mixing height the profiles are smoothed usually faster. If we have another peak value at level 3, then using the same K_z-profile, the mixing layer concentration will be evenly distributed within a few hours. In the HIRLAM grid, the final concentration profile, as well as the mass, will also be uniformly distributed throughout the first five levels above the surface. If K_z is increased to 50 $m^2 s^{-1}$ below hmix, the profile has become uniform in about one hour, while with a 100 times weaker mixing it takes 1.5 days.

1.11.3 Chemistry

The differential equations of atmospheric chemistry are stiff, containing a wide range of time scales which are difficult to treat numerically. Special integration methods (see a review in ZLATEV, 1995) for solving stiff systems have been developed. The classical, implicit methods for describing the interactions of reactive pollutants, where the equations are solved for each individual compound, are computationally expensive. It is therefore common to divide the simulated species into related groups or families, which have longer time scales than the individual members, and are easier to solve numerically. There are a lot of standard codes available, the best known of which, the Gear method, is based on the backward differentiation formulae; however it is too time-consuming for longer simulations.

The QSSA (quasi steady-state approximation) method, employed in the EMEP model and described in HESSTVEDT et al. (1978) and HOV (1983), is used in the HILATAR model. Consider a group of ordinary differential equations which describe the chemical transformation of N compounds (with concentration c_j)

$$dc_j/dt = Q_j(c_1,c_2 \ \ldots \ c_n), \ j=1,N. \tag{61}$$

The QSSA is based on the assumption that sufficiently accurate results can be achieved by treating the system (61) as a group of independent equations: during a short time step the concentrations of compounds c_j, $j = 1,N$, $j \neq k$, are assumed to stay fixed while they react with compound k. Thus we can omit the subscripts, and in the equation of the time dependency of concentration c

$$\partial c/\partial t = P - Lc, \tag{62}$$

the chemical production and loss terms P and L become constant over a time interval Δt, and (62) can be solved analytically. The solution depends on the photochemical lifetime $\tau = 1/L$ of the component, with the formulae:

$$c^{t+1} = (P/L)^t + (c^t - (P/L)^t) \exp(-L^t \Delta t), \quad \text{if } 0.1\Delta t \le \tau \le 100\Delta t, \tag{63}$$

$$c^{t+1} = (P/L)^{t+1}, \quad \text{if } \tau < 0.1\ \Delta t, \text{ a photostationary state exists,}$$

$$c^{t+1} = c^t + (P^t - L^t c^t)\ \Delta t, \quad \text{if } \tau > 100\ \Delta t,$$

where the superscript indicates time. The purely numerical tests have been omitted because in principle the code is a well-known EMEP scheme (IVERSEN et al., 1989; JAKOBSEN et al., 1995 and 1996), which is also used in the photo-oxidant codes of the RADM model (DENNIS et al., 1990), the EMEP MSC-W (SIMPSON, 1991) and the Danish Eulerian model (ZLATEV et al., 1990). The QSSA algorithm does not conserve mass exactly, a fact which is discussed shortly in Chapters 4.2 and 5.5.

2. Model Input

2.1 Meteorological fields

The meteorological input for the HILATAR model for simulations before 1998 consists of the 6-hour predictions of the HIRLAM weather prediction model with 0.5° horizontal and 6-h time resolution. The fields have been collected in a database covering the Baltic Sea drainage basin since 1991, to be available in air pollutant dispersion modelling studies. In 1993 and 1996 the geographical collection area has been increased. Since 1999 the data consists of 51 variables, 7 of them being 3-dimensional.

The database contains 21 surface parameters and 3-dimensional vertical profiles of the wind components, the specific humidity and temperature (see Table 5). The HILATAR model extends vertically up to about 3000 m, so before May 1992 data from the 7 lowest layers from the available 16 are included in our model simulations. In May 1992, the HIRLAM vertical grid was expanded to 31 levels, since when data from the 10 lowest vertical layers has been used.

Table 5. Meteorological data base for the grid model

<u>on 16 - 31 vertical layers</u>:	specific humidity q	
	temperature T	
	wind components u and v	
<u>At the surface:</u>		
pressure p_o	temperature at 0 m, T_o	topography
surface humidity	2 m temperature	u (10 m)
soil humidity	soil temperature	v (10 m)
deep soil humidity	temperature deep in soil	snow cover
sea/land mask	sea surface temperature	climatological snow
albedo	ice cover	clim. roughness
large-scale precipitation:	convective precipitation:	roughness z_o:
cumul. values and intensity	cumulative values and intensity	over land and water

The original data is in GRIB (gridded binary) code form, each time step in its own file, but these data are pre-processed on a monthly basis. The boundary layer parameters are calculated with a separate pre-processor in advance and saved as CRAY binary data, thus the GRIB library is not necessary for simulation applications.

For the use of the data base, several working tools have been developed. The tool set consists of a separate ABL pre-processor, and statistical and graphical visualisation programs. With these tools it is possible to calculate the boundary layer parameters or any HILATAR model internal parameters (vertical wind velocities, vertical mixing coefficients, dry deposition velocities or scavenging efficiencies), over different periods, to pick out selected time series, classify the data with e.g. time of the prediction or wind direction, calculate 1D trajectories and present the data on a map as numbers, wind rose presentations, curves, isolines or surface illustrations. The graphical programs use Disspla and UNIRAS libraries.

2.2 Emissions

As input data, the model requires either a gridded emission distribution or, if available, annual emissions (with data on their time variation) including exact knowledge of the location of each source and certain parameters characterising the stack and burning processes (for evaluation of the vertical dilution inside the emission box). Important parameters are those determining the effective height of the source according to the plume rise equations; the stack height and dimensions, temperature and mass volume of the smoke gas flux, etc. The emissions, (in units of molecules per unit volume per second) are added to the air of the grid point of the source. Grid emissions are diluted inside a layer, the thickness of which depends on the weather conditions. In convective situations they are mixed throughout the mixing layer depth. Because the grid size of the model is at least 10 km, the Briggs plume-rise equations as used and described, e.g., in NORDLUND at al. (1986) only give an estimate of the effective average height of the emission inside a grid box; the standard deviations of a gaussian plume as a function of the distance from the source are used as an other measure for evaluating the vertical dispersion of emissions in the grid. When detailed information about each emission source was not available, the emissions for each grid box were classified as areal sources with emission-specific vertical height profiles.

The time dependency of the emissions was calculated by weighting the annual emissions of each polluting sector (see Table 6) by time indices for every month, weekday and hour. For Finland, data from the FMI local air quality study emission inventories have been used in evaluating the monthly, weekly and diurnal time variation of the emission sources; for other areas the EMEP-model time variation indices (the same function for each country, because the more detailed GENEMIS indices were not available at the time) have been used.

The main inventories used were: FMI emission register (PIETARILA et al., 1996) for Finland, the stack- and initially district-based FMI inventory for Russia and Estonia, and the EMEP MSC-W inventory with a 50-km horizontal resolution and 2 emission height categories for other model areas. The Russian and Estonian emissions have been collected in co-operation with the Estonian environmental authorities and the institute SRI Atmosphera in St. Petersburg. The emission inventory has been further

augmented by the measurement projects of the Technical Research Centre of Finland (VTT) and the Technical University of Lappeenranta, with traffic emission inventories made at VTT.

For Estonia, St. Petersburg, Leningrad Oblast and South Karelia, the sulphur emissions used in the simulations totalled of 495 kt of SO_2. Of the 398 kt SO_2 stack emissions, about 250 stacks with 188 kt SO_2 emissions were located in Estonia, and 34 known stacks with 210 kt of SO_2 in St. Petersburg, Leningrad Oblast and South Karelia. For St. Petersburg the SRI Atmosphera reported total emissions of 61 kt SO_2, of which 57,6 kt were identified as being emitted at 14 main sources. According to a report by PLANCENTER (1991a), in the St. Petersburg city area there are about 36 000 sources, in the Leningrad Oblast area 105 900 identified sources. Thus, in the model simulations, the total St. Petersburg dispersed source emission estimate was assumed to be larger than the official value, 25 kt SO_2, of which known traffic emissions are 5920 t (MÄKELÄ, personal communication 1995).

The traffic emission inventory covering Estonia, Karelia, St. Petersburg and Leningrad Oblast was made for the year 1993 with the model described in MÄKELÄ (1990) and applied in MÄKELÄ & SALO (1994). The NH_3-emissions from the biggest farms of the Leningrad Oblast are treated individually, according to the information in MARKKANEN (1995), ETELÄ-KARJALAN MAASEUTUKESKUS (1994) and PLANCENTER (1991 b). Other dispersed emissions from geographical areas, for which detailed data were not available, are from the EMEP-inventory.

The Leningrad Oblast and Karelia emissions have been distributed to the districts, and inside the districts to the town and rural areas, using as the weighting factor the population amounts from data in KELLER et al. (1994). The Estonian dispersed emissions were provided by the Estonian authorities for each district. The Karelian areal emissions are the difference between the total emission and the sum of the point source emissions. However, this figure may be too low, because the Russian authorities do not include all diffused sources into their statistics. The areal emissions have mainly been assumed to be located in the principal towns.
A summary of the emissions is given in Table 6. The Finnish emissions are taken from the FMI emission inventory register (PIETARILA et al., 1996). The Estonian emissions are based on KIVIVASARA (1994), whose inventory was completed with several modifications during 1995, using the original data of the Estonian authorities, the results of VTT measurements (AUNELA et al., 1994) and special air quality model studies made at the FMI (RANTAKRANS et al., 1995; KIVIVASARA et al., 1994). The Russian emission inventory (Karelia, St. Petersburg and the Leningrad Area), described in HÄKKINEN et al. (1995), MILYAEV & YASENSKI (1997) and HONGISTO et al. (1995) has mainly been collected by the researchers of the SRI Atmosphera institute in St. Petersburg. The Kola Peninsula emissions are from the report MUR (1994). The total Kola Peninsula NO_x-emissions were 32 270 t NO_2 in 1993; in Table 6 traffic sources are not included, being summed to the gridded EMEP-emission inventory. The 50 km resolution EMEP emission inventory has been collected at the EMEP MSC-W with 1990 as the base year. The emissions for the year 1993 are scaled using each country's emission time series from BARRETT et al. (1995).

The geographical distribution of the emissions is presented in Fig. 4. Of the sulphur emissions, 20 % were located in the Kola Peninsula, 25.8 % in Estonia, St. Petersburg,

Leningrad Oblast and Karelia, 5.3 % in Finland and over 48 % in other model areas, mainly in the southern part, even though the major Central-European high emission-density areas are not included in the simulations. For oxidised nitrogen only 1.7 % was emitted in the Kola Peninsula (even under cold conditions and with 1.117 M inhabitants), while 10,1 % was emitted in Estonia, St. Petersburg, Leningrad Oblast and Karelia, 14 % in Finland and 74.2 % in the southern and western model areas.

Table 6 Annual emissions used in the model studies

Emission area	1000 t SO_2	1000 t NO_2	1000 t NH_3
Finland			
- road traffic	2353	91852	
- street traffic	1606	45732	
- T-dependent dispersed sources	7133	8136	
- T-independent disp. sources	6030	46122	42270
- stack sources	111232	90237	199
Finland sum	128354	272079	42469
Estonia, Karelia, St. Petersburg, Leningrad Oblast, areal emissions	99780	102540	
Estonia, stack-emissions	172000	34904	
St. Petersburg, Leningrad Oblast, South Karelia: stack emissions	322439	60189	
Kola Peninsula, North Karelia total emissions	491397	25472 + traffic	
EMEP-emissions and the rest of the simulation area	1178101	1453579	611538
total	2392071	1948763	654007

REFERENCES

ASMAN W.A.H. & JANSSEN A.J., 1987. A long range transport model for ammonia and ammonium for Europe. *Atmos. Environ. Vol. 21, No. 10* p. 2099-2119

ASMAN W.A.H., HARRISON, R.M. and OTTLEY C.J., (1994), Estimation of the net air-sea flux of ammonia over the southern bight of the North Sea. *Atmospheric Environment*, **28**, 3647-3654

AUNELA L., HÄSÄNEN E., KINNUNEN V., LARJAVA K., MEHTONEN A., SALMIKANGAS T., LESKELÄ J. and LOOSAAR J., 1994. Emissions from Estonian and Baltic oil-shale power plants. VTT Chemical technology, Environmental Technology, Final Report, Espoo 1994. 25 + 22 p.

BARRETT K., SELAND, Ø., FOSS A., MYLONA S., SANDNES H., STYVE H. and TARRASON L., 1995. European transboundary acidifying air pollution: Ten years calculated fields and budgets to the end of the first Sulphur Protocol. *EMEP MSC-W report 1995, Report 1/95. The Norwegian Meteorological Institute, Research Report no. 17,* 71 p + 199 p. appendices.

BARTNICKI J., OLENDRZYNSKI, K., ABERT K., SEIBERT P. and MORARIU B., 1990. Numerical approximation of the transport equation, Comparison of five positive definite algorithms. *IIASA working paper WP-90-10*, 32 p.

BENKOVITZ C. M., BERKOWITZ C. M., EASTER R. C., NEMESURE S., WAGENER R. and SCHWARZ S. E., 1994. Sulfate over the North Atlantic and adjacent continental regions: Evaluation for October and November 1986 using a three-dimensional model driven by observation-derived meteorology. *J. Geophys. Res., Vol. 99, No. D10*, pp. 20725-20756.

BOTT A., (1989). A positive definite advection scheme obtained by nonlinear renormalization of the advective fluxes. *Mon. Wea. Rev. Vol. 117, May 1989*, p. 1006-1015.

BRUTSAERT W., 1982. Evaporation into the atmosphere. Theory, history and applications. D. Reidel Publishing Company, Dordrecht Holland, 299 p.

BYTNEROWICZ, A., MILLER, P.R. & OLSZYK, D.M., 1987. Dry deposition of nitrate, ammonium and sulfate to a ceanothus crassifolius canopy and surrogate surfaces. *Atmos. Environ. Vol. 21, 8,* p. 1749-1757.

CARDENAS L., RONDON A., JOHANSSEN C. & SANHUEZA E., 1993. Effects of soil moisture, temperature and inorganic nitrogen on nitric oxide emissions from acidic tropical savannah soils. *J. Geophys. Res., Vol. 98, No. D8*, pp. 14783-14790.

CHANG T. Y., 1984. Rain and snow scavenging of HNO3 vapour in the atmosphere. *Atm. Env. Vol. 18, No. 1* p. 191-197.

CHANG T.,Y., 1986. Estimates of nitrate formation in rain and snow systems. *J. Geophys. Res*, Vol. 91, No. D2, p. 2805-2818.

CHIN M., JACOB D.J., GARDNER G.M., FOREMAN-FOWLER M.S., SPIRO P.A. and SAVOIE D.L., 1996. A global three-dimensional model of tropospheric sulfate. *J. Geophys. Res*, Vol. 101, No. D13, p. 18667-18690.

CHOCK D. P., 1991. A comparison of numerical methods for solving the advection equation - III. *Atm. Environ. Vol 25A, No. 5/6*, p. 853-871

CROWLEY W.P., 1968. Numerical advection experiments. *Mon. Wea. Rev., 96,* 1-11.

DAVIS W. E., DANA M. T., LEE R. N., SLINN W. G. N. and THORP J. M., (1992). Scavenging ratios based on inflow air concentrations. In: *Schwartz S. E. and Slinn W. G. N., (ed's) Precipitation scavenging and atmosphere-surface exchange Vol 1., The Georgii Volume: Precipitation Scavenging Process.* Hemisphere Publishing Corporation, Washington,Philadelphia, London, p. 447-458.

deMORE, W. B., SANDER S. P., GOLDEN D. M., HAMPSON R. F., KURYLO M. J., HOWARD C. J., RAVISHANKARA A. R., KOLB C.E. and MOLINA M. J., 1992. Chemical kinetics and photochemical data for use in stratospheric modeling, Evaluation number 11 (JPL 92-20), edited by NASA, and JPL Pasadena.

DENNIS R. L., BARCHET W. R. & SEILKOP S. K., 1990. Evaluation of the Regional Acid Deposition Model, RADM, with respect to NO_3^- air concentrations and deposition. In: *Kluge J. (ed.), EMEP workshop on the progress of transport modelling of nitrogen compounds, Potsdam FRG, 15-18 Oct. 1990*, Deutsher Wetterdienst, p. 62-65.

DIMITROULOPOULOU C. & MARS A.R.W., 1997. Modelling studies of NO_3 nighttime chemistry and its effects on subsequent ozone formation. *Atm. Environ.Vol. 31, No. 18*, p. 3041-3057.

ERISMAN, J.,W, 1994. Evaluation of a surface resistance parameterisation of sulphur dioxide. *Atm. Environ.Vol. 28, No. 16*, p. 2583-2594.

ERISMAN, J.W., van PUL, A. and WYERS, P., 1994. Parameterisation of a surface resistance for the quantifying of atmospheric deposition of acidifying pollutants and ozone. *Atm. Environ.Vol. 28, No. 16,* p. 2595-2607.

ETELÄ-KARJALAN MAASEUTUKESKUS (1994). Karjanlannan tehokkaampi hyödyntäminen Karjalan Kannaksen alueella. Loppuraportti 21.12.1994, 25 p. (in Finnish)

FEICHTER J., KJELLSTRÖM E., RODHE H., DENTENER F., LELIEVELD F. and ROELOFS G.-J., 1996. Simulation of the tropospheric sulfur cycle in a global climate model. *Atm. Environ.Vol. 30, No. 10/11,* p. 1693-1707.

FINLAYSON-PITTS B.J. & PITTS J.N.Jr., 1986. Atmospheric chemistry, Fundamentals and experimental techniques. John Wiley & Sons, Inc. New York, 1098 p.

FOWLER J.A., 1994. Net primary productivity in the terrestial biosphere: the application of a global model. *J. Geophys. Res., Vol. 99, No. D10*, p. 20773-20783.

FRAUDE F. & GOSCHNICK J., 1995. Obstructed wetting of combustion aerosol particles in the presence of organic pollutants. 230 in: *Anttila, P., Kämäri, J. and Tolvanen, M. (eds), Proc. of the 10th World Clear Air Congress, Finland, Vol 2.* The Finnish Air Pollution Prevention Society, Helsinki.

HASS H., 1991. Description of the EURAD Chemistry-Transport-Model Version 2 (CTM2). *Mittailungen aus dem Institut fur Geophysik und Meteorologie der Universität zu Köln. Herausgeber A. Ebel, F.M. Neubauer, P. Speth. Heft 83*, 100 p.

HEGG, D. A., 1985. The importance of liquid-phase oxidation of SO_2 in the troposphere. *J. Geogphys. Res. 90*: 3773-3779.

HEIKINHEIMO M.J. & HELLSTEN E., 1992. Grid point presentation of effective surface roughness length and mean wind speed. In: *Tammelin B., Säntti K., Peltola E., Neuvonen H., (ed.'s) BOREAS - North Wind - Pohjatuuli. An international experts meeting on wind power in icing conditions. Finnish Meteorological Institute, Weather Department /Technical Climatology,* p. 153-163.

HESSTVEDT E., HOV Ø. and ISAKSEN S.A., 1978. Quasi-steady-state approximations in air pollution modelling: Comparison of two numerical schemes for oxidant prediction. *Int. J. Chemical Kinetics, vol X,* p. 971-994.

HICKS B. B., BALDOCCHI D. D., MEYERS T. P., HOSKER Jr, R. P. and MATT D. R., 1987. A preliminary multiple resistance routine for deriving dry deposition velocities from measured quantities. *Water, Air and Soil Pollution 36 (1987),* p. 311-330.

HIRLAM, 1990. Hirlam Forecast model level 1. On-line documentation manual. Per Kållberg, (ed.), *SMHI S - 60176*, Norrköping, Sweden, June 1990.

HIRLAM 1996. HIRLAM documentation manual, System 2.5. Källen E.,(ed.), June 1996.

HOLTSLAG A. A. M., de BRUIN, E.I.F. & PAN, H.-L.1990. A high resolution air mass transformation model for short-range weather forecasting. *Mon. Weather Rev., 118, No. 8,* p. 1561-1575.

HOLTSLAG A. A. M. & NIEUWSTADT F. T. M., 1986. Scaling the atmospheric boundary layer. *Boundary-Layer Meteorology 36*, 201-209.

HONGISTO M., 1992 A simulation model for the transport, transformation and deposition of oxidised nitrogen compounds in Finland. 1985 and 1988 simulation results. *Finnish Meteorol. Inst. Contributions No. 9*, Helsinki, 114 p.

HONGISTO M., 1993. A simulation model for the transport, transformation and deposition of oxidised nitrogen compounds in Finland. Technical description of the model. *Finnish Meteorol. Inst. Air quality publications No. 14*, Helsinki, 55 p.

HONGISTO M., 1998. Hilatar, a regional scale grid model for the transport of sulphur and nitrogen compounds. FMI Contributions no 21, Helsinki, 152 p. Yliopistopaino, Helsinki, 1998. http://www.fmi.fi/research_air/air_25.html (October 2002)

HONGISTO M., KANGAS L., NORDLUND G.,, MARKKANEN K., HÄKKINEN A. J., KARTASTENPÄÄ R. & KIVIVASARA J., 1995. Model calculations of the influence on Finland of

air pollution sources in the areas of St. Petersburg, Leningrad Oblast Karelia and Estonia. In: *Proceedings of the10th World Clear Air Congress, Espoo-Finland May 28- June 2, 1995, Vol*

HOV, Ø., 1983. Numerical solution of a simplified form of the diffusion equation for chemically reactive atmospheric species. *Atmos. Environ. Vol. 17, No. 3*, p. 551-562.

HÄKKINEN A.J., MARKKANEN K., HONGISTO M., KARTASTENPÄÄ R., MILYAEV V., YASENSKY A.N., KUZNETSOV V.I., KOPP I.Z. and KIVIVASARA J., 1995. Emission in St. Petersburg, the Leningrad Area and Karelia. In*: Tolvanen M., Anttila P., Kämäri J. (ed's): Proceedings of the 10th World Clear Air Congress, Espoo-Finland May 28- June 2, 1995.Vol 1, Emissions and control.* The Finnish Air Pollution Prevention Society, 1995. Ext. abstract 103.

HÖFKEN K. D., MEIXNER F. and EHHALT D. H., 1988. Dry deposition of NO, NO_2 and HNO_3. In: *van DOP H. (ed.), Air pollution modeling and its application VI, Proc. the NATO/CCMS int. techn. meeting, April 6-10, 1987, Lindau, FRG*. Plenum press, NY, p. 15-22.

IVERSEN T., SALTBONES J., SANDNES H., ELIASSEN A. and HOV Ø., 1989. Airborne transboundary transport of sulphur and nitrogen over Europe - Model descriptions and calculations. *EMEP MSC-W Report 2/89. DNMI Technical Report No. 80.* DNMI, Oslo, Norway, 92 p.

IVERSEN T., HALVORSEN N.E., MYLONA S. and SANDNES H., 1991. Calculated budgets for airborne acidifying components in Europe. *EMEP MSC-W Report 1/91. DNMI Technical Report No. 91.* DNMI, Oslo, Norway, 80 p. + Appendices.

JAKOBSEN H.A., BERGE E., IVERSEN T. and SKÅLIN, R., 1995. Status of the development of the multilayer Eulerian model. a) Model description, b) a new method of calculating mixing heights, c) model results for sulphur transport and deposition in Europe for 1992 in the 50 km grid*. EMEP/MSC-W Note 3/95, DNMI Research Report no 21.* 69 p.

JAKOBSEN H.A., JONSON J.E. and BERGE E., 1996. Transport and deposition of sulphur and nitrogen compounds in Europe for 1992 in the 50 km grid by use of the multilayer Eulerian model. *EMEP/MSC-W Note 2/96*, 70 p.

JOFFRE S.M., 1988. Parameterisation and assessment of processes affecting the long-range transport of airborne pollutants over the sea. *Finnish Meteorological Institute, Contributions No. 1*, 49 p.

JOHANSSON C.,1989. Fluxes of NO_x above soil and vegetation. In *Andreae M.O. & SCHIMEL D.S. (ed.'s) Exchange of trace gases between terrestial ecosystems and the atmosphere*. John Wiley, New York, p. 229-246.

JONSEN J.,E. & BERGE E., 1995. Some preliminary results on transport and deposition of nitrogen compounds by use of the Multilayer Eulerian Model. *EMEP/MSC-W, Note 4/95*, 25 p.

JYLHÄ K., 1995. Deposition around a coal-fired power station during a wintertime precipitation event. *Water, air and soil pollution 85*, p. 2125-2130.

KELLER A.A., ISLIAEV R.A., MALEVANNY I.N., AGAFONOV N.T. and SILK T.A., 1994. Morbidity of the population in the Leningrad Oblast. Saint-Petersburg Innovation and Marketing Center, 4 p.

KIVIVASARA J., 1994. Eestin päästökartoitus vuodelle 1991 - Päästömallin kehittäminen. Teknillinen korkeakoulu, prosessi- ja metallitekniikan osasto, Puunjalostustekniikan laitos. DI-työ, 1994, 139+22 p.

KIVIVASARA J., RANTAKRANS E. and HAARALA S., 1994. Arvio Kundan sementtitehtaan aiheuttamista ilman rikkidioksidi- ja hiukkaspitoisuuksista. *Ilmatieteen laitos, Ilmanlaatuosasto, Helsinki 8.7.1994.* 18+9 p. (in Finnish)

LIGHTFOOT P.D., COX R. A., CROWLEY J.N., DESTRIAU M., HAYMAN G.D., JENKIN, M.E., MOORTGAT G.K. and ZABEL F., 1992. Organic peroxy radicals: kinetics, spectroscopy and tropospheric chemistry. *Atm. Environ., Vol 26 A, No. 10,* p. 1805-1964.

LINDFORS V., JOFFRE S.M. and DAMSKI J., 1991. Determination of the wet and dry deposition of sulphur and nitrogen compounds over the Baltic Sea using actual meteorological data. *Finnish Meteorological Institute, Contributions No. 4*, 111p.

LÖVBLAD G., ERISMAN J.W. and FOWLER D., (ed's), 1993. Models and methods for the quantification of atmospheric input to ecosystems. An international workshop on the deposition of acidifying substances in Göteborg 3-6 November 1992. *Nordiske Seminar og Arbejdsrapporter 1993:573*, The Nordic Council of Ministers, 221 p.

MARCHUK G.I., 1975. Methods of numerical mathematics. Springer-Verlag, New York, 316 p.

MARCHUK G.I., 1986. Mathematical models in environmental problems. In: Lions J.L., Papanicolaou G., Fujita H. & Keller H.,B., *Studies in mathematics and its applications, Vol 16.* Elsevier Science Publishers B.V., North-Holland-Amsterdam, 217 p.

MARKKANEN K., (1995). Personal communication and correspondence with Olli Valo, Kymen vesi- ja ympäristöpiiri.

MEIXNER, F.X., FRANKEN, H.H., DUIJZER, J.H. and AALST, R.M., 1988a. Dry deposition of gaseous HNO_3 to a pine forest. In: *van DOP, H. (ed.), Air pollution modeling and its application VI, Proc. the NATO/CCMS int. techn. meeting, April 6-10, 1987, Lindau, FRG*. Plenum press, NY, p. 23-35

MEIXNER, F.X., SLEMR, F. and RENNENBERG, H., 1988b. Biosphere-atmosphere exchange of nitrogen oxides. In: *BEILKE, S., MORELLI, J. & ANGELETTI, G., (eds.), CEC air pollution research report 14, Field measurements and their interpretation. Proceedings of a workshop organized within the framework of the concerted action 'Physico-chemical behaviour of atmospheric pollutants', Cost 611, held on Villefranche sur Mer, France 3-4 May 1988.* p. 19-24.

MEYERS T. P. & BALDOCCHI D. D, 1993a. Trace gas exchange above the floor of a deciduous forest, 2. SO_2 and O_3 deposition. *J. of Geophys. Res., Vol 98, No. D7,* p. 12631-12638.

MEYERS T. P. & BALDOCCHI D. D, 1993b. A comparison of models for deriving dry deposition fluxes of O_3 and SO_2 to a forest canopy. *Tellus, 40B,* p.270-284.

MEYERS T. P., HICKS B. B., HOSKER R. P. Jr., WOMACK J. D. and SATTERFIELD L.C., 1991. Dry deposition inferential measurement techniques - II. Seasonal and annual deposition rates of sulfur and nitrate. *Atmos. Env. Vol. 25A, No.10*, p.2361-2370.

MILYAEV V. B. and YASENSKI, A. N. 1997. Data collection and evaluation in Russia for GENEMIS. In: *Ebel A., Friedrich R. and Rodhe H., (ed's). Transport and chemical transformation of pollutants in the troposphere Vol. 7, Tropospheric modelling and emission estimation, chemical transport and emission modelling on regional, global and urban scales*. Springer-Verlag Berlin Heidelberg 1997, p. 297-305.

MUR, 1994. Katsaus Murmanskin alueen ilmakehää saastuttavien aineiden päästöihin vuonna 1993. Venäjän Federaation Ympäristönsuojelu- ja luonnonvarainministeriö, Murmanskin alueen ekologia- ja luonnonvarainkomitea. Murmansk 1994. Käännetty venäjänkielisestä alkuperäisraportista suomenkielelle, 16+70 p.

MÄKELÄ K. & SALO M., 1994. Traffic emissions in Russia and the Baltic States. St. Petersburg, Leningrad Oblast, Republic of Karelia, Estonia, Latvia and Lithuania. *VTT Research notes 1569*.49 p.

MÄKELÄ K., 1990. Eestin tieliikenteen pakokaasupäästöjen laskentajärjestelmä ELIISA, *VTT Tie ja liikennelaboratorio Tutkimusselostus 802.* VTT, Tallinnan Teknillinen korkeakoulu, Espoo. 44p.

MÖLLER, D., 1980. Kinetic model of atmospheric SO_2 oxidation based on published data. *Atm. Environ, Vol. 14*, p. 1067-1076.

MÖLLER D. and MAUERSBERGER G., (1992) Modelling of cloud water chemistry in polluted areas. In Schwarz, S.E. & SLINN W.G.N. (ed's). Precipitation scavenging and atmosphere-surface exchange. Vol 1 - The Georgii volume: Precipitation scavenging processes. Hemisphere Publishing Corporation, Washington. p. 551-562.

NAPAP, 1991, Irving, P.M., (ed.). Acid deposition: state of science and technology. Summary report of the U.S. National Acid Precipitation Assessment Program (NAPAP). U.S. Government Printing Office, 265 p.

NIKMO J., TUOVINEN J.-P., KUKKONEN J. and VALKAMA I., 1997. A hybrid plume model for local-scale dispersion. *Finnish Meteorological Institute, Publications on Air Quality 27,* 65 p.

NORDLUND, G., RANTAKRANS, E., TAALAS, P. & VAAJAMA, P., 1986. Savunouseman arvioiminen. Ilmatieteen laitos, ilmanlaatuosasto, 43 s. (in Finnish)

PADRO, J. & EDWARDS, G.C., 1991. Sensitivity of ADOM dry deposition velocities to input parameters: A measurements for SO_2 and NO_2 over three land use types. *Atmos. Ocean 29 (4),* p. 667-685.

PADRO, J., 1993. Seasonal contrast in modelled and observed dry deposition velocities of O_3, SO_2 and NO_2 over three surfaces. *Atmos. Environ. 27A: No.6,* p 807-814.

PADRO, J., NEUMANN H.H and den HARTOG, G., 1991. Dry deposition estimates of SO_2 from models and measurements over a deciduous forest in winter. Water, Air and Soil Pollution 68: p 325-339.

PERSSON C., LANGNER J and ROBERTSON L., (1994). Regional sprindnings-modell för Göteborgs och Bohus, Hallandas ock Älvsborgas län. Regional luftmiljöanalys för år 1991. *SMHI RMK Nr. 65, April 1994*, 76 p.

PHAM M., MÜLLER, J.-F., BRASSEUR G.P., GRANIER C. and MEGIE G., 1995. *J. Geophys. Res*, Vol. 100, No. D12, p. 26061-26092.

PIETARILA H., SALMI T., KIVIVASARA J., 1996. The Finnish National emission register. On-line documens, outputs and personal communication.

PLANCENTER LTD, 1991a. Environmental priority action programme for Leningrad, Leningrad region, Karelia and Estonia. Synthesis report. Ministry of the Environment of Finland, 193 p.

PLANCENTER LTD, 1991b. Environmental priority action programme for Leningrad, Leningrad region, Karelia and Estonia. Pre-feasibility study No. 6, Development of livestock farming waste management in the Leningrad Region. Ministry of the Environment of Finland, Appendix 1.

PRESS W. H., FLANNERY B. P., TEUKOLSKY S. A. & VETTERLING W.T., (1986). Numerical recipes, the art of scientific computing. Cambridge University Press, New York, 818 p.

PRUPPACHER H. R. & KLETT, J. D., 1980. Microphysics of clouds and precipitation. D.Reidel Publishing Company, Dordrecht, Holland, 714 p.

RANTAKRANS E., KARTASTENPÄÄ R., KIVIVASARA J., HAARALA S. and KARPPINEN A., 1995. Arvio Imatra-Svetogorskin alueen rikkilaskeumasta v. 1993. *Ilmatieteen laitos, Ilmanlaatuosasto, 13.6.1995*. 34+10 p. (in Finnish).

ROGERS R. R. & YAU M. K., 1989. A short course in cloud physics. In: *Ter Haar, D. (ed.), International series in natural philosophy, vol. 113,* Pergamon Press, Oxford, p. 74-77.

RUIJGROK W., VISSER H. and RÖMER, F.,G., (1992). The scavenging and wet deposition of acidifying components in Arnheim: 1984 - 1990. In: *Schwartz S.,E. and Slinn W. G. N., (ed's) Precipitation scavenging and atmosphere-surface exchange. Vol 1., The Georgii Volume: Precipitation Scavenging Process.* Hemisphere Publishing Corporation, Washington, Philadelphia, London, pp. 471-482.

SANDNES H., 1993. Calculated budgets for airborne acidifying components in Europe, 1985, 1987, 1988, 1989, 1990, 1991 and 1992. *EMEP/MSC-W Report 1/93, DNMI Technical Report no. 109*. 57 p. + appendices.

SASS B.H., 1992. A discussion on the proper choice of roughness length for heat and moisture illustrated by results from road temperature simulations. *LAM newsletter, No. 21, August 1992,* p. 142-149.

SCOTT B. C., 1982. Theoretical estimates of the scavenging coefficient for soluble aerosol particles as a function of precipitation type, rate and altitude. *Atmos. Environ. Vol. 16, No. 7,* p.1753-1762.

SEINFELD J. H., 1986. Atmospheric chemistry and physics of air pollution. John Wiley & Sons, 738 p

SELAND ∅, van PUK A., SORTEBERG A. and TUOVINEN J.-P., 1995. Implementation of a resistance dry deposition module and a variable local correction factor in the Lagrangian EMEP model. *EMEP/MSC-W Report 3/95*, 57 p.

SIMPSON D., 1991. Long period modelling of photochemical oxidants in Europe. Calculations for April-September 1985, April-October 1989. *EMEP/MSC-W Report 2/91. DNMI Technical Report No 92.* 64 p.

SIROIS, A. & BARRIE, L.A., 1988. An estimate of the importance of dry deposition as a pathway of acidic substances from the atmosphere to the biosphere in eastern Canada. *Tellus 40B*, p. 59-80.

SLEM F. & SEILER W., 1991. Field study of environmental variables controlling the NO emission from soil and the NO compensation point. *J. Geophys. Res., Vol 96, No. D7*, 13017-13031.

SLINN S. A. and SLINN W.G.N., 1980. Predictions for particle deposition on natural water surfaces. *Atmos. Environ. 14*, p. 1013-1016.

SLINN W.G.N., HASSE L., HICK B.B., HOGAN A.W., LAL D., LISS P.S., MUNNICH K.O., SEHMEL G.A. and VITTORRI O., 1978. Some aspects of the transfer of atmospheric trace constituents past the air-sea interface. *Atmos. Environ. 12*, p. 2055-2087.

SMOLARKIEWICZ P.K., 1983. A simple positive definite advection scheme with small implicit diffusion. *Mon. Wea. Rev. Vol 111*, p. 479-486.

STATISTICS, 1984. Statistics of radiosonde observations 1961-1980. Meteorological yearbook of Finland, Vol. 61-80, Part 3. Finnish Meteorological Institute, 174 p.

STULL R. B., 1988. An introduction to boundary layer meteorology. Kluwer Academic Publishers, Dordrecht, The Netherlands, 666 p.

TEN BRINK H.M., JANSSEN A. J., SLANINA J., (1988). Plume wash out near a coal-fired power plant: measurements and model calculations. *Atm. Envir., Vol 22, No. 1,* p. 177 -187.

TOURULA T., 1993. Kasvustovastuksen kokeellinen määrittäminen ja vertailu mallituloksiin. Helsingin yliopisto, Matemaattis-luonnontieteellinen tiedekunta, Meteorologian laitos, Pro gradu tutkielma, 58 s. (in Finnish)

TREMBACK C.J., POWELL J., COTTON W.R. and PIELKE R.A., 1987. The forward-in-time upstream advection scheme: Extension to higher orders. *Mon. Wea. Rev., 115*, 540-555.

TUOVINEN J-P., 1992. Turbulenttisen diffuusion K-teoriaan perustuva ilmansaasteiden leviämismalli. Teknillinen korkeakoulu, Tietotekniikan osasto, Teknillisen fysiikan koulutusohjelma. Diplomityö, (A dispersion model of air pollutants based on the K theory of turbulent diffusion). 109 p. (in Finnish)

van ULDEN A.P. & HOLTSLAG A.A.M., 1985. Estimation of atmospheric boundary layer parameters for diffusion applications. *J. Climate Appl. Meteor. Vol. 24,* p.1196-1207.

WALCEK, C.J., BROST R.A., CHANG J.S. and WESELY M.L., 1986. SO2, sulphate and HNO3 deposition velocities computed using regional landuse and meteorological data. *Atm. Environ., Vol 20, No. 5,* p. 949-964.

WALCEK, C. J. & TAYLOR, G.R., 1986. A theoretical method for computing vertical distributions of acidity and sulfate production within cumulus clouds. *J. of the atmospheric sciences, 15 Feb. 1986,* p. 339-355.

WESELY, M.L., 1988. Improved parameterisations for surface resistance to gaseous dry deposition in regional scale, numerical models. Atmospheric Sciences research laboratory, *US EPA, RTP, NC 27711*.

WESELY M.L. 1989. Parameterisation of surface resistances to gaseous dry deposition in regional-scale numerical models. *Atm. Environ., Vol 23, No. 6,* p. 1293-1304.

WESELY M.L., SISTERSON D.L., HART R.L., DRAPCHO D.L. and LEE L.Y., 1989. Observations of nitric oxide fluxed over grass. *J. of atmospheric Chemistry, 9,* p. 447-463.

WHELPDALE D.M. and KAISER M.S. (ed's), 1996. Global acid deposition assessment. *WMO Global Atmosphere watch, Environmental pollution monitoring and research programme report series No. 106, WMO - TD No. 777*, 241 p.

WILLIAMS R.M., 1982. A model for the dry deposition of particles to natural water surfaces. *Atmos. Environ. 16:8*, p. 1933-1938.

WILLIAMS E.J. & FEHSENFELD F.C., 1991. Measurement of soil nitrogen oxide emissions at three North American ecosystems. *J. of Geophys. Res., Vol. 96, No. D1*, p. 1033-1042.

WIRTZ K., ROEHL C., HAYMAN G. D., together with JENKING M. E. and the LACTOZ Steering Group, 1994. LACTOZ re-evaluation of the EMEP MSC-W photo-oxidant model. A joint EUROTRAC / EC project. EUROTRAC International Scientific Secretariat, Garmish-Partenkirchen, 45 p.

VOLDNER, E.C., BARRIE, L.A. & SIROIS, A., 1986. A literature review of dry deposition of oxides of sulphur and nitrogen with emphasis on longrange transport modelling in North America. *Atmos. Environ. Vol. 20, No. 11,* p.2101-2123.

YANENKO, N. N., 1971. The method of fractional steps. The solution of problems of mathematical physics in several variables. Springer-Verlag, Berlin, 160 p.

ZLATEV Z., BERCOWICZ, R., CHRISTENSEN J., ELIASSEN A., HOV O., IVERSEN T. and PRAHM L.P. 1990. An Eulerian air pollution model with non-linear chemistry. EMEP Workshop on the progress of transport modelling of nitrogen compounds. Potsdam 15-18 October 1990. pp. 30-58.

ZLATEV Z., 1995. Computer treatment of large air pollution models. Environmental science and technology library Vol. 2, Kluwer Academic Publishers, Dordrecht / Boston / London, 358 p.